PhD thesis

Investigating the association between P2X7 receptors, microglia and the actions of morphine

Stephen John Medhurst

A thesis submitted to the University of Edinburgh in accordance with the requirements for the Degree of Doctor of Philosophy in the Royal School of Veterinary Sciences.

2011

Author’s declaration

I declare that the work presented in this dissertation was carried out in accordance with the regulations of the University of Edinburgh. The work is original, except where indicated by specific reference in the text, and no part of the dissertation has been submitted for any other academic award. Any views expressed in the dissertation are those of the author.

Signed:.....

Date:.....

Abstract

P2X7 receptors belong to a family of membrane bound ion channels which are activated by extracellular ATP, resulting in the opening of a non-selective cation channel. After prolonged or repeated exposure to agonist, functional and cellular changes can occur, including the formation of a large pore, cell lysis and the release of mature, biologically active interleukin-1β. It is this diversity of functions that underlies the significance of this receptor in pain processing.

P2X7 receptors are expressed on microglia, which when activated, release a host of mediators which contribute to central sensitisation, a phenomenon associated with neuropathic pain. The role of P2X7 receptors in the activation of microglia is less well established and is the main subject of this thesis.

Before considering the interaction between P2X7 receptors and microglia, the first aim was to establish whether P2X7 receptors played a role in a pathological process known to be associated with microglial activation. An additional aim was to establish whether the site of action was in the central nervous system (CNS), where microglia are located. These aims were accomplished using a surgery-based rat model of neuropathic pain, the chronic constriction injury (CCI) model, and by comparing the effects of different P2X7 receptor antagonists when dosed peripherally or directly into the spinal cord. The results indicated that P2X7 receptor antagonists produced efficacy in the CCI model via a mechanism located in the CNS.

To further investigate the association between P2X7 receptors and microglia, a different experimental paradigm was explored. Chronically dosed morphine is known to activate microglia, the consequence of which is thought to underlie morphine tolerance and reduced morphine analgesia. By administering a P2X7 receptor antagonist to CCI-operated rats treated with chronic morphine, the interaction between the P2X7 receptor and morphine tolerance and analgesia was explored. The results showed that P2X7 receptor antagonism delayed morphine tolerance and increased the efficacy of low doses of morphine, suggesting an association between P2X7 receptors and microglia.

It was intended to confirm the interaction between a P2X7 receptor antagonist and morphine in another neuropathic pain model, namely varicella zoster virus-induced neuropathy. However due to a lack of reproducibility, this model was not used for pharmacological studies.

Having demonstrated an association between P2X7 receptor antagonist and morphine in a chronic pain setting, studies were initiated to explore whether this interaction occurred in other morphine-related behaviours. The effect on body weight, motor coordination and single dosed morphine-induced analgesia was assessed in rats co-administered with P2X7 receptor antagonist and morphine. Results demonstrated that the blockade of P2X7 receptors enhanced morphine acute dose-induced analgesia, but had no influence on motor-impairment and body weight.

The final part of the thesis used immunohistochemical and molecular techniques to confirm that microglia played a role in established allodynia induced by CCI-surgery and that P2X7 receptors directly influenced microglia-activation.

In conclusion, the data in this thesis has illustrated an association between centrally activated P2X7 receptors and microglia, as well as an association between the P2X7 receptor and morphine-induced tolerance and analgesia. It is possible that co-administration of a P2X7 receptor antagonist with morphine could reduce the effective dose of morphine clinically, thereby reducing the side effects of this commonly used analgesic.

Acknowledgements

Firstly, I would like to thank my supervisors, Dr. Bob Dalziel and Dr. Andy Billinton for all their help, guidance and constructive comments throughout my PhD studentship. I would also like to acknowledge GlaxoSmithKline for funding this study.

Thanks also to Dr John Davies, Dr Martin Gunthorpe and Dr Sharon Bingham for their infectious enthusiasm and encouragement in the latter stages of my PhD, and to Julie Egerton, Michal Sulikowski, David Wille, Daryl Walter and Vicky Hadden for advice with molecular biology, IHC, statistics, chemistry and DMPK respectively.

I would like to thank my family and friends for their love and support, especially my brother Andy, for his unending advice and encouragement. On a personal note, I would like to give special thanks to my wonderful wife, Katrina and my amazing children Henry and Katy for their support, patience and providing me with welcome distractions along the way.

Table of Contents

List of tables and figures

Abbreviations used in this thesis

5-HT	5-hydroxytryptophan
AC	Adenyl cyclase
AMPA	α-amino-3-hydroxy-5-methyl-4-isoxazolepropionic acid receptor
ANOVA	Analysis of variance
ATP	Adenosine tri-phosphate
BBG	Brilliant Blue G
b.i.d.	*Bins in die* (twice a day)
BDNF	Brain derived nerve factor
BSA	Bovine serum albumin
BzATP	3'-O-(4-benzoyl)benzoyl adenosine 5'-triphosphate
CaMKII	Calcium/ calmodulin-dependent protein kinase II
cAMP	Cyclic AMP
CCI	Chronic constriction injury
CCK	Cholecystokinin
CGRP	Calcitonin gene related protein
CNS	Central nervous system
COX	Cyclo-oxygenase
cpe	Cytopathic effect
CR3	Complement receptor 3
CSF	Cerebrospinal fluid
Ct	Cycle time
CX3C11	Frackalkine
CXCR1	Frackalkine receptor
DEPC	Diethylpyrocarbonate
DH	Dorsal horn
DMEM	Dulbecco’s modified Eagles medium
DMPK	Drug metabolism and pharmacokinetics
DMSO	Dimethyl sulphoxide
DPA	Dynamic plantar aesthesiometer
DRG	Dorsal root ganglia
EAA	Excitatory amino acid
EthBr	Ethidium bromide
ERK	Extracellular regulator kinase
FDA	Food and drug administration
GABA	γ-Aminobutyric acid

GAPDH	Glyceraldehyde 3-phosphate dehydrogenase
GFAP	Glial fibrillary acidic protein
GI	Gastro-intestinal
GLAST	Glutamate Aspartate Transporter
GLT-1	Glial glutamate transporter
GPCR	G-protein coupled receptor
GSK	GlaxoSmithKline
HEPES	4-(2-hydroxyethyl)-1-piperazineethanesulfonic acid
HIV	Human immunodeficiency virus
i.art.	Intra-articular
Iba-1	Ionised binding adaptor molecule-1
IHC	Immunohistochemistry
IL-1β	Interleukin 1β
IL-18	Interleukin 18
IL-6	Interleukin 6
IL-1ra	Interleukin-1 receptor antagonist
IMS	Industrial methylated spirit
iNOS	Inducible nitric oxide synthase
i.p.	Intra-peritoneally
i.pl.	Intra-plantar
IP10	Interferon gamma-induced protein 10 kDa
i.t.	Intrathecal
ITGAM	Integrin alpha M
i.v.	Intravenous
JNK	c-Jun N-terminal kinase
KO	Knock out
LC-MS/MS	Liquid chromatography-mass spectrometry-mass
LDS	Lactate dehydrogenase
LPS	Lipopolysaccharide
MAPK	Mitogen activated protein kinase
MCP-1	Monocyte chemotractant protein-1
MHC	Major histocompatability complex
MPE	Maximum possible effect
NGF	Nerve growth factor
NK-1	Neurokinin receptor 1
nm	Nanometer
NMDA	N-methyl-D-aspartate
NMDG	N-methyl-D-glucamine

NNT	Numbers needed to treat
NO	Nitric oxide
NSAID	Non-steroidal anti-inflammatory drug
ORF	Open reading frame
P2X	Purinergic receptor
PAG	Periaqueductal grey
PANX	Pannexin
PBR	Peripheral benzodiazapine receptor
PBS	Phosphate buffered saline
PEG	Polyethylene glycol
PFA	Paraformaldehyde
pfu	Plaque forming unit
PGE2	Prostaglandin E2 receptor
Pgp	P-glycoprotein
PHN	Post-herpetic neuralgia
PG	Prostaglandin
PKC	Protein kinase C
PLD	Phosholipase D
p.o.	*per os* (by mouth)
PWT	Paw withdrawal threshold
RT-PCR	Reverse transcription polymerase chain reaction
RVM	Rostral ventral medulla
s.c.	Subcutaneous
S.D.	Standard deviation
SEM	Standard error of the mean
SNI	Spare nerve injury
siRNA	Small interfering RNA
TLR	Toll-like receptor
TNFα	Tumour necrosis factor α
TRPV1	Transient receptor potential cation channel subfamily V member 1
UTP	Uridine-5'-triphosphate
v/v	Volume/volume percentage solution
VZV	Varicella zoster virus
w/v	Weight/volume percentage solution
WT	Wild type

Chapter 1

Introduction to chronic pain

1. Introduction to chronic pain

The current definition of pain is ‘An unpleasant sensory and emotional experience associated with actual or potential tissue damage, or described in terms of such damage’, as proposed by the International Association for the Study of Pain (www.iasp-pain.org).

The ability to sense pain is an essential component of the body’s normal defence mechanism and has two main purposes; firstly, it allows the organism to detect potential injury and triggers an appropriate protective response and secondly, it alerts the organism to previously injured tissue with an aim to prevent further injury.

The development of abnormal sensitivity in the somatosensory system however, results in pain of a more chronic nature. Pain is classed as ‘chronic pain’ when the symptoms outlast the normal time required for healing following tissue damage, or when it is associated with a pathological condition that does not heal.

Chronic pain affects millions of people worldwide, and is regarded by the World Health Organisation as a major reason for health related absence from work. Massive economic costs are also associated with chronic pain patients. In the United States the annual cost of chronic pain, including health care expenses, lost income and lost productivity, is estimated to be $100 billion (Dray and Perkins, 2010)

1.1.1 Inflammatory pain

Inflammatory pain occurs in response to tissue injury and the subsequent inflammatory response. To aid healing and repair of the injured body part, the sensory nervous system undergoes a profound increase in its responsiveness. For example, stimuli that were normally innocuous now produce pain (allodynia) and noxious stimuli become both exaggerated and prolonged (hyperalgesia). These heightened sensitivities are a result of plasticity in nociceptors and central nociceptive pathways.

Typically, inflammatory pain disappears after the resolution of the initial tissue injury. However, in chronic disorders, such as rheumatoid arthritis the pain persists for as long as inflammation is active. Non-steroidal anti-inflammatory drugs (NSAIDs) such as aspirin and ibuprofen are the most commonly prescribed drugs for

inflammatory pain (Vergne-Salle and Beneytout, 2010). These compounds inhibit arachidonic acid metabolism and prostaglandin production through inhibition of cyclo-oxygenase (COX) (Vane, 1971; Kawai, 1998), thereby eliminating the direct hyperalgesic and sensitising effects of these inflammatory mediators. However NSAIDs have limited efficacy in severe pain, due in part to the involvement of many inflammatory mediators capable of sensitising neurones (e.g. bradykinin), and also to side effects resulting from prostaglandin inhibition in other tissues, such as gastrointestinal bleeding (Goodwin, 1987), renal failure (Lifschitz, 1983) and cardiovascular effects (Waksman et al., 2007).

1.1.2 Neuropathic pain

Neuropathic pain is defined as "Pain initiated or caused by a primary lesion or dysfunction in the peripheral or central nervous system" by International Association for the Study of Pain (www.iasp-pain.org). Central neuropathic pain most commonly results from spinal cord injury, stroke or multiple sclerosis (Ducreux et al., 2006). Peripheral neuropathic pain results from lesions to the peripheral nervous system caused by mechanical trauma, metabolic disease, neurotoxic chemicals, infection or tumour invasion. It is found in a number of conditions including post-herpetic neuralgia (PHN), diabetic neuropathy, HIV-related neuropathies and trigeminal neuralgia.

The resulting sensory symptoms are very heterogeneous across patients. Sensory loss, spontaneous pain, allodynia and hyperalgesia are distinct symptoms of neuropathic pain all of which adversely affect the quality of a patients' daily life.

Neuropathic pain often responds poorly to commonly used analgesics and to standard doses of opioid analgesics (Tremont-Lukats et al., 2000), and so antiepileptic drugs, such as carbamazepine, lamotrigine, gabapentin and pregabalin, or tricyclic antidepressants, e.g. amitriptyline, and selective re-uptake inhibitors such as duloxetine, are often used to treat a wide range of neuropathic pain disorders (Mico et al., 2006; Zaremba et al., 2006). Although these treatments are available, the efficacy of these drugs in neuropathic pain is poor. In addition, there is generally a low patient responder rate to these agents meaning that there is a large patient group

with unmet medical need, therefore highlighting the requirement for novel effective analgesics in this area.

The two most common features of neuropathic pain are hyperalgesia, which can be separated into primary and secondary hyperalgesia, and allodynia. Primary hyperalgesia occurs following sensitisation of primary afferents i.e. peripheral sensitisation (Hargreaves et al., 1988; Millan, 1999), whereas secondary hyperalgesia is an increased sensitivity in areas surrounding the damaged tissue and is due to central sensitisation (Reichling and Levine, 1999; Millan, 2002). Central sensitisation is also thought to be responsible for allodynia. Peripheral and central sensitisation are discussed further in sections 1.2 and 1.3.

1.1.3 Nociceptive processing

Pain from mechanical, chemical or thermal nociceptive stimulation is transmitted from peripheral nociceptors *via* primary afferent neurons to the dorsal root ganglion (DRG) and into the dorsal horn of the spinal cord (see Figure 1). In the dorsal horn, the primary afferent neurons make synaptic contact with secondary neurons which send afferent projections to supraspinal sites. Secondary afferents either make a second synapse in thalamic nuclei which subsequently make synaptic contact with tertiary neurons, or synapse with neurons in the brainstem, including pariaqueductal gray (PAG) and the nucleus raphe magnus, areas involved in descending endogenous modulation. Tertiary neurons from the thalamus send afferent fibres to the somatosensory cortices which are involved in the sensory quality of pain and to limbic structures which are involved in the emotional component of pain (Gauriau and Bernard, 2004).

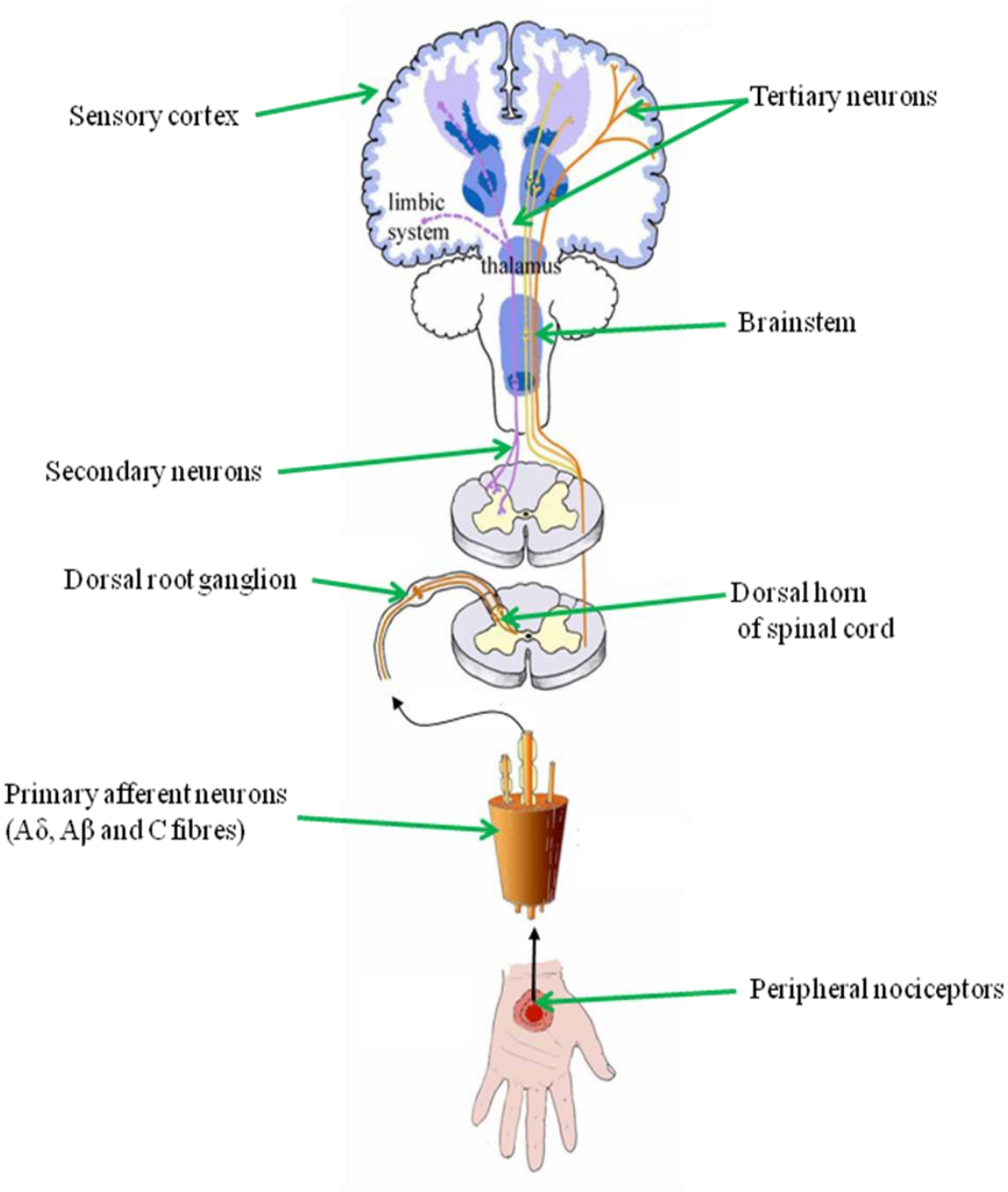

Figure 1. Diagram showing main pathway for sensory information from the periphery to the cortex (Modified from perioperativepain.com accessed on 20/08/10).

1.1.3.1 Peripheral nociceptors

Peripheral nociceptors are free nerve endings in the skin, muscle, articulation, fascia, and viscera that respond to nociceptive stimulation. Unlike other types of receptors, peripheral nociceptors can respond to multiple stimulus modalities, including temperature, mechanical and chemical stimuli (Bessou and Perl, 1969; Beck et al., 1974; Van and Gybels, 1981). The nociceptors are responsible for the transduction and transmission of the nociceptive signal.

1.1.3.2 Primary afferents

Primary afferent fibres transmit sensory information from the peripheral nociceptors to the spinal cord. Fibres that innervate regions of the head and body arise from cell bodies in the trigeminal and DRG respectively. They are categorised based on their myelination, the modality of stimulation that evokes a response and the characteristics of the response (see Table 1).

Fibre type	Fibre diameter (µM)	Myelination	Conduction velocity (m/s)	% primary afferents	Sensation following fibre activation
Aδ 	2-6	Thin	12-30	10	Noxious, sharp, prickling pain
Aβ 	>10	Thick	30-100	20	Non-noxious light touch
C 	0.4-1.2	None	0.05-2	70	Noxious, diffuse, persistent and poorly localised pain

Table 1. Characteristics of primary afferent fibres.

1.1.3.3 The role of the spinal cord in nociceptive processing

The different primary afferent fibres enter the spinal cord and terminate in specific laminae depending on density and myelination (Rexed, 1952) (see Figure 2). The first six laminae represent the principal site of modulation of pain by ascending and descending pathways, and make up the dorsal horn. The primary afferent fibres synapse onto second order neurones which have cell bodies in the dorsal horn.

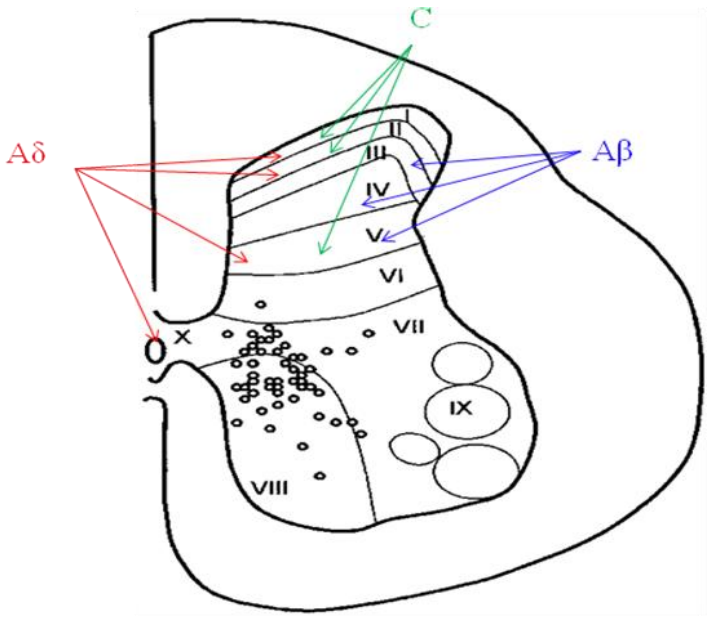

Figure 2. Diagram of Rexed's laminae of the spinal cord indicating the main laminae for the termination of fibres. The central terminals of primary afferents (Aδ, C and Aβ) occupy highly ordered spatial locations (I-X) in the dorsal horn.

1.1.3.4 The role of the brain in nociceptive processing

Neurones ascend from the spinal cord in a number of different tracts all ending at different destinations. These tracts include the spinothalamic tract which conveys information to the thalamus, a key structure in determining the type, temporal pattern, intensity and for cutaneous input, the topographical localisation of pain. These neurons then project to the primary somatosensory cortex and allow conscious localisation and characterisation of painful stimuli. The spinomesencephalic tract terminates in the PAG followed by the hypothalamus or amygdala (Millan, 1999).

These regions are known to modulate the emotional component associated with pain perception. Other ascending pathways include the spinoparabrachial tracts, the spinohypothalamic tract and the spinoreticular tract. Ascending pathways are responsible for the discrimination between differing sensory inputs and the affective qualities of pain (Millan, 1999; Hunt and Mantyh, 2001).

Pain perceived by a patient is the net result of peripheral and central neuronal activity and is the final outcome of complex mechanisms that modulate the nociceptive afferent signal. In addition to the excitatory mechanisms, like central and peripheral sensitisation, which will be discussed later, there are descending influences which can be inhibitory or facilitatory and originate from the brainstem (Millan, 2002; Vanegas and Schaible, 2004). These pathways can reduce or enhance the flow of nociceptive signals through the dorsal horn of the spinal cord and have been implicated in regulating pain sensitivity (Millan, 2002).

Descending inhibitory pathways have been shown to originate from several regions including the PAG and nucleus raphe magnus. These regions have important serotinergic and noradrenergic pathways which recruit enkephalinergic interneurons in the spinal cord to produce analgesia. Other areas include the corticodiencephalic and diencephalic system, the mesencephalic, periventricular grey areas, medullary centres, and from the locus coeruleus (Mayer and Price, 1976; Basbaum and Fields, 1984; Sagen and Proudfit, 1987; Bonica, 1990; Fields et al., 1991). Stimulation of areas of the brain known to be involved in descending inhibition, such as the PAG results in a negative modulation of pain. This has been demonstrated when painless surgery was carried out experimentally in animals when the PAG was stimulated (Reynolds, 1969).

Descending facilitation has been largely shown to originate within the rostroventral medulla (RVM) (Porreca et al., 2002). Numerous studies have implicated the RVM as a prominent source of descending modulation of nociception (Zhuo and Gebhart, 1992; Zhuo and Gebhart, 1997; McNally, 1999; Urban and Gebhart, 1999). For example low intensity focal brain electrical stimulation in the RVM region produced pain facilitation and high intensity stimulation produced an inhibition of tail flick reflex or dorsal horn activity (Zhuo and Gebhart, 1992).

Furthermore low dose microinjection of glutamate into the RVM facilitated pain and high dose inhibited the activity of spinal dorsal horn neurons (Zhuo and Gebhart, 1990; Zhuo and Gebhart, 1991; Urban and Gebhart, 1998). Other data also suggests that descending facilitation of nociceptive processing is mediated, in part, by 5-HT pathways from the RVM acting at spinal 5-HT3 receptors (McCleane et al., 2003; Oatway et al., 2004).

The RVM consists of 3 classes of neurons based on response characteristics to nociceptive stimuli. 'Off cells' pause in their firing immediately before a withdrawal response to nociceptive stimuli occurs and produce an inhibition of nociceptive input and nocifensive response. 'On cells' accelerate firing immediately before the nociceptive reflex occurs and activate a descending facilitation of nociceptive processing within RVM and projection to the spinal cord (Fields et al., 1983; Zhuo and Gebhart, 1990; Heinricher and Roychowdhury, 1997). Neutral cells show no electrophysiological response to nociception.

Activity in both ascending and descending pathways appears to be essential for the maintenance of chronic pain states (Nichols et al., 1999; Porreca et al., 2002).

1.2 Peripheral sensitisation

Sensitisation of primary afferents can occur following tissue injury or inflammation, or through direct activation. This phenomenon results in the release of chemicals and inflammatory mediators, like bradykinin, prostaglandins, 5-HT, nitric oxide (NO), acetylcholine, adenosine-5'-triphosphate (ATP) and protons from neurons, blood vessels and immune cells (Kress and Reeh, 1996; McMahon et al., 2006). These substances act directly on primary afferent neurones, causing pain or sensitisation (Kress and Reeh, 1996) or indirectly via inflammatory cells (including macrophages, mast cells, fibroblasts and synoviocytes) which act on primary afferent neurons via the release of cytokines such as Interleukin-1β (IL-1β) and Tumour necrosis factor-α (TNF-α) (Bianchi et al., 1998). Once released, IL-1β causes sensitisation of afferents by a variety of different mechanisms. These mechanisms include the stimulation of prostaglandin E_2 (PGE_2) release from inflammatory cells (Dayer et al., 1986), inducing nerve growth factor (NGF) (Yoshida and Gage, 1992;

Safieh-Garabedian et al., 1995) and upregulating substance P levels in neurones (Jonakait et al., 1990; Hart et al., 1991).

Part of the inflammatory response is also driven by the release of intracellular contents from damaged cells thereby releasing a number of inflammatory mediators including histamine, 5-HT (Leon et al., 1994) and cytokines (see section 1.4.5.) which excite primary afferents. These substances also induce vasodilation and extravasation of plasma proteins which increase sensitisation further.

Overall, direct and indirect mechanisms lead to a greater release of glutamate and substance P from central afferent terminals resulting in hyperexcitability, a reduced threshold for activation, inputs from low threshold stimuli and an increase in spontaneous firing (Woolf, 1983; Woolf and Thompson, 1991; Xu et al., 1992; Ma and Pei, 2007). Additionally, silent nociceptors that were previously quiescent are activated (Coggeshall et al., 1983; Schaible and Schmidt, 1988).

1.3 Central sensitisation

Central sensitisation is triggered by persistent nociceptor afferent input as a result of tissue damage or peripheral inflammation. It may result from many mechanisms including modulation of NMDA receptors (Mayer et al., 1999), dynorphin (Vanderah et al., 2001a), AMPA/ kainate receptor (Kest et al., 1997), CGRP (Powell et al., 2000) and cyclooxygenase (Powell et al., 1999) all promoting neurotransmitter release and/or post-synaptic potentiation of sensory transmission.

The result is a state of hypersensitivity where low-intensity stimuli, which are innocuous under normal conditions, are able to initiate pain sensations. This mechanism has a protective purpose by sparing injured body parts from further injury while healing occurs (Woolf and Walters, 1991). There are a variety of physiological changes that occur following persistent nociceptor input: a reduction in the threshold for activation of dorsal horn neurones; an increase in the responsiveness of dorsal horn neurones to the periphery and an expansion of the peripheral receptive field of dorsal horn neurones (Hylden et al., 1987; Woolf, 1991). Alterations in neuronal receptive field properties were first investigated by examining the cutaneous

receptive fields of flexor motor neurones following peripheral tissue injury or brief, high-threshold afferent inputs (Woolf and Wall, 1986).

The ability of the primary afferent barrage to initiate central sensitisation has been demonstrated in a variety of studies injecting capsaicin into both rats and man (LaMotte et al., 1992; Nozaki-Taguchi and Yaksh, 1998). The injection evokes secondary hyperalgesia which describes hyperalgesia in a region well outside the injection area, and is believed to arise purely from central sensitisation rather than peripheral sensitisation.

In chronic pain states, plastic changes in either the primary afferents or the dorsal horn may also occur, leading to increased central sensitisation. For example, 'phenotypic switch' enables Aβ-fibres to contribute to inflammatory hypersensitivity by switching their phenotype to one resembling C-fibres, by expressing substance P and other modulators (Neumann et al., 1996). This results in low-intensity stimulation inducing excitability in dorsal horn neurones (Neumann et al., 1996; Cotrina and Nedergaard, 2009). Large myelinated afferent fibres also change behaviour, by growing from the deep dorsal horn where they normally terminate into lamina II, where C-fibres terminate (Woolf, 1991; Koerber et al., 1994; Baba et al., 1999).

All of the physiological changes detailed above result in a state of hypersensitivity where low-intensity stimuli, which are innocuous under normal conditions, are able to initiate pain sensations.

1.4 Glia

Until recently glia (Greek for 'glue'), were considered as having a merely supporting function to neurons, regulating ionic environment and removing debris. It is now widely accepted that these cells share many characteristics of neurons and play a key role in the induction and maintenance of central sensitisation (Watkins et al., 1997; Colburn and Deleo, 1999; Milligan et al., 2003a). Glia also express receptors for many neurotransmitters and neuromodulators and synthesize and release numerous mediators in much the same way as neurons do.

1.4.1 Glial cell types

The term glia encompasses 3 main cell types (see Figure 3) which make up approximately 70% of the total cell population in the brain and spinal cord:

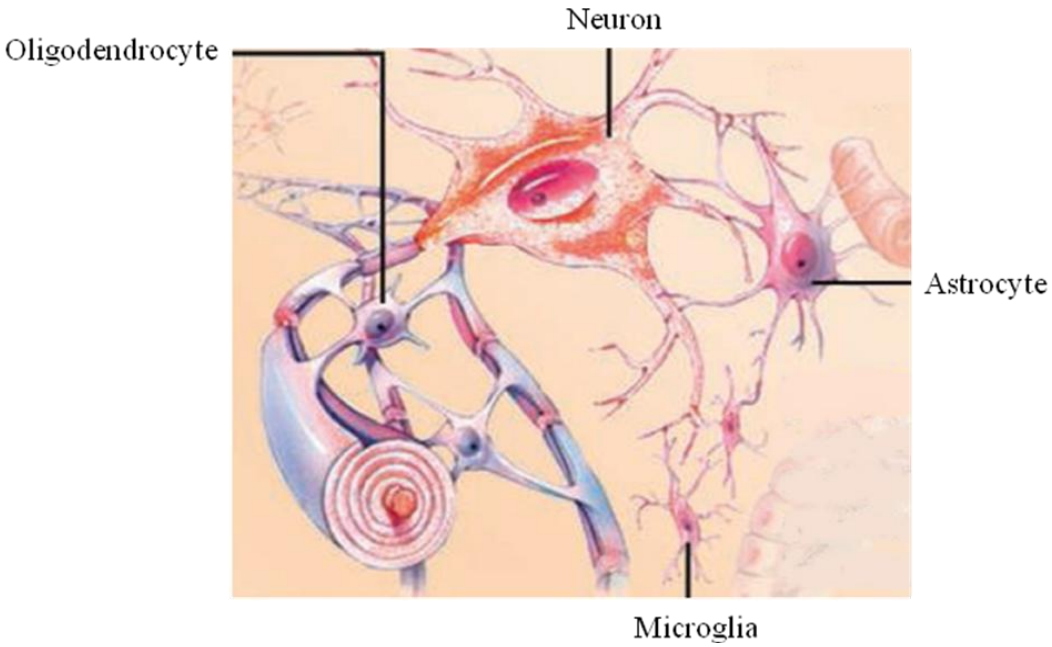

Figure 3. Diagram showing the three main types of glia cells (Miller, 2005).

Oligodendrocytes which synthesize myelin sheaths for multiple neurones (Peters, 1964) allowing fast nerve conduction.

Microglia which account for 5-10% of the total glial cell population, are known as the resident macrophages of the CNS and are the first cell type to respond to injury (Kreutzberg, 1996; Stoll and Jander, 1999). At rest microglia display a characteristically ramified morphology with numerous branching processes (Soltys et al., 2001) actively sensing their microenvironment. When activated however the cells proliferate and change in morphology from ramified to amoeboid shape (Tsuda et al., 2005). In this new form, microglia perform new functions including neural regeneration, phagocytosis and release of proinflammatory cytokines (Andersson et al., 2005; Persson et al., 2005). On activation there is also an increase in expression of certain markers specific to microglia, for example major histocompatability

complex II (MHC II), integrin alpha (ITGAM, also known as cluster of differentiation molecule 11b or CD11b) and ionised calcium binding adapter molecule 1 (Iba-1) (Eriksson et al., 1993; Hayes et al., 1987).

Astrocytes, the most numerous of all glial cells, are star-shaped cells with a central cell body and long processes extending in all directions. These processes make connections with neuronal synapses (Bushong et al., 2002), the vasculature (Abbott et al., 2006) and other astrocytes (Blomstrand et al., 1999; Guthrie et al., 1999) and play a key role in neuronal activity. They are responsible for the clearance of transmitters, such as glutamate and GABA from synaptic clefts, but also have the ability to release proinflammatory cytokines such as IL-1β, IL-18 and TNF-α, excitatory amino acids and growth factors (Araque et al., 1999). On activation there is an increase in expression of certain specific markers of astrocytes including glial-fibriliary acidic protein (GFAP).

1.4.2 Glia activators

Astrocytes and microglia are activated by a variety of mediators from a variety of sources (see Table 2). The outcomes of activation are very similar whichever source induced it (Watkins and Maier, 2003)

Glia activating mediators	Source	References
Excitatory amino acids	Activated nociceptive primary afferents	(Aicher et al., 1997)
ATP		(Tsuda et al., 2005)
Substance P		(Marriott, 2004)
Glutamate		(Snyder and Kim, 2004)
CGRP		(Priller et al., 1995)
Fractalkine		(Verge et al., 2004)
NO	Spinal cord secondary neurons	(Holguin et al., 2004)
Prostaglandins		(Watkins et al., 2001)
Fractalkine		(Verge et al., 2004)
Gangliosides	Cell injury	(Min et al., 2004)
Lysophosphatidic acid		(Watkins, 2007)
Nuclear components		(Watkins, 2007)
Heat shock proteins.		(Hutchinson et al., 2007)
Proinflammatory substances	Neighbouring glia	(Watkins, 2007)
Proinflammatory cytokines	Chronic morphine	(Raghavendra et al., 2002)
Proinflammatory cytokines	Invading viruses and bacteria	(Milligan et al., 2001)

Table 2. Table summarising the key mediators which activate glia and some of the sources which induce their release.

Some of these activating substances, including ATP and repeated administration of morphine, have particular importance to this thesis and will be discussed in more detail in sections 1.5 and 1.7 respectively.

Certain activators are considered as key neurone-glial signalling molecules. These include chemokines such as fractalkine, which has been extensively used to characterise glial activation. Fractalkine (also known as CX3C11) is expressed on extracellular surfaces of spinal neurones (Verge et al., 2004) and act on fractalkine receptors (CXCR1) which are predominantly expressed by spinal microglia and are upregulated in neuropathic pain states (Lindia et al., 2005; Milligan et al., 2008; Shan et al., 2007; Verge et al., 2004). Interestingly fractalkine only activates microglia when unbound from neurones after neuronal challenge (Chapman et al., 2000) as illustrated by a dramatic reduction in membrane fractalkine in DRG and spinal cord neurons (Zhuang et al., 2007). The involvement of fractalkine in pain transmission has been demonstrated by the enhanced pain responsivity observed when the chemokine is injected intrathecally (Milligan et al., 2008). Suggestions that this pain facilitation occurs via microglia activation and release of proinflammatory cytokines and NO have also been made, as the chemokine-induced pain can be blocked by minocycline, an inhibitor of activated microglia, IL-1 receptor antagonist and a nitric oxide inhibitor (Milligan et al., 2008). Supporting this hypothesis, fractalkine has been shown to induce IL-1β release from the spinal cord (Johnston et al., 2004). Finally, fractalkine has also been reported to upregulate the expression of the purinergic P2X4 receptor (Wieseler-Frank et al., 2004) suggesting an involvement in microglia priming in response to ATP. This role has particular significance to this thesis and will be discussed in more detail in Chapter 3.

Other chemokines thought to be key neurone-glial signalling molecules include interferon-inducible protein of 10 kDa (IP-10) and monocyte chemoattractant protein -1 (MCP-1) which are rapidly induced and released from damaged neurons and activate glia (Gao and Ji, 2010).

When considering receptors for substances released by damaged neurons, there is a group of receptors known as pattern recognition receptors. The pattern recognition receptors researched most are the toll-like receptors (TLRs). For

example, in response to nerve injury, TLR1, 2 and 4 have each been reported to be up-regulated in the CNS (Tanga et al., 2004; Tanga et al., 2005), linked to production of proinflammatory cytokines (e.g. TNF and IL-1) and chemokines (e.g. MCP-1) (Owens et al., 2005).

1.4.3 Glial activation

When activated, as well as morphological changes, proliferation and increased expression of cell surface markers, glia also release a host of neuroexcitatory substances including proinflammatory cytokines (TNF, IL-1 and IL-6), reactive oxygen species, nitric oxide, prostaglandins, excitatory amino acids (primarily glutamate) and ATP (Tikka and Koistinaho, 2001; Svensson et al., 2005). All these released substances were classically assumed to derive solely from neurons, hence the majority of previous pain literature did not focus on a contribution of glia to the effects observed.

1.4.4 Role of glial cells in regulation of pain

It was in 1991 that Garrison first made a link between pain and glial activation by demonstrating astrocyte activation in a neuropathic pain model by using the astrocyte-specific marker GFAP (Garrison et al., 1991), an effect that could be blocked with analgesics such as the NMDA receptor antagonist MK-801 (Garrison et al., 1994). Since then glia activation has been identified in a wide range of preclinical models of chronic pain, such as inflammation (Raghavendra et al., 2004b; Sweitzer et al., 1999) , nerve injury (Colburn et al., 1999) and bone cancer (Schwei et al., 1999; Zhang et al., 2005a) using various markers, including Iba-1 (Ji and Suter, 2007).

Many behavioural studies using different animals models of chronic pain have also demonstrated the importance of glia in pain transmission, by showing that selective glial inhibitors reduce hyperalgesia or allodynia (Meller et al., 1994; Watkins et al., 1997; Sweitzer et al., 2001).

Fluorocitrate which selectively disrupts the Krebs energy cycle in glia (Fonnum et al., 1997), has been shown to block hyperalgesia in a range of models including sciatic inflammatory neuropathy (Milligan et al., 2003b), intrathecal delivery of viral

components (Milligan et al., 2000; Milligan et al., 2001) and subcutaneous formalin (Watkins et al., 1997).

Minocycline also inhibits microglial function and has been shown to pre-emptively block the production and release of proinflammatory cytokines in neuropathic pain models (Raghavendra et al., 2003a), and also block the induction of hypersensitivity (Raghavendra et al., 2003a; Ledeboer et al., 2005a). These authors also showed that minocycline had little effect on hypersensitivity once activation had been established, indicating that microglia have more of a role in the development of pain states than in the maintenance of pain. This may be due to microglia producing a more rapid response to injury, whereas the astrocyte response was more delayed. It was suggested that early microglial activation led to astrocyte activation which then served to maintain the hypersensitivity and consequently the pain. These theories have since been put into question with a perseverative role for microglia having recently been reported (Hains and Waxman, 2006; Tawfik et al., 2007). Hains and Waxman (2006) observed that minocycline reversed nerve-injury induced hypersensitivity 4 weeks after surgery and Tawfik et al. (2007) observed propentofylline, a glial inhibitor, reversing hypersensitivity with an increase in activated protein level, using ITGAM (CD11-b), up to day 42 post-nerve injury.

Other microglia inhibitors shown to block hyperalgesia are methotrexate (Hashizume et al., 2000) and ibudilast, which have been shown to attenuate mechanical allodynia in three neuropathic pain models: the chronic constriction injury model (CCI), the spinal nerve injury model (Chung) and Taxol-induced allodynia model (Ledeboer et al., 2006).

The mechanisms by which glia modulates pain are very complex. Briefly, the substances released from activated glia excite spinal neurons and cause exaggerated release from sensory neurons that synapse in the dorsal horn of pain transmitters, such as reactive oxygen species, nitric oxide, prostaglandins, excitatory amino acids or growth factors. It is important to note that the involvement of glia in pain processing seems to be limited to pathological hypersensitivity with no effect on basal, acute pain processing.

There is increasing evidence suggesting a specific role of microglia in the development of neuropathic pain states (for recent reviews see Watkins et al., 2005; Watkins, 2007) and some authors suggest that microglia are responsible for the initiation of neuropathic pain states (Ledeboer et al., 2005a; Cui et al., 2008; Mika et al., 2009a). It is hypothesised that released proinflammatory factors such as IL-1, TNF, IL-6 from microglia play a substantial role in central sensitisation leading to neuropathic pain (Hanisch, 2002; Ledeboer et al., 2005b; Zanjani et al., 2006; Mika, 2008).

Although oligodendrocytes and astrocytes are found in close apposition to neurons, microglia have gained more attention, in part because nerve injury-induced microglial changes are more robust than that of the other two glial cells types (Ji and Suter, 2007). Microarray studies also show that the most regulated genes following nerve injury are expressed in spinal microglia (Griffin et al., 2007) and nerve injury also induces a profound proliferation of spinal microglia (Echeverry et al., 2008). Microglia are predominantly and profoundly activated ipsilaterally in the lumbar spinal cord after peripheral nerve injury (Coyle, 1998; Mika et al., 2009a; Piao et al., 2006). Furthermore, minocycline has been shown to inhibit the release of neuroexcitatory substances from microglia (Tikka and Koistinaho, 2001). Due to other glial inhibitors also attenuating hyperalgesia in models of neuropathic pain the proportion of contribution that each glial cell type has is less clear and illustrates the complexity of the relationship between glia and pain transmission.

Added complexity exists when considering the plethora of events that occur from subsequent actions of the released substances, for example released NO will elevate glial release of other inflammatory mediators, like glutamate, ATP, prostaglandin E2 and cytokines (Bal-Price and Brown, 2001). Discussing each consequential action individually is beyond the scope of this thesis.

Yet further complexity arises with more and more glial-released substances being identified. For example D-serine, an endogenous ligand for the glycine modulatory site on NMDA receptors, is released from microglia which causes an enhancement of C-fibre mediated excitation of pain responsive neurons (Guo et al., 2006).

Of all the substances released by glia, proinflammatory cytokines appear to have a major impact on pain processing and will be a focus of this thesis. It has been reported that pretreatment with minocycline attenuated gp120-induced increases in IL-1β and TNF-α mRNA in spinal cord and accumulation of these cytokines in CSF (Ledeboer et al., 2005a) with similar results being shown in the spinal nerve transection model (Raghavendra et al., 2003a; Raghavendra et al., 2003b). Further evidence of the association of glia and cytokines include minocycline inhibiting activated p38 mitogen-activated protein kinase (MAPK) in microglial cells (Tikka and Koistinaho, 2001), a key regulator of cytokine expression.

1.5 Purinergic receptors

ATP is one of the major substances released by damaged and dying cells and is considered as an intrinsic 'danger signal' triggering the activation of nearby microglia (Di, 2006). Microglia are exquisitely responsive to extracellular ATP, whether released by cellular damage, nearby astrocytes or neurons from either synaptic or nonsynaptic regions (Davalos et al., 2005; Di, 2006). Detection of extra-cellular ATP causes rapid convergence of microglial processes toward its source (Davalos et al., 2005) and also release of plasminogen, a protein which enhances NMDA receptor function (Inoue et al., 1994). It has also been shown that an intraspinal administration of microglia that have been activated by ATP produced allodynia in naïve rats (Tsuda et al., 2003). The receptors for ATP which are present on microglia are purinergic receptors, also known as purinoceptors.

1.5.1 Purinoceptors

Purinoceptors are a large family of receptors that include ligand-gated ion channel receptors and G-protein coupled metabotropic receptors. The receptors are activated by purines, heterocyclic aromatic organic compounds, which include adenosine, ATP and uridine-5'-triphosphate (UTP).

It was in 1972 that purinergic transmission was first proposed (Burnstock, 1972), following the identification of ATP as the neurotransmitter in non-adrenergic and non-cholinergic nerves supplying the gut and urinary bladder (Burnstock et al., 1970). It was later that the receptors were reclassified to those responding to

adenosine (P1) and those that were activated by ATP (P2). P1 receptors have been further subdivided on the basis of molecular, biochemical and pharmacological evidence into adenosine A1, A2a, A2b and A3 receptors, all of which couple to G proteins and mediate their actions via adenylate cyclase (AC). The P2 receptor family were divided into ionotropic P2X and metabotropic P2Y receptors on the basis of pharmacology and molecular biology. There are now 7 subtypes of ionotropic P2X receptors named P2X1-P2X7 and 8 subtypes of metabotropic P2Y (P2Y1, 2, 4, 6, 11-14). Although there is increasing evidence for the contribution of P2Y receptors to pain processing, including P2Y1, 2, 4 and 6 mRNA expression in DRG neurones (Burnstock, 2007) and receptor activation inhibiting spinal pain transmission (Okada et al., 2002), it is out of the scope of this thesis to discuss their contribution further.

1.5.2 P2X receptors

P2X receptors are membrane bound ion channels that are activated by the binding of extracellular ATP, resulting in the opening of a non-selective cation channel. The P2X subunit proteins are 384 (P2X4) to 595 (P2X7) amino acids long and have two hydrophobic regions which span the plasma membrane. Separating these 2 domains is the majority of the polypeptide on the extracellular side of the membrane and the NH2 and COOH terminals are presumed to be cytoplasmic. The transmembrane regions are thought to form the ion conduction pore and undergo conformational changes during receptor activation.

The ATP binding site on P2X receptors is located in the extracellular domain and there have been many mutagenetic studies revealing some of the residues involved in ATP binding to P2X receptors, for example the binding site of the P2X1 receptor has been shown to lye close to the channel vestibule (Ennion et al., 2000) and the site for P2X2 receptor has been found proximal to the first transmembrane domain (Jiang et al., 2000b).

Intracellularly the amino acid sequence and length of the C-terminal domain vary across the P2X receptor family and are 36-48% identical to one another. All P2X receptors form functional homomeric channels, with the possible exception of P2X6 as the protein may be insufficiently glycosylated in heterologous expression systems to form functional channels. There is also evidence for heteromultimeric

assemblies of P2X subunits, including P2X1/2, P2X1/4, P2X1/5, P2X2/3, P2X2/6, P2X4/6 and P2X7/4 which confer further different properties. Table 3 summarises the distribution and general properties of homomeric P2X receptors.

Receptor	First described (tissue/date)	ATP potency (~EC50; μM)	Main distribution	Main function	Relevance to disease states	References
P2X1	Rat vas deferens (1994)	1	Smooth muscle, platelets, CNS tissue, vas deferens, spinal cord, sensory ganglia	Smooth muscle contraction, platelet activation, regulation of renal function	Thrombosis, possible role in male infertility	(Hu and Hoylaerts, 2010)
P2X2	Rat pheochromocytoma cells (1994)	10	Smooth muscle, CNS tissue, retina, GI and bladder tissue, autonomic and sensory ganglia	Modulation of synaptic function and sensory transmission		(Keceli and Kubo, 2009)
P2X3	Rat DRG (1995)	1	Sensory neurones and ganglia	Sensory neurotransmission	Possible role in chronic inflammatory and neuropathic pain, bladder hyper-reactivity	(Jarvis, 2003)
P2X4	Rat ganglia, brain and endocrine tissue (1996)	10	(Most ubiquitously expressed) CNS (including microglia), bladder, GI tract, uterus, testis, colon	Modulation of cytokine, BDNF release from microglia, control of haemodynamic responses	Chronic inflammatory and neuropathic pain	(Tsuda et al., 2009)
P2X5	Rat sympathetic ganglia and heart (1996)	1	Skeletal muscle, gut, bladder, thymus, skin, spinal cord	None identified		(Ruan and Burnstock, 2005)
P2X6	Rat cervical ganglia and brain (1996)	1	Overlaps with distribution of P2X4	None identified		(Jones et al., 2004)
P2X7	Rat brain (1996)	1000	Cells of haemopoetic origin: immune and glial cells	Proinflammatory cytokine release, cell proliferation, apoptosis, activation of PLD, shedding of L-selectin	Chronic inflammatory and neuropathic pain	(Chessell et al., 2005)

Table 3. A summary of the key information about P2X receptors

1.5.3 P2X receptors and pain

When released following inflammation or nerve injury, ATP has effects on neuronal and non-neuronal cells via different purinergic receptors depending on where the receptor is expressed.

P2X2 and P2X3 receptors are expressed on primary afferents (Lewis et al., 1995) and when activated increase the release of glutamate, GABA and glycine in the dorsal horn (Gu and MacDermott, 1997; Rhee et al., 2000; Sawynok et al., 1993). The expression of P2X3 receptors has been shown to increase following a peripheral nerve injury (Novakovic et al., 1999). Acting on P2X2 receptors, ATP also acts as a mediator of fast excitatory neurotransmission through co-release with GABA (Jo and Schlichter, 1999). Further evidence confirming a key role of neuronally expressed purinergic receptors in pain processing is gained from an *in vivo* study, in which a dual P2X2/3 and P2X3 antagonist, A-317491, reduced hyperalgesia in inflammatory and neuropathic pain models (McGaraughty and Jarvis, 2005).

ATP also activates P2X receptors on non-neuronal cells, namely glia and macrophages. A P2X receptor of particular importance is the P2X4 receptor as it was the first purinergic receptor shown to be markedly upregulated on spinal microglia after nerve injury (Tsuda et al., 2003). In addition to this, mice treated spinally with a P2X4 antisense oligonucleotide and mice lacking the P2X4 receptor showed attenuated tactile allodynia after nerve injury (Tsuda et al., 2009; Tsuda et al., 2003; Ulmann et al., 2008). Moreover, it was found that spinal administration of P2X4-stimulated microglia caused otherwise normal rats to develop allodynia (Tsuda et al., 2003). Postulated mechanisms by which P2X4 receptors cause neuropathic pain include increasing intracellular Cl^- in spinal lamina 1 neurons (Coull et al., 2005), microglial release of brain-derived neurotrophic factor (BDNF) (Coull et al., 2005; Trang et al., 2009), increased levels of spinal fibronectin (Nasu-Tada et al., 2006), activation of p38 MAPK resulting in release of TNF and IL-6 (Burnstock, 2009) and the release of cytokines that can enhance synaptic transmission (Tsuda et al., 2003). The above evidence indicates that P2X4 receptor plays a key role in pain signalling in the spinal cord under pathological conditions (Trang et al., 2006).

Importantly it has been shown that P2X7 receptors on microglia are also involved in neuropathic pain and is the main subject of this thesis.

1.6 The P2X7 receptor

1.6.1 Structure

The P2X7 receptor, known then as the cytolytic P2Z receptor (Gordon, 1986; Burnstock, 1990) was first described as the receptor that mediated the permeabilising action of ATP on mast cells and large conductance in macrophages. The full length cDNAs were first cloned from rat brain in 1996, followed by human monocytes and mouse microglia (Surprenant et al., 1996) . The human P2X7 receptor gene was localised by *in situ* hybridisation to chromosome 12q24, within 130 kb of the gene for the homologous P2X4 receptor. The P2X7 subunit protein is 595 amino acids long, the longest of the P2X receptor family, and is 35-45% identical to the other P2X receptors (Surprenant, 1996).

The most striking difference between the P2X7 receptor and other P2X receptors is the longer intracellular COOH terminal. A lipopolysaccharide (LPS)-binding site has been identified close to the carboxy terminus of the receptor, whereby the receptor is able to translate inflammatory signals to signal transduction events. The region between residues 551 and 581 has been identified as essential for trafficking and cell surface expression of the P2X7 receptor. The ATP binding site is suggested to be located within the anti-parallel six-stranded beta-pleated sheet, nearby a cysteine-rich region of the extracellular domain of the receptor (see Figure 4).

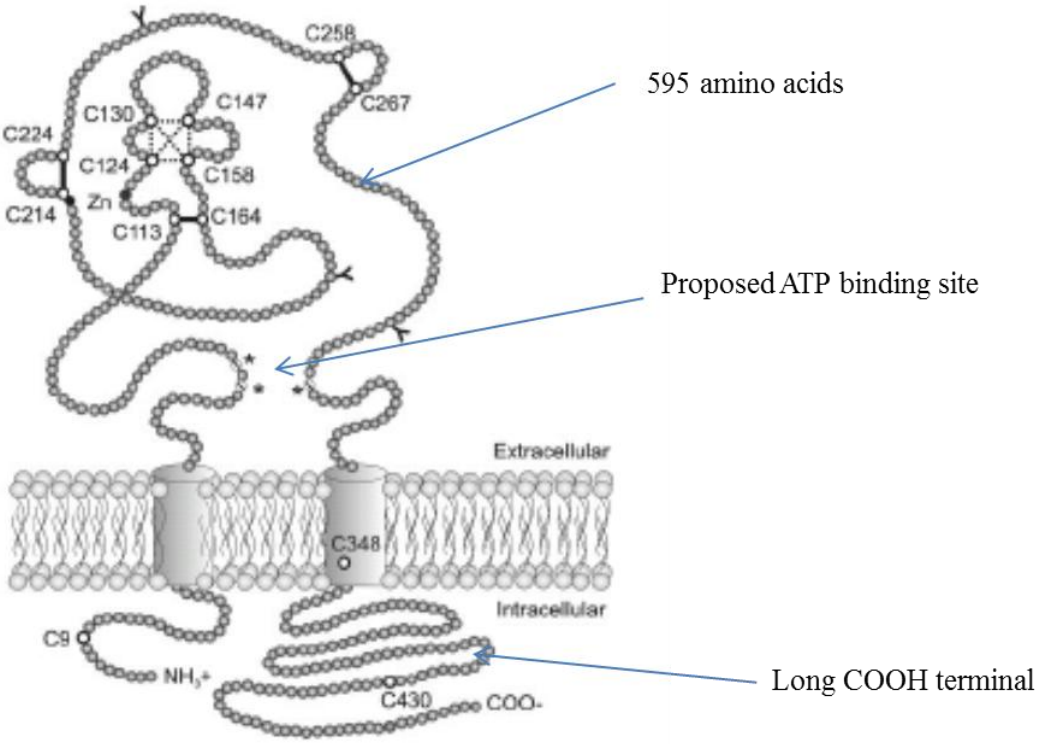

Figure 4. The molecular topology of the P2X7 receptor

1.6.2 P2X7 receptor distribution

P2X7 receptors are widely distributed. They are expressed on many cells of haematopoietic lineage (Romagnoli et al., 2008) including mast cells, lymphocytes, erythrocytes, fibroblasts, and macrophages (Surprenant, 1996), and Schwann cells (Colomar and Amedee, 2001). Within the central nervous system, P2X7 receptors are predominantly localized on microglia (Visentin et al., 1999; Choi et al., 2007; Takenouchi et al., 2009). The expression of P2X7 receptors on astrocytes remains controversial; some reports suggest their expression (John et al., 2001; Panenka et al., 2001; Duan et al., 2003; Suadicani et al., 2006) and others suggest the lack of expression (Rappold et al., 2006; Yu et al., 2008; Jabs et al., 2007). Some also believe that the contribution of P2X7 receptors to astrocytic physiology is considered negligible since astrocytic P2X7 receptor protein levels have been more elusive to establish (Cotrina and Nedergaard, 2009). It is fair to say that further investigations

are required to fully understand the relevance of P2X7 expression on astrocytes. There is some evidence for P2X7 expression in oligodendrocytes (Matute et al., 2007), but the significance of this also requires further attention.

In contrast to the conflicting reports on astrocytic expression, P2X7 receptors can be unequivocally detected in microglia at the mRNA and protein levels (Cotrina and Nedergaard, 2009) and for this reason will be referred to, in this thesis, as the predominant expression site of P2X7 receptors. Furthermore, microglia, and not astrocytes, have been identified as the main source of IL-1β in the CNS (Konsman et al., 1999; Chauvet et al., 2001) and microglia have also been specifically shown to express IL-1β in LPS-stimulated mixed glial cell cultures (Mingam et al., 2008), making this glial cell type more relevant when considering chronic pain.

Whether P2X7 receptors are expressed on neurones is controversial with some studies suggesting neuronal expression (Papp et al., 2004; Sperlagh et al., 2006) and others suggesting not (Sim et al., 2004; Chu et al., 2010). Controversy mostly exists due to the poor specificity of primary antibodies and ligands targeting the rats P2X7 receptor (Anderson and Nedergaard, 2006) as they showed immunoreactivity in P2X7 knock-out mice (Kukley et al., 2004; Sim et al., 2004).

1.6.3 Pharmacology of P2X7 receptor

Studies investigating the pharmacology of P2X receptors have been hampered due the limited characterisation of ligands and poor specificity of compounds. For example, many studies use suramin and pyridoxalphosphate-6-azophenyl-2'-4'-disuphonate (PPADS). However, suramin produces non-P2X effects at low concentrations (Voogd et al., 1993) and PPADS interacts with multiple P2X and P2Y receptors subtypes (Burnstock and Knight, 2004). Further complicating factors include the same antagonist producing different responses in different assays. For example in electrophysiology studies, calmidazolium is a potent inhibitor of P2X7 receptors, but it has no effect in assays measuring channel uptake using the dye YO-PRO which is commonly used for investigating P2X7 receptors (Virginio et al., 1997). Technique dependent differences between different laboratories, due to the large number of variables within each study also exist. For example there are inconsistencies in concentration of the challenging agonist used, the number of

applications, the constituents of the bathing solution, and the pre-incubation times for antagonists.

More recently however, the identification of more selective antagonists, primarily through the drug discovery programmes of pharmaceutical companies, has considerably aided the characterisation of the individual receptor subtype.

1.6.3.1 P2X7 receptor agonists

The fundamental pharmacological difference between the P2X7 receptor and the other purinergic receptors is the low potency of ATP at P2X7 receptors (Sperlagh et al., 2006). Levels of ATP found extra-cellularly under normal physiological conditions are not sufficient to activate the P2X7 receptor. Another difference is that the potency of ATP analogue BzATP is greater than ATP at the P2X7 receptor (Bianchi et al., 1999). BzATP is often used instead of ATP in pharmacological studies due to the large amount of ATP required to activate the receptor often making the ATP solutions acidic. The endogenous agonist for P2X7 receptors is the free acid form of ATP (ATP4-) which was first proposed following the assumption that the inhibition of P2X7 by divalent cations represented an alteration in the concentration of ATP (Cockcroft and Gomperts, 1980). The potency of ATP and BzATP varies across species with potency at rat > human >> mouse (Chessell et al., 1998). The difference between rat and mouse is likely to be due to changes of single amino acids (Michel et al., 2008).

1.6.3.2 P2X7 receptor antagonists

The early P2X antagonists, suramin, PPADS, oxidised-ATP and TNP-ATP all block P2X7 receptors but with lower potency than at the other subtypes (Evans et al., 1996; Chessell et al., 1998; North and Surprenant, 2000).

There are however a number of more selective antagonists including KN-62 (1-[N, O-bis(5-isoquinolinesulphonyl)-N-methyl-L-tyrosyl]-4-phenylpiperazine) which is an antagonist of $Ca^{2+/}$calmodulin-dependent protein kinase II (CaMKII) but which at lower concentrations selectively blocks human P2X7 receptors. KN62 exhibits marked species selectivity (Humphreys et al., 1998) being considerably more potent at the mouse receptor (IC50 = 200-400 nM) than the rat receptor (IC50 = ~10 µM).

Brilliant Blue G (BBG), a coloured dye, also blocks P2X7 receptors and exhibits a higher potency at the rat receptor (IC_{50}=10 nM) than the human receptor (IC_{50}= 200nM). At higher concentrations (IC50 = 2 to > 30 μM) BBG does have activity at other P2X receptors, but at lower concentrations it can be considered selective (Jiang et al., 2000a). Finally, calmidazolium, an inhibitor of cyclic nucleotide-gated receptor, also shows greater potency at rat receptors than human, and interestingly only inhibits the ionic channel of receptors, whilst having no effect on the large diameter pore form (Virginio et al., 1997) the significance of which is discussed in the next section.

Through drug discovery research, a number of high-affinity P2X7 receptor antagonists have been described and although they do not escape the orthologue specificity issue, they do have improved subtype specificity (see review Friedle et al., 2010). Studies have demonstrated efficacy with selective P2X7 receptor antagonists in a large number of different animal models of chronic pain.

The drug companies that have most recently published exemplars include Pfizer (Chen et al., 2010), GlaxoSmithKline (Abberley et al., 2010; Chambers et al., 2010; Gleave et al., 2010) and Abbott Laboratories (Donnelly-Roberts et al., 2009; Honore et al., 2009). In this regard, of the 220 patent applications relating to P2X7 receptor modulation filed with the United States Patent and Trademark Office since 2001, 150 of them have been filed in the last 3 years. This indicates the rapidity with which this area of focus is expanding (Friedle et al., 2010). As discussed later in the thesis, there are many reports demonstrating that these P2X7 receptor-selective ligands significantly reduce allodynia in animal models of neuropathic pain providing direct evidence of the involvement of P2X7 receptors.

P2X7 function is also inhibited by ions, including Ca^{2+}, Mg^{2+} (Surprenant, 1996) Zn^{2+}, Cu^{2+} and protons (H^{+}) (Virginio et al., 1997; Michel et al., 1999). This inhibition is thought to be mediated either directly via the P2X7 receptor itself (Liu et al., 2008; Jiang, 2009) or indirectly, via the chelation of the effective agonist, ATP^{4-} thereby reducing the relative concentrations of ATP (North, 2002).

1.6.4 P2X7 receptor activation

The low affinity of ATP for P2X7 receptors infers a potential pathological role for P2X7 receptors when large amounts of ATP are released. *In vitro*, P2X7 receptors have been shown to have an almost unique response to ATP acting differently depending on the level of exposure of agonist.

During a brief activation, P2X7 receptors behave as classical non-selective cation channels allowing the bidirectional flux of Na^+, Ca^{2+} and K^+ ions (Surprenant, 1996) (see Figure 5). The channel activates rapidly and currents show little desensitisation during applications lasting for many seconds. The time course of closure of the channel following agonist activation slows with each subsequent agonist application. This is related to the agonist potency and is thought to be due to a slow dissociation of agonist from the receptor rather than being an intrinsic property of the ion channel (Hibell et al., 2001). The peak current amplitude is also not stable, and often steady increases are recorded with each addition of agonist. The extent of these changes is species dependent (Michel et al., 1999; Hibell et al., 2001).

At high agonist concentrations, sustained or repeated activation of the receptor results in a dramatic change in the receptor in which a large diameter transmembrane pore opens that is permeable to large molecules (Surprenant et al., 1996). This is reflected by either dramatic growth of current amplitude, by sustained tail currents, or by both (Chessell et al., 1997; Chessell et al., 2001). This occurrence often results in cell lysis (Zanovello et al., 1990; Zheng et al., 1991), resultant lactate dehydrogenase (LDH) release and is the reason why the P2X7 receptor had previously been referred to as the ‘cell death receptor’.

This dramatic structural change is often measured using plate-based fluorescence readers due to an increase in the permeation of extracellular dyes, such as YOPRO and ethidium bromide (EthBr), that fluoresce once bound to nucleic acids within the cell. The formation of the pore has also been measured electrophysiologically as a progressive increase in the permeability of a large cation NMDG (Virginio et al., 1999a). YO-PRO and NMDG entry have been widely used as assays measuring P2X7 receptor activation, but controversy exists as to how

similar the processes are that induce their entry (Jiang et al., 2005; Martinez-Francois et al., 2002; Yan et al., 2008).

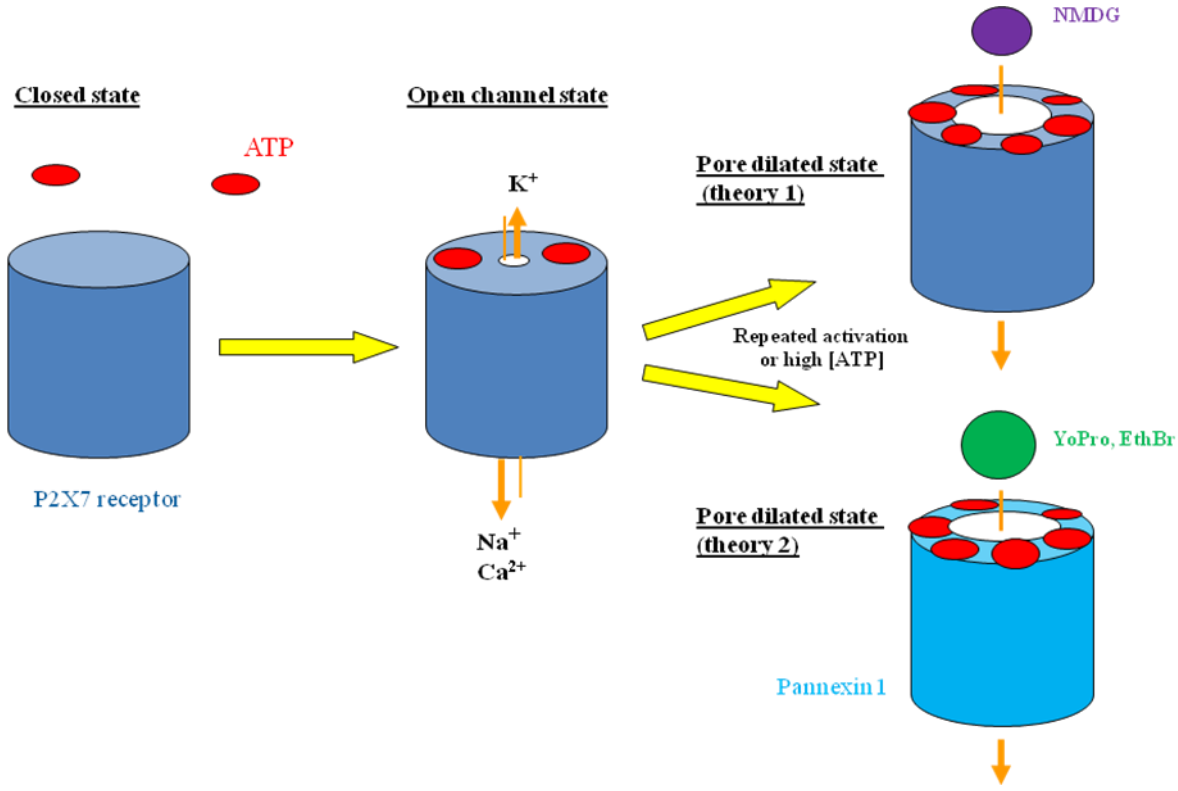

Figure 5. Diagram illustrating the two theories of P2X7 receptor activation.

There is much debate as to the form and mechanisms involved in pore formation and two main theories exist.

Theory 1: It was initially hypothesised that the channel of the receptor undergoes a progressive dilation, resulting in an increase in the size of the transmembrane pathway and hence allows the permeability of larger molecules (Virginio et al., 1999b). It was thought likely that the dilation was mediated through the P2X7 receptor itself as the pore exists in many different expression systems; HEK293 (Surprenant, 1996; Rassendren et al., 1997), mouse microglial cell line (Chessell et al., 1998), granulocytic cells (Suh et al., 2001), rat peritoneal mast cells (Tatham and Lindau, 1990) and human THP-1 cells (Donnelly-Roberts et al., 2004). This theory also seemed likely due to considerable overlap in pharmacology between the channel and the pore with many agents blocking both, including Brilliant blue G (Jiang et al.,

2000a), and many of the newer tool molecules (Honore et al., 2006; Stokes et al., 2006). Studies suggest that it is the elongated C-terminal tail of the P2X7 receptor that contributes to the formation of the large pore, as truncations abolish the receptor transition (Surprenant, 1996; Smart et al., 2003). However given that the pore dilation has also been described for P2X2 and P2X4 receptors (Khakh et al., 1999; Virginio et al., 1997), the difference in C-terminal length is clearly not the only determinant.

Theory 2: The main alternative theory for P2X7-induced pore formation centres around the hypothesis that P2X7 activation initiates the formation of separate pore-forming protein complexes in the membrane. Evidence for this theory include the finding that calmidazolium and a monoclonal antibody to the P2X7 receptor only blocked the ionic channel with no effect on YO-PRO uptake (Virginio et al., 1997; Chessell et al., 2001). More recent work has also shown P2X7-induced pore formation is dependent upon a cascade of events involving the release of second messengers (Faria et al., 2010), and activation of, in particular p38 MAPK (Donnelly-Roberts et al., 2004), and caspase pathways (Donnelly-Roberts et al., 2004). The observed involvement of pannexin-type hemi-channels in the formation of the pore, particularly centering on pannexin-1 (Pelegrin and Surprenant, 2006; Locovei et al., 2007) has also added considerable evidence to this theory. Pannexins are mammalian proteins that are similar, in general structure, to the non-mammalian innexins that form gap junctions in invertebrates (Panchin et al., 2000). Three pannexins (Panx1, Panx2, Panx3) have been identified (Panchin, 2005; Barbe et al., 2006). Panx1 was co-immunoprecipitated with the P2X7 protein following co-expression in HEK293 cells (Pelegrin and Surprenant, 2006) and there is functional evidence using small interference RNA (siRNA) that panx1 is the molecular correlate of the P2X7-activated pore (Pelegrin and Surprenant, 2006).

Whatever the molecular basis for pore formation, there is no doubt that P2X7 receptor activation causes a massive disruption in cytoplasmic ion homeostasis which leads to range of considerable and complex cell responses. Other than ion influx, P2X7 activation has been shown to activate caspase 1 (Kahlenberg and Dubyak, 2004), activate MAPK (Donnelly-Roberts et al., 2004), extracellular regulated kinase

(ERK) (Gendron et al., 2003), phospholipase-D (Gargett et al., 1996; Humphreys and Dubyak, 1996), nuclear factor of activated T lymphocytes (Ferrari et al., 1997b; Aga et al., 2002), shedding of L-selectin (involved in adhesive interactions and rolling behaviour of lymphocytes on endothelial cells) (Jamieson et al., 1996) and lead to membrane blebbing (irreversible loss of plasma membrane) (Verhoef et al., 2003), microvesical shedding and cell death (North, 2002).

The complexity of P2X7 activation also encompasses the knock-on effects of all the activities listed above. For example when P2X7 stimulation upregulates MAPK several biochemical process relevant to other pathological states are then regulated. To date there are three major signalling protein families involved in the MAPK cascades; ERK1/2 kinases, which are mainly involved in cellular growth and proliferation (Li et al., 2007); JNK/stress-activated protein kinases which are involved in cellular stress from exposure to inflammatory cytokines (Rincon et al., 2000) and p38 kinase which is activated upon exposure to inflammatory cytokines, endotoxin and often leads to apoptotic cell death (Ono and Han, 2000; Bu et al., 2006).

In addition to the actions above, P2X7 receptor activation has also been linked with release of the excitatory neurotransmitter glutamate and inhibition of glutamate uptake (Papp et al., 2004; Morioka et al., 2008) . The involvement of P2X7 receptor in modulation of the proliferation capability of microglia has also been reported (Bianco et al., 2006), adding more complexity to the mechanisms by which P2X7 receptors are involved in microglia response to injury.

The process not listed above which is a major consequence of receptor activation is the release of mature, biologically active interleukin-1β (IL-1β), a potent inflammatory cytokine (Perregaux and Gabel, 1994; Ferrari et al., 1997a). P2X7 activation by ATP has been argued as being the most potent stimulus for the release of IL-1β (Di, 2006).

1.6.5 IL-1β release from P2X7 receptor activation

Microglia were the first cell type in which coupling of the P2X7 receptor to IL-1β release was formally shown (Ferrari et al., 1996). Much of the current understanding of the close links between purinergic receptors and neuroinflammation

originates from the finding of high level expression of P2X7 receptors on microglia and their association with the maturation and release of IL-1β from microglia (Di et al., 2009).

IL-1β is a proinflammatory cytokine that is part of the Interleukin-1 family. When ATP binds to P2X7 receptors the resultant reduction of intracellular K^+ ions activates a cysteine protease, caspase-1 (previously known as Interleukin-1 converting enzyme, ICE) (Perregaux and Gabel, 1994; Kahlenberg and Dubyak, 2004). This enzyme cleaves the inactive precursor molecule to IL-1β, called pro-IL-1β into the mature, active form (Kostura et al., 1989; Thornberry et al., 1992). IL-1β release can be prevented by the inhibition of caspase-1 (Watanabe et al., 1998), and the inhibition of the ATP-binding cassette-1 (ABC-1), suggesting a role of anion flux in the release of IL-1β (Hamon et al., 1997). The proposed methods of IL-1β release include; secretion via endosomes (Andrei et al., 1999), secretion via microvesicle shedding (MacKenzie et al., 2001), or the export by transporters, such as ABC transporters (Hamon et al., 1997).

1.6.6 Evidence for IL-1β and P2X7 receptor involvement in pain processing

Once mature IL-1β is released via P2X7 receptor activation, it has numerous downstream effects including the induction of inflammatory mediators including nitric oxide synthase (iNOS), cyclooxygenase 2 (COX-2) (Samad et al., 2001), the production of superoxide products (Parvathenani et al., 2003) and TNF- α (Woolf et al., 1997), all of which have well described roles in the generation or maintenance of pain.

The significance of IL-1β release is demonstrated by the fact that an IL-1 receptor antagonist (IL-1ra) reduces thermal hyperalgesia and mechanical allodynia in a mouse neuropathic pain model (Sommer et al., 1999). IL-1β has further importance as its release, after P2X7 activation, has been shown to cause an increase in the expression levels of P2X7 receptors in astrocytes (Narcisse et al., 2005).

The role of the P2X7 receptor in pain is well defined *in vivo*. Data from studies of P2X7 receptor KO mice (Labasi et al., 2002; Chessell et al., 2005) supports a pain mediating role since P2X7 knock-out (KO) mice show less chronic inflammatory

and nerve- injury induced pain relative to wild-type controls. This is further supported by data showing that numerous selective P2X7 receptor antagonists demonstrate anti-hyperalgesic properties in multiple experimental models of nerve injury (Honore et al., 2006; Nelson et al., 2006; Carroll et al., 2007; McGaraughty et al., 2007; Nelson et al., 2008; Donnelly-Roberts et al., 2009; Honore et al., 2009; Abberley et al., 2010; Chen et al., 2010). The effects of modulating P2X7 receptors have also been demonstrated in electrophysiological experiments, with a reduction in noxious evoked activity of spinal neurones after administration of a P2X7 receptor antagonist (McGaraughty et al., 2007). Clinically-relevant evidence demonstrating the role of P2X7 receptors in pain also exists and includes the increase in P2X7 receptor expression in DRG sections from patients suffering with persistent neuropathic pain (Chessell et al., 2005).

Supporting evidence for the association between P2X7 receptors and IL-1β was demonstrated by the reduction of IL-1β release from blood samples or plated cells from P2X7 knockout mice following ATP/BzATP stimulation of LPS (Solle et al., 2001; Labasi et al., 2002; Chessell et al., 2005) and from selective P2X7 receptor antagonists (Abberley et al., 2010). Recently, Honore et al., (2009) also showed a lack of effect of a P2X7 receptor antagonist in an inflammatory model conducted in IL-1αβ KO mice further suggesting that anti-hyperalgesic effects of P2X7 receptor antagonists are mediated by IL-1 blockade.

1.6.6.1 Significance of central P2X7 receptors

The prevention of P2X7 receptor activation on microglia thereby reducing cytokine release and consequently synaptic transmission is now recognised as a potential therapeutic approach. As described above a number of pharmaceutical companies are attempting to identify selective and potent small molecule antagonists which may provide a novel treatment of pain. One important property of these compounds however, which has not been clearly defined, is how important it is that these antagonists can cross the blood brain barrier and access the CNS.

Clearly the role of activated central glia in chronic pain through regulation of IL-1β and perhaps glutamate suggests the importance of a spinal site of action;

however the significance of antagonists being centrally penetrant has not been specifically described so far. This is an area that is investigated within this thesis.

As well as having a potential utility for treatment of neuropathic pain, P2X7 receptor antagonists may have utility in other clinical applications. Theoretically, by preventing microglia activation any other pathological event associated with this occurrence may be blocked by P2X7 receptor antagonists. As detailed in Table 2 microglia are also activated by chronic morphine administration. There is speculation therefore that pro-nociceptive activities of glial activation may account in some way for the tolerance seen with prolonged opioid use and the reduction of efficacy in opioids. Preventing tolerance and enhancing the efficacy of opioids, could therefore be a different clinical application of P2X7 receptor antagonists and is an area considered in this thesis.

1.7 Opioid receptors

1.7.1 Introduction

Opioids play a central role in nociception. Endogenous opioids provide an anti-nociceptive tone and regulate the experience of pain (Marvizon et al., 2010), and exogenous opioids have become the ‘gold standard’ analgesic to which all others are compared. Opioids have been used in the treatment of pain for thousands of years with some dating the first use of opioid poppy extracts for analgesia back to 3000 BC (Hutchinson et al., 2007). In spite of such widespread use, current opioid therapeutics can result in unfavourable side effects and are not beneficial in all types of pain. Novel approaches are being developed aiming to optimise the treatment of pain by opioids. These approaches consider the physiochemical, pharmacokinetic and pharmacodynamic properties of the opioid as well as the pharmaceutical formulation and route of administration (Christrup et al., 2009).

1.7.2 Opioid receptors

Opioid receptors belong to the class A (Rhodopsin) superfamily of G protein coupled receptors (GPCRs). Like all GPCRs the opioid receptors contain seven hydrophobic transmembrane domains interconnected by short loops and display an

extracellular N-terminal domain and intracellular C-terminal tail. The opioid receptor family consists of four receptors: μ, δ, κ and opioid-like receptor 1 (ORL1 receptor). Receptors are highly homologous with transmembrane domains and intracellular loops best conserved (86-100%) (Waldhoer et al., 2004).

1.7.2.1 Opioid receptor distribution

All four receptors are widely, but differentially, distributed throughout the central and peripheral nervous systems and in endocrine and immune cells. Drugs modulating their activity can therefore induce a variety of physiological and behavioural effects. For example, opioids acting in the brain stem reduce the sensitivity of the respiratory centre to CO_2 causing respiratory depression (Ling et al., 1985), opiates in the medulla can cause vomiting and cough suppression (Bolser, 2006) and in the periphery opiates constrict pupils by acting on the oculomotor nucleus (Murray et al., 1983) or cause constipation by acting on the smooth muscle of the gut (Holzer et al., 2009).

Up to 75% of the opiate receptors are found pre-synaptically on the c-fibre terminal of the dorsal horn (lamina I and II) and are predominantly of the μ and d-type (Besse et al., 1990). The contribution of μ, δ and κ receptors to the total opiate binding throughout the spinal cord is estimated at 70, 24 and 6% respectively at a predominantly (> 70%) presynaptic location (Besse et al., 1990). It is not surprising therefore that opioid receptors, particularly μ receptors, mediate analgesia in the spinal cord. This is also reflected by the fact that the most potent opioids are the μ ligands. The main mechanisms of spinal opioid analgesia, whether it be endogenously or exogenously mediated, is via activation of presynaptic opioid receptors.

Opioid receptors are also located in the 5-HT and noradrenergic nuclei of the brain stem and midbrain including the raphe nuclei, the RVM, the PAG and the locus coeruleus (Przewlocki and Przewlocka, 2001).

1.7.2.2 Opioid receptor ligands

All 4 opioid receptors are activated by endogenous opioid peptides, of which there are close to 30, including endorphin (μ receptor peptide), enkephalin (δ receptor

peptide), dynorphin (κ receptor peptide) and nociceptin (ORL-1 peptide) (Weber et al., 1983).

The exogenous opioids comprise a chemically diverse group of compounds that differ in many physical and pharmacological properties, including metabolic stability, opioid receptor specificity, receptor on/off rates, hydrophobicity, receptor efficacy as agonists, antagonists and inverse agonists and interaction with receptors other than members of the opioid GPCRs. Exogenous opioids include the morphinans, drugs based upon the structure of the opium poppy-derived alkaloids, which consist of partial agonists (oxycodone, hydrocodone, morphine, codeine and heroin), the opripavines (buprenorphine and etophine) and the antagonists (naloxone and naltrexone). Fentanyl and related derivatives, like remifentanil, are more μ selective than morphinans with fast on and off actions making them the preferred choice during surgery or childbirth.

The fundamental mechanism by which opioid analgesia is accomplished is through an inhibitory action on peripheral and central neurons within spinal and supraspinal sites, however what is unusual about opioid receptors is the significant differences seen in mechanisms when opioids are dosed chronically, compared to the mechanisms when dosed acutely.

1.7.3 Activation following acute administration

1.7.3.1 Spinal mechanisms

Opioid receptors normally couple to inhibitory G-proteins, namely G_i or G_o, to inhibit neuronal depolarisation (Waldhoer et al., 2004). Upon receptor activation, GDP is transferred to GTP leading to the separation of the α from the βγ subunit of the G protein which leads to an interaction with multiple cellular effector systems. For example, adenyl cyclase (AC) activity is inhibited and less cAMP is produced as a result. In turn, voltage-dependent calcium channels are inhibited and inwardly rectifying potassium channels are activated which inhibit neurotransmitter release (Ikeda et al., 2002) (see Figure 6). In primary afferent C fibres the activation of opioid receptors results in hyperpolarisation, decreased firing which inhibits glutamate and substance P release from the central termini of these fibres in the

dorsal horn of the spinal cord resulting in decreased neuronal excitability (Freye and Latasch, 2003; Harrison et al., 1998). Spinally applied morphine has been shown to reduce substance P and CGRP release after noxious stimulation (Go and Yaksh, 1987). Activation by spinal administration may elicit anti-nociception by pre-synaptic modulation of the activity of primary afferent fibres as well as by post-synaptic inhibition of dorsal horn neurons (Kohno et al., 1999; Marker et al., 2005; Zhou et al., 2008). The remaining post-synaptic receptors, through the same coupling mechanisms, inhibit neuronal firing and hyperpolarise the dendrites of projection neurones, interneurones and disinhibit inhibitory interneurones; the net result is further inhibition of the C-fibre induced activity. Opioids also activate the PKC and MAPK cascades which affect cytoplasmic events and transcriptional activity of the cells (Williams et al., 2001).

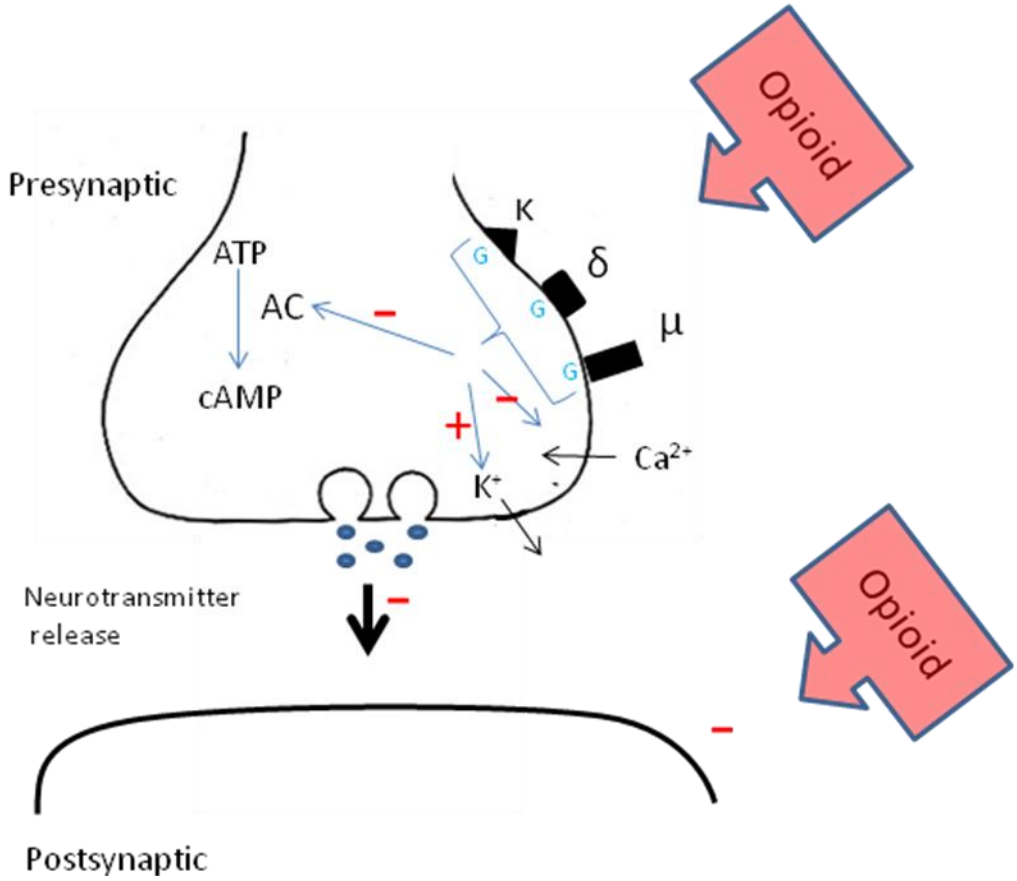

Figure 6. Schematic illustrating the key mechanisms of action for acute opioids

1.7.3.2 Supraspinal mechanisms

Supraspinal mechanisms for analgesia are still poorly understood but are thought to involve disinhibition which occurs through opioid inhibition of inhibitory neurons, such as GABA-containing cells.

When activated, supraspinal receptors alter the level of activity in descending pathways to the spinal cord, thereby contributing to the reduced spinal nociceptive activity. Exogenous injection of morphine into either the PAG or the RVM causes anti-nociception via increased activity in inhibitory descending controls terminating in the dorsal horn of the spinal cord (Fields, 2000; Heinricher and Neubert, 2004). Two theories exist for the mechanism of action. The first is that supraspinal morphine reduces the descending controls which filter sensory messages at the spinal level which normally allow pain messages to be extracted from the incoming barrage. The second theory is that morphine turns on descending controls associated with anti-nociception, i.e. 'off cells' and turns off controls associated with pro-nociception i.e. 'on cells'. In this way, reduction of an inhibition leads to a facilitation in a circuit.

Opioids also have actions at other supraspinal sites such as thalamic levels, the amygdala and the sensory cortex which are relevant to emotional and sensory aspects of analgesia (Dickenson and Suzuki, 2005).

1.7.4 Chronic administration of opioid and the development of tolerance

Even though opioids remain the analgesics of choice in both acute and chronic pain, a major limitation to their long term use is the development of tolerance, which remains one of the most unwanted effects of opioid therapy. Tolerance describes a pronounced decrease in analgesia during prolonged administration of opioid drug, an effect which demands an increase in dose to maintain a sufficient analgesic effect (Foley, 1995). A consequence of elevating the dose is an increase in side effects, such as respiratory depression. It is therefore highly desirable to avoid or at least attenuate the development of tolerance.

The development of opioid tolerance in humans varies depending on the route of administration. Intriguingly the development of tolerance also depends on the disease states for which the opioids are prescribed. For example tolerance is not observed

towards constipation and miosis, however it does develop to respiratory depression, nausea and sedation, which is a clinical advantage (Freye and Latasch, 2003).

In terms of analgesic tolerance, which forms the main focus of this thesis, patients with terminal malignancies experience an escalation in pain as their disease progress. This situation makes it difficult to distinguish between the development of opioid tolerance and an increase requirement for opioids for efficacious treatment of their pain (Gebhart, 1990). In other pain-related conditions however, the advent of tolerance is a very distinct, well characterised problem that requires continuous assessment for each individual patient. Tolerance is also observed in animal studies (Ossipov et al., 2003; Ossipov et al., 2004; Vanderah et al., 2001c) but despite considerable progress, the exact molecular and cellular mechanisms mediating this phenomenon are complex, unclear and remain controversial.

Multiple hypotheses exist which attempt to explain the mechanisms behind tolerance and many of the hypotheses are potentially intertwined making interpretation very complex. To summarise the key mechanisms in a clear manner, they have been grouped into three sections: desensitisation and down-regulation, plasticity of opioid signal transduction and opioid-induced pain facilitation mechanisms.

1.7.4.1 Desensitisation and down-regulation of opioid receptors

Prolonged opioid activation results in receptor phosphorylation by G protein coupled receptor kinases (Cvejic et al., 1996; Chakrabarti et al., 1997; Appleyard et al., 1999) and cAMP-induced kinases (Harada et al., 1990) followed by the binding of regulatory proteins, called β-arrestins (Ferguson et al., 1996; Pitcher et al., 1998). β-arrestin binding has two consequences; firstly it uncouples the opioid receptor from the G-protein, which desensitises the receptor (Zhang et al., 1996; McLaughlin et al., 2004), and secondly it targets the receptors to clathrin-coated pits which initiates receptor internalisation (Holt et al., 2003).

A decrease in functional cell surface receptors as a result of prolonged agonist exposure is a common characteristic for GPCRs. Upon receptor internalisation the receptor may be recycled to the membrane leading to resensitisation (Harrison et al.,

1998; Littleton, 2001), or targeted for degradation, leading to receptor down-regulation (Waldhoer et al., 2004).

Evidence for this theory is mostly from *in vitro* studies (Chang et al., 1982; Zadina et al., 1993) and is well established. *In vivo* data however introduces inconsistencies. Evidence includes the observation that β-arrestin knock-out mice do not develop morphine tolerance (Bohn et al., 2002). However other *in vivo* approaches show conflicting data. Some suggest μ-receptors are down regulated (Bhargava and Gulati, 1990), whereas other groups show μ-receptors are up-regulated (Abdelhamid and Takemori, 1991; Rothman et al., 1991). There is also evidence suggesting this effect depends on the agonist used, for example DAMGO, which induces receptor internalisation (He et al., 2002; Kieffer and Evans, 2002) elicits less tolerance compared to morphine which does not induce receptor internalisation in the majority of reports (Sternini et al., 1996; Kovoor et al., 1997; Finn and Whistler, 2001; Whistler et al., 1999; Blanchet and Scher, 2002). In addition, murine κ opioid receptors do not internalise (Schultz et al., 1997) but display analgesic tolerance.

The β-arrestin knock out data has also been put into question with the realisation that β-arrestin also functions as a scaffolding molecule essential for the membrane recruitment of many signalling molecules, for example MAP kinases, c-jun N-terminal kinase (Ma and Pei, 2007) suggesting that β-arrestin may have a role in tolerance which is independent of receptor internalisation. This conflicting data makes it difficult to assess the role of receptor down-regulation but it appears unlikely that a loss of opioid receptors can account for the totality of opioid tolerance.

1.7.4.2 Plasticity of opioid signal transduction

Chronic morphine initiates an array of integrated convergent adaptations that occur downstream from the receptor, including changes in cytoplasmic signalling events involving Gα and βγ subunits as well as opioid receptor pleiotropy. It is proposed that these complex adaptations are directly related to tolerance and/or form part of many associated mechanisms of tolerance.

Whereas opioid receptors normally couple to inhibitory G-proteins, when dosed chronically, signalling pathways alter considerably and result in a switch of signalling

from inhibitory G_i/G_o to stimulatory G_s signalling (Chakrabarti et al., 2005; Gintzler and Chakrabarti, 2006).

The mechanisms by which the switch occurs involves neuroadaptive changes in signal transduction mediated by different protein kinases such as MAPK, PKC, cAMP dependent protein kinase and others (Liu and Anand, 2001). These changes include the augmented PKC-mediated phosphorylation of both AC, leading to increased stimulatory responsiveness to Gβγ (Chakrabarti et al., 1997; Chakrabarti et al., 1998; Chakrabarti and Gintzler, 2003; Chakrabarti et al., 2005), and Gβγ which increases the availability and potency to stimulate AC (Mao et al., 1995b; Mayer et al., 1995; Chakrabarti et al., 2001; Chakrabarti and Gintzler, 2003; Chakrabarti et al., 2005). Other examples include the increase in membrane translocation of PKC (Chakrabarti et al., 2005) and altered activity of regulatory G-protein signalling proteins (Zachariou et al., 2003; Xu et al., 2004; Garzon et al., 2005; Xie and Palmer, 2005).

The excitatory actions associated with a switch includes the increase in AC synthesis (Chakrabarti et al., 1998; Rivera and Gintzler, 1998) or 'AC superactivation' (Wang and Gintzler, 1995; Wang and Gintzler, 1997) and corresponding increase in cAMP which leads to an increase in Ca^{2+} leading to, for example, an increase neurotransmitter release (Gintzler et al., 1987; Gintzler and Xu, 1991). Increased levels of extracellular calcium have been observed in brain and spinal cord tissues of mice chronically exposed to morphine (Welch and Olson, 1991).

It has been proposed that these neurochemical adaptations to long term morphine exposure occur in an attempt to reinstate the initial steady state condition. For example the AC superactivation would neutralise the opioid-induced inhibition of AC, and the augmented AC stimulatory signalling and increased interaction with G_s would neutralise the opioid-induced inhibitory signalling. One shortcoming of this theory is that enhanced effects of increased cAMP levels should influence the efficacy of many other receptor systems whose major function is to suppress cAMP production and so puts this theory into doubt (King et al., 2005).

1.7.4.3 Opioid-induced facilitation mechanisms

Theories also exist that chronic morphine exposure enhances excitation via a variety of mechanisms which thereby counteracts morphine analgesia. Tolerance may therefore be considered as the requirement of additional opioid to overcome enhanced pain to maintain a consistent level of analgesia (Colpaert, 1996; Laulin et al., 1999). Some of the mechanisms are described below.

1.7.4.3.1 Excitatory neurotransmitter release

As a result of increased extracellular calcium from the signalling adaptations summarised above, neurotransmitter release from primary afferent terminals is enhanced during chronic opioid exposure. A number of these neurotransmitters will be excitatory, for example CGRP and substance P, and when released from primary afferent nerve terminals will increase synaptic transmission in the spinal cord and produce pain or 'paradoxical pain' (Vanderah et al., 2000a; Vanderah et al., 2001a; Gardell et al., 2002; Ossipov et al., 2003). Other identified neuroplastic changes which enhance excitatory transmission include an increase in spinal dynorphin levels (Takemori et al., 1992).

Morphine-induced paradoxical pain is demonstrated in animal studies (Yaksh and Harty, 1988; Trujillo and Akil, 1991; Vanderah et al., 2000b; Vanderah et al., 2001b; Vanderah et al., 2001c; Gardell et al., 2002; Trang et al., 2002) and reported in the clinic (Doverty et al., 2001; Ossipov et al., 2004; White, 2004). Experimental evidence for this hypothesis includes those studies in which drugs known to abolish hyperalgesia in pain models, also abolish tolerance to opioids and opioid-induced pain, these include calcium channel blockers, NMDA antagonists (Trujillo and Akil, 1991; Elliott et al., 1994), NK-1 antagonist, nitric oxide synthase inhibitors (Bhargava and Thorat, 1996), kinase inhibitors and cyclooxygenase inhibitors (Ossipov et al., 2003; Ossipov et al., 2004).

The effect of NMDA antagonists however, might also be due to additional involvement of NMDA receptors in tolerance, as opioids are known to stimulate intracellular PKC which phosphorylates the NMDA receptor thereby causing a functional antagonism (Srivastava et al., 1995). The NMDA receptor is considered critical in the maintenance of morphine tolerance (Mayer et al., 1999). Chronic

morphine also down-regulates glutamate transporter whilst an activator of the glutamate transporter attenuated morphine tolerance (Tai et al., 2007). Clinically, NMDA antagonists such as ketamine and dextromethorphan have been used to minimise tolerance development during opioid treatment.

1.7.4.3.2 Role of CCK in tolerance

A receptor associated with opioid-induced facilitation is the cholecystokinin (CCK) receptor. The distribution of CCK and CCK receptors overlap with the distribution of endogenous opioids and opioid receptors suggesting a modulatory role (Ghilardi et al., 1992). Administration of CCK produces hyperalgesia, suggesting a pro-nociceptive role (Jeftinija et al., 1981; Hong and Takemori, 1989), and blocks opioid-induced anti-nociception, suggesting a counteracting influence (Faris, 1985). CCK antagonists enhance opioid-induced anti-nociception (Watkins et al., 1985; Stanfa and Dickenson, 1993; Vanderah et al., 1994) and also inhibit morphine tolerance (Dourish et al., 1988; Kellstein and Mayer, 1991; Bhargava, 1994). CCK is upregulated in brain and spinal cord during the development of morphine tolerance (Ding and Bayer, 1993; Zhou et al., 1993). In terms of mechanism, CCK may maintain excitatory neurotransmitter release by eliciting a mobilisation of Ca^{2+} from intracellular stores thereby counteracting the opioid induced inhibition of depolarisation-induced Ca^{2+} influx into the primary afferent neurons (Stanfa and Dickenson, 1993). Data suggest that CCK is also likely to act through the activation of pro-nociceptive systems arising from the RVM (Heinricher and Neubert, 2004).

1.7.4.3.3 Role of descending pain facilitatory system

As central sensitisation associated with morphine-induced pain facilitation produces hyperalgesia, enhanced release of CGRP and increases in FOS expression in the spinal cord (Gardell et al., 2002; Xie et al., 2005), exposure to chronic morphine may also elicit activation of descending pathways arising from the RVM. Manipulations of the RVM not only abolish facilitation and enhance excitatory neurotransmitter release but also abolish morphine-induced paradoxical pain and anti-nociceptive tolerance (Yaksh et al., 1986; Celerier et al., 2000; Vanderah et al., 2000a; Gardell et al., 2002; Ossipov et al., 2003; Ossipov et al., 2004). Lesions to the

dorsolateral funiculus (DLF) blocked morphine-induced hypersensitivity (Vanderah et al., 2001c) suggesting that the descending facilitatory system may also play a part. The lesions to the DLF also prevented the release of CGRP and prevented the up-regulation of spinal dynorphin (Vanderah et al., 2001b).

Descending facilitation increases the expression of spinal dynorphin which acts as an endogenous pro-nociceptive agent that promotes increased release of excitatory neurotransmitters from primary afferent neurons (Dubner and Ruda, 1992). Dynorphin was originally identified as an endogenous K-opioid agonist which had anti-nociceptive properties under certain conditions (Ossipov et al., 1994). Considerable evidence now indicates that enhanced expression of spinal dynorphin is pro-nociceptive (Dubner and Ruda, 1992; Vanderah et al., 1996; Laughlin et al., 1997). Antiserum to dynorphin not only abolishes enhanced neurotransmitter release and nerve injury-induced hyperalgesia (Wagner and Deleo, 1996; Malan et al., 2000; Wang et al., 2001) but also abolishes opioid induced abnormal pain and anti-nociceptive tolerance (Malan et al., 2000; Vanderah et al., 2000b; Gardell et al., 2002; Ossipov et al., 2003; Ossipov et al., 2004). Elevations in spinal dynorphin are also seen in conditions of opioid-induced pain states (Gardell et al., 2002; Vanderah et al., 2000a). This suggests that dynorphin may be providing a positive feedback loop that amplifies further sensitisation (Faden, 1992; Koetzner et al., 2004).

There is also evidence suggesting that the PAG region is important in the development of morphine tolerance. For example, repeated microinjections of morphine into the region produce tolerance (Tortorici et al., 1999; Morgan et al., 2005) and profound changes in PAG neurons, including a decrease in opioid activation of potassium channels (Ingram et al., 1998; Hack et al., 2003; Bagley et al., 2005).

1.7.4.3.4 The involvement of glia and cytokines

As suggested above there are similarities between the pathophysiological mechanisms involved in neuropathic pain and tolerance. These include the broad similarities such as the involvement of pain facilitation, the diminished efficacy of opioids and abnormal pain (Mao et al., 1994; Mayer et al., 1999), but also more intricate mechanisms like P38 MAPK activation and the involvement of excitatory

substances like EAAs, NO and prostaglandins (Sung et al., 2003; Ozawa et al., 2001). It was this recognition of the similarities that led to the discovery of glial involvement in modulating opioid actions (Mayer et al., 1995; Mayer et al., 1999).

The involvement of glia and cytokines in morphine tolerance was first recognised in 1988 when proinflammatory cytokines (identified then as 'unspecified proteins') were elevated after morphine treatment of astrocyte enriched cultures or brain slices (Ronnback and Hansson, 1988). It was not until 2001 that this association was confirmed and characterised by observing an up-regulation of GFAP in the spinal cord in rats that had been chronically dosed with morphine (Song and Zhao, 2001). In addition when these rats were challenged by the glial metabolic inhibitor fluorocitrate the GFAP staining was reversed and morphine tolerance was attenuated. This has been confirmed and extended by other investigators using different glia inhibitors, such as propentofylline (Raghavendra et al., 2004a), minocycline (Mika et al., 2007) and ibudilast (Hutchinson et al., 2009). Increases in other glial markers have also been observed, including those specifically for microglia (Raghavendra et al., 2002; Cui et al., 2006; Tai et al., 2006; Hutchinson et al., 2009).

Other evidence for morphine activating glia include membrane ruffling and activation of extracellular signal-regulated kinase (Takayama and Ueda, 2005) and microglial P38 MAPK (Liu et al., 2006; Cui et al., 2006) with inhibitors of these pathways reversing morphine tolerance (Cui et al., 2006; Parkitna et al., 2006). The presence of opioid receptors, including μ receptor on glia further suggests a possible direct interaction (Chang et al., 1998).

The chemokine fractalkine, postulated as a neuron-glial signalling molecule (Watkins et al., 2007b), has also been implicated in tolerance with the observation that repeated morphine administration leads to the release of fractalkine from neurons and to tolerance which is attenuated by co-administration of anti-CXCR1 antibody (Johnston et al., 2004). Further support for the interaction between morphine and glia is provided by observations that the production of NO and proinflammatory cytokines occurs following morphine-induced glial activation (Stefano et al., 1998;

Raghavendra et al., 2002; Johnston et al., 2004; Tawfik et al., 2005; Watkins et al., 2005; Tai et al., 2006; Hutchinson et al., 2008a).

There is a wealth of information associating increased levels of proinflammatory cytokines with morphine tolerance. This includes the use of transgenic mice with impaired IL-1 signalling which exhibit reduced morphine tolerance (Shavit et al., 2005) and the use of cytokine antagonists which reinstate morphine analgesia in morphine tolerant rats (Gul et al., 2000; Raghavendra et al., 2002; Johnston et al., 2004; Shavit et al., 2005; Mika et al., 2009b). There is also evidence for proinflammatory cytokine transcription, translation and protein release being elevated in spinal cord in response to chronic morphine (Raghavendra et al., 2002; Johnston et al., 2004; Raghavendra et al., 2004a; Hutchinson et al., 2008a; Hutchinson et al., 2009).

Cytokines also act indirectly to affect morphine tolerance. For example, they induce the release of CCK (Ohgo et al., 1992) which activates astrocytes, thus stimulating more proinflammatory cytokine release which further enhances tolerance (Watkins et al., 1984). IL-1 also induces COX2 production, blockade of which has been shown to delay morphine tolerance (Deciga-Campos et al., 2003). Chronic morphine administration also causes the release of chemokines, like fractalkine perhaps by rapid sensitisation of glutamatergic NMDA receptors (Mao and Mayer, 2001). Glutamate can induce fractalkine cleavage (Chapman et al., 2000) allowing the formation of a diffusible signal from neurones to activate more microglia to release proinflammatory cytokines (Johnston et al., 2004). Evidence for this includes co-administration of anti-CXCR1 antibody attenuating tolerance related behaviours (Johnston et al., 2004).

Apart from cytokines, morphine tolerance has also been associated with the down regulation of glial GLAST and GLT-1 glutamate transporters leading to an up-regulation of excitatory amino acids (Mao et al., 2002; Tai et al., 2006). This finding illustrates the large number of mechanisms that glia can potentially impact on, and thereby have some association with the majority of theories detailed above. For example, pain enhancing effects of neuronally derived spinal dynorphin have been

linked to selective activation of microglial p38 MAPK kinase leading to the release of PGE2 and IL-1 (Laughlin et al., 2000; Svensson et al., 2005).

Taking all this evidence into account, an overall hypothesis for the involvement of glia in morphine tolerance can be formulated. Chronic morphine activates glia directly by releasing excitatory substances including proinflammatory cytokines, or indirectly by regulating neural plasticity (e.g. uptake of GABA and glutamate). This creates pain facilitation thereby counterbalancing morphine-induced analgesia and promoting analgesic tolerance.

Although there is evidence for the involvement of glial cells in morphine tolerance, less is known about the specific role of glial cell subtypes and the contribution each subtype makes to the process. As many of the tool antagonists used in glial research are not selective for astrocytes or microglia it has been difficult to distinguish between the two cell types. Recently however, it has been demonstrated that the morphine-induced up-regulation of a microglia marker, but not an astrocyte marker was diminished after minocycline and pentoxifylline administration supporting a specific role of microglia (Mika et al., 2009b). Further evidence suggesting the interaction between morphine and microglia is the ability of morphine to prime microglia for enhanced production of TNF-α (Chao et al., 1994).

By investigating the role of P2X7 receptors on morphine tolerance, given that they are primarily expressed on microglia, the contribution of this specific glial cell type can be assessed. As P2X7 receptors have a key role in the production of proinflammatory cytokines such as IL-1β (Takenouchi et al., 2009) and TNF (Suzuki et al., 2004), and have been shown to produce efficacy in neuropathic pain models (Abdi et al., 2010; Honore et al., 2009; Donnelly-Roberts et al., 2009) there is a strong possibility that these receptors have some involvement in the mechanism behind morphine tolerance. Although there is already clear evidence implicating a role of a different purinergic receptor, P2X4 in morphine tolerance (Horvath et al., 2010b), the role of P2X7 has not been fully elucidated.

1.7.5 Enhancing opioid efficacy

As detailed above, some proposed mechanisms of tolerance suggest that it is increased neuronal excitation induced by chronic morphine dosing that counteracts

the analgesic properties resulting in tolerance. It is therefore conceivable that via these same mechanisms acute morphine analgesia, or the analgesia prior to tolerance developing could be enhanced if co-administered with compounds that block morphine-induced excitation.

This has been demonstrated in the literature using several drugs, also known to block neuropathic pain. Ketamine, the NMDA receptor antagonist has been shown to enhance the analgesic effects of fentanyl (Celerier et al., 2000) and several calcium channel blockers including mibefradil and amlodipine have also been shown to enhance the anti-nociceptive effects of acute morphine (Dogrul et al., 1997; Dogrul and Yesilyurt, 1998; Dogrul et al., 2001; Dogrul et al., 2002). In terms of blocking glia, an enhancement of efficacy of morphine has also been shown in naïve rats when co-dosed with IL-1 receptor antagonist (Shavit et al., 2005; Hutchinson et al., 2008a) and ibudilast (Hutchinson et al., 2009). To date there are no published studies investigating the effect of P2X7 receptors on the efficacy of acute morphine in naïve rat and this is investigated as part of this project.

The effect that blocking glia has on morphine efficacy might also help explain the clinical finding that opioids are less effective in treating chronic pain than acute pain (Kalso et al., 2004; McCleane and Smith, 2007; Rosenblum et al., 2008). Resolving this problem would lead to the improvement in the treatment of millions of patients with chronic pain. In neuropathic pain, resistance to morphine is well characterised (Porreca et al., 1998; McQuay, 2002) and the mechanisms of the decreased analgesic potency are not fully understood (Przewlocki and Przewlocka, 2001; Przewlocki and Przewlocka, 2005). The majority of studies demonstrate that neuropathy-induced hyperalgesia leads to a decrease in the anti-nociceptive potency of morphine (Mao et al., 1995b; Christensen and Kayser, 2000). However other reports suggest that peripheral nerve injury increases the anti-nociceptive potency of morphine (Backonja et al., 1995; Catheline et al., 1996).

Theories exist to explain the lower effectiveness of morphine in neuropathic pain. For example, it was suggested that a reduction in the number of presynaptic opioid receptors following degeneration of primary afferent neurons caused by nerve damage was the main mechanism (Porreca et al., 1998). RVM sites have also been

implicated as they are opioid sensitive and alter after nerve injury suggesting that supraspinal changes may also contribute to the changed effectiveness of opioids after nerve damage (Kovelowski et al., 2000).

Evidence also exists suggesting a role of morphine-induced excitation. This includes the findings that the anti-analgesic action of CCK is enhanced after nerve injury (Nichols et al., 1995) and that gabapentin has been shown to enhance the effectiveness of morphine in neuropathic rats (Matthews and Dickenson, 2002).

The role that glia and cytokines may have on the reduced analgesic effect of morphine in neuropathic pain has also been considered. Uncontrolled activation of microglial cells after injury can lead to altered activity of opioid systems or opioid-specific signalling (Speth et al., 2002; Przewlocki and Przewlocka, 2005). It has been reported that the microglial inhibitor minocycline, and the cytokine inhibitor pentoxyfylline, enhanced the effect of a single dose of morphine administered to CCI-operated rats and mice (Mika et al., 2007). This suggests that P2X7 receptor antagonists may also act in the same way by preventing microglial activation and thereby potentiate the efficacy of morphine in CCI-operated rats. This has not been previously reported and is investigated in this PhD.

1.8 Animal models of pain

Animal models provide pivotal systems for preclinical studies of pain and serve as an experimental basis for mechanistic investigations and for the pre-clinical assessment of novel analgesics. There are a wide variety of animal models of pain that are commonly used to understand pain processing mechanisms in all pain states. Animal models can be generally classified as acute nociceptive models, inflammatory pain models or neuropathic pain models.

1.8.1 Models of nociception

Models of nociception are used to assess the anti-nociceptive potential of drugs in ‘naïve rats’ (defined as rats that have not been manipulated in any way). These models rely on the application of a noxious stimulus (thermal, mechanical, electrical or chemical) to a convenient body part (usually hindpaw, tail or abdomen) to evoke a nocifensive withdrawal or to other simple behaviours that can be easily scored.

Examples include, the tail flick reflex model, in which heat is focussed on the tail and the animal flicks its tail to escape the stimulus (D'Amour and Smith, 1941) or the paw pressure model, in which a mechanical pressure is exerted on to the paw until a paw withdrawal threshold is obtained (Skingle et al., 1990). Some of the evoking stimuli used in these classical assays are also used in neuropathic and inflammatory pain assays when measuring hypersensitivity.

Analgesic drugs, such as opioids, and anaesthetic drugs are effective in these models, however common 'pain-killers' such as non-steroidal anti-inflammatory drugs (NSAIDs) are not, as these drugs interact with mechanisms that develop during pathological conditions.

For a review on acute nociceptive models see (Le et al., 2001). Acute pain studies detailed in this project measure paw withdrawal reflex using an analgesymeter and are described in more detail in Chapter 6.

1.8.2 Models of inflammatory pain

Inflammatory pain can be modelled by injecting inflammatory agents into the hind paw or into specific joints and recording nocifensive behaviours. Inflammatory agents include; formalin (Dubuisson and Dennis, 1977) and capsaicin (Gilchrist et al., 1996) acting on TRPV1 receptors, and also substances that more generally activate the immune system, e.g. carageenan, complete Freunds Adjuvant, urate crystals and zymosan (Chapman et al., 1985).

1.8.3 Models of neuropathic pain

Animal models of neuropathic pain typically comprise of 'surgery-based neuropathic pain assays' in which peripheral nerves are transected or ligated, and 'painful disease assays' which attempt to induce the disease, injury or physiological state itself.

1.8.3.1 Surgery based neuropathic pain assays

The first behavioural assay of neuropathic pain involved complete nerve transection and resulted in autotomy behaviour which is the self-mutation of digits (Wall et al., 1979). Due to animal healthcare issues, partial nerve injury models were

developed which also better mimicked more common clinical conditions, such as DRG avulsion injury and trigeminal neuralgia.

The first partial nerve injury model was the chronic constriction injury (CCI) model in which catgut ligatures were loosely tied around the sciatic nerve proximal to the sciatic trifurcation degeneration (Bennett and Xie, 1988) (see Figure 7). This constriction of the nerve results in intraneural oedema which strangulates the nerve, a focal ischemia, and an axonal degeneration. As a consequence, this model results in chemical and heat-evoked hyperalgesia, as well as cold and mechanical allodynia, and some symptoms of spontaneous pain which lasts for a period of more than 2 months (Bennett and Xie, 1988; Attal et al., 1990). The CCI model will be described more detail in Chapter 2 as it is the principal model used in this thesis.

Other partial nerve injury models include: the Seltzer model, where a tight ligature is tied around part of the sciatic nerve (Seltzer et al., 1990); the Chung model, which involves tightly ligating L5 and L6 spinal nerves (Kim and Chung, 1992) and the spared nerve model, which involves tightly ligating the tibial and common peroneal branches of the sciatic nerves, but leaving the sural branch intact (Decosterd and Woolf, 2000) (see Figure 7).

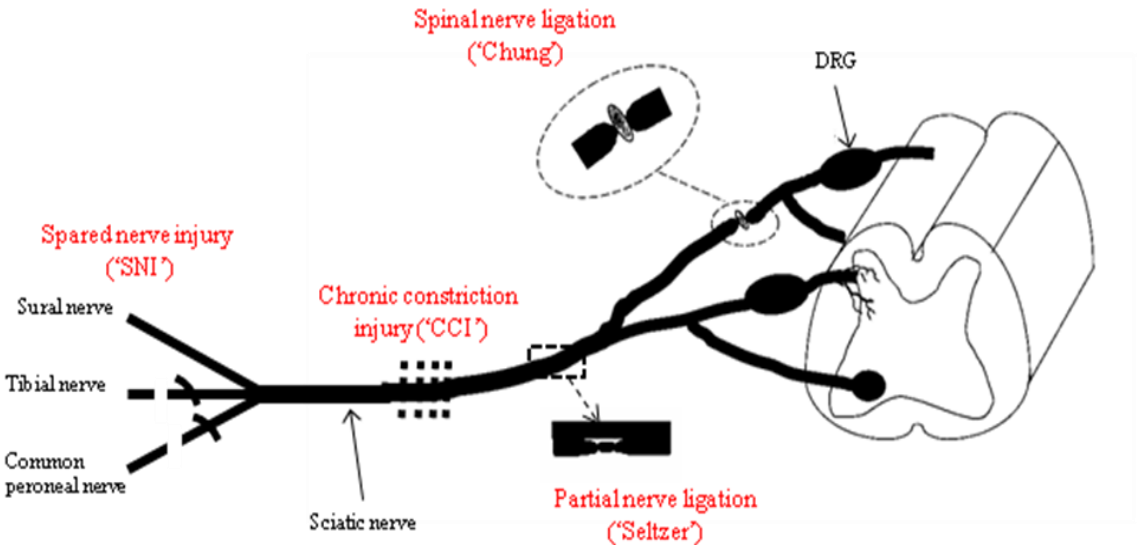

Figure 7. Diagram representing the main surgery-based models of neuropathic pain.

All surgery-based models produce a heightened responsiveness similar to that seen in neuropathic pain patients (Kim et al., 1997; Bennett and Xie, 1988; De et al., 2004) and are sensitive to clinically relevant drug treatments (Attal et al., 1991; Hunter et al., 1997; Abdi et al., 1998; Esser and Sawynok, 2000; Pelissier et al., 2003; De et al., 2004).

1.8.3.2 Painful disease assays

When it was realised that the surgery based models were too general and did not mimic the more common clinical pain syndromes well enough, 'painful disease assays' were developed which attempted to induce the disease, injury or physiological state itself.

Examples of these models include a model of painful diabetic neuropathy which involves the administration of streptozotozin, a toxin which kills insulin-secreting islet of Langerhans pancreatic cells. Administration of this toxin produces the rapid development of hyperglycaemia, as well as thermal and mechanical hyperalgesia and allodynia (Courteix et al., 1993). Models of bone cancer pain have also been developed and involve injecting 'cancer cells' into bones resulting in allodynia which is reversed by clinically used compounds (Medhurst et al., 2002). The final example is a model of post-herpetic neuralgia, the chronic pain associated with shingles, which involves the administration of the varicela-zoster virus (VZV), the virus responsible for the condition (Fleetwood-Walker et al., 1999). Within this PhD it was necessary to compare data between the surgery based neuropathic pain model (CCI) and a painful disease model. The VZV-induced allodynia model was chosen and will be described in more detail in Chapter 4.

1.8.3.3 Behavioural tests of neuropathic pain in animals

Many patients with neuropathic pain present with hyperalgesia and allodynia. Our knowledge of pain in the patient rests exclusively on the patient's ability to use language. Animals however cannot speak thus there is no objective indication of their pain sensations. Experiments on animals must therefore rely on the nocifensive withdrawal reflexes evoked by painful stimuli.

It should also be noted however that chronic-pain syndromes in humans often feature dramatic changes in overall quality of life and include a wide variety of complex behaviours including attention, memory, depression, anxiety, motivation and sleep. In response to this alternative non-reflexive models are beginning to be developed that reflect these co-morbidity symptoms, however only stimulus-evoked stimuli producing hyper-reflexia were used in this project.

Neuropathic pain studies mostly use tests of heat hyperalgesia, in which paw withdrawal latencies to a radiant heat stimulus are measured; cold allodynia, in which mini-withdrawals or ‘paw flicks’ to cutaneous administration of acetone are recorded; or mechano-hyperalgesia and mechano-allodynia, in which paw withdrawal thresholds to increasing pressure are measured. The stimulus used for the neuropathic pain studies contained in this thesis is mechano-hyperalgesia and mechano-allodynia and uses two different methods or ‘read-outs’, namely an analgesymeter and von Frey hairs respectively and are described in more detail later in the thesis.

1.9 Aims of the thesis

In this thesis *in vivo*, molecular and immunohistochemical techniques have been utilised to investigate the role of P2X7 receptors in neuropathic pain and the interaction that P2X7 receptors have with a variety of morphine-induced actions. The aims were:

- to demonstrate that efficacy by P2X7 receptor antagonists in the CCI model of neuropathic pain is dependent on compounds having the ability to penetrate the CNS
- to demonstrate an interaction between P2X7 receptors and morphine that influences morphine-induced analgesia, when chronically and acutely dosed, and morphine-induced tolerance
- to compare responses from animals co-dosed with P2X7 and morphine in two contrasting models of neuropathic pain
- to identify whether an interaction exists between P2X7 receptors and morphine-induced effects that are non-analgesic related
- to investigate the potential mechanisms for the interaction between the P2X7 receptor and morphine using immunohistochemistry and molecular techniques.

Chapter 2

Investigating the site of action of P2X7 receptor antagonists in the chronic constriction injury model of neuropathic pain

2. Investigating the site of action of P2X7 receptor antagonists in the chronic constriction injury model of neuropathic pain

2.1 Introduction

The localisation of P2X7 receptors to predominantly immune cells of haemopoetic lineage, e.g. mast cells, lymphocytes, erythrocytes, fibroblasts and macrophages and the unique properties of the receptor in mediating cytokine release (Perregaux and Gabel, 1994; Solle et al., 2001; Kahlenberg and Dubyak, 2004) has focused research efforts on the involvement of P2X7 receptor in mediating inflammatory pain.

Although one publication showed that activation of P2X receptors in the spinal cord could elicit allodynia (Fukuhara et al., 2000), it was not until 5 years later that a centrally- mediated pain state was considered. Chessell et al. (2005) reported the lack of neuropathic hypersensitivity in P2X7 receptor KO mice using the Seltzer model. In the same paper it was also reported that the P2X7 receptor was up-regulated in injured nerves from chronic neuropathic pain patients. In the same year Zhang et al. (2005b) also demonstrated electrophysiologically the functional expression of P2X7 receptors in non-neuronal cells from the dorsal root ganglia.

These studies led to an increase in work focusing on purinergic signalling in neuropathic pain with the use of selective P2X4 and P2X7 receptor antagonists. For example, P2X7 receptor antagonists were shown to have efficacy in the Chung model of spinal nerve ligation, the CCI model and a chemotherapy-induced neuropathic pain model (Nelson et al., 2006; Honore et al., 2006; Carroll et al., 2007). Conflicting data was also reported however with, Broom et al. (2008) demonstrating a P2X7 receptor antagonist that was unable to reverse L5 spinal nerve ligation-induced tactile allodynia when given therapeutically, and Ando et al. (2010) showing a ‘non-significant tendency’ of reversal of mechanical allodynia in the Seltzer model of neuropathic pain.

One important property of P2X7 receptor antagonists which has not been clearly defined is how important it is that these antagonists can cross the blood brain barrier and access the CNS. One potential reason for the lack of attention is due to the initial bias to inflammatory diseases which are primarily driven by peripheral mechanisms and therefore central penetration was not considered relevant. There are indications in the literature that CNS penetrating P2X7 receptor antagonists produce efficacy in neuropathic pain models, for example compound A-438079 is reported to have a brain to blood ratio of 2:1 and produces efficacy in two nerve injury models and a chemotherapy-induced pain model (McGaraughty et al., 2007). It was also illustrated in electrophysiological studies that A-438079 reduced the activity of spinal neurons in neuropathic rats. Although this data suggests the importance of CNS penetration, there is no definitive *in vivo* data demonstrating that central penetrance is critical for a P2X7 receptor antagonists to exert an effect and is an area that is investigated within this chapter.

It has been reported that spinal administration of IL-1 receptor antagonist results in reduced nociception in animal models of inflammatory and nerve-injury induced pain (Ferreira et al., 1988; Maier et al., 1993; Sommer et al., 1999). This data suggests an alternative approach to establishing the importance of central penetrance of P2X7 receptor antagonists by dosing the compounds via the intrathecal route.

The aims of this chapter was to compare the effects of a centrally penetrant and a peripherally-restricted P2X7 receptor antagonist in a neuropathic pain model, when dosed both systemically and centrally. Pharmacokinetic analysis was also carried out to determine drug levels in blood and brain tissues. The primary objective was to establish the potential site of action for P2X7 receptors in neuropathic pain.

The neuropathic pain model chosen to test the P2X7 receptor antagonist was the sciatic nerve chronic constriction injury model using withdrawal threshold to von Frey hairs as the behavioural readout. According to a study comparing five models of peripheral nerve injury, the CCI provides reliable and reproducible results when using this readout (Dowdall et al., 2005). This concurs with the experience of the GSK laboratory.

Two potent and selective P2X7 receptor antagonists were assessed in the CCI model: GSK1370319 (N-[(2,4-dichlorophenyl)methyl]-1-methyl-5-oxo-L-prolin-amide) and GSK2039841 (2-oxo-N-(phenylmethyl)-4-imidazolidine-carboxamide). Table 4 details the chemical structure of both compounds as well as other parameters relevant to this thesis. As well as being chemically distinct, the two compounds also differ in other parameters including potency at the P2X7 receptor. Potencies were measured by the GSK Neurosciences *in vitro* department using the ethidium bromide uptake assay in recombinant cells expressing either human or rat P2X7 receptors (Michel et al., 2006). The assay is a competition assay using the natural ligand, ATP. As described in Chapter 1 activation of ATP leads to formation of a large pore in the cell wall and it is the level of ethidium bromide dye within the cell that is measured using fluorescence. The resultant pIC50s of both compounds suggest that GSK2039841 is more potent than GSK1370319. *In vitro* selectivity assays were also run in recombinant cells and demonstrated that the compounds had no effect on other receptors, including those within the P2X receptor family.

The two compounds also differ in their CNS penetration. CNS penetration describes the ability of compounds to cross the blood-brain barrier, the separation between circulating blood and the cerebro-spinal fluid (CSF). The barrier occurs along capillaries and consists of tight junctions that do not exist in normal circulation. It is endothelial cells that restrict the diffusion of microscopic objects (e.g. bacteria) and large hydrophilic molecules into the cerebro-spinal fluid, whilst allowing the diffusion of small hydrophobic molecules. The significance of CNS penetration is of particular importance when targeting diseases associated with the brain (e.g. Alzheimer's disease) or when trying to avoid centrally-mediated side effects for peripherally orientated diseases. In table 4, CNS penetration of both compounds is presented as brain: blood ratios and assumes the term 'CNS penetration' refers to penetration into both the brain and spinal cord, even though ratios were only calculated from compound exposure in the blood and brain. The exposures used for calculating the current ratios were obtained from rats used in a number of pain studies run by the GSK Neuroscience *in vivo* department. In this instance, the difference in CNS penetration maybe due to GSK2039841 having a

higher P glycoprotein (Pgp) efflux ratio. Pgp is a member of the superfamily of ATP-binding cassette transporters which transport a variety of molecules across the blood/ brain barrier. The higher the efflux ratio the more the compound is a substrate for the transporter and the more likely it is to be continuously transported out of the CNS and be less centrally penetrant. The Pgp efflux ratio was measured by the GSK Neurosciences DMPK department.

	Structure	Potency (pIC50 in rat)	Pgp efflux ratio	Brain: blood ratio
GSK1370319	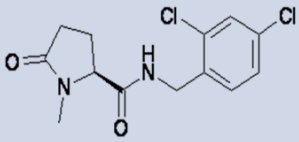	6.4	1.1:1	0.5:1
GSK2039841	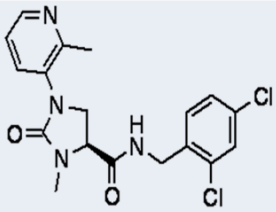	7.2	4.9:1	0.05:1

Table 4. Chemical structure, potency, Pgp efflux ratio and brain: blood ratios of the P2X7 receptor antagonists GSK1370319 and GSK2039841.

Before proceeding with the assessment of these novel compounds in the CCI model, the model was first characterised to ensure that my results are consistent with the literature and other operators that use the model within GSK.

2.2 Methods

2.2.1 Animals

All experimental procedures involving animals were conducted in compliance with the Home Office Guidance on the operation of the Animals (Scientific Procedures) Act 1986 under the authority granted in personal and project licenses, and were reviewed and approved by the GlaxoSmithKline Procedures Review Panel. All animals were housed under standardised environmental conditions (12 hour light/dark cycle, 21 °C and 55% humidity) and allowed free access to food and water. Rats were given at least 5 days acclimatisation prior to use. In all studies the number of animals and intensity of noxious stimuli were the minimum necessary, as determined by power calculations, to demonstrate consistent effects of drug treatments. This information applies to all *in vivo* procedures detailed in this thesis. Details of strain, weight and supplier are included in appropriate method sections.

2.2.2 Chronic constriction injury (CCI) model

The chronic constriction injury model (CCI) is a model of nerve damage-induced allodynia/hyperalgesia which has been shown to share pathophysiology with a variety of neuropathic pain conditions observed in the clinic (Bennett and Xie, 1988).

2.2.2.1 Surgery

Male Random-hooded rats (200-250 g; Charles River, UK) were anaesthetised via the inhalation route with isoflurane mixed with oxygen (3:1). Rats were placed in a specialised anaesthetic induction chamber into which the isoflurane/ oxygen mixture was introduced. When showing the recognised signs of anaesthesia (loss of pedal withdrawal reflex, loss of eye reflex, decline in heart and lung function) rats were removed from the chamber and placed on a heated mat to maintain the body temperature of the rat at approximately 37 °C. To maintain anaesthesia throughout the surgical procedure, the nose of the rat was placed into a specialised anaesthetic mask to allow the continuous exposure of isoflurane/ oxygen mixture. Ensuring the rat was fully anaesthetised (see signs of anaesthesia above) an incision was made at

mid thigh level and the common left sciatic nerve was exposed via blunt dissection. Four loose ligatures of chromic gut (4.0, Braun) were tied loosely around the nerve with 1 mm spacing between each (Bennett and Xie, 1988) before the wound was closed and secured with suture clips. After completing the surgical procedure, rats were placed in a heated chamber (~40 °C) to recover from anaesthesia before being placed in a new cage with other operated rats. The surgical procedure was identical for sham operated rats except the sciatic nerve was not ligated. Rats were allowed between 8-10 days to recover from the surgery before behavioural testing was carried out.

2.2.2.2 Behavioural testing

Compounds were tested for their ability to reverse CCI-induced allodynia by measuring paw withdrawal thresholds (PWTs) using an ascending series of von Frey filaments (Stoelting, Wood Dale, IL; Figure 8). These filaments were presented to a hind paw using a method previously described by Field et al. (1997).

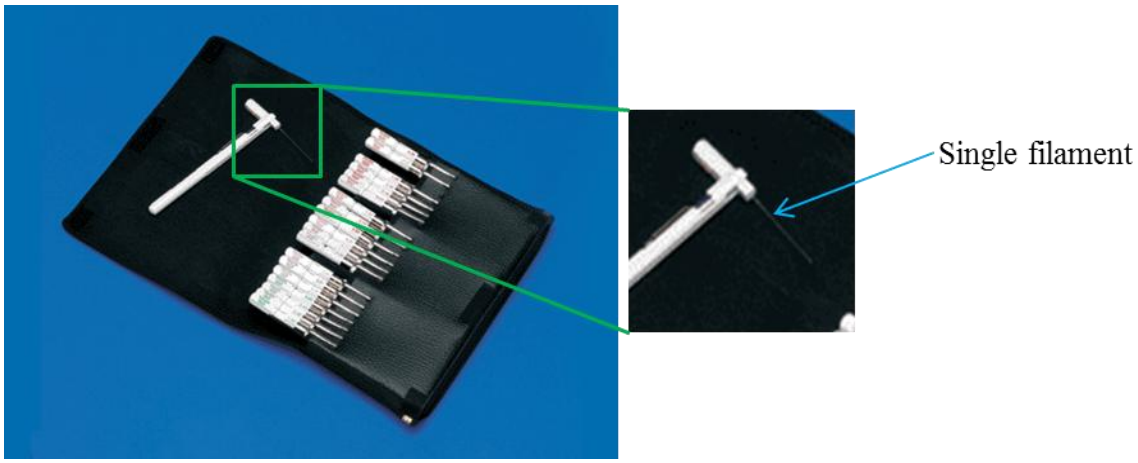

Figure 8. Photograph of a series of von Frey filaments with a range of pressure they exert when bent of 0.0001 g to 500 g. A section is enlarged to show the detail of a single filament

Rats were first placed in a raised clear Perspex boxes on a perforated metallic platform and left to acclimatise for 5 minutes. When animals were settled the filaments were applied to the middle region of the plantar surface of the hind paw ipsilateral to the nerve ligation with sufficient force to result in buckling of the

filament. Each filament was applied for approximately 3-5 seconds until a withdrawal response was observed. If a withdrawal was not observed the next higher filament was tested. The lowest filament to give a withdrawal was recorded as the response after confirmation with re-application of lower and/or higher filaments within the range tested (range: 1.4 g to 26 g) (Field et al., 1997). The filament exerting a pressure of 26 grams was chosen as the cut-off filament as accurate readings are not possible with successive filaments due to filament thickness not allowing adequate bending when presented to the surface of a rat paw.

Readings were taken prior to surgery, to establish a naïve baseline reading for each rat; post-surgery, to establish robust levels of allodynia/ hyperalgesia; and during the dosing period typically 1 hour after the morning dose. In some studies additional readings were taken after the dosing period. To ensure all rats included in a drug study were considered allodynic a 'non-responder cut-off' was introduced. Any CCI-operated rat responding to the 10 g hair or above was not included in the study. This cut-off was chosen for non-responding rats as it is often the lowest pressure an un-operated rat responds to.

2.2.2.3 Testing compounds

Compounds were administered only when a robust level of allodynia had been established, as defined by paw withdrawal thresholds of CCI-operated rats consistently being significantly lower than sham-operated rats (< approximately 8 g). When this level had been reached the rats were ranked according to their latest reading and randomised into dosing groups according to Latin square design. Compounds were generally dosed orally by gavage at a volume of 5 ml/kg. In one experiment compounds were dosed intrathecally using a similar technique to that described previously by Hylden and Wilcox (1980). Rats were anaesthetised via the inhalation route with isoflurane mixed with oxygen (3:1) using an anaesthetic mask. The compounds were then delivered in a volume of 10 µl between L4 and L5 regions of the spinal cord using a 50 µl Hamilton syringe with a 27 g x 12 mm luer needle as shown in Figure 9.

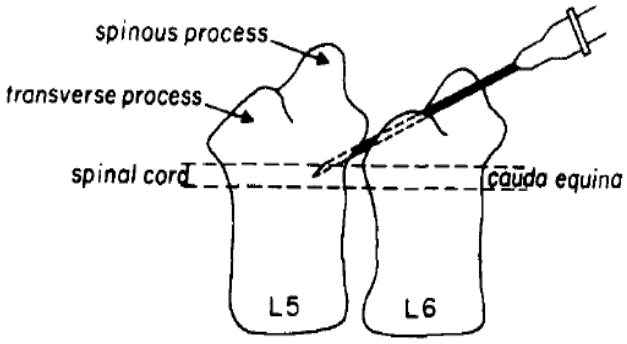

Figure 9. Diagram showing insertion of needle into the intervertebral space between L5 and L6 (Hylden and Wilcox, 1980).

Oral dosing studies required twice a day dosing (b.i.d.) which was conducted at 0900 ±1 h and 2100 ±1 h. To minimise repetition, the protocol details for each study (i.e. the compounds tested, the doses administered and the days that testing was carried out) are reported in the results section. All studies were performed with the operator blind to which treatment each rat received. At the end of the study all rats were euthanised using CO_2 inhalation.

2.2.2.4 Data analysis

Paw withdrawal threshold data are presented graphically as log mean ±SEM in grams with typically, n=9 rats per dosing group. The log transformation of the data was adopted to reduce the disproportionality of the uneven intervals between the von Frey hairs. If data was not logged there would potentially be positive bias to a positive response, i.e. more rats withdrawing to lower hairs as the intervals of lower hairs is less. Statistical analysis was carried out on logged PWTs either comparing responses from CCI-operated rats to sham-operated rats or comparing responses from drug dosed groups with vehicle treated groups using Repeated Measures ANOVA, followed by Planned LSD comparisons, where $p<0.05$ was considered significant (Medhurst et al., 2008).

2.2.3 Compound details

This section contains compound details for all *in vivo* studies included in this thesis. GSK1370319 (N-[(2,4-dichlorophenyl)methyl]-1-methyl-5-oxo-L-prolin-amide) and GSK2039841 (2-oxo-N-(phenylmethyl)-4-imidazolidinecarboxamide) were synthesised at GlaxoSmithKline, Harlow, UK and made up in 1% (w/v) methylcellulose and water (oral dosing) and 1% DMSO/ 49.5% PEG200/ 49.5% saline (intrathecal dosing). Pregabalin and gabapentin were purchased from ChemPacific, Baltimore and made up in 1% (w/v) methycellulose and water. Duloxetine was synthesised at GlaxoSmithKline, Harlow, UK and made up in 1% (w/v) methycellulose. Venlafaxine was synthesised by Toronto Research Centre (cat. V120000) and made up in 1% (w/v) methylcellulose and water. Minocycline was obtained from Sigma (M9511) and made up in 1% (w/v) methylcellulose and water for oral dosing and saline (0.9% sodium chloride) for subcutaneous dosing. All compounds made up in 1% (w/v) methylcellulose and water were first added to a mortar and ground using a pestle in a few drops of vehicle. When a paste had been formed the remaining vehicle was added to produce a smooth suspension ready for oral dosing. Morphine was obtained as morphine sulphate salt pentahydrate from Sigma (M8777) and dissolved in saline. Capsaicin was obtained from Sigma (M2028) and made up in 10% ethanol, 10% Tween and 80% saline (w/v) respectively.

2.2.4 Pharmacokinetic analysis

Where relevant, blood and brain samples were taken following the final behavioural reading to determine drug concentrations. Following the post-dose reading, rats were euthanised using CO_2 inhalation before blood and brain samples were taken. 50 µl of trunk blood was diluted with 50 µl 0.1 M HEPES (4-(2-hydroxyethyl)-1-piperazineethanesulfonic acid, a commonly used buffer) or water, frozen on cardice and stored at -80 °C prior to analysis. Brains were removed, washed in fresh cold saline, blotted on tissue paper and frozen in glass tubes on cardice and stored at -80 °C prior to analysis.

Blood and brain samples were analysed by colleagues in the Neurosciences CEDD DMPK department using a specific LC-MS/MS assay. On the day of analysis,

diluted blood samples, control blood aliquots (100 µl aliquots 1:1 blood:water) and brains were removed from the freezer and thawed. Calibration standards containing the test compounds and blanks were prepared using the control blood. Brain tissue was homogenised and diluted with HEPES. The samples, standards and blanks were extracted by protein precipitation using 250 µl of precipitation solvent (80:20 acetonitrile:10 mM ammonium acetate, native pH containing internal standard). Aliquots of the resulting supernatant were analysed by reverse phase LC-MS/MS using a heat assisted electrospray interface in positive ion mode. Concentration data (µM) was expressed as mean ±SD.

2.3 Results

2.3.1 Model characterisation studies

Operator variability is an inherent problem when comparing *in vivo* data between individuals due to the multitude of slight differences that each individual inadvertently adds into the protocol. It is therefore critical before running any drug studies that the model is characterised. The first study was to assess the time-course that any behavioural phenotype might follow. Having established the most appropriate time for dosing compounds, 4 pharmacological studies were completed testing 3 different drugs used clinically for treating neuropathic pain. This was to confirm the models utility for pharmacological studies, to compare with literature and in-house data and to identify the most suitable standard for subsequent studies.

2.3.1.1 Time course study

In this initial CCI study, 14 rats underwent CCI surgery and 10 rats were sham operated as detailed in section 2.2.2.1. Von Frey hair testing was carried out as detailed in section 2.2.2.2 on the day prior to surgery (baseline reading), and on days 7, 11, 15, 18 and 22 post-surgery.

When rats were tested for mechanical allodynia using von Frey hairs prior to surgery (day 0), all 24 rats produced a mean paw withdrawal threshold (PWT) of 21.5 ±1.3 g (Figure 10). This baseline reading was similar to data produced from other lab members at GSK and the literature thereby allowing the study to continue and the surgical technique to go ahead.

7 days post-CCI surgery, the PWTs produced from 14 CCI-operated rats decreased to 7.1 ±1.7 g. This value was shown to be statistically different from the baseline reading from the corresponding group of rats, suggesting the onset of allodynia. There was also a small decrease in PWTs from sham-operated rats to 15.0 ±2.6 g, but this was not statistically significant from the corresponding baseline reading (Figure 10). These levels of PWT remained consistent for both CCI-operated and sham-operated rats throughout the time-course. CCI-operated rats producing PWT with a range of means of 4 to 8.7 g and sham-operated rats produced means of

17-20 g. When statistically comparing the PWTs of CCI-operated and sham-operated rats over the time course a significant difference was observed on all test days post-surgery up to day 22. The difference between the two groups on day 22, also known as the 'window of allodynia', was considered sufficient to be modulated by drug treatment in subsequent studies.

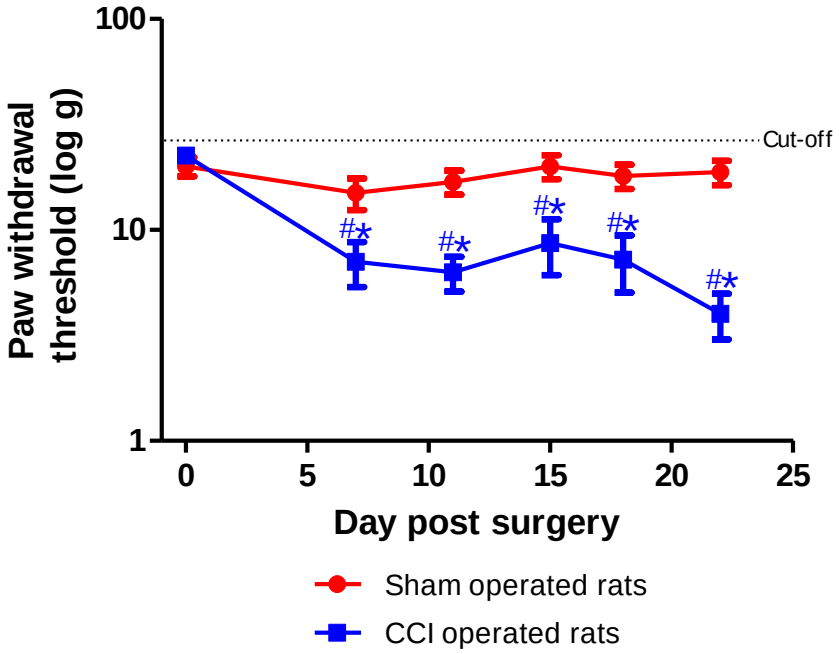

*Figure 10. Effect of loosely ligating the left sciatic nerve of male Random-hooded rats on paw withdrawal threshold following von Frey filament application. Data are log mean ±SEM in grams for sham operated rats (n=10) and CCI-operated rats (n=14). # denotes p<0.05 using repeated measures ANOVA followed by post-hoc Fisher's LSD test compared to corresponding baseline reading. * denotes p<0.05 using ANOVA followed by Planned LSD Comparisons compared to responses from sham-operated rats.*

2.3.1.2 Effect of gabapentin and pregabalin on CCI-induced allodynia when dosed for 5 days

To confirm that two clinically used drugs were efficacious in the CCI model, gabapentin and pregabalin were tested at doses previously shown to be efficacious.

27 rats underwent CCI surgery and 8 rats were sham operated. Von Frey hair testing was carried out on the day prior to surgery and on day 9, 14 and 17 post-surgery. On day 20, after CCI-operated rats had been ranked and assigned a dose

group, they were dosed with gabapentin (30 mg/kg, p.o., b.i.d., n=8), pregabalin (30 mg/kg, p.o., b.i.d., n=8) or vehicle (1% (w/v) methylcellulose, p.o., b.i.d., n=8) for 5 days. The sham operated rats were also dosed with vehicle (1% methylcellulose, p.o., b.i.d., n=8) for 5 days. Testing was conducted 1 hour post-morning dose on day 1, 3 and 5 of the dosing period which corresponded to day 20, 22 and 24 post-surgery.

Prior to surgery (day 0) all rats produced a mean paw withdrawal threshold (PWT) of 21.8 ±1.1 g (Figure 11). Although this value gives a good indication of baseline reading for the whole group of rats the meaned number is not illustrated on the accompanying graph for this study. This is due to the baseline readings having already been divided into the appropriate dosing groups.

On day 9, 14 and 17 post-surgery, the PWTs from CCI-operated rats had significantly decreased to 8.3 ±0.7 g, 3.5 ±0.4 g and 3.5 ±0.3 g respectively, whereas the sham-operated group produced PWTs of 14.9 ±3.5 g, 15.3 ±3.2 g and 18 ±3 g which were not significantly different to baseline readings. The differences between CCI and sham and the differences from baseline readings suggest that a suitable ‘window of allodynia’ was observed to continue with drug testing.

On day 17 it was observed that 3 CCI-operated rats met the exclusion criteria of PWT > 10 g and so were not included in the study. The remaining CCI-operated rats were dosed with the test compounds.

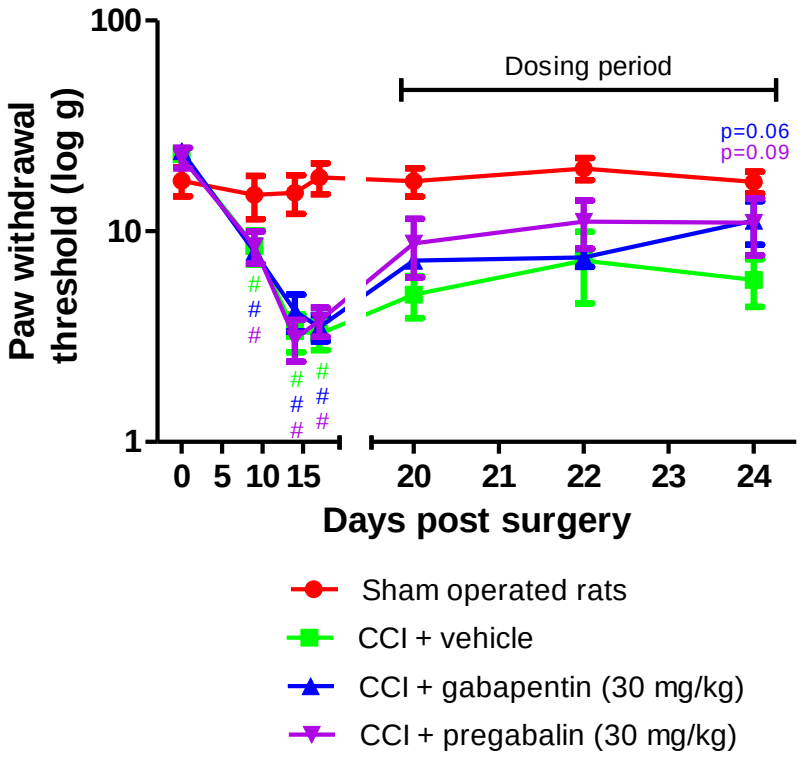

Figure 11. Effect of gabapentin (30 mg/kg, p.o., b.i.d. for 5 days) and pregabalin (30 mg/kg, p.o., b.i.d. for 5 days) on paw withdrawal threshold of CCI-operated rats following von Frey filament application. Data are log mean ±SEM in grams with 8 rats in each group. # denotes p<0.05 using Repeated Measures ANOVA followed by Fisher's LSD post hoc test comparing to baseline for only predose readings. During the dosing period, groups receiving drug were also statistically compared with the vehicle treated rats using Repeated Measures ANOVA, followed by Planned LSD comparisons, however no significance was observed.

On the 3 test days during the dosing period, sham operated rats continued to produce PWTs which were not different to baseline readings, namely 17.3 ±2.7 g, 19.9 ±2.4 g and 17.1 ±2.0 g respectively, suggesting the surgical procedure itself had no effect on PWT. CCI-operated rats that were dosed with vehicle continued to demonstrate allodynia, throughout the dosing period with a PWT range of 5.0 ±1.1 g to 7.3 ±2.7 g. In contrast, CCI-operated rats dosed with gabapentin produced elevated PWT on days 1, 3 and 5 of the dosing period of 7.3 ±0.5 g, 7.5 ±0.7 g and 11.3 ±2.6 g respectively however these values were not significantly different to PWTs produced from vehicle treated rats. Rats dosed with pregabalin produced a similar

profile to gabapentin, producing elevated PWTs of 8.8 ±2.7 g, 11.1 ±2.8 g and 11.0 ±3.3 g on day 1, 3 and 5 respectively but were not significantly different from responses from vehicle treated rats. Although both gabapentin and pregabalin failed to reverse CCI-induced allodynia when orally dosed at 30 mg/kg b.i.d. for 5 days, a trend to significance was evident on the last day producing p values of p=0.06 and p=0.09 respectively.

2.3.1.3 Effect of gabapentin and pregabalin on CCI-induced allodynia when dosed for 8 days

To obtain a statistically significant effect with gabapentin and pregabalin it was decided to extend the dosing period from 5 days to 8 days. 27 rats underwent CCI surgery and 8 rats were sham operated. Von Frey hair testing was carried out on the day prior to surgery and on day 5, 14 and 19 post-surgery. On day 21, after the CCI-operated rats had been ranked and assigned a dose group, they were dosed with gabapentin (30 mg/kg, p.o., b.i.d., n=8), pregabalin (30 mg/kg, p.o., b.i.d., n=8) or their vehicle (1% (w/v) methylcellulose, p.o., b.i.d., n=8) for 8 days. The sham operated rats were also dosed with vehicle (1% methylcellulose, p.o., b.i.d., n=8) for 8 days. Testing was conducted 1 hour post-dose on day 1, 5 and 8 of the dosing period which corresponded to day 21, 25 and 28 post-surgery. A post-dose reading was also taken on day 33 post-surgery.

Prior to surgery (day 0) all rats produced a mean paw withdrawal threshold (PWT) of 22.5 ±1.0 g which decreased to 4.4 ±0.4 g 19 days post-surgery in 24 CCI-operated rats (Figure 12). The 8 rats receiving sham operation continued to produce higher PWTs as expected, for example 21.3 ±2.4 g on day 19. The difference between CCI and sham readings suggested that a suitable ‘window of allodynia’ was obtained to continue with drug testing. To reduce repetition, in this and all subsequent studies the significant changes from baseline readings to post-CCI-surgery will not be shown graphically or mentioned in the text.

On day 19 it was observed that 3 CCI-operated rats met the exclusion criteria of PWT > 10 g and so were not included in the study. The remaining CCI-operated rats were divided into 3 groups with similar PWTs and dosed with the test compounds.

During the dosing period, sham operated rats continued to produce PWTs which were not different to baseline readings (16.9-21 g). CCI-operated rats dosed with vehicle continued to produce low PWTs (4.8-5.5 g), with no significant difference from the pre-dose readings.

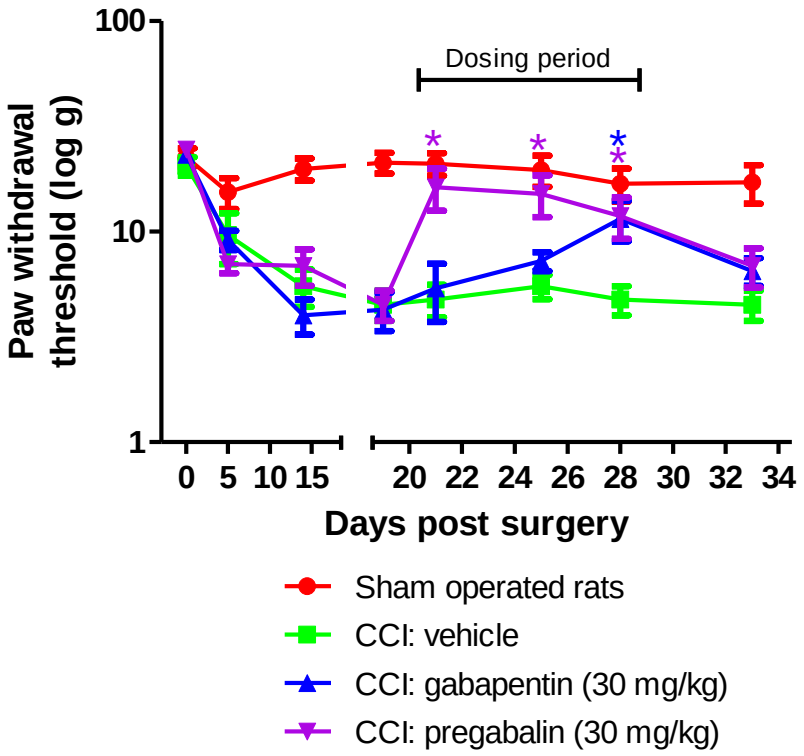

*Figure 12. Effect of gabapentin (30 mg/kg, p.o., b.i.d. for 8 days) and pregabalin (30 mg/kg, p.o., b.i.d. for 8 days) on paw withdrawal threshold of CCI-operated rats following von Frey filament application. Data are log mean ±SEM with 8 rats in each group. * denotes p<0.05 comparing drug treated rats with vehicle treated rats using Repeated Measures ANOVA followed by Planned LSD comparisons.*

When tested on days 1, 5 and 8 of the dosing period, CCI-operated rats dosed with gabapentin produced elevated PWTs of 5.4 ±1.7 g, 7.3 ±0.8 g and 11.5 ±2.5 g respectively. On this occasion, the PWT of drug treated rats on the final day of dosing were significantly different from the value obtained from the corresponding vehicle treated group. Also, in contrast from the previous study, pregabalin produced a significant effect on each test day of the dosing period (16.3 ±3.7 g, 15.1 ±3.4 g and 11.9 ±2.6 g for day 1, 5 and 8 respectively).

To ascertain the length of effect of the two standards, an additional post-dose reading was taken. Neither gabapentin nor pregabalin had a post-dose effect, with low PWTs being produced which were not significantly different to the vehicle dosed CCI-operated rats.

2.3.1.4 Effect of gabapentin and venlafaxine on CCI-induced alldoynia when dosed for 8 days

To ensure the positive response from gabapentin in the previous study was reproducible and to confirm efficacy with a different class of compound, gabapentin was re- tested alongside venlafaxine. Venlafaxine, a 5-HT-norepinephrine reuptake inhibitor, is an anti-depressant known to work clinically in alleviating neuropathic pain symptoms (Collins and Chessell, 2005).

24 rats underwent CCI surgery and 8 rats were sham operated. Von Frey hair testing was carried out one day prior to surgery and on day 13 and 19 post-surgery. On day 20, after CCI-operated rats had been ranked and assigned a dose group, they were dosed with gabapentin (30 mg/kg, p.o., b.i.d., n=8), venlafaxine (30 mg/kg, p.o., b.i.d., n=8) or their vehicle (1% (w/v) methylcellulose, p.o., b.i.d., n=8) for 8 days. The sham operated rats were also dosed with vehicle (1% (w/v) methylcellulose, p.o., b.i.d., n=8) for 8 days. Testing was conducted 1 hour post-morning dose on day 1, 4 and 8 of the dosing period which corresponded to day 20, 23 and 27 post-surgery. A post-dose reading was also taken on day 29 post-surgery.

Prior to surgery (day 0) all rats produced a mean paw withdrawal threshold (PWT) of 23.2 ±0.8 g which decreased to 5.2 ±0.5 g 19 days post-surgery in 24 CCI-operated rats (Figure 13). The 8 rats receiving sham operation continued to produce high PWT as expected, for example 21.3 ±2.4 g on day 19.

On day 19 it was observed that 4 CCI-operated rats met the exclusion criteria of PWT > 10g and so were not included in the study. The remaining CCI-operated rats were divided into 3 groups and dosed with test compounds.

During the dosing period, sham operated rats continued to produce PWTs which were not different to baseline readings (19.9-23.3 g). CCI-operated rats dosed with vehicle continued to produce low PWTs (4.3-5.5 g), with no significant difference from the pre-dose readings.

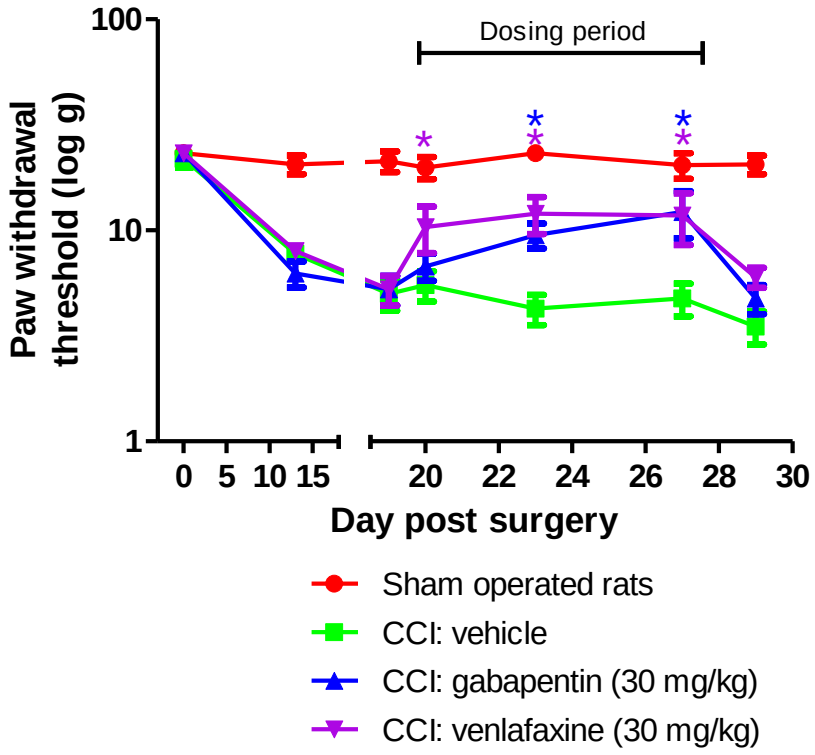

*Figure 13. Effect of gabapentin (30 mg/kg, p.o., b.i.d. for 8 days) and venlafaxine (30mg/kg, p.o., b.i.d. for 8 days) on paw withdrawal threshold of CCI-operated rats following von Frey filament application. Data are log mean ±SEM with 8 rats in each group. * denotes p<0.05 comparing drug treated rats with vehicle treated rats using Repeated Measures ANOVA followed by Planned LSD comparisons.*

In this study, gabapentin again reversed allodynia, as illustrated by significant increases in PWT as compared to the vehicle dose group, but this time the drug showed efficacy on day 4 of dosing as well as the final day of dosing producing PWTs of 7.3 ±0.8 g and 11.5 ±2.5 g respectively. Venlafaxine also significantly reversed CCI-induced allodynia on all test days when comparing to the response from vehicle dosed rats, producing PWTs of 10.4 ±2.6 g, 12.0 ±2.4 g and 11.8 ±3.2 g respectively on days 1, 4 and 8 of the dosing period. A reading was taken from all rats 2 days after the dosing period, however neither gabapentin nor venlafaxine

produced PWT which were significantly different to the vehicle dosed CCI-operated rats.

By producing a reproducible time-course of CCI-induced allodynia and demonstrating efficacy from testing 3 clinically used standards (gabapentin, pregabalin and venlafaxine) the CCI model was considered sufficiently characterised to allowing subsequent testing of novel compounds. It was also decided to use pregabalin as a positive control in subsequent orally dosed CCI studies.

2.3.2 P2X7 receptor antagonist studies

Having successfully characterised the CCI model, the effects of two novel P2X7 receptor antagonists on CCI-induced allodynia were compared when dosed systemically and centrally.

For all subsequent CCI studies it was decided that sham-operated rats would not be included. This decision was made by considering the robustness of the negative effect from sham operated rats in the studies described above and a large set of in-house data, versus the ethical considerations of using more rats. Sham data is also not included in any statistical analysis, as comparisons are made to responses from vehicle treated rats only.

2.3.2.1 Effect of P2X7 receptor antagonists, GSK1370319 and GSK2039841 on CCI-induced allodynia when dosed systemically

60 rats underwent CCI surgery and no rats were sham operated. Von Frey hair testing was carried out on the day prior to surgery and on day 14 and 24 post-surgery. On day 27, after rats had been ranked and assigned a dose group they were dosed with P2X7 receptor antagonist GSK1370319 (2, 20, 50 mg/kg, p.o., b.i.d., n=10/group), the structurally distinct P2X7 receptor antagonist GSK2039841 (20 mg/kg, p.o., b.i.d., n=10), pregabalin (30 mg/kg, p.o., b.i.d., n=10) or their vehicle (1% methylcellulose, p.o., b.i.d., n=10) for 8 days. Testing was conducted 1 hour post-morning dose on day 1, 4 and 8 of the dosing period which corresponded to day 27, 30 and 34 post-surgery. Following the final reading, rats were euthanised using CO_2 inhalation and blood and brain samples were taken to determine drug concentration.

Prior to surgery all rats produced a mean PWT of 23.3 ±0.7 g which reduced to 5.8 ±0.3 g 24 days post-CCI surgery hence demonstrating a robust allodynic response. On day 24 there were no CCI-operated rats that met the exclusion criteria of PWT > 10g and so all 60 rats were included in the study.

The doses of P2X7 receptor antagonist were chosen by considering the potency of the compounds at the rat P2X7 receptor, as well as other *in vivo* data produced in other pain models by GSK *in vivo* pain group (data not shown). Blood samples were taken at the end of the study to confirm drug concentration, as any pharmacokinetic differences between the two compounds could impact the concentration of compound at the target site. Brain samples were also taken to confirm the central penetration status of both compounds.

Throughout the dosing period, rats dosed with vehicle continued to show allodynia, producing PWTs with a range of 5.2-5.4 g, which were not significantly different to the pre-dose PWT (Figure 14). PWTs from rats dosed with GSK1370319 (2 mg/kg) also remained low and were not significantly different from the responses obtained from vehicle dosed rats, producing a PWT range of 6.9-7.3 g. This data suggests that at the lowest dose tested, GSK1370319 had no effect on CCI-induced allodynia. In comparison to this however, when PWTs were taken from rats that received higher doses of GSK1370319 the PWTs increased as the dosing period continued. At 20 mg/kg GSK1370319, PWT on days 4 and 8 of the dosing period increased to 8.2 ±1.2 g and 11.9 ±2 g respectively which were significantly different to the responses from the corresponding vehicle dosed rats. A significant effect on days 4 and 8 was also seen in rats dosed with GSK1370319 at 50 mg/kg producing PWTs of 11.1 ±2.1 g and 12.7 ±2.4 g respectively.

In complete contrast to the efficacy seen with GSK1370319 however GSK2039841 had no effect on PWT on any of the testing days when dosed at 20 mg/kg b.i.d. The PWTs produced on days 1, 4 and 8 were 6 ±2.2 g, 6.0 ±0.9 g and 5.8 ±0.6 g respectively and were not significantly different to the PWTs produced by the rats dosed with vehicle. Interestingly, this data appears to demonstrate completely opposing effects from two compounds known to be potent, selective P2X7 receptor antagonists.

Finally the positive control, pregabalin, produced a significant effect on days 4 and 8 of the dosing period which were similar to results previously generated hence validating the study.

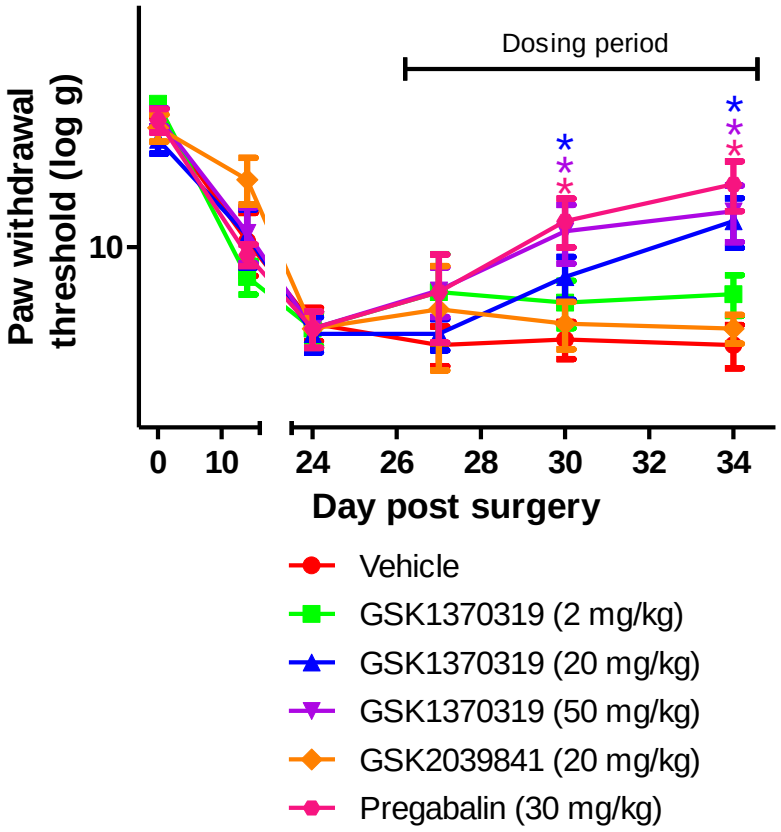

*Figure 14. Effect of P2X7 receptor antagonists GSK1370319 (2-50 mg/kg, p.o., b.i.d. for 8 days) and GSK2039841A (20 mg/kg, p.o., b.i.d. for 8 days) on paw withdrawal threshold of CCI-operated rats following von Frey filament application. Pregabalin (30mg/kg, p.o., b.i.d. for 8 days) was included in this study as a model standard. Data are log mean ±SEM with 10 rats in each group. *denotes $p<0.05$ comparing drug treated rats with vehicle treated rats using Repeated Measures ANOVA followed by Planned LSD comparisons.*

Blood and brain samples were taken from 3 rats dosed with the higher doses of GSK1370319 (50 mg/kg) and with GSK2039841 (20 mg/kg) and analysed by colleagues in the Neurosciences CEDD DMPK department. The mean blood concentrations of GSK1370319 and GSK2039841 were 23.0 ±7.8 µM and 3.4 ±0.7 µM respectively and the mean brain concentrations of GSK1370319 and GSK2039841 were 12.4 ±4.7 µM and 0.2 ±0.06 µM respectively.

2.3.2.2 Effect of P2X7 receptor antagonists, GSK1370319 and GSK2039841 on CCI-induced allodynia when dosed intrathecally.

To investigate the hypothesis that P2X7 receptor antagonists need to access the CNS to produce efficacy in the CCI model, a study was conducted in which GSK1370319, the centrally penetrant P2X7 receptor antagonist and GSK2039841, the peripherally restricted P2X7 receptor antagonist were dosed directly onto the spinal cord. The hypothesis was that the previously inactive GSK2039841 should produce efficacy when dosed centrally demonstrating that the lack of efficacy was due to the peripheral route of administration as opposed to a general inactivity. GSK1370319 should also produce efficacy indicating that the efficacy seen previously was due to a central site of action. A positive control was included in this study to ensure that the compounds were dosed accurately onto the spinal cord. Morphine was intrathecally dosed at 20 µg in a 10 µl volume, a dose known to have effects when dosed via this route (Westin et al., 2010).

50 rats underwent CCI surgery and no rats were sham operated. Von Frey hair testing was carried out on the day prior to surgery and on day 9, 20 and 26 post-surgery. On day 27, after rats had been ranked and assigned a dose group randomly they were dosed intrathecally under isoflurane anaesthesia, with P2X7 receptor antagonist GSK1370319 (100 µM, n=9), GSK2039841 (100 µM, n=9) or their vehicle (1% (w/v) DMSO, 49.5% (v/v) PEG200/ 49.5% (v/v) saline, n=8). The doses of P2X7 receptor antagonist were chosen to ensure the spinal cord was saturated by both compounds. In addition to dosing the P2X7 receptor antagonists, morphine (20 µg, n=9) or vehicle (saline, n=8) were also dosed to provide a model standard. Von Frey hair testing was conducted 30 minutes post-intrathecal dose. Following the final

reading, rats were euthanised using CO_2 inhalation and blood and brain samples were taken to determine drug concentration.

Prior to surgery all rats produced a mean PWT of 25.1 ±0.5 g which reduced to 5.5 ±0.3 g 26 days post-CCI surgery (Figure 15). On day 26 it was observed that 7 CCI-operated rats met the exclusion criteria of PWT > 10g and so were not included in the study. The vehicle treated rats continued to produce PWTs of approximately 5 g with no significant difference from the pre-dose readings.

When dosed intrathecally, GSK1370319 produced a significant effect compared to the vehicle response producing a PWT of 11.4 ±2 g. When the previously inactive compound, GSK2039841 was dosed intrathecally, it produced a significant effect compared to the vehicle producing a PWT of 8.4 ±0.6 g. The model standard morphine was also active as expected producing a PWT of 12.9 ±3.3 g thereby validating the study.

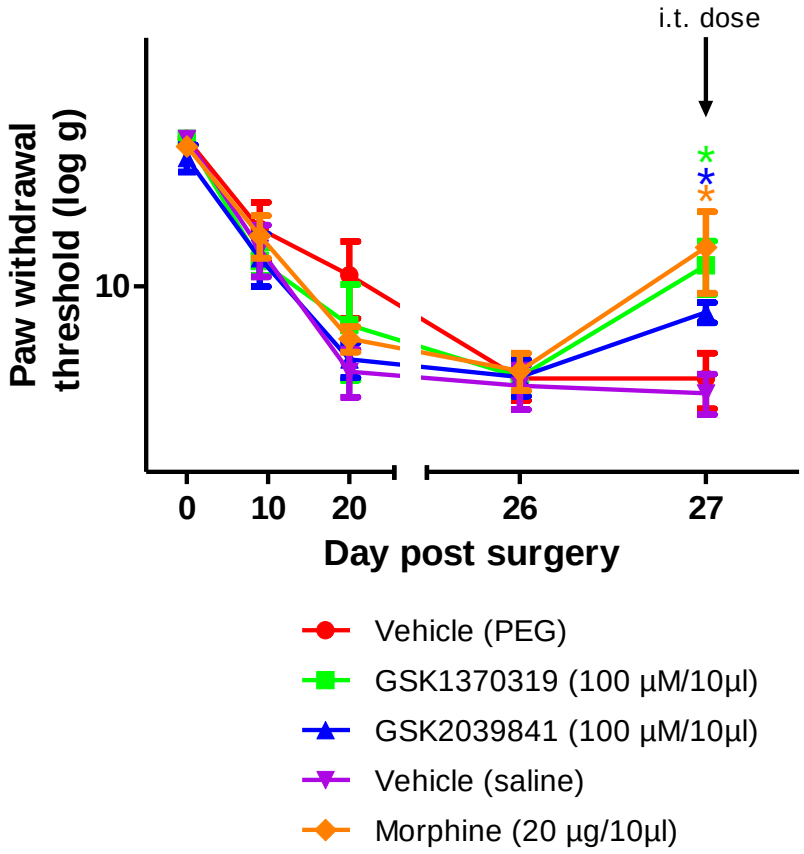

*Figure 15. Effect of P2X7 receptor antagonists GSK1370319 (100 µM in 10 µl i.t.) and GSK2039841A (100 µM in 10 µl i.t.) on paw withdrawal threshold of CCI-operated rats following von Frey filament application. Morphine (20 µg in 10 µl i.t.) was included in this study as a model standard. Data are log mean ±SEM with 9 rats in each drug dosed group and 8 rats in each vehicle dosed group. * denotes p<0.05 comparing drug treated rats with appropriate vehicle treated rats using Repeated Measures ANOVA followed by Planned LSD comparisons.*

To confirm that neither compound entered the blood stream, thereby confounding the interpretation, and that there was evidence of compound in the CNS, blood and brain samples were taken at the end of the study for analysis by the Neurosciences CEDD DMPK department. The mean blood concentrations of GSK1370319 and GSK2039841 were 0.004 ±0.001 µM and 0.002 ±0.001 µM respectively and the mean brain concentrations were 0.003 ±0.001µM and 0.0001 ±0.00001 µM respectively, the significance of which is discussed in the next section.

2.4 Discussion

There is currently no direct *in vivo* evidence that selective P2X7 receptor antagonists show efficacy in a neuropathic pain model due to a central site of action. This chapter therefore explores the potential role of centrally expressed P2X7 receptors in the etiology of neuropathic pain by comparing the efficacy of a peripherally restricted and a centrally penetrant P2X7 receptor antagonist in the CCI model of neuropathic pain. Before considering the assessment of novel compounds in an *in vivo* model however, the model requires characterisation.

To characterise the CCI model, it was initially intended to establish the time course of the allodynia that rats would experience after causing injury to the sciatic nerve, and to compare the results with similar reports in the literature. One of the biggest difficulties with this approach however was the variation in the methods used. Although authors describe using the CCI model there were many variables. The biggest variable, was how authors obtained the behavioural readout, for example different devices were used, such as an analgesymeter (Woodhams et al., 2007), an aethesiometer (Ando et al., 2010) or algometer (Dowdall et al., 2005) which all mechanically deliver a more substantial stimulus than a von Frey hair and so cannot be directly compared. Even in studies using von Frey hairs there is a variation in how the hairs are used, from testing % frequency to each hair (Chaplan et al., 1994) and therefore not reporting the paw withdrawal threshold data or measuring a paw withdrawal threshold (Field et al., 1999a). Having identified papers that do use similar methods however, it appears that the level of allodynia, of approximately 5 g, reached in the current study is comparable (Honore et al., 2006; Medhurst et al., 2008; Hsieh et al., 2010; Pradhan et al., 2010). Using this readout, Hsieh et al. (2010) also reported that drug testing commenced at 3 weeks after surgery suggesting this might be the maximum allodynic response they achieved thereby agreeing with the data presented here. It is also important to highlight that this data is very similar to data produced at GSK by different operators using the same method. The time course data has not only been shown to compare well with appropriate literature but has also

provided the valuable information regarding the most appropriate time for pharmacological testing.

When assessing the data generated with the clinically used drugs, it was also difficult to compare directly with the literature. This was not only due to the reasons mentioned above, but also due to the wide variety of dosing regimes used for testing the compounds. The variables included the doses used, the route of administration and the frequency of dosing. The principal aim of the present studies was to ensure that the compounds showed efficacy compared to vehicle response and to ascertain which standard was most appropriate to use as a positive control in subsequent studies.

Gabapentin, originally developed as an anticonvulsant, has been widely used off-label for a number of years in the treatment of neuropathic pain until the FDA approved its use for this condition. This decision came after significant pain relief was observed in two large scale clinical studies in painful diabetic neuropathy and post-herpetic neuralgia (Backonja et al., 1998; Rowbotham et al., 1998). To combat the effects of patent loss and inevitable erosion of market share due to generic gabapentin, Pfizer subsequently developed a follow-up compound. This compound, called pregabalin, was believed to be an improved product and has since been tested in many animal models of pain (Field et al., 1999a; Field et al., 1999b; Han et al., 2007).

In the first study gabapentin and pregabalin failed to show any efficacy, although there was a non-significant tendency of reversal on the 5th day of dosing. The lack of effect may be due to the variable vehicle response making it harder to achieve an effect with statistical significance. The data also suggested that a significant effect might be observed if the dosing period was extended. The dosing period was therefore increased in the next study and efficacy was observed after 8 days of dosing. Some publications report efficacy with gabapentin in the CCI model after one dose (Hsieh et al., 2010; Nakazato-Imasato and Kurebayashi, 2009), however in many of these incidences, the dose is often very high which not only puts selectivity into question, but may also introduce potential side effects, for example sedation (Collins and Chessell, 2005), which could complicate the behavioural response.

Studies undertaken in GSK (not published) have shown that the doses used for the current CCI studies are not overtly sedative.

Interestingly, when comparing the second study to the first study, pregabalin appeared to be more efficacious with a maximum efficacy seen on day 1. This apparent inconsistency might be explained by the operator gaining more experience and inadvertently improving the surgical technique and behavioural testing technique. This can be further illustrated by the reduction in SEM values in each of the groups. It is also worth re-iterating the inherent variability which is seen in *in vivo* studies with certain variables being unavoidable between studies, for example a different batch of rats and subtle differences in environment.

To ensure the efficacy seen with gabapentin was reproducible and to confirm efficacy with a different class of compound, venlafaxine, a 5-HT-norephinephrine reuptake inhibitor was tested. As with gabapentin and pregabalin there are many case reports available in the literature highlighting the efficacy of venlafaxine as a treatment for neuropathic pain (Pernia et al., 2000; Sumpton and Moulin, 2001). In the current study venlafaxine produced a significant effect on each test day of the dosing period. There are no directly similar reports of venlafaxine being tested in a similar method, however one group has reported efficacy in CCI model using a thermal readout (Lang et al., 1996) and another group reported anti-hyperalgesic properties in a chemotherapy-induced painful neuropathy (Marchand et al., 2003). In this final characterisation study gabapentin again significantly reversed CCI-induced allodynia thereby confirming the efficacy observed in the first drug study.

By demonstrating efficacy with 3 clinically used compounds, the CCI model was considered fully characterised with sufficient information accrued to continue with testing novel compounds.

To investigate the role of centrally expressed P2X7 receptors in the generation of neuropathic pain the effect of two P2X7 receptor antagonists GSK1370319 and GSK2039841 on CCI-induced allodynia was assessed. GSK1370319, a centrally penetrant compound produced a highly significant and dose-related reversal of CCI-induced allodynia. Paw withdrawal thresholds were significantly increased when compared to the vehicle response on days 5 and 8 when GSK1370319 was orally

dosed at 20 mg/kg and 50 mg/kg. Analysis of blood and brain samples taken after testing on the final day of dosing confirmed central penetrance of GSK1370319 producing a resultant brain: blood ratio of 0.5 ±0.02:1.

This result supports previous findings from several publications demonstrating efficacy in neuropathic pain models with small molecule P2X7 receptor antagonists (Honore et al., 2006; Nelson et al., 2006; Perez-Medrano et al., 2009). However, as previously mentioned there is conflicting literature which report a lack of effect with P2X7 (Broom et al., 2008; Ando et al., 2010). These discrepancies may be due to differences in selectivity and potency of the compounds being used. BBG, used by Ando et al. (2010) has been shown to selectivity inhibit P2X7 receptor with nanomolar affinity (Jiang et al., 2000a). Broom et al. (2008) used a compound, that had shown selectivity over P2X4 receptors, but in-house data showed a pIC50 of 6.8 at rat P2X4 receptors with this compound. Considering other variables, it appears there are several differences between the papers in terms of the how the neuropathic models were conducted. Broom et al. (2008) used the Chung model of spinal nerve ligation and Ando et al. (2010) uses the Seltzer model of partial sciatic nerve ligation, whereas the Nelson et al. (2006) and Honore et al. (2006) who have published positive data with P2X7 receptor antagonists quote data from the CCI model. The difference in neuropathic pain model might go some way in explaining the difference in results, but what is more fundamental is the difference in readout. Broom et al. (2008) and Ando et al. (2010) use electronic devices as opposed to the hand-held von Frey hairs which are considered much more sensitive and determine allodynia at much low pressures. It is possible therefore that the anti-allodynia properties of P2X7 receptor antagonists might only exist at the lower end of stimulation. Another explanation for the negative data might be the dosing regimes adopted. Indeed, in contrast to the chronic dosing used in the current studies, both Broom et al. (2008) and Ando et al. (2010) rely on a single dose. However, this is unlikely to be a valid explanation as other authors have produced efficacy with only a single dose of a P2X7 receptor antagonist (Honore et al., 2006; Nelson et al., 2006; Perez-Medrano et al., 2009)

An alternative explanation for the lack of efficacy of some antagonists, is the possibility that the dose of compound may not have achieved sufficient CNS penetration to gain efficacious levels at a central site of action. This was explored in the current study by testing a compound known to be peripherally restricted. In contrast to GSK1370319, GSK2039841 had no effect on CCI-induced allodynia even after 8 days dosing. The PK status of both compounds was also confirmed by analysing blood and brain samples taken after the final reading on day 8. The mean blood concentrations of GSK1370319 and GSK2039841 were 23.0 ±7.8 µM and 3.4 ±0.7 µM respectively.

When considering this large difference in blood concentration between the two compounds, one potential explanation for the differences in behavioural effect could simply be the disparity in the blood concentrations of compound. As mentioned earlier there is a difference with the potency of each compound at the P2X7 receptor which needs to be taken into account. To standardise the data to make comparisons more reliable, the number of multiples of the pIC50 present in the blood is calculated for each compound. When considering the data in this way, an additional parameter known as the 'free concentration' needs to be considered. The 'free drug concentration' of each compound is the % of the compound which does not get bound to protein and is therefore available to act on the target site. The free concentration data is produced from an *in vitro* DMPK assay (performed by the GSK DMPK department) and produces a % value which can be used to determine the free concentration in the blood samples for individual studies. To standardise the exposures of compounds in the blood the necessary calculation is dividing the free concentration of compound by the IC50. The results show a concentration 12 x IC50 of GSK2039841 and a 17 x IC50 of GSK1370319 present in the blood suggesting that there is a similar surplus of both compounds in the periphery regardless of the differences in peripheral exposure. This is a simple, crude way of examining the data but it aids interpretation if used cautiously. If the concentration of GSK2039841 was close to or below the IC50 it could be argued that a reduced concentration is the reason why it did not work.

To confirm the lack of CNS penetration, brain samples were also analysed at the end of the study. Concentrations of GSK1370319 and GSK2039841in the brain were 12.4±4.7 µM and 0.2±0.06 µM respectively. The resultant brain: blood ratios for GSK1370319 and GSK2039841 were 0.5 ±0.02:1 and 0.05 ±0.01:1 confirming that GSK2039841 was less brain penetrant than GSK1370319 and confirming previous data (table 4). Within GSK Neurosciences CEDD, a brain:blood ratio of less than 0.05:1 is considered the cut-off when deciding whether compounds are brain penetrant or non-brain penetrant. This cut-off takes several influencing factors into account including the accuracy of the mass spectrometer and possible blood contamination on brain samples. The ratio from samples from rats dosed with GSK2039841 falls into this category confirming the lack of CNS penetration.

With a ‘surplus’ of GSK2039841 and GSK1370319 in the periphery and a lack of only GSK2039841 in the brain, the differential activity between the compounds lends to the hypothesis that efficacy is being driven by CNS concentration.

To confirm this hypothesis, a study was conducted in which the peripherally restricted compound was administered directly onto the spinal cord. It has previously been shown that intra-spinal injection of the P2X7 receptor antagonist OxATP in the peri-traumatic zone in a weight drop model of traumatic spinal cord injury, reduced spinal cord damage (Wang et al., 2004). Even though this data suggested a beneficial effect with a P2X7 receptor antagonist administered via this route, this was not confirmed by assessing the anti-allodynic profile. In fact, this approach is novel as there are no records found in the literature of acquiring a nociception readout after central administration of a selective P2X7 receptor antagonist.

In contrast to the lack of efficacy when dosed systemically, GSK2039841 significantly reversed CCI-induced allodynia after a single local administration to the spinal cord confirming that efficacy is being driven by a central action. GSK1370319 also produced efficacy when dosed centrally confirming that a central action was, at least in part, responsible for the efficacy observed with this centrally penetrant compound when dosed systemically.

To confirm that neither compound entered the blood stream and that there was some trace of compound in the CNS, blood and brain samples were taken at the end

of the study and analysed by GSK DMPK department. This data confirmed that insufficient compound was present in the blood to have any effect peripherally, as determined by comparing to the compounds IC50s. Although there were minimal concentrations of compound in the brain, caution is required when comparing blood and brain concentrations as there are many complicating parameters which confound the data generated from brain samples. There are two important parameters to consider, firstly the continually circulating cerebrospinal fluid (CSF) flow rates which would potentially dilute the small locally dosed volume and secondly the distance the compound is required to travel between the injection site and the brain. One other consideration is that the compound may well be acting in the spinal cord, as opposed to the brain suggesting the brain concentration might not be relevant. It is possible to take CSF samples however the protocol had not been optimised in-house. Even with the known concentrations of compounds in the CSF, similar complications would need to be considered when interpreting the data. The main conclusion taken from pharmacokinetic data is that the efficacy produced from both compounds was not caused by compound being present in the periphery.

The current studies confirmed and extended previous results on the anti-allodynic effect of P2X7 receptor antagonists in neuropathic pain models. Moreover we report the importance of P2X7 compounds reaching a central site in order to be efficacious.

Having discussed the site of action, it is important to consider the potential mechanisms of action that P2X7 receptor antagonists might be adopting to elicit their effect. The data reported in this chapter alone does not directly implicate any specific mechanism; however it does lend support to the postulated role of P2X7 in the release of IL-1β and/or glutamate in activated glia within the CNS (Donnelly-Roberts and Jarvis, 2007). Since P2X7 receptors are found predominantly on glial cells (Ferrari et al., 1997b; Hide et al., 2000; Zhang et al., 2005b; Ferrari et al., 2006; Inoue, 2006) the current findings highlight the importance of glial-neuronal interactions and it is this interaction which forms the main focus of this thesis. What is clear from the studies detailed however, is that the P2X7 receptor should no longer be considered as only being involved in responses to inflammation.

Chapter 3

Investigating the interaction between P2X7 receptors and morphine-induced tolerance and morphine-induced efficacy in nerve-injured rats

3. Investigating the interaction between P2X7 receptors and morphine-induced tolerance and morphine-induced efficacy in nerve-injured rats

3.1 Introduction

Having demonstrated efficacy with the P2X7 receptor antagonist, GSK1370319 in the CCI model of neuropathic pain in the previous chapter, it was considered whether P2X7 receptors could play an important role in morphine tolerance, given previous proposals that neuropathic pain and opioid tolerance shared common mechanisms (Mayer et al., 1999; Mika, 2008; Watkins et al., 2009).

The working hypothesis was that a P2X7 receptor antagonist could interfere with morphine tolerance in neuropathic rats by suppressing microglia activation. Support for this hypothesis was suggested by data demonstrating an increase in immunostaining of GFAP, a marker for astrocytes, in the spinal cord following chronic morphine administration (Song and Zhao, 2001) and evidence that chronic morphine administration could activate microglia (Raghavendra et al., 2002; Cui et al., 2006). The hypothesis was explored in behavioural studies by chronically co-administering the P2X7 receptor antagonist GSK1370319 in conjunction with morphine to rats that had undergone neuropathic surgery. The majority of previous studies have focused on the association of microglia on either morphine tolerance in naïve rodents or on hyperalgesia in nerve-injured rats, with only a few publications combining both paradigms. This is therefore the first investigation into the effect of a P2X7 receptor antagonist on morphine tolerance in rats that have undergone neuropathic surgery.

In addition to the possible effects on morphine tolerance, it was also considered whether P2X7 antagonism could affect morphine analgesia in neuropathic rats. Early literature on morphine analgesia in neuropathic pain was contradictory. Several studies had demonstrated that neuropathy-induced hyperalgesia led to a decrease in anti-nociception to morphine (Mao et al., 1995a; Christensen and Kayser, 2000),

whereas other studies reported an increased in morphine efficacy (Backonja et al., 1995; Catheline et al., 1996). Later studies however strongly suggested that morphine had a decreased analgesic efficacy in neuropathic pain (Fundytus et al., 2001; Raghavendra et al., 2002) to the extent that resistance to morphine became a recognised characteristic of neuropathic pain (Porreca et al., 1998; McQuay, 2002). The mechanisms for this phenomenon are not fully understood (Przewlocki and Przewlocka, 2001; Przewlocki and Przewlocka, 2005), although the involvement of glia and cytokines has been suggested (Sweitzer et al., 2001; Raghavendra et al., 2002; Raghavendra et al., 2003b; Raghavendra et al., 2004a; Mika et al., 2007; Tawfik et al., 2007). It is therefore feasible that antagonising P2X7 receptors and preventing microglial activation could enhance morphine-induced analgesia in nerve-injured rats. This hypothesis was explored by assessing paw withdrawal threshold following von Frey hair stimulation of CCI-operated rats co-dosed with GSK1370319 and a submaximal dose of morphine. The potentiation of morphine efficacy has been demonstrated previously in naïve rats using microglia inhibitors but, as far as the author is aware, there are no reports showing this effect with a P2X7 receptor antagonist in nerve injured rats.

Before progressing with the drug combination studies, the most appropriate doses of morphine to use in tolerance and efficacy studies needed to be established. This was accomplished by administering a range of morphine doses to CCI-operated rats and selecting the most suitable dose depending on the level of efficacy observed.

In summary, this chapter uses behavioural pharmacological techniques to explore the hypothesis that P2X7 receptor antagonism blocks microglial activation, thereby removing a counter-regulatory system and thus reducing morphine tolerance and increasing morphine efficacy in nerve-injured rats.

3.2 Method

3.2.1 CCI method

All studies contained within this chapter used CCI-operated Random-hooded male rats. For details of the surgical procedure and the methodology for the behavioural testing with von Frey hairs please refer to sections 2.2.2.1 and 2.2.2.2 respectively.

3.2.2 Testing compounds

As previously described, GSK1370319 was dosed orally at 5 ml/kg in 1% (w/v) methylcellulose as detailed in section 2.2.2.3. Morphine was obtained as morphine sulphate salt pentahydrate from Sigma (M8777) and dosed subcutaneously at 3 ml/kg in 0.9% (w/v) saline. In combination studies GSK1370319 was generally dosed 30 minutes before morphine administration and behavioural testing was generally conducted 30 minutes post-morphine administration.

3.2.3 Data analysis

More extensive statistical analysis was required for combination studies compared to previous CCI studies. Although repeated ANOVA followed by Planned comparison was used as before, more comparisons were made between different groups.

One analysis compared responses from drug dosed groups to groups receiving both vehicles and a separate analysis was conducted comparing responses between groups co-dosed with morphine + vehicle and groups co-dosed with morphine + GSK1370319. To highlight the different comparisons clearly, in some instances the same data has been represented in more than one graph.

The final statistical analysis assessed the potential interaction between morphine and GSK1370319. Ordinarily when combination data is statistically analysed, graphs are created from large datasets consisting of dose response curves to a variety of different doses in different combinations to ascertain whether the relationship between the two compounds is additive or synergistic. Additive describes a relationship that is simply the sum of the effect they would have if dosed alone, whereas synergistic describes the relationship in which the effect of the co-

administration of two compounds is greater than the individual effects being added together. Due to the studies detailed in this chapter only comparing one or two combinations, a thorough statistical analysis is less feasible. It is possible however, even with this limited dataset, to carry out more basic statistics using the ANOVA test with Planned Comparisons. All data was first log transformed before it was compared. The paw withdrawal thresholds (PWTs) from GSK1370319 + vehicle and morphine + vehicle dosed groups were statistically compared with responses from both groups dosed with vehicle + vehicle and GSK1370319 + morphine. A caveat to this statistical analysis is the lack of consideration to artificial boundaries that are introduced by virtue of using von Frey hairs. The statistics do not take into account the relationship each response has with the maximum possible effect (i.e. the cut-off of 26 g) or the minimum effect (i.e. the vehicle response). This caveat therefore needs to be considered when interpreting this type of analysis.

3.2.4 Pharmacokinetic analysis

In some instances, blood samples were taken from rats at the end of the study. The details of how the samples were taken, prepared and analysed are similar to previous studies and described in section 2.2.4.

3.3 Results

3.3.1 The effect of morphine on CCI-induced allodynia

Von Frey hair testing was carried out on 60 rats one day before each rat underwent CCI surgery. Testing was then carried out 19 days post-surgery before rats were ranked and assigned a dose group. On day 20, rats were dosed with morphine (0.3, 1, 3, 10 mg/kg, s.c., b.i.d., n=10 per group) or vehicle (saline, s.c., b.i.d., n=10 per group) for 8 days. The doses of morphine were chosen as a range commonly used in the literature (Raghavendra et al., 2002; Tawfik et al., 2005; Hutchinson et al., 2009). Pregabalin (30 mg/kg, p.o., b.i.d., vehicle of 1% (w/v) methylcellulose, n=10) was also dosed for 8 days to act as a study control. Testing was conducted on days 1, 3, 6 and 8 of the dosing period, 30 minutes post-morning dose for morphine treated rats and 1 hour post-dose for pregabalin treated rats. The testing days corresponded to day 20, 22, 25 and 27 post-surgery.

Prior to surgery, all 60 rats produced a mean baseline PWT of 23.6 ±0.6 g reading which was reduced to 2.9 ±0.2 g 19 days post-CCI-surgery (Figure 16). In this study there were no CCI-operated rats that met the exclusion criteria of PWT > 10 g and so all 60 rats were included in the study.

Rats treated with vehicle continued to produce low PWTs ranging from 2.8-4.1 g with no significant difference from the pre-dose readings on day 19. When dosed at 0.3 mg/kg, morphine had no effect on PWT compared to vehicle response producing a PWT range of 6.5-8.4 g. When dosed at 1 mg/kg however, morphine produced a significant effect on day 3 producing a PWT of 9.4 ±2.3 g, but no significant effect on days 1, 5 or 8.

When dosed at 3mg/kg, morphine produced a significant effect on days 1 and 3 producing PWT of 13.5 ±2.8 g and 13.1 ±2.5 g respectively. Interestingly as the dosing period continued the PWTs reduced to 7.2 ±1.7 g and 3.6 ±1.2 g on days 5 and 8. The reduction of efficacy as morphine dosing continued suggested the onset of tolerance at this dose.

Tolerance was more apparent when morphine was dosed at 10 mg/kg. On days 1 and 3, rats dosed with 10 mg/kg morphine produced PWTs of 23.8 ±1.5 g and

15.9 ±2.4 g respectively and these values dramatically decreased to 4.2 ±1.6 g and the 1.4 ±0.5 g respectively on days 5 and 8.

Intriguingly, the final PWT from the rats dosed with the highest dose of morphine was shown to be significantly lower than the PWT obtained from the vehicle dosed group producing a PWT of 1.4 ±0.5 g. This suggested that morphine was having a deleterious effect on the rats and appeared to be making the rats more allodynic.

Finally, pregabalin, the study control, produced a significant effect on all testing days of the dosing period producing a PWT range of 10.0-11.9 g.

In summary, morphine (3 and 10 mg/kg, s.c., b.i.d.) significantly reversed CCI-induced allodynia on days 1 and 3 of the dosing period. This efficacy decreased as morphine dosing continued suggesting the onset of tolerance. On the final day of dosing, morphine appeared to significantly exacerbate CCI-induced allodynia. At lower doses, morphine produced minimal efficacy at 1mg/kg and no efficacy when dosed at 0.3 mg/kg.

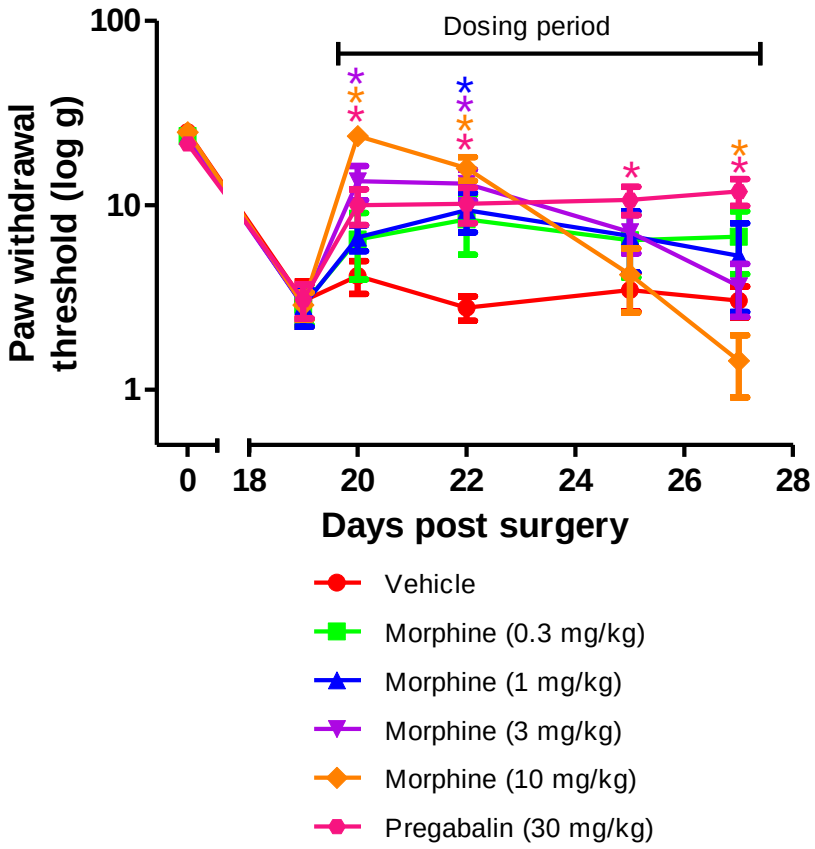

*Figure 16. Effect of μ opioid receptor agonist morphine (0.3-10 mg/kg, s.c., b.i.d. for 8 days) on paw withdrawal threshold of CCI-operated rats following von Frey filament application. Pregabalin (10 mg/kg, p.o., b.i.d. for 8 days) was included in this study as a model standard. Data are log mean ±SEM with 10 rats in each group. *denotes $p<0.05$ comparing drug treated rats with vehicle treated rats using Repeated Measures ANOVA followed by Planned LSD comparisons.*

3.3.2 The effect of GSK1370319 on morphine-induced tolerance and morphine-induced analgesia in CCI-operated rats

Von Frey hair testing was carried out on 60 rats one day before each rat underwent CCI surgery. Testing was then carried out 18 days post-surgery before rats were ranked and assigned a dose group. On day 21, rats were dosed with the following combination of compounds or vehicles twice a day for 8 days (n=10 per each group):

- Vehicle of GSK1370319 (1% (w/v) methylcellulose, p.o.), 30 minutes later, the vehicle of morphine (saline, s.c.)
- Vehicle of GSK1370319 (1% (w/v) methylcellulose, p.o.), 30 minutes later, morphine (0.3 mg/kg, s.c.)
- Vehicle of GSK1370319 (1% (w/v) methylcellulose, p.o.), 30 minutes later, morphine (10 mg/kg, s.c.)
- GSK1370319 (5 mg/kg, p.o.), 30 minutes later, the vehicle of morphine (saline, s.c.)
- GSK1370319 (5 mg/kg, p.o.), 30 minutes later morphine (0.3 mg/kg, s.c.)
- GSK1370319 (5 mg/kg, p.o.), 30 minutes later morphine (10 mg/kg, s.c.)

The doses of morphine were chosen from the previous study as a low non-efficacious dose and a high dose which produced tolerance. The dose of GSK1370319 was chosen as one that lay between a maximum effect (i.e. 20 mg/kg) and a non-effective dose (2 mg/kg) to allow any potential additive effect to be observed.

Testing was conducted 30 minutes post-morning dose of morphine or saline on day 1, 3, 5 and 8 of the dosing period which corresponded to day 21, 23, 25 and 28 post-surgery.

Prior to surgery (day 0) all 60 rats produced a mean PWT of 23.6 ±0.6 g which decreased to 4.7 ±0.3 g 18 days post-surgery confirming that the CCI surgery had induced allodynia.

In this study there were no CCI-operated rats that met the exclusion criteria of PWT > 10 g and so all 60 rats were included in the study.

Throughout the dosing period, rats dosed with both vehicles continued to show allodynia producing PWTs with a range of 3.2-4.6 g (Figure 17). In rats dosed with GSK1370319 + saline however, there was a significant increase in PWT producing a range of 6-8.4 g on all 4 test days. Although the range of PWTs appeared low, they were still significantly different to the threshold obtained from the rats treated with both vehicles.

When rats were dosed with 10 mg/kg morphine + vehicle of GSK1370319, CCI-induced allodynia was significantly reversed throughout the dosing period when compared to the vehicle dosed rats. When comparing this effect with the response from rats dosed with 10 mg/kg of morphine in the previous study (section 3.3.1) the profiles of the responses are different. Although the first two readings are similar, 20.4 ±2.4 g and 16.2 ±2.4 g compared to 23.8 ±1.5 g and 15.9 ±2.4 g, the decline of efficacy (i.e. tolerance) was considerably less in this study. As an illustration of this, the PWT on the final test day was 10.9 ±2.8 g in the current study versus 1.4 ±0.5 g in the previous study, with vehicle controls both being approximately 3 g in both cases. A possible explanation for this difference, other than inherent variability, was that the rats were affected by the additional oral dose in this current study.

Rats co-dosed with morphine (10 mg/kg) + GSK1370319 (5 mg/kg) produced a different profile to the group dosed with morphine + vehicle, showing a lack of the decreasing efficacy. The initial responses were similar to responses from the morphine + vehicle group, producing PWT of 19.2 ±2.6 g and 21.7 ±2.2 g for the first two time-points. However, instead of decreasing as morphine dosing continued, the level of threshold remained constant producing PWTs of 19.3 ±2.3 g and 20.3 ±2.4 g on days 5 and 8 of the dosing period. Interestingly, when the two groups of rats receiving 10 mg/kg morphine were statistically compared there was a significant difference on days 5 and 8 of the dosing period (Figure 18). It therefore appeared that GSK1370319 prevented the onset of tolerance.

When rats were dosed with 0.3 mg/kg morphine + vehicle, CCI-induced allodynia was significantly reversed on days 3, 5 and 8 of the dosing period producing PWT of 8.7 ±0.9 g, 7 ±0.3 g and 5.4 ±0.7 g respectively (Figure 17). The profile of this response was again different from the morphine dose response study in which this dose had no effect and maybe due to the additional drug administration.

Similarly to the morphine (0.3 mg/kg) + vehicle group, a significant increase in PWTs on days 3, 5 and 8 was also seen from rats co-dosed with morphine (0.3 mg/kg) + GSK1370319, producing PWTs of 8.7 ±1.5 g, 13.0 ±2.4 g and 11.9 ±2.5 g respectively (Figure 17). When the responses from rats dosed with morphine (0.3 mg/kg) in the presence and absence of GSK1370319 were compared, a

significant difference was observed on the final day of dosing (Figure 18). This result suggested that GSK1370319 may have potentiated the effect of morphine. Further statistical analysis of the final day potentiation showed that there was no significant interaction between the two compounds producing a p=0.5.

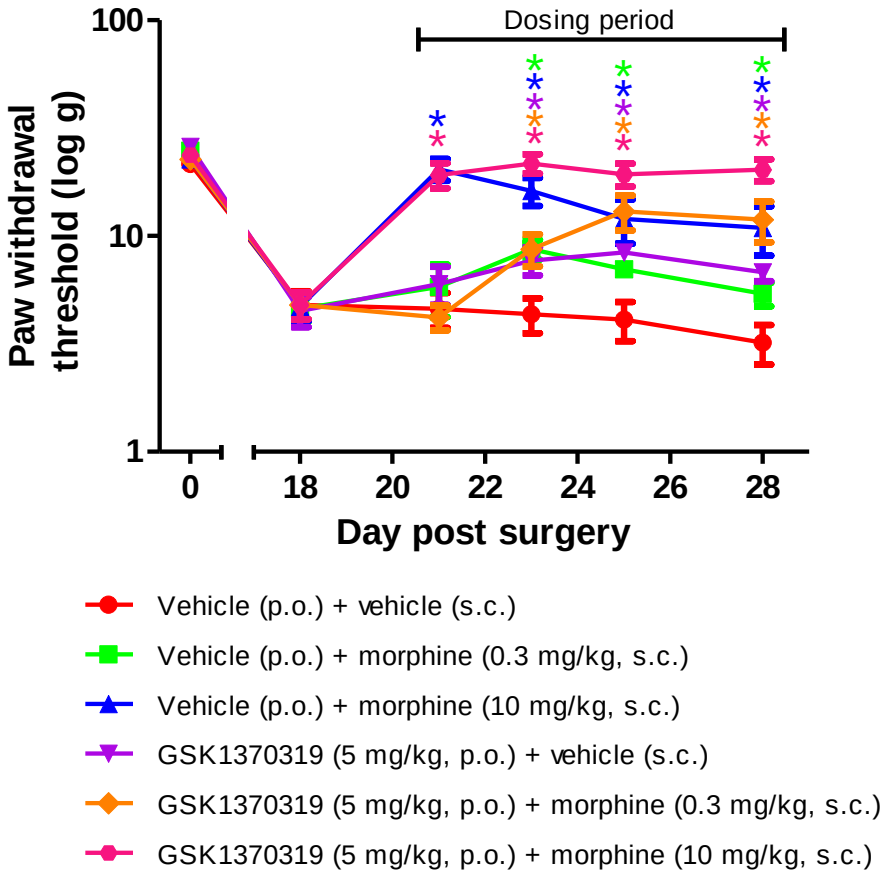

*Figure 17. Effect of co-dosing P2X7 receptor antagonist GSK1370319 (1 and 5 mg/kg, p.o., b.i.d. for 8 days) and μ opioid receptor agonist morphine (10 mg/kg, s.c., b.i.d. for 8 days) on paw withdrawal threshold of CCI-operated rats following von Frey filament application. Data are mean ±SEM with 10 rats in each group. *denotes p<0.05 using Repeated Measures ANOVA followed by Planned LSD comparisons comparing all groups to veh+veh dosed group.*

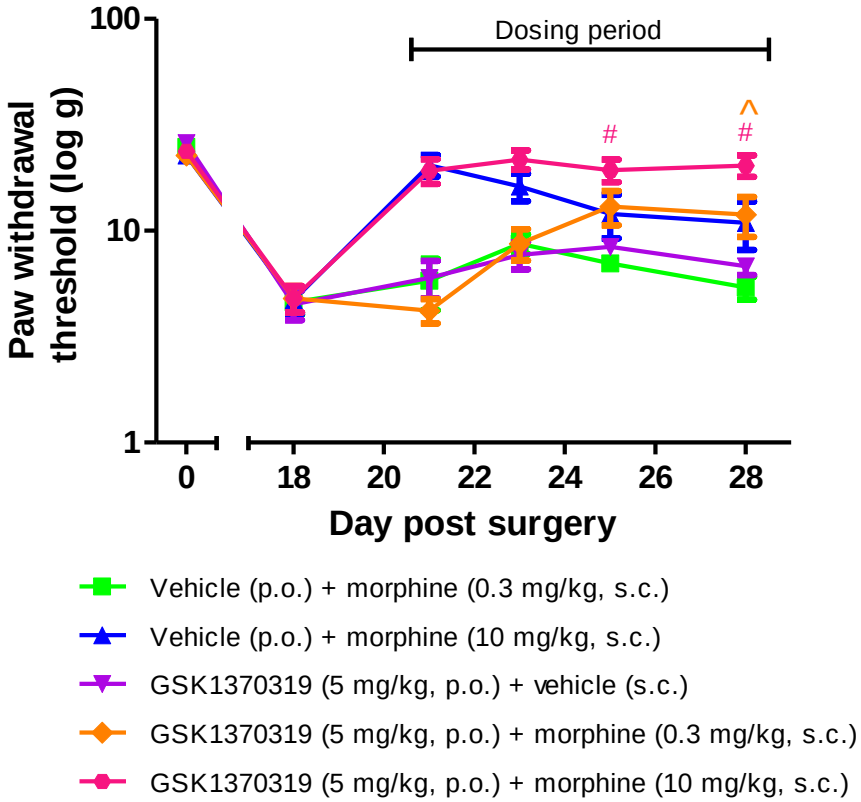

Figure 18. Effect of co-dosing P2X7 receptor antagonist GSK1370319 (1 and 5 mg/kg, p.o., b.i.d. for 8 days) and μ opioid receptor agonist morphine (10 mg/kg, s.c., b.i.d. for 8 days) on paw withdrawal threshold of CCI-operated rats following von Frey filament application. Data are mean ±SEM with 10 rats in each group. # denotes p<0.05 comparing 'GSK1370319 5 mg/kg + morphine 10 mg/kg' and 'vehicle p.o. + morphine 10 mg/kg' treated rats using Repeated Measures ANOVA followed by Planned LSD comparisons. ^ denotes p<0.05 comparing 'GSK1370319 5 mg/kg + morphine 0.3 mg/kg' and 'vehicle and morphine 0.3 mg/kg' treated rats using Repeated Measures ANOVA followed by Planned LSD comparisons.

In summary, this data suggests that when morphine is co-dosed with P2X7 receptor antagonist GSK1370319, the onset of tolerance was prevented, but the efficacy of a low dose of morphine appeared to be improved. These two findings are explored further in the next two studies.

3.3.3 The effect of repeat administration of different doses of GSK1370319 on morphine-induced tolerance in CCI-operated rats

The ability of GSK1370319 to prevent the onset of tolerance was further investigated by incorporating a longer dosing period. An extended dosing period was used to ensure a more significant tolerance to morphine occurred compared to the previous study and thereby potentially increasing the difference in responses between the groups dosed with morphine + GSK1370319 and morphine + vehicle. A lower dose of GSK1370319 was also included to increase the likelihood of demonstrating a significant interaction.

Von Frey hair testing was carried out on 60 rats one day before each rat underwent CCI surgery. Testing was then carried out 18 days post-surgery before rats were ranked and assigned a dose group. On day 21, rats were dosed with the following combination of compounds or vehicles twice a day for 12 days:

- Vehicle of GSK1370319 (1% (w/v) methylcellulose, p.o.), 30 minutes later the vehicle of morphine (saline, s.c.) n=9
- Vehicle of GSK1370319 (1% (w/v) methylcellulose, p.o.), 30 minutes later morphine 10 mg/kg, s.c.) n=10
- GSK1370319 (1 mg/kg, p.o.), 30 minutes later the vehicle of morphine (saline, s.c.) n=10
- GSK1370319 (5 mg/kg, p.o.), 30 minutes later the vehicle of morphine (saline, s.c.) n=10
- GSK1370319 (1 mg/kg, p.o.), 30 minutes later morphine (10 mg/kg, s.c.) n=10
- GSK1370319 (5 mg/kg, p.o.), 30 minutes later morphine (10 mg/kg, s.c.) n=10

Testing was conducted 30 minutes post-morning dose of morphine or saline on day 1, 3, 5, 8, 10 and 12 of the dosing period which corresponded to day 21, 23, 25, 28, 30 and 32 post-surgery.

Following the final reading, rats were euthanised using CO_2 inhalation and blood samples were taken to determine drug concentration. Lumbar spinal cord

samples were also dissected out and snap frozen in liquid nitrogen for subsequent RT-PCR studies detailed in Chapter 6.

Prior to surgery (day 0), all 60 rats produced a mean PWT of 23.6 ±0.6 g which decreased to 5.1 ±0.3 g 18 days post-surgery. Throughout the dosing period, rats dosed with both vehicles continued to show allodynia producing PWTs with a range of 3.1-4.2 g (see Figure 19).

When rats were co-dosed with 1 and 5 mg/kg GSK1370319 + saline, the PWTs produced on day 1, 3 and 5 were significantly different to the PWTs from rats receiving both vehicles, suggesting that these low doses of GSK1370319 had significantly reversed allodynia. Caution is required when interpreting these positive responses however, as the PWT are still considered low, with a range of 5.5-8.7 g, and significance may only be as a result from unusually low responses from the vehicle dosed rat on those days.

The responses from rats dosed with 10 mg/kg morphine + vehicle showed a familiar profile of tolerance starting with a PWT of 21.7 ±2.2 g on day 1 of dosing and continually decreasing to 1.82 ±0.57 g on day 12 of dosing (Figure 19). In this study morphine was only significantly different from vehicle treated rats on days 1, 3 and 5 of the dosing period.

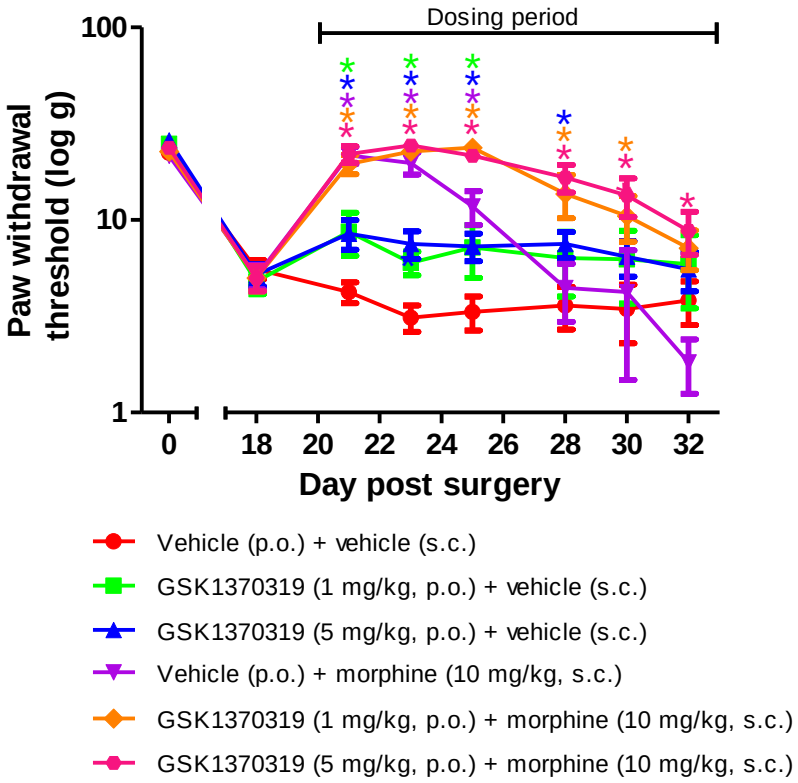

*Figure 19. Effect of co-dosing P2X7 receptor antagonist GSK1370319 (1 and 5 mg/kg, p.o., b.i.d. for 12 days) and μ opioid receptor agonist morphine (10 mg/kg, s.c., b.i.d. for 12 days) on paw withdrawal threshold of CCI-operated rats following von Frey filament application. Data are mean ±SEM with 10 rats in each group (n=9 for vehicle treated group). *p<0.05 using Repeated Measures ANOVA followed by Planned LSD comparisons comparing all drug dosed groups to 'vehicle p.o. + vehicle s.c.' dosed group.*

When rats were co-dosed with 1 or 5 mg/kg GSK1370319 (1 or 5 mg/kg) + morphine (10 mg/kg), tolerance was still evident but the profile of the response was different. It appeared that the peak effect prior to the decline in efficacy remained as a plateau for approximately 5 days before the efficacy started to decline. This resulted in the tolerance that followed being delayed and thus shifting the profile to the right when compared to the profile of tolerance of rats dosed with morphine + vehicle (Figure 19). Substantial differences in responses were therefore observed between rats dosed with morphine + vehicle and both groups of rats dosed with morphine + GSK1370319. For example on day 8, compared to the PWT of rat dosed with

morphine + vehicle (4.4 ±1.5 g), rats dosed with morphine + 1 and 5 mg/kg GSK1370319 produced PWTs of 13.7 ±3.5g and 16.6 ±2.7 g respectively. When statistically compared the results from GSK1370319 dosed rats were significantly different on days 5, 8, 10 and 12 compared to the group dosed with vehicle (Figure 20).

Whereas the previous study suggested that tolerance was completely abolished, the extension of the dosing period has demonstrated that tolerance is actually delayed. Furthermore, the response profiles of the two groups of rats receiving GSK1370319 and morphine were very similar even though the rats received doses of GSK1370319 that differed by five-fold. This suggests that the effect may have reached an optimum level, making it unlikely that higher doses of GSK1370319 would have more of an effect.

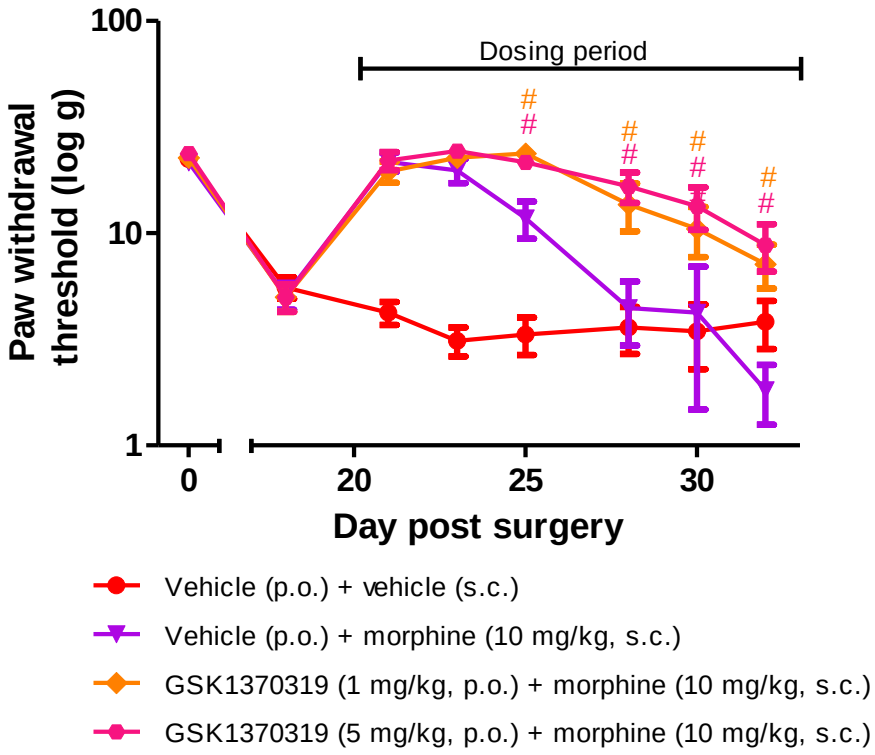

Figure 20. Effect of co-dosing P2X7 receptor antagonist GSK1370319 (1 and 5 mg/kg, p.o., b.i.d. for 12 days) and μ opioid receptor agonist morphine (10 mg/kg, s.c., b.i.d. for 12 days) on paw withdrawal threshold of CCI-operated rats following von Frey filament application. Data are mean ±SEM with 10 rats in each group (n=9 for vehicle treated group). #p<0.05 comparing 'GSK1370319 1 mg/kg + morphine' and 'GSK1370319 5 mg/kg + morphine' to 'vehicle p.o. + morphine 10 mg/kg s.c.' treated rats using Repeated Measures ANOVA followed by Planned LSD comparisons.

Although this data is primarily concerned with the effect of GSK1370319 on morphine tolerance, the data can also be interpreted in an alternative way. On days 8, 10 and 12 of dosing, due to the effect of tolerance, morphine had no significant effect when compared to the response from vehicle treated rats. When co-dosed with GSK1370319 however, a significant effect was observed suggesting that the morphine efficacy has been enhanced. When considering the data in this way it is clear that there is a relationship between GSK1370319 and morphine, however it is unclear whether this relationship is additive or synergistic. Further statistical assessment indicated that the interaction between morphine and 1 mg/kg GSK1370319 was not significant producing p values of 0.23, 0.13 and 0.08 on days

8, 10 and 12 respectively. The interaction between morphine and 5mg/kg GSK1370319 was also not significant producing p values of 0.11, 0.14 and 0.06 on days 8, 10 and 12 respectively. Although there was no statistical evidence of synergy between the compounds, there appears to be a trend towards significance on the final day of dosing with P values approaching the 5% value suggesting further exploration would be worthwhile.

One potential explanation for the effect that P2X7 receptor antagonist has on morphine-induced tolerance could be a modification in the pharmacokinetic clearance or distribution of morphine rather than a pharmacodynamic change in efficacy. To investigate this, blood samples were taken from 3 rats dosed with GSK1370319 (5mg/kg) + vehicle, vehicle + morphine and GSK1370319 (5mg/kg) + morphine (10mg/kg) on days 1, 5 and 12 of the dosing period and drug concentration of both compounds was determined. Table 5 summarises the results.

Treatment	Day of dosing	[morphine] (µM)	[GSK1370319] (µM)
GSK1370319 + vehicle	1	n/a	7.7 ±1.0
	5	n/a	6.5 ±2.9
	12	n/a	6.8 ±0.9
Vehicle + morphine	1	3.2 ±0.3	n/a
	5	5.2 ±0.6	n/a
	12	3.7 ±1.1	n/a
GSK1370319 + morphine	1	2.7 ±0.3	6.8 ±1.0
	5	3.8 ±0.09	11.1 ±4.6
	12	4.1 ±0.6	8.5 ±1.1

Table 5. Blood concentrations of morphine and GSK1370319 (µM) from rats dosed with GSK1370319 (5 mg/kg, p.o.), morphine (10 mg/kg, s.c.) and a combination of both for 12 days b.i.d. Samples were taken after the behavioural reading on days 1, 5 and 12 of the dosing period. Data represented as mean ±SD with n=9 per group.

It can be seen from table 5 that there was no significant change in morphine concentration with the co-administration of GSK1370319 or vice versa. Thus altered morphine pharmacokinetics cannot account for the delay in tolerance observed as a consequence of P2X7 receptor antagonist co-administration.

3.3.4 The effect of single administration of GSK1370319 on the development of morphine tolerance in CCI-operated rats

To investigate whether the effect of GSK1370319 on tolerance was dependent on the compound being repeatedly dosed, the P2X7 receptor antagonist was administered as a single dose on different days during the 8 day period of morphine dosing. The aim of this study was to see whether a single dose of GSK1370319 could affect different stages of the development of morphine tolerance.

Von Frey hair testing was carried out on 50 rats one day before each rat underwent CCI surgery. Testing was then carried out 23 days post-surgery before rats were ranked and assigned a dose group. On day 24, rats were dosed with the following combination of compounds or vehicles on the specific days during the dosing period (n=10 per group):

- Vehicle of morphine (saline, s.c., b.i.d. for 8 days), 30 minutes after the vehicle of GSK1370319 (1% (w/v) methylcellulose, p.o., once a day) on days 1, 5 and 8 of the dosing period.
- Morphine (10 mg/kg, s.c., b.i.d. for 8 days), 30 minutes after the vehicle of GSK1370319 (1% (w/v) methylcellulose, p.o., once a day) on days 1, 5 and 8 of the dosing period
- Morphine (10 mg/kg, s.c., b.i.d. for 8 days), 30 minutes after GSK1370319 (5 mg/kg, p.o., once a day) on day 1, and vehicle of GSK1370319 (1% (w/v) methycellulose, p.o., once a day) on days 5 and 8 of the dosing period
- Morphine (10 mg/kg, s.c., b.i.d. for 8 days), 30 minutes after GSK1370319 (5 mg/kg, p.o., once a day.) on day 3, and vehicle of GSK1370319

(1% (w/v) methycellulose, p.o., once a day) on days 1 and 8 of the dosing period

- Morphine (10 mg/kg, s.c., b.i.d. for 8 days), 30 minutes after GSK1370319 (5 mg/kg, p.o., once a day) on day 8, and vehicle of GSK1370319 (1% (w/v) methycellulose, p.o., once a day) on days 1 and 5 of the dosing period

In summary, 4 groups were dosed for 8 days with morphine (10 mg/kg, b.i.d., s.c.) and one other group dosed with vehicle (saline). These groups were then pre-dosed with GSK1370319 (5 mg/kg) on the morning of either day 1, 5 or 8 of the 8 day dosing period and with vehicle (1% (w/v) methylcellulose) on all other dosing occasions. Testing was carried out on days 1, 5 and 8 of the dosing period. Testing was conducted 30 minutes post- morning dose of morphine or saline on day 1, 5 and 8 of the dosing period which corresponded to day 24, 28 and 31 post-surgery.

Prior to surgery (day 0) all 50 rats produced a mean PWT of 23.3 ±0.7 g which decreased to 4.4 ±0.3 g 23 days post-surgery. In this study there were no CCI-operated rats that met the exclusion criteria of PWT > 10g and so all 50 rats were included in the study.

Throughout the dosing period, rats dosed with both vehicles continued to show allodynia producing PWTs with a range of 3.9-4.4 g (see Figure 21). When rats were dosed with morphine (10 mg/kg) + vehicle, PWT significantly increased on day 1 of dosing (22.7 ±2.3 g) and decreased during the dosing period producing a PWT of 12.7 ±2.4 g on day 5 and 7.2 ±0.9 g on day 8, indicative of tolerance.

When morphine-dosed rats were pre-dosed with GSK1370319 on days 1 and 5 the profile of tolerance was no different to that produced by rats dosed with morphine + vehicle. For example, on day 1 and 5 the PWT from rats dosed with morphine + GSK1370319 was 26.0 ±0 g and 12.6 ±2.5 g respectively, compared to PWT from rats co-dosed with morphine + vehicle of 22.7 ±2.3 g and 12.7 ±2.4 g respectively. This data suggests that the P2X7 receptor antagonist had no effect on the development of tolerance when GSK1370319 was dosed acutely at this dose. Furthermore, the lack of any difference between these groups at subsequent time-

points suggests that the P2X7 receptor antagonist also had no lasting effect on the development of tolerance.

In contrast however, morphine-dosed rats receiving GSK1370319 on day 8 produced a different profile. The PWTs of these rats remained stable at 16.2 ±2.7 g, as opposed to declining like other morphine-dosed groups. Not only was this response significantly different to rats receiving morphine + vehicle, the PWT continued to be significantly different to vehicle treated rats. This data suggests that a single dose of P2X7 receptor antagonist has influenced the maintenance of morphine-induced tolerance as opposed to the development of morphine-induced tolerance. Statistics investigating the interaction between both compounds was not feasible in this study as a critical control group for the analysis was not included in the design of the study, i.e. groups of rats dosed with vehicle + GSK1370319.

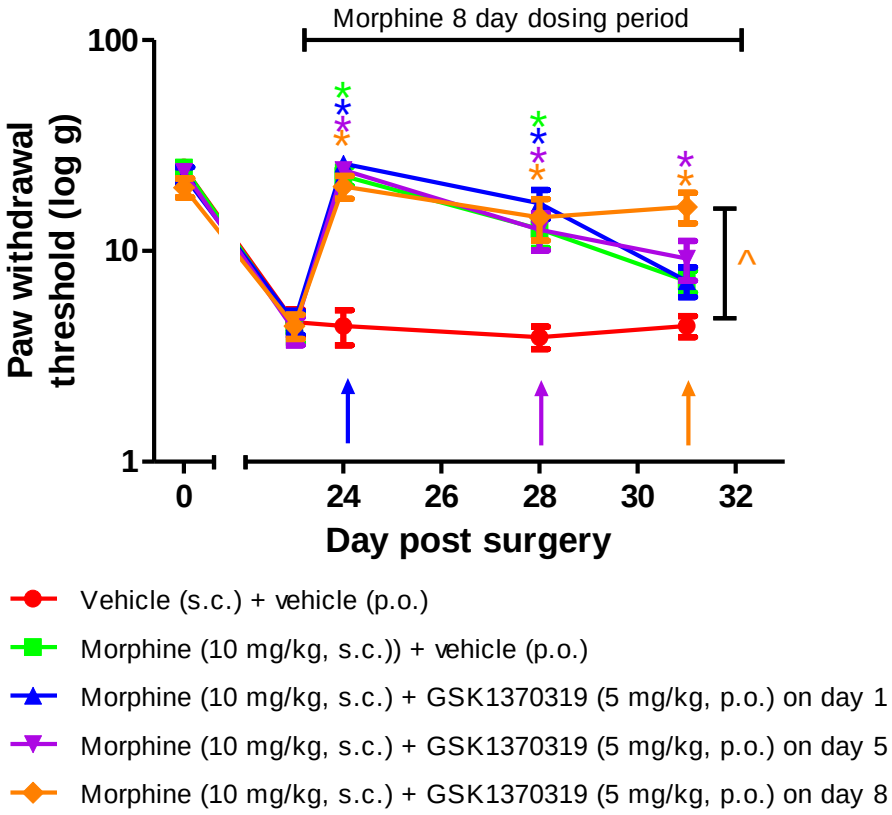

*Figure 21. Effect of a single dose of P2X7 receptor antagonist GSK1370319 (5 mg/kg, p.o.) on paw withdrawal threshold of CCI-operated rats pre-dosed with μ opioid receptor agonist morphine (10 mg/kg, s.c., b.i.d. for 8 days). Data are mean ±SEM with 10 rats in each group. *p<0.05 comparing to 'vehicle s.c. + vehicle p.o.' treated rats using Repeated Measures ANOVA followed by Planned LSD comparisons. ^p<0.05 comparing 'morphine (10 mg/kg) + GSK1370319 (5 mg/kg)' and 'morphine (10 mg/kg) + vehicle' using Repeated Measures ANOVA followed by Planned LSD comparisons.*

3.3.5 The effect of GSK1370319 on morphine-induced efficacy in CCI-operated rats

To explore the potentiation of morphine analgesia further, CCI-operated rats were co-dosed with GSK1370319 and two submaximal doses of morphine. To explore potential synergy between the two compounds an additional submaximal dose of GSK1370319 was also included.

Von Frey hair testing was carried out on 60 rats one day before each rat underwent CCI surgery. Testing was then carried out 18 days post-surgery before rats were ranked and assigned a dose group. On day 21, rats were dosed with the

following combination of compounds or vehicles twice a day for 8 days (n=8 per group):

- Vehicle of GSK1370319 (1% (w/v) methylcellulose, p.o.), 30 minutes later the vehicle of morphine (saline, s.c.)
- Vehicle of GSK1370319 (1% (w/v) methylcellulose, p.o.), 30 minutes later morphine (0.3 mg/kg, s.c.)
- Vehicle of GSK1370319 (1% (w/v) methylcellulose, p.o.), 30 minutes later morphine (1 mg/kg, s.c.)
- GSK1370319 (1 mg/kg, p.o.), 30 minutes later the vehicle of morphine (saline, s.c.)
- GSK1370319 (5 mg/kg, p.o.), 30 minutes later the vehicle of morphine (saline, s.c.)
- GSK1370319 (1 mg/kg, p.o.), 30 minutes later morphine (0.3 mg/kg, s.c.)
- GSK1370319 (5 mg/kg, p.o.), 30 minutes later morphine (1 mg/kg, s.c.)

Testing was conducted 30 minutes post-morning dose of morphine or saline on day 1, 3, 5 and 8 of the dosing period which corresponded to day 21, 23, 25 and 28 post-surgery.

Prior to surgery (day 0) all 60 rats produced a mean PWT of 23.8 ±0.6 g which decreased to 4.6 ±0.5 g 18 days post-surgery. On day 18 it was observed that 3 CCI-operated rats met the exclusion criteria of PWT > 10g and were not included in the study.

Throughout the dosing period, rats dosed with both vehicles continued to show allodynia, producing PWTs with a range of 1.9-2.6 g (see Figure 22). Paw withdrawal thresholds were also unaffected by administration of GSK1370319 (1 and 5 mg/kg) + vehicle (s.c.) throughout the dosing period, producing a range of PWTs of 2.4-5.6 g. This suggested that when co-dosed with vehicle, GSK1370319 at these doses had no effect on CCI-induced-allodynia.

When morphine was dosed alone at 0.3 mg/kg, a dose previously shown to be sub-maximal, significant efficacy was observed on days 3 and 8 post-dose, producing PWTs of 5 ±0.9 g and 4 ±0.6 g respectively. Although these doses appear to have

produced significant effects, it is worth noting that in this instance vehicle responses were unusually low, thereby increasing the likelihood that low responses from drug dosed groups are statistically significant.

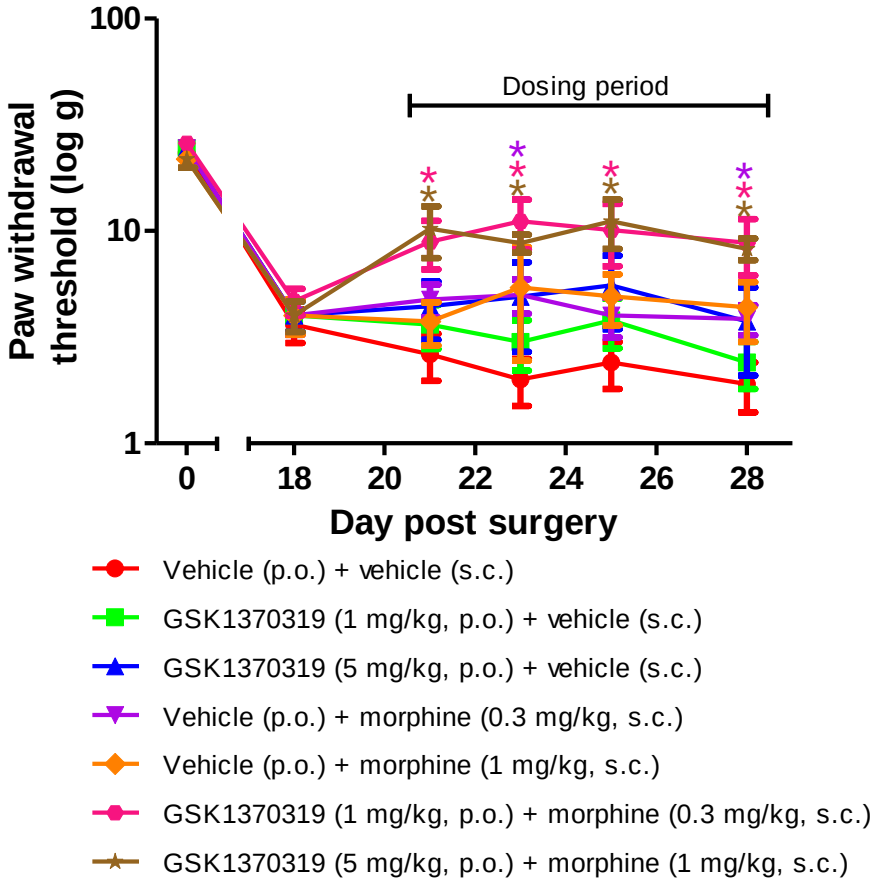

*Figure 22. Effect of co-dosing P2X7 receptor antagonist GSK1370319 (1 and 5 mg/kg, p.o., b.i.d. for 8 days) and μ opioid receptor agonist morphine (0.3 and 1 mg/kg, s.c., b.i.d. for 8 days) on paw withdrawal threshold of CCI-operated rats following von Frey filament application. Data are mean ±SEM with 8 rats in each group. *p<0.05 comparing to 'vehicle p.o. + vehicle s.c.' treated rats using Repeated Measures ANOVA followed by Planned LSD comparisons.*

When rats were dosed with morphine (0.3 mg/kg) + GSK1370319 (1 mg/kg) a significant reversal of allodynia was observed on every test day (day 1, 3, 5 and 8) of the dosing period when compared to the responses from the group dosed with both vehicles, producing PWTs of 8.9 ±2.3 g, 11.1 ±2.9 g, 10.1 ±3.3 g and 8.8 ±2.6 g

respectively. These higher thresholds were also in contrast to the minimal efficacy achieved by morphine when co-dosed with vehicle. When responses from group of rats dosed with the morphine (0.3 mg/kg) + GSK1370319 (1 mg/kg) were statistically compared to the groups dosed with both vehicles, there was no significant difference (Figure 23). Although a significant effect had only been achieved when both compounds were combined compared to when they were each co-dosed with a vehicle, the statistics suggest there is no significant effect of these doses when combined.

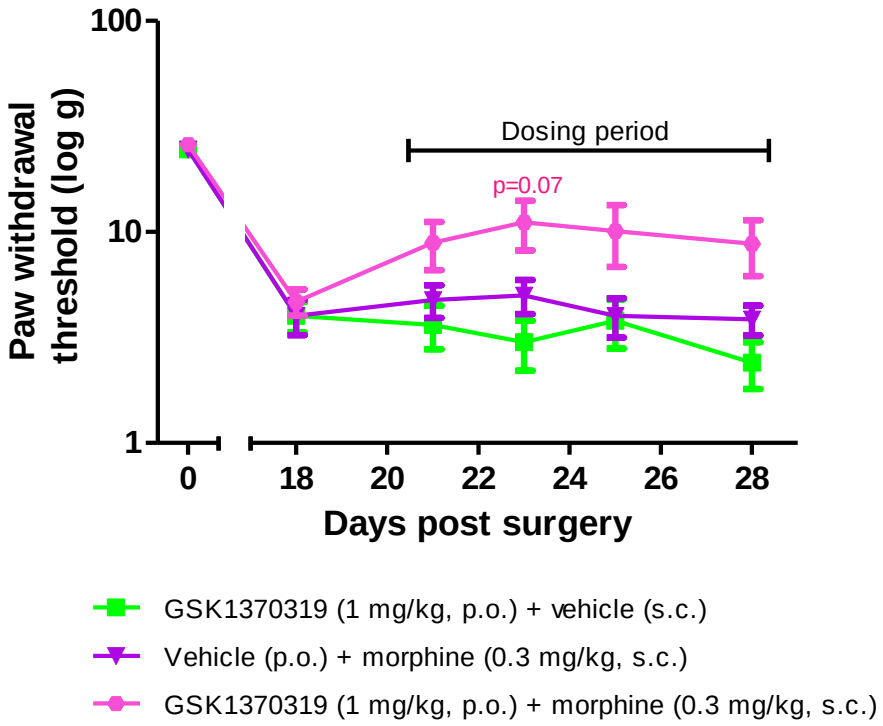

Figure 23. Effect of co-dosing P2X7 receptor antagonist GSK1370319 (1 mg/kg, p.o., b.i.d. for 8 days) and μ opioid receptor agonist morphine (0.3 mg/kg, s.c., b.i.d. for 8 days) on paw withdrawal threshold of CCI-operated rats following von Frey filament application. Data are mean ±SEM with 8 rats in each group. #p<0.05 comparing to 'vehicle + morphine 0.3 mg/kg' treated rats using Repeated Measures ANOVA followed by Planned LSD comparisons.

When rats were co-dosed with the higher doses of morphine + GSK1370319, a significant effect was also seen throughout the dosing period, producing PWTs of 10.3 ±2.8 g, 8.8 ±0.8 g, 11.1 ±2.9 g and 8.3 ±1 g on days 1, 3, 5 and 8 respectively

(Figure 24). This was in contrast to the lack of efficacy achieved by morphine (1 mg/kg) + vehicle and GSK1370319 + vehicle. When responses from rats co-dosed with morphine + vehicle were statistically compared with responses from rats dosed with morphine + GSK1370319 a significant difference was observed on days 1, 3 and 8 of the dosing period (Figure 24).

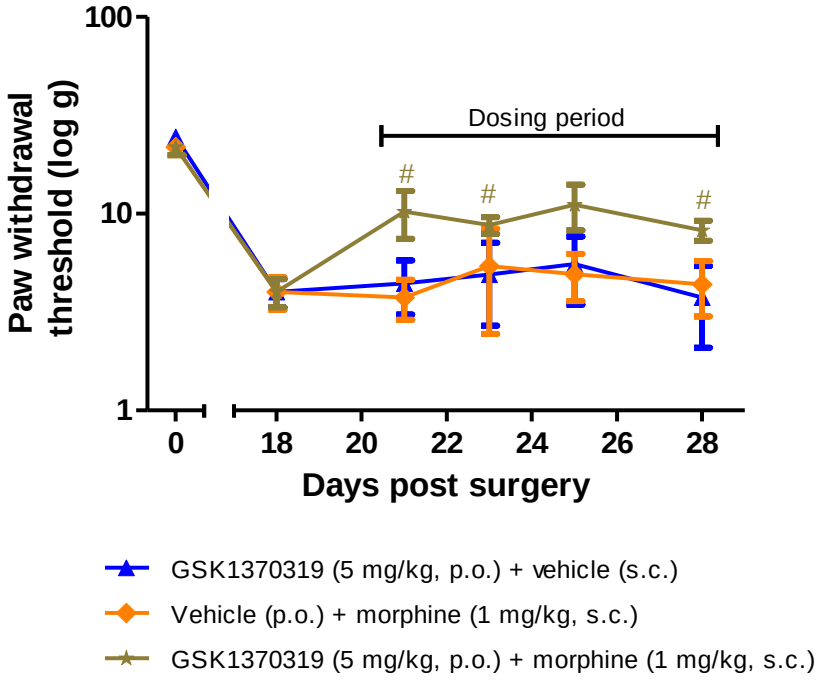

Figure 24. Effect of co-dosing P2X7 receptor antagonist GSK1370319 (5 mg/kg, p.o., b.i.d. for 8 days) and μ opioid receptor agonist morphine (1 mg/kg, s.c., b.i.d. for 8 days) on paw withdrawal threshold of CCI-operated rats to von Frey filament application. Data are mean ±SEM with 8 rats in each group. #p<0.05 comparing to 'vehicle + morphine 1 mg/kg' treated rats using Repeated Measures ANOVA followed by Planned LSD comparisons.

When statistically considering the interaction between the two compounds however, analysis showed that there was not a significant interaction between the compounds, producing p values of 0.3 on days 1, 3 and 8. Although an interaction was not borne out in the statistics, the considerable differences observed in thresholds from rats dosed with either compound alone versus the thresholds from rats dosed with the compounds in combination adds confidence that there is value in exploring this relationship further.

3.4 Discussion

Although the similarities between morphine tolerance and neuropathic pain are widely acknowledged, most reports in the literature determine mechanisms using either tolerance or neuropathic pain models. In the current studies however, the role of P2X7 receptor mediated microglia activation is explored in a combined rodent model of neuropathic pain and morphine tolerance thus examining both allodynia and tolerance simultaneously. It is believed that the studies presented in this chapter are the first to investigate the effects of P2X7 receptor antagonist on morphine tolerance in nerve-injured rats.

Before progressing to combination studies the most suitable dose of morphine was identified by conducting a morphine dose response study. After an initial highly significant efficacy when morphine was dosed at 3 and 10 mg/kg, efficacy decreased as the number of morphine doses increased. This response was indicative of tolerance at these doses. From this data it was decided that the most suitable systemic dose of morphine for subsequent tolerance studies was 10 mg/kg, a dose also commonly used in the literature for tolerance studies (Raghavendra et al., 2002; Raghavendra et al., 2004a; Mika et al., 2007; Horvath et al., 2010a).

Interestingly, some authors have shown a difference in the profile of morphine tolerance between sensitised and non-sensitised rats. Raghavendra et al. (2002) for example showed that neuropathic pain surgery enhanced the development of morphine tolerance when compared to sham-operated responses. The authors suggested this was due to enhanced proinflammatory immune responses at the lumbar spinal cord which was counteracting the analgesic effects of morphine. This theory therefore supports the postulated role of P2X7 receptors in morphine tolerance.

Although not borne out statistically, it appeared that the profiles of the tolerance obtained from rats dosed with 3 and 10 mg/kg of morphine were different. The 10mg/kg dose produced a higher maximum efficacy and the decline of effect appeared to occur faster. This observation agrees with data in naïve rats in which the rate of tolerance increased as the dose of morphine increased (Hutchinson et al., 2008b).

It has also been observed in the literature that the development of morphine tolerance is dependent on the route of administration. When dosed intrathecally, tolerance developed after 3 days compared to 6 days when dosed subcutaneously (Tawfik et al., 2005). According to the authors, the hastened tolerance following i.t. delivery indicated a stronger effect on glial cell activation and further development of anti-allodynic tolerance. This explanation again supports a potential role for the P2X7 receptor in the mechanisms involved in tolerance.

In two separate studies detailed in this chapter, morphine tolerance, produced by repeated systemic dosing of 10 mg/kg morphine, was delayed when rats were co-dosed with GSK1370319. As P2X7 receptors are predominantly expressed on microglia, the involvement of this glial cell type is therefore implicated. The involvement of glia in tolerance has been reported in the literature, albeit in naïve animals. A variety of glial inhibitors or inhibitors of the proinflammatory substances that glia release have been shown to suppress morphine tolerance all using a variety of different protocols, including fluorocitrate (Song and Zhao, 2001), minocycline (Cui et al., 2008), propentofylline (Raghavendra et al., 2004a), IL-1 receptor antagonist (Johnston et al., 2004) and pentoxifylline (Mika et al., 2009b).

Little literature exists investigating microglial involvement in morphine tolerance in nerve-injured rats. In one paper however, an association has been made between astrocytes and morphine tolerance in the L5 spinal nerve transection model (Tawfik et al., 2005). An enhanced elevation of GFAP protein levels, using Western blot analysis, was detected in morphine treated nerve-injured rats compared to vehicle treated nerve-injured rats. However, the authors stated that it was not possible to use the same methodology to detect ITGAM, a microglia marker and the effect was not mirrored in mRNA analysis.

Using the same neuropathic model, Raghavendra et al. (2002) demonstrated that a cocktail of IL-1ra, soluble TNF receptor and anti-IL6 (i.t.) co-dosed with morphine (s.c.) for 5 days increased the efficacy of a further i.v. dose of morphine once the rats had been made tolerant. Although this data does not implicate glia directly, the cytokines being inhibited are those known to be released from glia. This data also gives no indication of the interaction between the compounds during the

development of tolerance as only one data point post-chronic morphine was recorded. In the current study the time-course of the interaction is evident showing that tolerance is being delayed by approximately 3 days in rats dosed with both compounds.

It has been reported, using the CCI model in mice, that repeat dosing with microglia inhibitors minocycline and pentoxifylline attenuated morphine anti-nociceptive tolerance (Mika et al., 2009b). Other than the species difference, the main difference from the present study was that the inhibitor administration started pre-emptively to the surgery and several days before morphine dosing commenced. This design resulted in glial activity being impacted before neuropathic-induced allodynia was apparent and therefore complicating the interpretation of how the inhibitors could affect additional microglial activity from chronic morphine administration. The effect of glial inhibitors on the development of CCI-induced allodynia might also impact the progression of morphine tolerance. In the current study, co-dosing morphine and GSK1370319 after CCI-induced allodynia had developed focused the attention on the effect of the antagonist on morphine-induced tolerance. The current data therefore indicates that approaches that inhibit microglial activation, directly impact morphine tolerance irrespective of the rats being neuropathic. How this effect compares with a pre-emptive dosing regimen in rats would however be an interesting follow-up study to consider.

It is believed this is the first study implicating the involvement of the P2X7 receptor in morphine tolerance in nerve-injured rats. Recently however Zhou et al. (2010) found that the dye Brilliant Blue G, a P2X7 receptor antagonist, increased the efficacy of a subsequent dose of morphine (5 mg/kg, i.p.) in naïve rats that were morphine tolerant (6 days of 10 mg/kg morphine s.c.). This effect only occurred when BBG was co-dosed during the tolerance development phase, and not when tolerance had already developed, suggesting that spinal P2X7 receptors contribute to the induction, but not the maintenance of morphine tolerance. Similar conclusions were found in studies in naïve rats in which minocycline failed to reverse morphine tolerance once it had been well established (Cui et al., 2008). In contrast to these published findings tolerance appeared to be blocked on the final day of an 8 day

morphine dosing period after a single administration of GSK1370319. Further studies are required to investigate this fully however, as the interaction between the two compounds was not statistically significant suggesting that the maintained efficacy may have been due to an additive effect of both compounds.

The association between morphine tolerance and purinergic receptors has also recently been confirmed by reports that an antisense oligonucleotide to P2X4 blocked tolerance to systemically administered morphine in naïve rats (Horvath et al., 2010b). Although naïve rats have been used in both of the recent purinergic related papers, the findings aid the validation of the data reported in this chapter.

One potential explanation for the delay in tolerance would be a modification of pharmacokinetic clearance or distribution of morphine when co-dosed with GSK1370319, rather than a pharmacodynamic change. To investigate this, concentrations of both morphine and GSK1370319 in the blood of rats dosed with both compounds alone and compounds in combination were quantified. There were no significant changes in morphine or GSK1370319 blood concentration when dosed alone or in combination suggesting that the results were not accounted for by higher compound exposure and therefore more likely to be a pharmacodynamic association between the P2X7 receptor and the development of morphine tolerance.

In contrast to the efficacy and tolerance achieved with 3 and 10 mg/kg morphine in the initial morphine dose response study, when morphine was dosed at 0.3 and 1mg/kg minimal efficacy was produced. The minimal efficacy observed at these doses is in agreement with literature (Raghavendra et al., 2002). There are also other studies suggesting that the efficacy of morphine is decreased in rodents that have undergone neuropathic surgery compared to naïve rats (Mao et al., 1995b; Fundytus et al., 2001; Raghavendra et al., 2002). However this has not been explored in the current research studies as sham rats were not included. Interestingly, it has also been reported clinically that neuropathic pain is less responsive to opioid analgesia (Cherny et al., 1994). Several theories have been proposed to explain this finding. It was first suggested that lower effectiveness of morphine in neuropathic pain might be due to the reduced number of presynaptic opioid receptors following degeneration of primary afferent neurons caused by nerve damage (Porreca et al., 1998) or due to the

sensitisation arising from neuropathic pain (Tawfik et al., 2005). More recently however it has been speculated that uncontrolled activation of microglia due to a neuropathic insult counteracts the beneficial analgesic properties of morphine (Watkins et al., 2005; Mika et al., 2007; Watkins et al., 2007a). Indeed, the restoration of the analgesic activity of morphine has been shown in neuropathic pain models by propentofylline and pentoxifylline (Sweitzer et al., 2001; Raghavendra et al., 2002; Raghavendra et al., 2003b; Raghavendra et al., 2004a; Mika et al., 2007; Tawfik et al., 2007).

There is a suggestion from the current data that GSK1370319 may enhance the efficacy of morphine, however the statistics do not show a significant interaction between the two compounds. The increased efficacy might therefore be a result of an additive effect as opposed to a synergistic relationship. The lack of statistical significance for an interaction was unexpected when comparing paw withdrawal thresholds of the rats dosed with morphine and GSK1370319 individually and when dosed in combination. For example, the sum of the mean PWT from rats dosed with GSK1370319 (1 mg/kg) + morphine (0. 3 mg/kg) alone on day 3 was 8g which is considerably less than the actual responses from rats dosed with both compounds (11.1 g). Caution does need to be taken when mean PWTs are added together as errors of the mean are not considered. In this instance, however the authors consider that a comparison of the mean data does add confidence that a synergistic interaction might exist if a larger dataset was generated and a full isobolographic analysis was completed. One potential explanation for the disparity between the actual thresholds obtained versus the interaction statistics could be the disproportionality of the intervals of pressures that each von Frey hair exerts. One way of avoiding this complication is using a behavioural readout that generates continuous data, for example a thermal readout or data generated from an analgesymeter (see section 4.2.1.3.2). Continuous data can also be converted to % maximum possible effect (% MPE), a format more amenable for statistical analysis compared to von Frey hair data which is complicated by variable intervals between hairs.

If synergy was demonstrated it would suggest that an enhancement of morphine analgesia via P2X7 receptor antagonism could be due to the suppression of CCI-

induced spinal glial activation. As far as the author is aware there are no published studies demonstrating an enhancement of morphine-induced analgesia in nerve-injured rats with co-administration of a P2X7 receptor antagonist. There is a report however demonstrating that pre-emptive and repeated treatment with the microglia inhibitor, minocycline improved the response to a single dose of morphine in CCI-operated rats (Mika et al., 2007). Positive synergistic results between a P2X7 receptor antagonist and morphine would also complement published data in naïve rats which demonstrate a potentiation of morphine-induced analgesia by microglial inhibitors such as minocycline (Hutchinson et al., 2008b) and ibudilast (Hutchinson et al., 2009) as well as cytokine inhibitors, like IL-1 receptor antagonist (Johnston et al., 2004; Shavit et al., 2005). The clinical implications could be considerable if increased efficacy was achieved with submaximal doses of morphine that do not produce side effects.

An additional area of interest worth pursuing is that of morphine-induced hyperalgesia. This phenomena has frequently been reported in the literature and some believe it manifests behaviourally as anti-nociceptive tolerance (Mao et al., 1995a; Celerier et al., 2000; Vanderah et al., 2001a; Ossipov et al., 2003; Johnston et al., 2004). Although this has not been investigated in the current research, evidence for this paradoxical occurrence is observed in the initial morphine dose response study. On the final day of the 8 day dosing period, rats withdrew their paws at a significantly lower threshold than rats dosed with vehicle suggesting the rats were becoming more allodynic. Several mechanisms have been proposed to explain opioid-induced hyperalgesia, including activation of descending facilitation from the RVM, as well as spinal dynorphin-dependent enhancement of CGRP release from primary afferent fibres (Vanderah et al., 2001c; Gardell et al., 2002). There is also evidence suggesting that morphine-induced hyperalgesia is partly driven by microglia (Johnston et al., 2004) or products released by activated microglia (Shavit et al., 2005) and if this is the case, the pain caused from chronic morphine administration observed in the clinic might be resolved by the co-administration with a P2X7 receptor antagonist.

The cellular and molecular mechanisms involved in the interaction between the P2X7 receptor and morphine-induced tolerance and analgesia are extremely complex and inter-related. The behavioural data described within this chapter do not contribute directly to the elucidation of any specific mechanisms however, other than the involvement of the P2X7 receptors and microglia. It is difficult to investigate specific mechanisms using only behavioural techniques as it is likely that the experimental protocol would require the administration of 3 or more compounds to each rat. With appropriate control groups included, the study would become impracticable. Non-behavioural techniques such immuno-histochemistry and molecular biology however can be used to investigate mechanisms and these techniques are discussed further in Chapter 6. Potential mechanisms involved in the purinergic involvement in morphine activities include many ATP-related mechanisms, glial regulation of glutamatergic NMDA receptor changes, the involvement of proinflammatory cytokines and enhanced p38 MAPK signalling and are discussed in Chapter 1.

In conclusion, the data shown in this chapter provides the first evidence that repeated systemic dosing of a P2X7 antagonist attenuates the development of morphine-induced tolerance in nerve-injured rats. In addition, data is presented which suggests that P2X7 receptor antagonism may also potentiate the analgesic effect of morphine, however further studies are required to confirm this. Collectively this data suggests that the suppression of glial activation by P2X7 receptor antagonism could increase the clinical usefulness of opioids. Co-administration of morphine and a P2X7 receptor antagonist could potentially reduce the necessity of using doses of morphine that are associated with side effects.

Chapter 4

Investigating the interaction between P2X7 receptor antagonists and morphine in a disease-related model of neuropathic pain

4. Investigating the interaction between P2X7 receptor antagonists and morphine in a disease-related model of neuropathic pain

4.1 Introduction

Having already shown a positive interaction between a P2X7 receptor antagonist and morphine in a surgery based nerve-injury model, it was important to confirm this finding in an alternative neuropathic pain model with a different aetiology.

The three most widely used models of neuropathic pain all involve ligation and/or sectioning of one or more nerves in the rodents and all produce similar signs of neuropathic pain with similar time courses (Kim et al., 1997). Whilst surgery based models are more relevant to rare pain syndromes, such as causalgia or phantom limb pain, they are less relevant for more common neuropathic syndromes, such as peripheral diabetic neuropathy, cancer pain and post-herpetic neuralgia. Hence there was a new wave of disease-induced neuropathic models that have been developed (Mogil, 2009). These models are not induced by surgical manipulation, but attempted to induce the disease or physiological state itself to produce allodynia or hyperalgesia. These include the streptozocin-induced diabetic neuropathy model (Courteix et al., 1993), models of bone cancer pain (Schwei et al., 1999; Medhurst et al., 2002), HIV (and anti-retroviral)-induced painful neuropathy (Wallace et al., 2007a) and a model of post-herpetic neuralgia (Fleetwood-Walker et al., 1999).

Differences have been reported when efficacy from the same compound has been compared between two types of model. For example, one publication reports that P2X7 receptor antagonist A-740003 was more efficacious in the Chung surgery-induced nerve-injury model compared to a chemotherapy-induced neuropathic pain model (Honore et al., 2006). Another example highlights an increase in efficacy of morphine in the streptozocin–induced allodynia model compared to the CCI surgery-induced model (Field et al., 1999a; Field et al., 1999b). These differential effects between models suggest that there could be separate aetiologies and

pathomechanisms that are associated with the development of allodynia/ hyperalgesia or the involvement of particular targets is different. As these differences demonstrate, a need to test molecules in both a surgery based model and a disease-induced model of neuropathic pain was considered important to get a better understanding of the mechanism of action of a P2X7 antagonist.

The disease-related model chosen for these studies was the varicella zoster virus (VZV)-induced allodynia model of post-herpetic neuralgia (PHN), the pain experienced by some patients with herpes zoster. It was decided to develop this model within GSK as a patient population with PHN are often used as the first clinical study for assets targeted at neuropathic pain.

Herpes zoster, or shingles, is an infection of the nervous system caused by the varicella zoster virus (VZV), the same alpha-herpes virus responsible for chicken pox. After the acute infectious period of chicken pox, VZV remains latent in the sensory ganglia, often for decades, before reactivating in susceptible individuals to produce shingles (Kennedy et al., 1998; Cohrs et al., 2004). The process of reactivation is unclear but is thought to occur as a result of a decline in cellular immunity to VZV with aging or immune-suppression (Gershon and Steinberg, 1979; Burke et al., 1982).

Pain is the prevailing symptom of herpes zoster of which PHN, a debilitating neuropathic-type pain, persists for months to years after the resolution of the characteristic rash (Dworkin and Schmader, 2003). In the clinic PHN is characterised by the development of chronic hyperalgesia and mechanical allodynia accompanied by spontaneous pain usually of a burning or aching nature, but has also been described as sharp, piercing, throbbing or stabbing (Nurmikko, 1995). Clinical-virological correlations suggest that the range of symptoms probably results from injury to the dorsal horn (DH) of the spinal cord and dorsal root ganglia as well as injury to the peripheral nervous system (Fields et al., 1998). PHN is therefore principally regarded as a neuropathic pain and can be characterised by neuronal hyperexcitability in damaged areas of the nervous system (Rowbotham and Fields, 1996).

It remains unclear how latent VZV infection interacts with the neurone to induce the molecular changes required that lead to hyperexcitability. When VZV is reactivated from latency the localised rash and pain affects only one cutaneous dermatome, suggesting that VZV virions must migrate from the DRG along sensory nerves to the periphery (Fields et al., 1998). As the virus descends from the DRG, its replication and associated inflammatory response may damage axons and peripheral nerves leading to the generation of ectopic impulses (Argoff et al., 2004). In addition to this, similar unprovoked discharge may occur from hypersensitive nerve sprouts that are produced from the regrowth of the damaged axons (Woolf et al., 1992). It is this excessive peripheral activity that is thought to lead to hyperexcitability of the dorsal horn, also known as central sensitization. Altered CNS signal processing then results in lower activation thresholds displaying exaggerated responses to stimuli producing the clinical symptoms of spontaneous pain, hyperalgesia and allodynia (Ji and Woolf, 2001).

Evidence from post-mortem studies showing ongoing inflammation in PHN patients (Watson et al., 1991) suggests an inflammatory component to the disease. It is widely known that activated glial cells (microglia and astroglia) play a major role in facilitating pain transmission in the spinal cord by releasing cytokines (Watkins et al., 2001; Watkins and Maier, 2003), but this has yet to be demonstrated in a virus-induced animal model.

Not only does this model fit the criteria of being non-surgery based, there are also reports implicating microglia as a primary mediator of herpes virus induced oxidative damage (Schachtele et al., 2010). This might therefore have some significance when exploring the interaction between morphine, P2X7 receptor antagonists and microglia. Finally, as the VZV-induced allodynia model attempts to mimic a prevalent clinical pain syndrome the data would have relevance to the clinic.

Due to the species specificity of varicella zoster virus, identification of rodent models had been particularly challenging. The first rat model of VZV infection was described by Sadzot-Delvaux et al. (1990) who found long term persistence of the virus in the DRG and neurons after inoculation of virus both subcutaneously and into the footpad. Fleetwood-Walker et al. (1999) then adapted this model and reported

persistent allodynia and hyperalgesia up to 35 days following the injection of human VZV in the rat hindpaw. This model was characterised further by Dalziel et al. (2004) and Hasnie et al. (2007) by establishing the duration of VZV-induced allodynia, comparing different viral strains and by attenuating the allodynia with clinically useful analgesic drugs. As far as the author is aware there are no other publications characterising the potential pathomechanisms behind VZV-induced allodynia.

The intended objective was to compare the effects of combining the P2X7 receptor antagonist, GSK1370319 and morphine in this model with the data produced by the CCI model reported in the previous chapter. Once any differences had been established, the potential reasons for these would be explored. For example, the level of involvement of microglia or cytokines, like IL-1β, has in the pathomechanism of each model could be established.

The first approach was to determine the levels of proinflammatory cytokines, and in particular IL-1β, in spinal cord samples from VZV-injected and CCI-operated rats over the time course in the absence of any compound dosing. These levels would then be compared when GSK1370319 and morphine are dosed separately and co-dosed. The detection of cytokines in the spinal cord would be carried out using Meso Scale Discovery multi-array technology via electrochemiluminescence.

The second approach would be determining the levels of microglia in the spinal cord via immunohistochemical techniques using Iba-1, a commonly used marker for detecting activated microglia. The levels of activated microglia would then be compared between the VZV-induced allodynia model and the CCI model with and without pre- treatment with GSK1370319 and morphine.

The VZV protocol involves several different techniques, including the culturing of infected and non-infected cells, the inoculation procedure and the behavioural testing, it was therefore important to ensure that the behavioural response was sufficiently robust and reproducible before embarking on investigative pharmacological studies. Therefore, as with the CCI model, the model was characterised by running an allodynia time-course study followed by the testing of standard compounds known to work clinically for the treatment of PHN.

4.2 Studies to establish VZV-induced allodynia

4.2.1 Method

4.2.1.1 Preparation of viral inoculum

MEWO cells (a human melanoma cell line; ATCC, VA, USA) were grown on SelecT (automated cell culture robot, The Automation Partnership, Cambridge) and maintained in Dulbecco's modified Eagle's medium (DMEM; Gibco BRL) supplemented with 10% (v/v) foetal calf serum, 1% (v/v) glutamine and 1% (v/v) essential amino acids.

MEWO cells were infected with VZV (Dumas strain; kindly donated by Dr. R. Dalziel, University of Edinburgh) when ~ 60% confluent (Figure 25a) and grown in T175 flasks (in DMEM with 2% (v/v) foetal calf serum, 1% (v/v) glutamine and 1% (v/v) essential amino acids). The infected cells were harvested when exhibiting 80% cytopathic effect (cpe). Cpe refers to the destruction of normal cell architecture due to viral lytic infection and is characterised by the presence of vacuoles and granules (Figure 25b). The cytopathic profile of the infected cells was decided upon by visual assessment using a microscope. Virus-infected cells were removed from the flask surface using Accutase, a non-mammalian alternative to trypsin, a proteolytic enzyme commonly used in cell culture techniques for this purpose. The cell suspension was then centrifuged at 252 x gravity, 4 °C for 15 minutes and the resulting pellet was resuspended in 150 µl PBS before being injected into the rat as a 50 µl volume containing 4-8 x 10^6 VZV-infected MEWO cells. Uninfected cells were prepared and injected in the same way to act as a control (i.e. sham treated rats).

Figure 25a) Figure 25b)

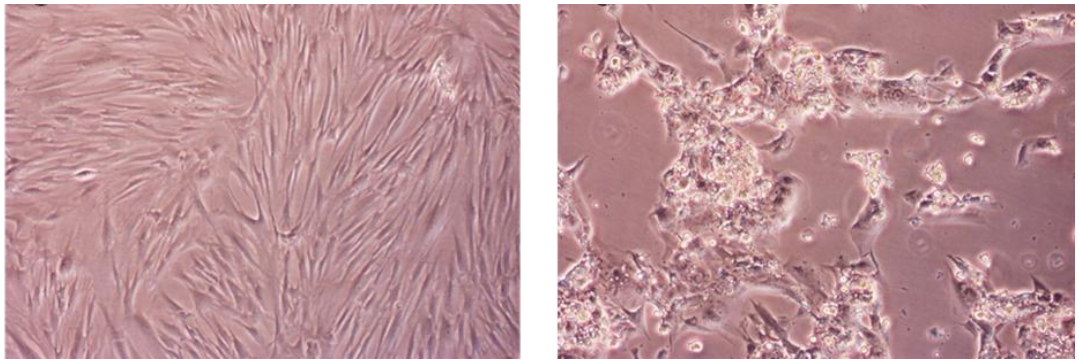

Figure 25. Uninfected MEWO cells approximately 60% confluent, magnification x 40, b) Dumas strain of VZV-infected MEWO cells at approximately 80% cytopathic effect, magnification x 40.

4.2.1.2 Injection of viral inoculum

Male Random-hooded rats (200-240 g prior to inoculation; Charles River, UK) were anaesthetised via the inhalation route with isoflurane: oxygen (3:1). Rats were placed in a specialised anaesthetic induction chamber into which the isoflurane/ oxygen mixture was introduced. When the rat was showing the recognised signs of anaesthesia (loss of pedal withdrawal reflex, loss of eye reflex, decline in heart and lung function) the rats were removed from the chamber and placed on a heated mat to maintain the body temperature of the rat at approximately 37 °C. To maintain anaesthesia throughout the procedure, the nose of the rat was placed into a specialised anaesthetic mask to allow the continuous exposure of isoflurane/ oxygen mixture. Ensuring the rat was fully anaesthetised (see signs of anaesthesia above), 50 µl of inoculum was injected into the glabrous skin of the left hind paw using a 21 g or 19 g bore needle.

4.2.1.3 Behavioural assessment

4.2.1.3.1 Assessing mechanical allodynia using von Frey hairs

VZV-induced mechanical allodynia was assessed by using an ascending series of von Frey filaments presented to both ipsilateral and contralateral hind paw to record paw withdrawal thresholds (PWTs) using method previously described in section 2.2.2.2.

Readings were taken prior to inoculation to establish a baseline, post-inoculation to establish robust levels of allodynia and on specific days during the dosing period, typically 1 hour after the morning dose. To ensure all rats included in a drug study were considered allodynic a 'cut-off' was introduced which was based on a hair pressure which naïve rats can respond to. Any rat responding to the 10 g hair or above was not included in the study.

4.2.1.3.2 Assessing mechanical hyperalgesia

In some studies it was necessary to measure mechanical hyperalgesia, by using an analgesymeter (Ugo Basile, Italy). The device exerts a force that increases at a constant rate and is continuously monitored by a pointer moving along a linear scale (Skingle et al., 1990) (see Figure 26). Following von Frey hair testing, rats were loosely scruffed and the ipsilateral paw was placed on a small plinth under a cone shaped 'pusher'. When activated the pressure increased from 0 to 250 g until the rat withdrew its paw and the paw withdrawal threshold (PWT) was read off the scale. Data for each treatment group was presented as mean ±SEM in grams.

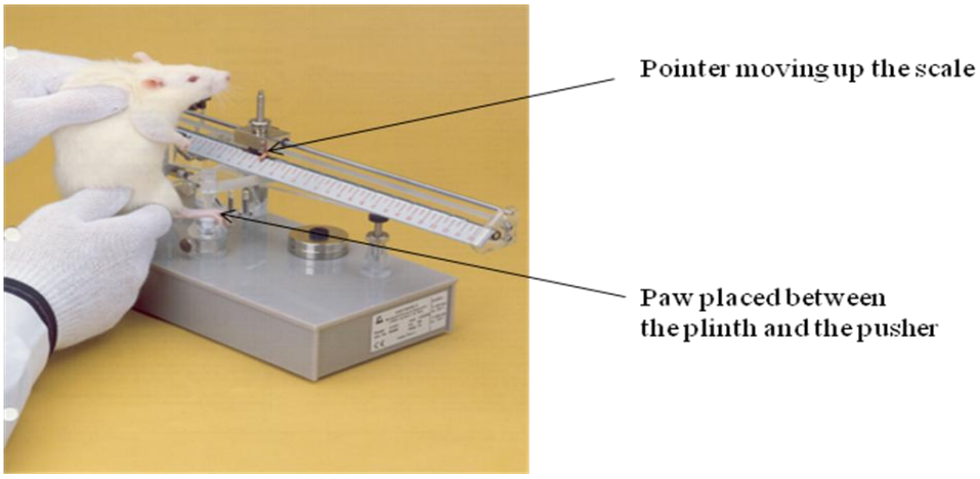

Figure 26. The analgesymeter (Ugo Basile, Italy) was used to measure mechanical hyperalgesia in VZV-injected rats.

4.2.1.3.3 Assessing dynamic allodynia

In one study, rats were tested for dynamic allodynia using the method described by Field et al. (1999b). Before von Frey hair testing was carried out and after the rats had habituated to the chambers, a 'fluffed up' cotton bud was presented to the plantar surface of the rat paw in a stroking motion from heel to toe for 15 seconds or less. The time that the rat withdrew the paw from the stimulus in a sudden motion was recorded. This procedure was repeated 3 times with 5 minutes interval between each trial to produce a mean paw withdrawal latency for each rat.

4.2.1.3.4 Assessing mechanical allodynia using an aesthesiometer

In two studies, mechanical allodynia was assessed using the Dynamic Plantar Aesthesiometer ('DPA', Ugo Basile), a device which delivers a constant pressure via a blunt metal probe to the plantar surface of rat or mouse paws (Figure 27).

The rats were placed in testing chambers with mesh flooring for 10 minutes, to habituate to their surroundings. When the rats were settled, the probe unit was carefully slid under the rat so that the probe, when activated, would advance upwards and be positioned in the middle of the foot pad towards the toes. When the device was activated, the probe advanced towards the rats' foot at 0-50 g in 10 seconds and the paw withdrawal threshold was automatically recorded. Three readings were taken from each rat to obtain an average. Abnormally sensitive rats were defined as those with initial PWTs of less than 20 g and were excluded from the study.

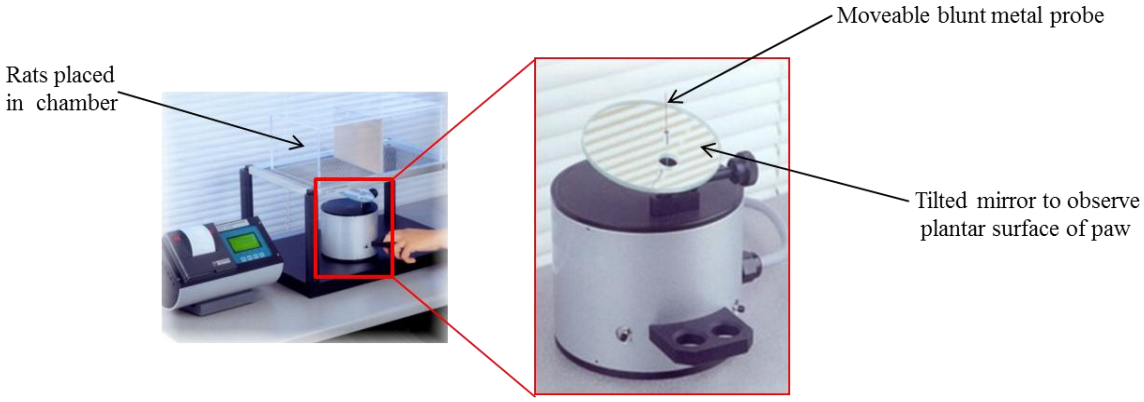

Figure 27. A photo of the Dynamic Plantar Aesthesiometer and enlargement photo of the probe unit.

4.2.1.4 Data analysis

All studies were performed with the operator blind to which rats had received infected or non-infected cells. Paw withdrawal threshold data using von Frey hairs were presented graphically as log mean ±SEM in grams. The log transformation of the data was adopted to reduce the diproportionality of the uneven intervals between the von Frey hairs. Paw withdrawal threshold data using the analgesymeter and the aesthesiometer was presented as mean ±SEM in grams. Data from the dynamic allodynia readout were presented as mean ±SEM in seconds. Statistical analysis for all behavioural tests was carried out on raw data comparing responses from VZV-injected rats to sham-injected rats, using Repeated ANOVA followed by Planned LSD comparisons, where $p<0.05$ was considered significant.

4.2.2 Results for behavioural studies

The intention was to first characterise the model by establishing the time-course of allodynia followed by the assessment of standard compounds known to be effective for treating PHN, for example gabapentin (Rowbotham et al., 1998) and pregabalin (Sabatowski et al., 2004).

4.2.2.1 Time course study 1

Following the protocol above, 15 rats received VZV-infected cells and 7 rats received uninfected cells. On day of inoculation, MEWO cells were passage 21 when infected with the Dumas strain of VZV. Von Frey hair testing was carried out and 4 days prior to inoculation (i.e. day -3 and -4 baseline readings), and on days 3, 6, 8, 9, 13, 16, 20 and 23 post-inoculation. Baseline readings from day -4 were used to divide the rats into the 2 treatment groups to ensure the groups had similar pre-inoculation readings.

When rats were tested for mechanical allodynia using von Frey hairs prior to infection (day -3 and -4), all rats produced mean ipsi- and contra-lateral paw withdrawal thresholds (PWTs) of 23.8±1.0 g and 21.5±1.3 g respectively. These baseline readings were similar to those produced from other neuropathic pain studies reported in Chapter 2 and 3 and also by other members of the *in vivo* pain group at

GSK. There was also no difference between the ipsilateral and contralateral baseline readings as expected, thereby allowing the study to continue and inoculation to proceed.

Three days post-inoculation, the ipsi- and contra-lateral PWTs produced from VZV-injected rats decreased from the baseline readings to 11.3 ±2.5 g and 14.5 ±2.4 g (Figure 28). Although this response suggested the onset of VZV-induced allodynia, the response from sham-treated rats also decreased in both paws, producing PWTs of 14.5 ±4.1 g and 12 ±3.8 g respectively. This lack of differentiation in response between virus-injected and sham-treated rats continued for all subsequent time-points. On day 9 post-inoculation, the data appeared most differentiated, with ipsilateral readings of VZV-injected rats and sham-treated rats of 6.1 ±1.1 g and 14.3 ±4.2 g, there was however no statistical significance (p=0.13).

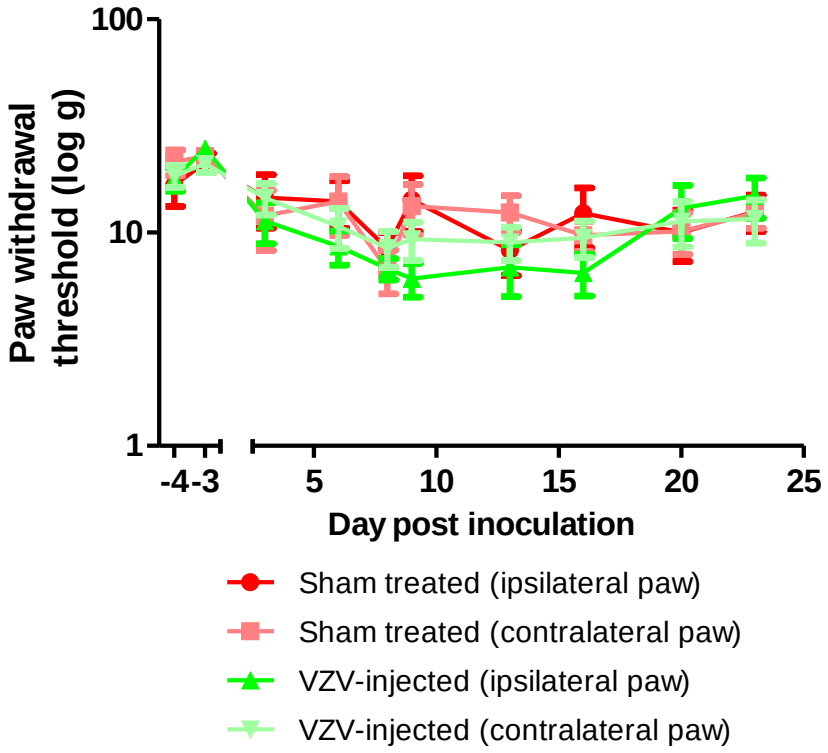

Figure 28. Effect of injecting VZV (Dumas strain) - infected MEWO cells into the left paw (intra-plantar) on paw withdrawal thresholds of male Random-hooded rats following von Frey filament application. Data are log mean ±SEM with n=7 for sham treated group and n=15 for VZV-injected group. Statistical analysis was completed using Repeated Measures ANOVA comparing to responses from sham treated rats, however there was no significant effect.

In this initial study there appeared to be no significant difference in the responses between rats injected with infected cells and rats injected with uninfected cells. Even though there was a statistically significant difference between pre- and post-inoculation on the majority of time-points, the 'window of hyperalgesia' between VZV-injected rats and sham treated rats was too small to consider using the model for compound testing in its current form. It was therefore decided to optimise the model to produce an allodynic response sufficient enough to allow compound testing to proceed.

During the optimisation process, literature was assessed and variables were methodically changed in an attempt to obtain VZV-induced allodynia. Following the first study, it was decided to change the rat strain from Random-hooded rats to Wistar rats, the strain used in the original paper by Fleetwood-walker et al. (1999), in case there was strain specificity. In addition to this change, several minor experimental improvements were made, including an increase in the n number for the sham group to try and reduce the variability and the addition of an extra group of untreated rats (i.e. naïve rats) to allow an appropriate statistical comparator for the sham operated group. Two small amendments were also implemented in the cell culture technique. Firstly, MEWO cells were infected at a lower passage, in case the health of the cells had declined as the number of passages increased. Secondly, the cell suspension was tritriated more thoroughly to allow a smaller, less invasive needle to be used to inoculate the rats, in case it was the needle insertion which produced the allodynic response in the sham treated rats. Finally, two additional behavioural readouts were included to compare directly with data found in the literature. Hasnie et al. (2007) reported a significant effect using the same method of VZV inoculation, by measuring static allodynia using an electronic 'von Frey device' which delivers a more intense stimulus and also by measuring dynamic allodynia, which involve lightly stroking the plantar surface of the paw.

4.2.2.2 Time course study 2

Male Wistar rats (180-200 g prior to inoculation; Charles River, UK) were used for the second time course study. 16 rats received VZV-infected cells ('VZV-injected'), 16 rats received uninfected cells ('sham treated') and 8 rats remained un-injected ('untreated'). On the day of inoculation, MEWO cells were passage 10 when infected with VZV. The infected cell suspension was titriated well before administration producing a smoother suspension and thereby allowing a finer needle to be used for the injection (i.e. 23 g). In addition to von Frey testing being carried out on days 3, 7, 9 and 11 post-inoculation; mechanical hyperalgesia measurements using the analgesymeter (method in section 4.2.1.3.2) were taken on days 9, 11 and 14 post-inoculation, and dynamic allodynia measurements (method in section 4.2.1.3.3) were taken on days 3, 7, 9 and 11. The analgesymeter was used as a substitute to the device used by Hasnie et al. (2007) for measuring mechanical allodynia. Although it was a different device the important factor for the purposes of optimisation is that a higher pressure stimulus was presented to the paws.

When rats were tested for mechanical allodynia using von Frey hairs there was no significant difference between responses from naive rats, VZV-injected rats or sham treated rats on any test day (Figure 29). PWTs from untreated rats on day 3, 7, 9 and 11 post-inoculation were 14.5 ±2.1 g, 18.4 ±2 g, 20.9 ±1.9 g and 14.4 ±1.7 g respectively. On the same days PWTs from sham treated rats were 21.8 ±1.7 g, 20.3 ±2.0 g, 21 ±2 g and 21.2 ±1.9 g respectively. Finally, PWTs from VZV-injected rats were 14.2 ±2.2 g, 15.6 ±2.3 g, 20.1 ±1.8 g and 17.6 ±1.8 g respectively.

This data suggests that injecting VZV-infected cells into rat paws has not produced mechanical allodynia when measured with von Frey hairs, even after introducing changes from the first time-course study.

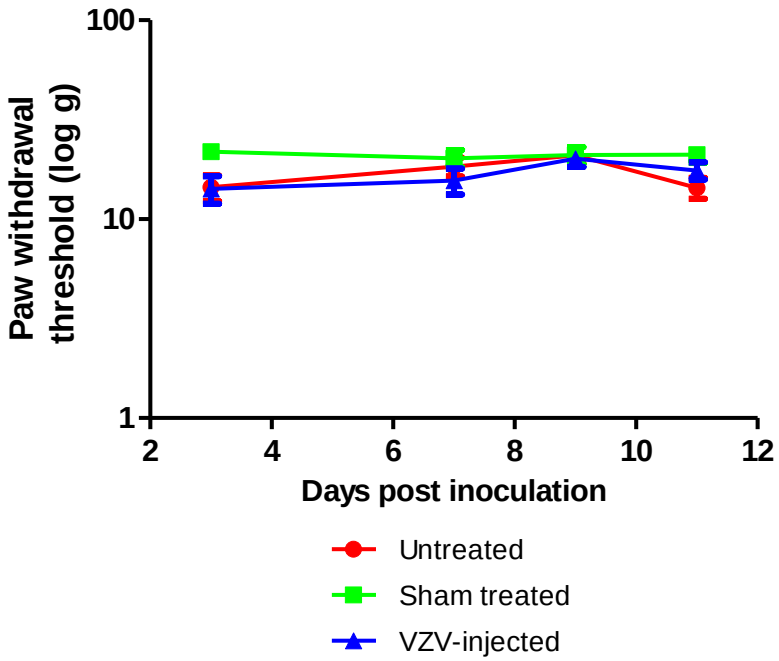

Figure 29. Effect of injecting VZV (Dumas strain) - infected MEWO cells into the left paw (intra-plantar) on paw withdrawal thresholds of male Wistar rats following von Frey filament application. Data are log mean ±SEM with n=8 for untreated group, n=16 for sham treated group and n=16 for VZV-injected group. Statistical analysis was completed using Repeated Measures ANOVA comparing to responses from untreated rats, however there was no significant effect.

To investigate the effect on paw withdrawal threshold of rats injected with VZV when a higher pressure is exerted onto the paw, an analgesymeter was used on days 9, 11 and 14 post-inoculation. Although a more intense stimulus was presented to the paw there was still no significant difference between responses from untreated rats, sham treated rats or VZV-injected rats on any of the test days (Figure 30). PWTs from untreated rats on days 9, 11 and 14 post-inoculation were 212 ±5 g, 210 ±4 g and 230 ±8 g respectively. On the same days PWTs from sham treated rats were 214 ±5g, 209 ±5g and 223 ±6g respectively. Finally, PWTs from VZV-injected rats were 207 ± 4g, 182 ±7 g and 218 ±8 g respectively. On day 11, there appeared to be some differentiation between the responses from the rats injected with infected cells compared to the other two groups; however this difference was not statistically

significant when the entire dataset was taken into account and a reduction of 20 grams in this assay would not be considered as a robust effect.

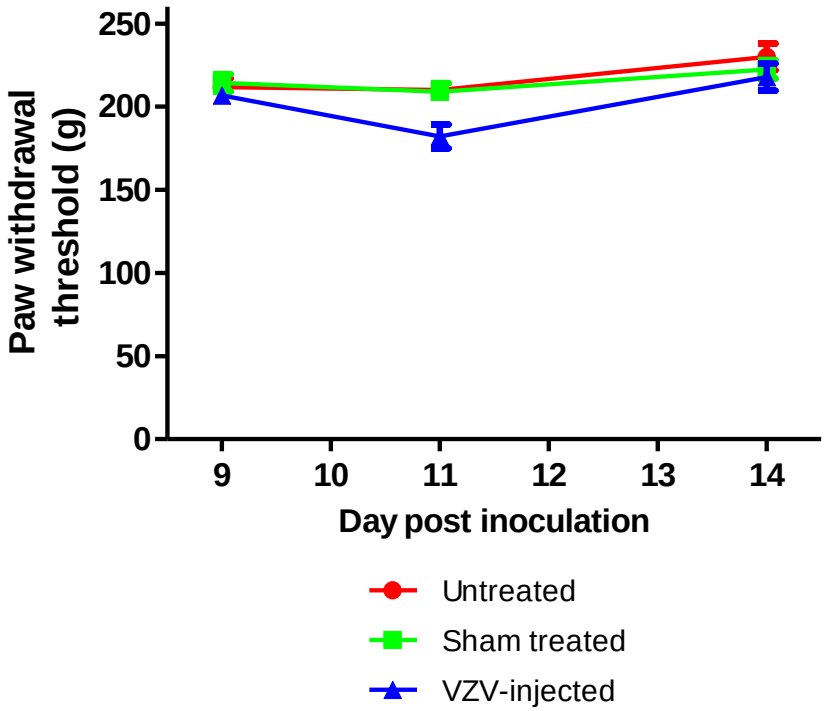

Figure 30. Effect of injecting VZV (Dumas strain) - infected MEWO cells into the left paw (intra-plantar) on paw withdrawal thresholds of male Wistar rats using the analgesymeter. Data are mean ±SEM with n=8 for untreated group, n=16 for sham treated group and n=16 for VZV-injected group. Statistical analysis was completed using Repeated Measures ANOVA comparing to responses from untreated rats, however there was no significant effect.

Finally, when rats were tested for dynamic allodynia a lack of significance was also seen in all groups on all of the test days (Figure 31). Paw withdrawal latencies (PWLs) from untreated rats on day 3, 7, 9 and 11 post-inoculation were 12.0 ±1 sec, 12.1 ±1 sec, 13.0 ±1 sec and 12.9 ±1 sec respectively. On the same days PWLs from sham treated rats were 13.9 ±0.2 sec, 13.4 ±0.4 sec, 13.8 ±0.5 sec and 12.9 ±1 g respectively. Finally, PWLs from VZV-injected rats were 11.8 ±0.6 sec, 11.8 ±0.6 sec, 12.4 ±0.7 sec and 12.8 ±0.5 sec respectively. These data suggested that

injecting VZV-infected cells into the paws of rats did not produce dynamic allodynia, contrary to the literature (Hasnie et al., 2007).

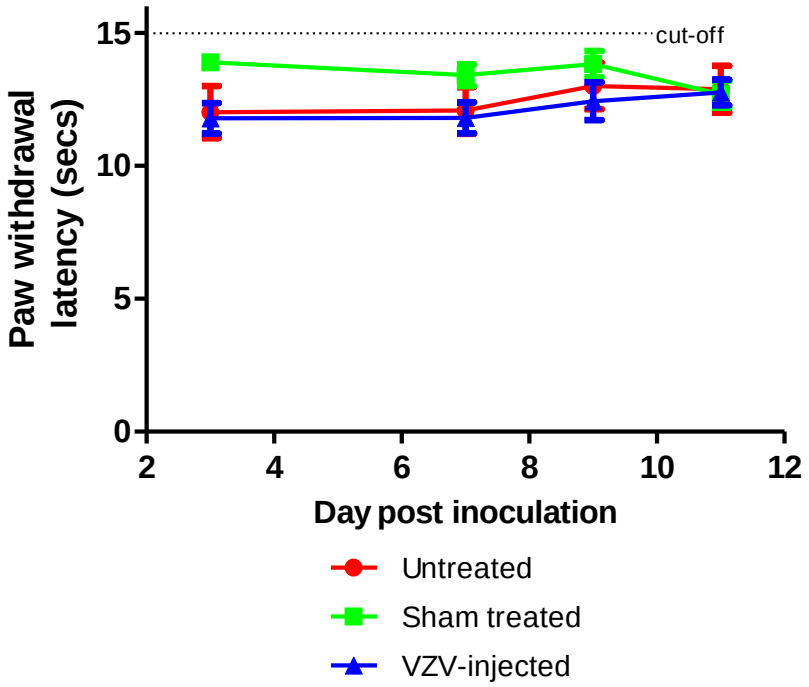

Figure 31. Effect of injecting VZV (Dumas strain) - infected MEWO cells into the left paw (intra-plantar) of male Wistar rats on paw withdrawal latencies to a lightly stroked cotton bud. Data are mean ±SEM with n=8 for untreated group, n=16 for sham treated group and n=16 for VZV-injected group. Statistical analysis was completed using Repeated Measures ANOVA comparing to responses from untreated rats, however there was no significant effect.

Due to the negative results generated in study 1 and 2, further model optimisation was required and other adjustable variables needed to be identified. A discrepancy that exists in the limited literature on models of VZV-induce allodynia is the strain of host cell. In studies 1 and 2 it was decided to use human melanoma cell line (MEWO) that had been used by Sadzot-Delvaux et al. (1990) in the first publication on VZV infection in rats and later by other groups (Zerboni et al., 2005). Several other publications however, including one authored by Sadzot-Delvaux (1995) used fibroblast cell lines instead which are also known to be permissive to VZV (Merville-Louis et al., 1989; Garry et al., 2005; Hasnie et al., 2007). Having

searched the literature there was no known reason for a particular preference of cell line, however to continue the optimisation of this method, a fibroblast cell line (MRC5) was obtained, prepared, infected and injected in the same way that MEWO cells were for the first two studies.

4.2.2.3 Time course study 3

Male Wistar rats (200-240 g prior to inoculation; Charles River, UK) were used in time course study 3. Following the method for study 2, 15 rats received VZV-infected cells, 10 rats received uninfected cells and 10 rats remained untreated. The main difference from the previous studies is that MRC5 cells were used instead of MEWO cells. The cells were treated exactly the same as the MEWO cells however and were 60% confluent when infection was carried out (see Figure 36a). Von Frey hair testing was carried out 1 day prior to inoculation (baseline reading), and on days 4, 6, 8, 13, 15 and 18 post-inoculation. Paw pressure testing using the analgesymeter was carried out on days 13 and 15 post-inoculation. Baseline von Frey hair readings were used to divide the rats into the 3 treatment groups to ensure the groups had similar pre-inoculation readings.

When rats were tested for mechanical allodynia using von Frey hairs there was no significant difference between responses from untreated rats, sham treated rats or VZV-injected rats on any of the test days (Figure 32). The ranges of PWTs from untreated, sham treated and VZV-injected rats for all time-points post-inoculation were 22.7-23.8 g, 20.5-24.9 g and 18.8-20.8 g respectively. These data suggested that injecting MRC5 cells infected with VZV into rat paws, did not produce mechanical allodynia when measured with von Frey hairs, a similar result to when MEWO cells were used.

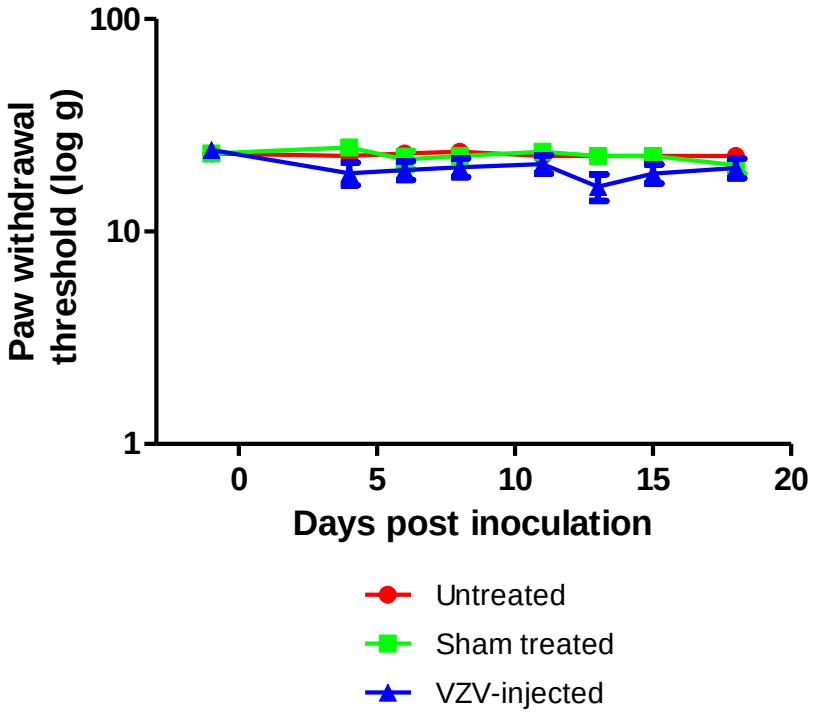

Figure 32. Effect of injecting VZV (Dumas strain) - infected MRC5 cells into the left paw (intra-plantar) on paw withdrawal thresholds of male Wistar rats following von Frey filament application. Data are mean ±SEM with n=10 for untreated group, n=10 for sham treated group and n=15 for VZV-injected group. Statistical analysis was completed using Repeated Measures ANOVA comparing to responses from untreated rats, however there was no significant effect.

Similar data were also observed when measuring the paw withdrawal thresholds using the analgesymeter (Figure 33). PWTs of both untreated rats and sham treated rats on days 13 and 15 were 210 ±10 g and 200 ±10 g respectively. PWTs of VZV-injected rats were 170 ±10 g and 180 ±10 g respectively and although lower values were produced than the other two groups there was no statistically significant difference. This data again demonstrated a lack of hypersensitivity when stimulating the rats with a higher pressure.

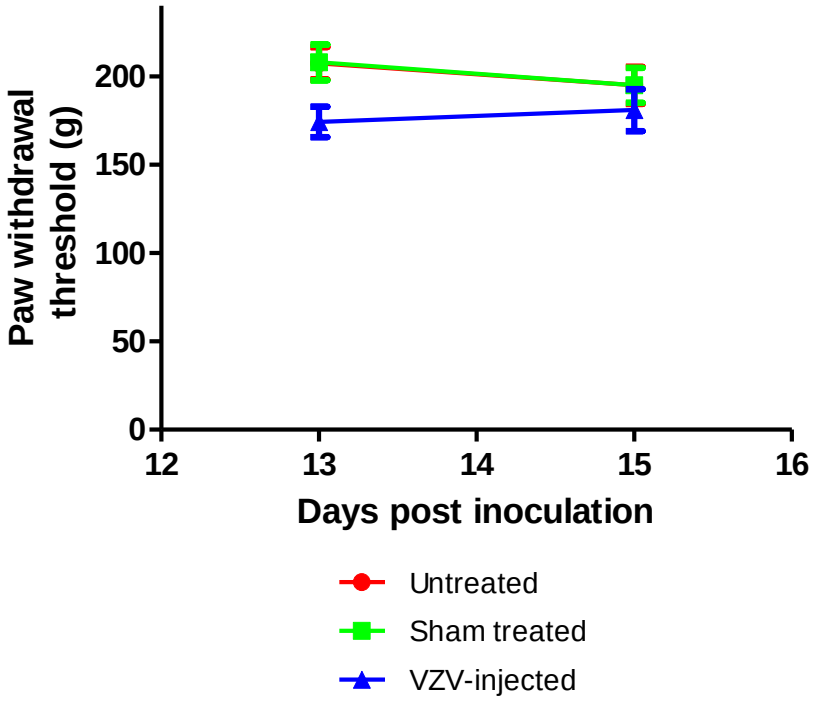

Figure 33. Effect of injecting VZV (Dumas strain) - infected MRC5 cells into the left paw (intra-plantar) on paw withdrawal thresholds of male Wistar rats using an analgesymeter. Data are mean ±SEM with n=10 for untreated group, n=10 for sham treated group and n=15 for VZV-injected group. Statistical analysis was completed using Repeated Measures ANOVA comparing to responses from untreated rats, however there was no significant effect.

The variable to consider for the next study was the strain of virus used. In the previous studies the Dumas strain had been used which is a clinical isolate for which the VZV sequence is known (Davison and Scott, 1986) and was the strain used by Fleetwood-Walker et al. (1999). An alternative strain that is commonly used is the Ellen strain which is a highly passaged laboratory strain (Moffat et al., 1998) and was used by Dalziel et al. (2004) when the model was further characterised.

As well as the change of virus strain there were two experimental variables that were changed for time course study 4. Previously Accutase had been used in the cell culture harvesting process, to remove cells from the inner surface of the flasks. Accutase works by combining protease and collagenolytic activities to shed particles from the surface of cells. There was a possibility that the particles being shed may be

essential for the viral mechanism of infection. For this reason, accutase was no longer used and the cells were removed mechanically by gently scraping them off the surface using a cell scraper. In addition, it was thought that the cells in previous studies might not be confluent enough for the virus to spread from one cell to the next so in future studies the cells were grown to greater confluence.

4.2.2.4 Time course study 4

Male Wistar rats (200-230 g prior to inoculation; Charles River, UK) were used in time course study 4. 14 rats received VZV-infected cells, 11 rats received uninfected cells and 10 rats remained untreated. Three changes to the protocol occurred in study 4. Firstly, a change of virus strain from Dumas to Ellen (kindly donated by Dr. R. Dalziel, University of Edinburgh), although the virus was treated in exactly the same manner as the Dumas strain. Secondly, the MRC5 cells were more confluent at time of infection (~80% confluent as opposed to 60%). Finally, when harvesting, the cells were gently removed mechanically from the flask surface using cell scrapers. Von Frey hair testing was carried out 1 day prior to inoculation (baseline readings), and on days 3, 6, 8, 10, 13, 15 and 17 days post-inoculation. Paw pressure testing using the analgesymeter was carried out on days 6, 8, 10 and 13 post-inoculation. Baseline von Frey hair readings were used to divide the rats into the 3 treatment groups to ensure the groups had similar pre-inoculation readings.

When rats were tested for mechanical allodynia using von Frey hairs there was no significant difference between responses from untreated rats, sham treated rats or VZV-injected rats on any of the test days (Figure 34). The ranges of PWTs from untreated, sham treated and VZV-injected rats for all time-points post-inoculation were 22.7-23.8 g, 20.5-24.9 g and 18.8-20.8 g respectively. This data suggested that MRC5 cells injected with Ellen, did not produce mechanical allodynia when measured with von Frey hairs.

This data suggested that using MRC5 cells infected with the Ellen strain of VZV was also unable to evoke mechanical allodynia when measured with von Frey hairs, in similar way to when the Dumas strain were used.

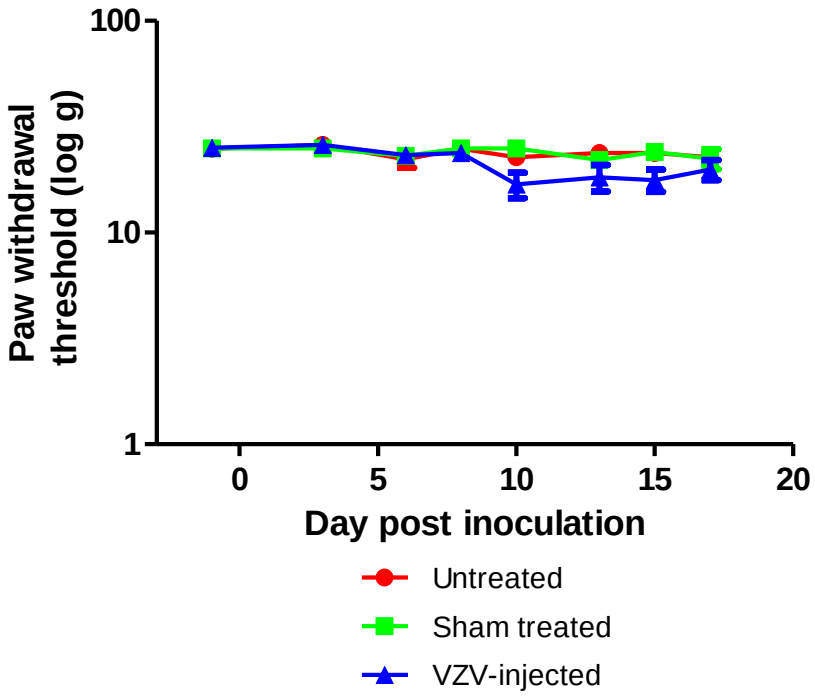

Figure 34. Effect of injecting VZV (Ellen strain) - infected MRC5 cells into the left paw (intra-plantar) on paw withdrawal thresholds of male Wistar rats following von Frey filament application. Data are mean ±SEM with n=10 for untreated group, n=11 for sham treated group and n=14 for VZV-injected group. Statistical analysis was completed using Repeated Measures ANOVA comparing to responses from untreated rats, however there was no significant effect.

Similar data was observed when measuring the paw withdrawal thresholds using the analgesymeter (Figure 35). The range of PWTs from untreated rats on all test days was 199-230 g and the range of PWT from sham treated rats was 193-232 g. Finally, the range of PWTs from VZV-injected rats was 198-221 g, therefore demonstrating a lack of hypersensitivity when compared to the other two groups.

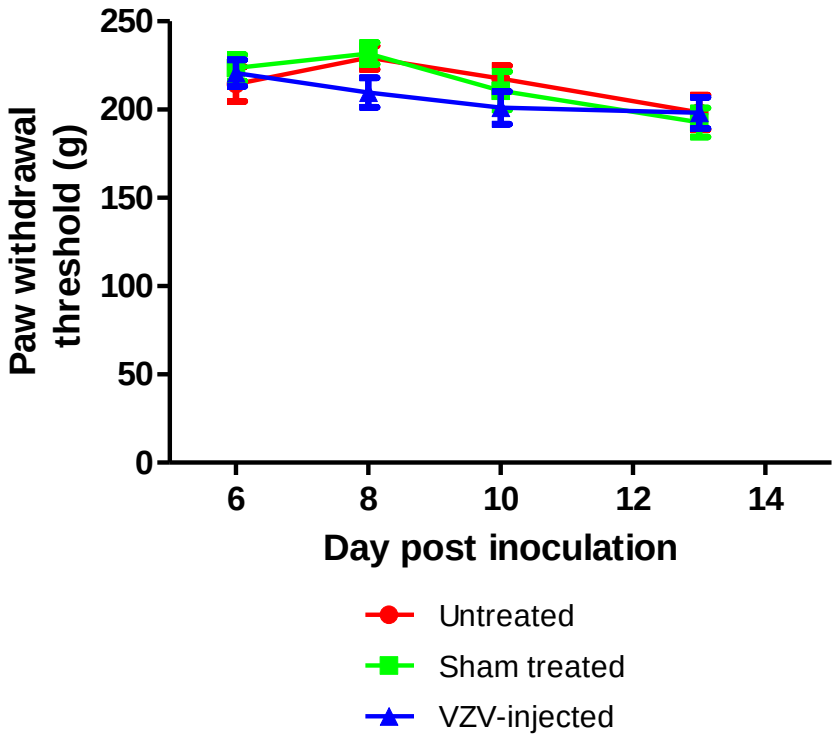

Figure 35. Effect of injecting VZV (Ellen strain) - infected MRC5 cells into the left paw (intra-plantar) on paw withdrawal thresholds of male Wistar rats using an analgesymeter. Data are mean ±SEM with n=10 for untreated group, n=11 for sham treated group and n=14 for VZV-infected group. Statistical analysis was completed using Repeated Measures ANOVA comparing to responses from untreated rats, however there was no significant effect.

When considering new variables to change, the clinical disease was considered in greater detail to try and identify other important factors that could be taken into account when developing a pre-clinical model. The overall incidence of Herpes zoster is ~3/1000 of the population per year rising to 10/1000 per year by 80 years of age (Johnson and Whitton, 2004). Although it is known that not all sufferers of herpes zoster develop post-herpetic neuralgia, the risk of PHN also increases dramatically with age, from 3-4% in adults aged 30-49 years, to 21% in 60-69-year-olds, to 29% in 70-79-year-olds and to 34% in adults over the age of 80 years (Dworkin and Portenoy, 1996). To incorporate this knowledge pre-clinically, rats that were 4 weeks older than previously used rats were used in time course study 5.

Two additional minor experimental variables were also included. Firstly, the confluency of the host cells was increased further and the cut-off used in the allodynia readout was increased to 60 g from 24 g, in an attempt to better mimic the higher pressure used in the allodynia technique described in other papers (Fleetwood-Walker et al., 1999; Dalziel et al., 2004).

4.2.2.5 Time course study 5

Male Wistar rats (370-380 g prior to inoculation; Charles River, UK) were used in time course study 5. Following the method for study 4, 8 rats received VZV-infected cells and 8 rats received uninfected cells. Three changes to the protocol occurred in study 5 from previous studies. The first difference was the size of the rats from approximately 220 g to 375 g. The corresponding approximate ages of these two body weights are 5 weeks and 9 weeks (Research Models and Service Catalogue, 2010, Charles River) which is a suitable age difference for testing this hypothesis. Compared to other studies, MRC5 cells were more confluent at time of infection, being ~95% confluent as opposed to 60% (see Figure 36b), but cytopathic effect remaining at approximately 80% (Figure 36c). Von Frey hair testing (with increased cut-off to 60 g) and paw pressure readings were carried out on days 3, 7, 10, 14 and 17 days post-inoculation.

Figure 36a) Figure 36b) Figure 36c)

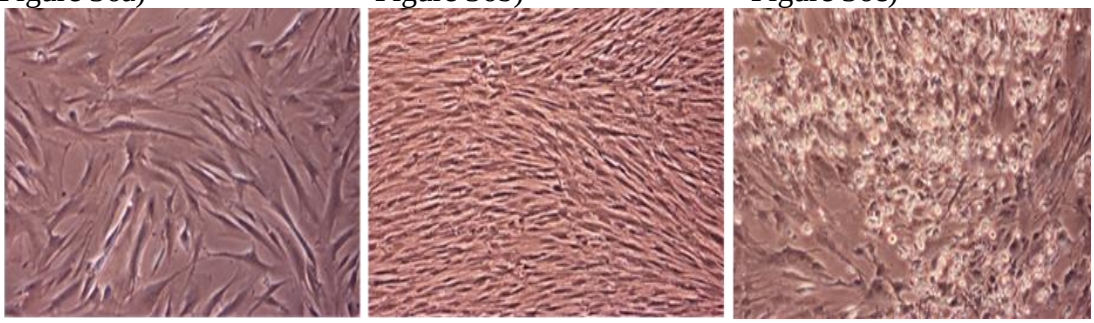

Figure 36. Uninfected MRC5 cells approximately 60% confluent, magnification x40, b) Uninfected MRC5 cells approximately 95% confluent, magnification x 40, c) Ellen strain of VZV-infected MRC5 cells at approximately 80% cytopathic effect, magnification x40.

When rats were tested for mechanical allodynia using von Frey hairs up to 60 g, there was no significant difference between responses from untreated rats, sham treated rats and VZV-injected rats on any of the test days (Figure 37). The ranges of PWTs from sham treated and VZV-injected rats for the time-points post-inoculation were 33-60 g and 37-56 g respectively.

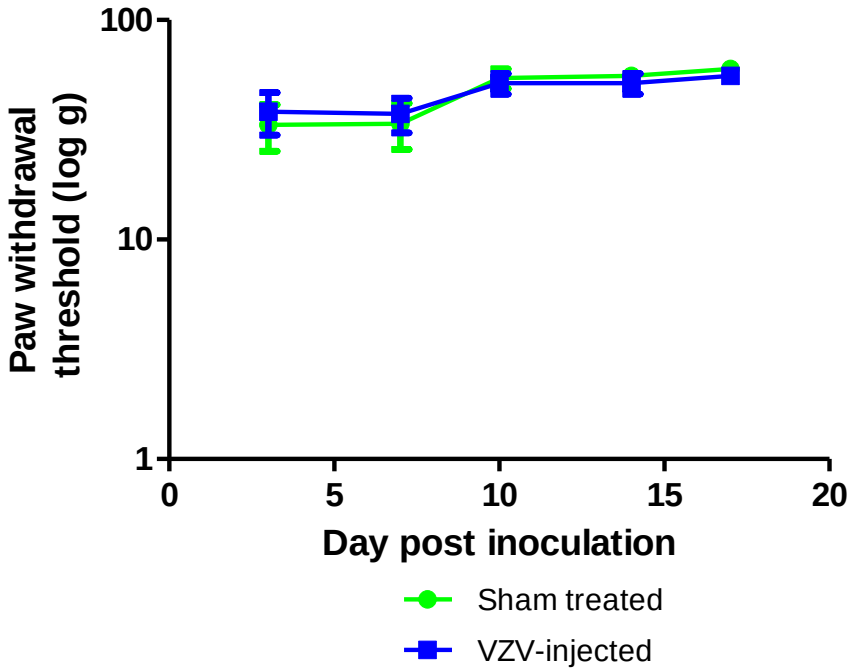

Figure 37. Effect of injecting VZV (Ellen strain) - infected MRC5 cells into the left paw (intra-plantar) on paw withdrawal thresholds of male Wistar rats (~380 g body weight) following von Frey filament application. Data are mean ±SEM with n=8 for sham treated group and n=8 for VZV-injected group. Statistical analysis was completed using Repeated Measures ANOVA comparing to responses from sham treated rats, however there was no significant effect.

When measuring paw withdrawal threshold using the analgesymeter however, there was a significant difference between responses from VZV-injected and uninfected cell-injected rats effect on days 7 and 10 post-inoculation, which resolved by day 14 (Figure 38). The PWTs from VZV-injected and sham treated rats on day 7 was 196 ±9 g and 126 ±8 g respectively and on day 10 was 189 ±9 g and 138.1 ±6 g respectively. After changing many variables, this was the first time that any

statistically significant effect had been observed. The resolution by day 14 however was concerning as differentiation between infected and non-infected groups in the literature is reported to continue for at least 34 days, as reported by Fleetwood-Walker et al. (1999) or 80 days, as reported by Dalziel et al. (2004) albeit using different behavioural readouts.

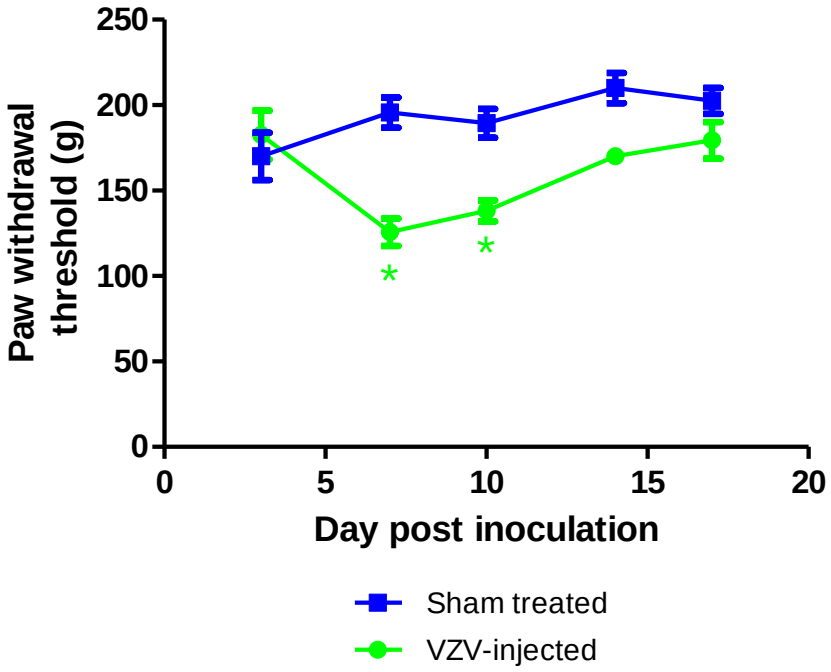

*Figure 38. Effect of injecting VZV (Ellen strain) - infected MRC5 cells into the left paw (intra-plantar) on paw withdrawal thresholds of male Wistar rats using an analgesymeter. Data are mean ±SEM with n=8 for sham treated group and n=8 for VZV-injected group. *p<0.05 using Repeated Measures ANOVA followed by Fisher's LSD post hoc test comparing to responses from untreated rats.*

With a positive effect in this study, albeit at only 2 timepoints, it was decided to use the same strain of host cell and the same strain of virus, but increase the amount of virus being injected into the rats to attempt to enhance the positive response.

4.2.2.6 Time course study 6

Male Wistar rats (270-290 g prior to inoculation; Charles River, UK) were used in study 6. Following the method for study 5, 8 rats received VZV-infected cells and

4 rats received uninfected cells. The main change to this protocol compared to study 5 was the volume of inoculum injected into the rats increased from 50 µl to 100 µl. Von Frey hair testing and paw pressure readings were carried out 1 day prior to inoculation and on days 6, 9, 12, 15, 20, 26 and 34 days post-inoculation.

When rats were tested for mechanical allodynia using von Frey hairs up to 60 g, there was no significant difference in the responses from sham-treated or VZV-injected rats on any of the test days (Figure 39). The ranges of PWTs from sham-treated and VZV-injected rats for all time-points post-inoculation were 32-52 g and 33-52 g respectively.

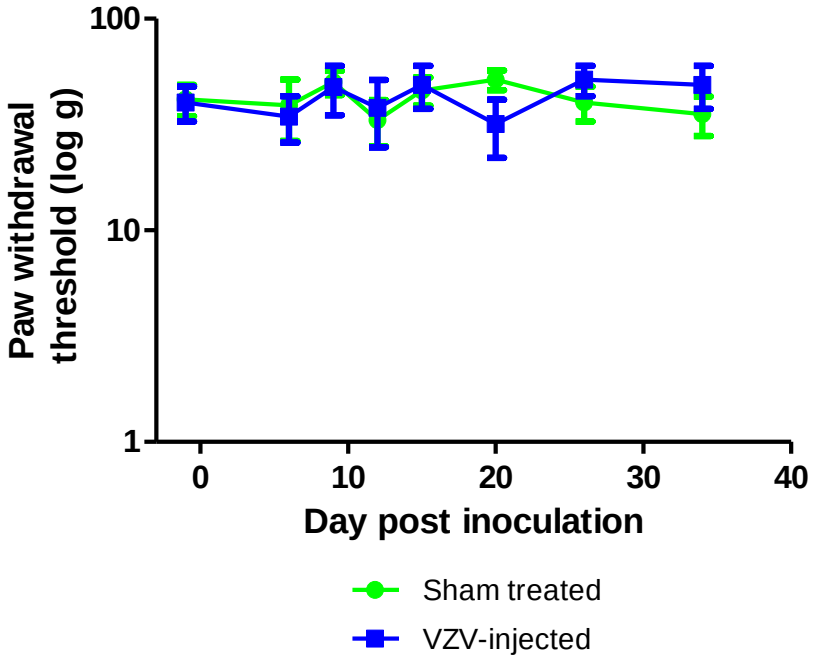

Figure 39. Effect of injecting VZV (Ellen strain) - infected MRC5 cells into the left paw (intra-plantar) on paw withdrawal thresholds of male Wistar rats following von Frey filament application. Data are mean ±SEM with n=4 for sham treated group and n=8 for VZV-infected group. Statistical analysis was completed using Repeated Measures ANOVA comparing to responses from sham treated rats, however there was no significant effect.

Similar data was observed when measuring the paw withdrawal thresholds using the analgesymeter (Figure 40). The ranges of PWTs from sham treated and VZV-

injected rats were 140-185 g and 114-180 g on all test days. Interestingly, the PWTs from both groups decreased over the time-course, there is no explanation for this other than rats exhibiting an anticipatory response as they become more familiar with the apparatus and potentially painful stimulus. This significance of this decrease however was minimal for current purposes as the objective was to achieve differentiation between VZV-injected and sham treated rats.

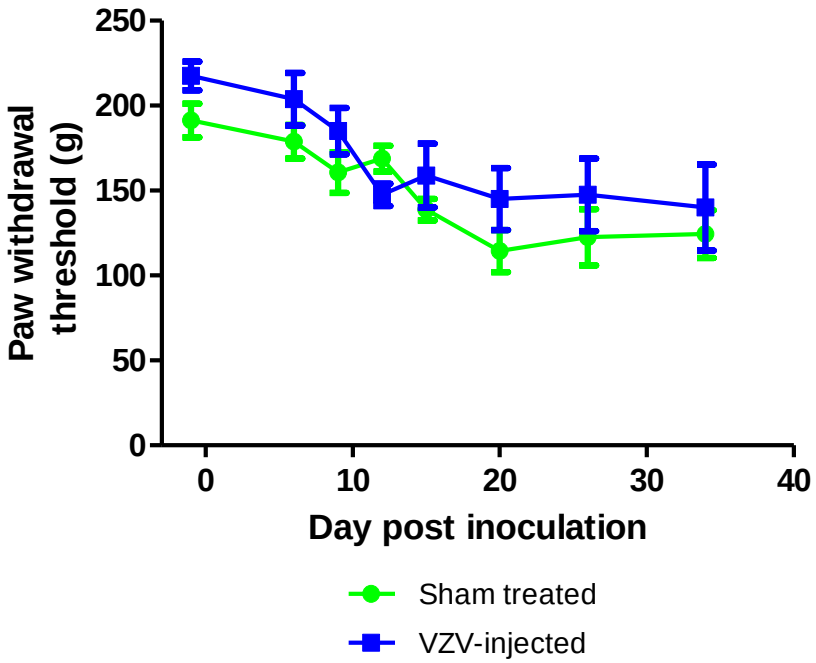

Figure 40. Effect of injecting VZV (Ellen strain) - infected MRC5 cells into the left paw (intra-plantar) on paw withdrawal thresholds of male Wistar rats using an analgesymeter. Data are mean ±SEM with n=4 for sham treated group and n=8 for VZV-injected group. Statistical analysis was completed using Repeated Measures ANOVA comparing to responses from sham treated rats, however there was no significant effect.

Having considered several individual experimental variables, the broader circumstances were considered. It was widely known that variations in data generated from similar studies occur between different laboratories. Specific explanations for these differences are often difficult to identify, but subtle differences such as methods

of husbandry, variety of food, levels of humidity and noise etc may be important. To address this, the next study used virus prepared from a lab that had shown success with this model, but also to have the rats injected and housed in the same lab. The chosen lab was at Edinburgh University by personnel who routinely run this assay and who were involved in the original publication (Dalziel et al., 2004).

4.2.2.7 Time course study 7

The cells were prepared by Dr. R. Dalziel in the same way the cells were prepared for when positive data had previously been generated. The injections were carried out in two groups of rats by myself and 'operator 2' and all behavioural testing performed by myself.

Male Wistar rats (240-460 g prior to inoculation; Charles River, UK) were used in this study. MRC5 cells were prepared and infected with Ellen strain of VZV by Dr. Dalziel in a similar way to previous studies that produced an effect. Rats were anaesthetised with halothane before 50 µl of infected cells (85% infectivity) were injected intra-plantar into the left paw. Operator 2 injected 8 rats, I injected 7 rats and 5 rats were left untreated. Von Frey hair testing was carried out 1 day prior to inoculation and 8 days post-inoculation using the same method used for all previous time course studies.

There was no significant difference on either test day, between responses obtained from untreated rats or VZV-injected regardless of the operator (Figure 41). The ranges of PWTs from untreated rats and VZV-injected rats for all time-points post-inoculation were 32-52 g and 33-52 g respectively.

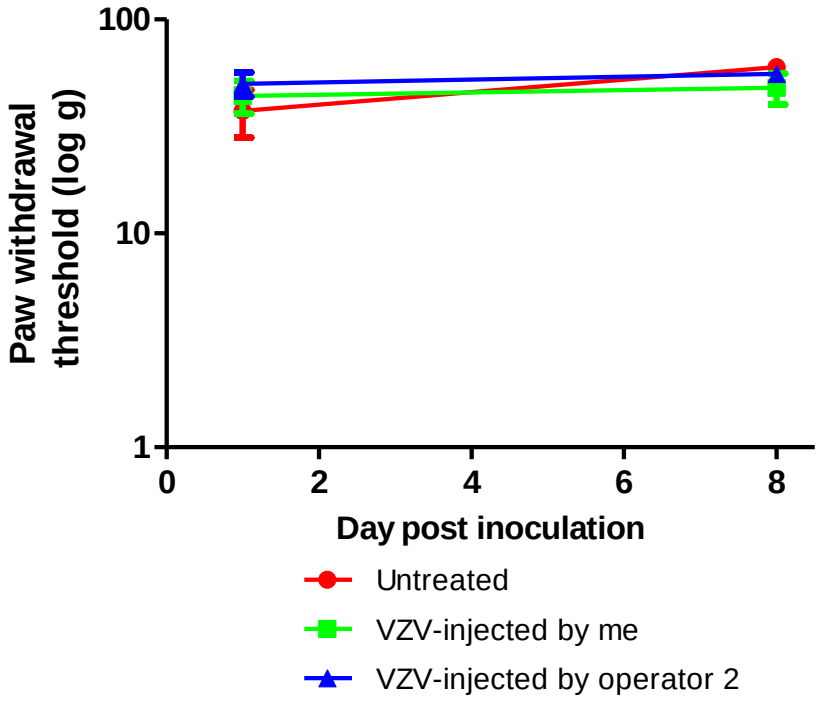

Figure 41. Comparing the effect of 2 different operators injecting VZV (Ellen strain) - infected MRC5 cells into the left paw (intra-plantar) on paw withdrawal thresholds of male Wistar rats following von Frey filament application. Data are mean ±SEM with n=5 for untreated groups, n=8 for group of rats injected with VZV by me and n=9 for group of rats infected with VZV by operator 2. Statistical analysis was completed using Repeated Measures ANOVA comparing to responses from untreated rats, however there was no significant effect.

These results suggested that any inadvertent differences that may have existed in the method used at GSK from the original method used by Dalziel et al. (1999) were not significant enough to negatively affect the data.

The final set of individual experimental variables that were changed for the final time course, were an attempt to increase the active viral load within the rat. This was done by firstly increasing the virus concentration within the inoculum and secondly, by reducing the cytopathic effect of the infected cells to ensure that the health of the cells had not deteriorated so excessively that the cells no longer had the ability of infecting the rats. The significance of the viral titre has been discussed in the

literature with one report claiming that differences in viral inoculum concentration could be responsible for the lack of significant effect (Delaney et al., 2009).

4.2.2.8 Time course study 8

Male Wistar rats (270-290 g prior to inoculation; Charles River, UK) were used in study 8. Following the method for study 6, 10 rats received VZV-infected (Ellen strain) cells (MRC-5 strain) and 8 rats received uninfected cells. Two changes to the protocol occurred in study 8 from previous studies. The first difference was that the inoculum was as concentrated with infected cells as possible with very little media present before PBS was added. The second difference was that the cytopathic effect (cpe) of the inoculum was reduced to 60% from 80% to ensure some live cells were present to infect the rats. Von Frey hair testing and paw pressure readings were carried out 1 day prior to inoculation and on days 4, 7, 17, 21 and 26 days post-inoculation.

There was no significant difference between the responses from sham treated and VZV-injected on any of the test days (Figure 42). The range of PWTs from both groups of rats for all time-points post-inoculation was 47-60 g.

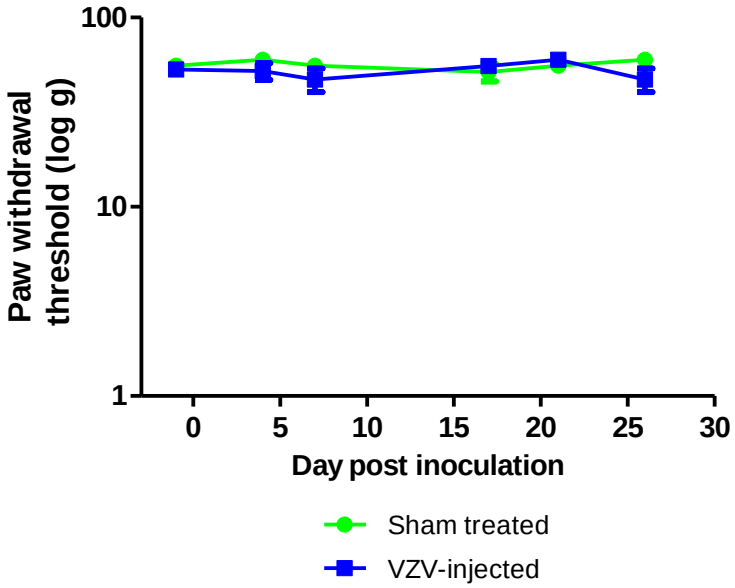

Figure 42. Effect of injecting 100 µl (instead of 50 µl) VZV (Ellen strain) - infected MRC5 cells into the left paw (intra-plantar) on paw withdrawal thresholds of male Sprague-Dawley rats following von Frey filament application. Data are mean ±SEM with n=8 for sham treated group and n=10 for VZV-injected group. Statistical analysis was completed using Repeated Measures ANOVA comparing to responses from sham treated rats, however there was no significant effect.

Similarly when PWTs were recorded using the analgesymeter, there was no significant difference between the responses from either group of rats on any of the test days (Figure 43). The ranges of PWTs from both groups of rats for all time-points post-inoculation was 153-196 g.

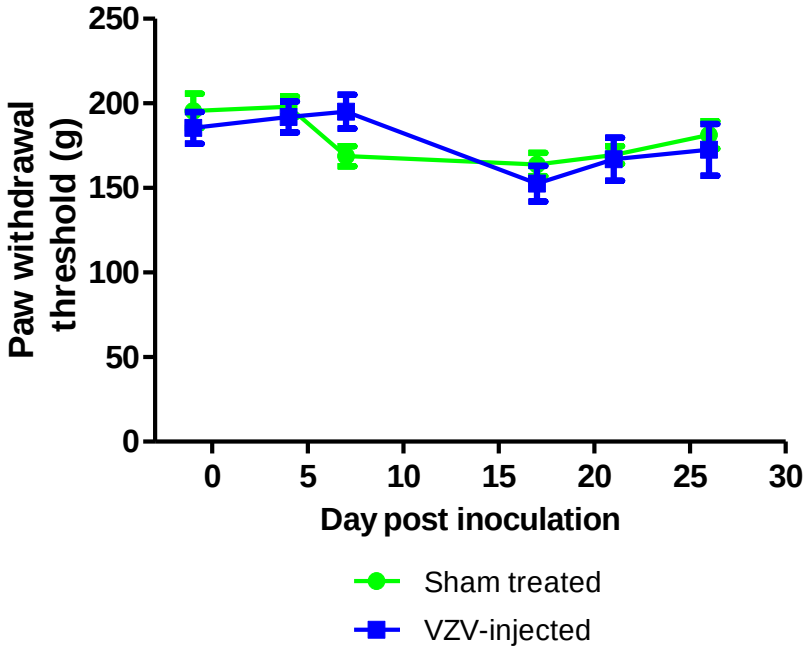

Figure 43. Effect of injecting 100 µl (instead of 50 µl) VZV (Ellen strain) - infected MRC5 cells into the left paw (intra-plantar) on paw withdrawal thresholds of male Sprague-Dawley rats using an analgesymeter. Data are mean ±SEM with n=8 for sham treated group and n=10 for VZV-injected group. Statistical analysis was completed using Repeated Measures ANOVA comparing to responses from sham treated rats, however there was no significant effect.

After changing several individual variables in the previous 8 studies, the final behavioural study was to take a different approach. If the virus was unable to evoke a response in the rat by itself due to its effect being too subtle, perhaps there was a possibility that the virus might produce an effect in rats that were already hypersensitive. Injecting capsaicin, the pungent component of hot chilli peppers, intra-dermally into the heel of rats produces a secondary mechanical and thermal allodynia/hyperalgesia in the footpad distal to the site of injection (Gilchrist et al., 1996). This is thought to involve sensitisation of dorsal horn neurones in the spinal cord (Gilchrist et al., 1996). As this proposed central site of action is similar to that proposed for the VZV-induced allodynia model (Cohrs et al., 2004), it seemed appropriate to investigate the effect of the virus on the secondary hyperalgesia induced by capsaicin.

Before assessing the effect the VZV virus had on the sensitivity of the rats paw to an injection of capsaicin, it was important to identify the most appropriate dose of capsaicin to use. In-house data had repeatedly shown that 10 µg of capsaicin in a 10 µl injection produced a maximum response and was often the dose used in literature (Medhurst et al., 2007; Bassani et al., 2005). For the purposes of this study however, a response lower than maximal was preferred to prevent any effect of the virus being masked.

In both the capsaicin dose response study and the capsaicin/ VZV combination study, hyperalgesia was assessed using the Dynamic Plantar Aesthesiometer (DPA, Ugo Basile) a device which delivers a constant pressure via a blunt metal probe to the plantar surface of rat paws (see methods in section 4.2.1.3.4). This equipment had historically been used within GSK for measuring secondary hyperalgesia due to the high-throughput nature of the readout.

4.2.2.9 Capsaicin dose response study

Paw withdrawal threshold (PWTs) were taken from 28 male Wistar rats (230-350 g, Charles River, UK) using the DPA. After a baseline reading, all rats were anaesthetised via the inhalation route with isoflurane mixed with oxygen (3:1) through a face mask. When rats were fully anaesthetised, capsaicin was injected into the heel at 3 different concentrations (0.3, 1, 3 µg in a 10 µl dosing volume) or vehicle (10% (v/v) ethanol, 10% (v/v) Tween, 80% (v/v) saline in a 10 µl dosing volume).

Twenty minutes after the injection, the rats were placed in the testing chambers for the 10 minute habituation period before PWTs we re-taken as described above.

The average baseline paw withdrawal threshold (PWTs) from all rats was approximately 40 g (Figure 44). When rats were dosed with vehicle there was no significant difference in PWT from the baseline threshold producing a PWT of 38±3.8 g. When rats were dosed with capsaicin at 0.3, 1 and 3 µg however PWTs were significantly lower producing PWTs of 31.3±4.8 g, 31.2±5.5 g and 28.4±3.9 g respectively. From this data it was decided that 3 µg would be the dose used in the subsequent exploratory study as the response appears less variable than the other 2

doses. Comparing this data with in-house data (not shown) using 10 µg, it also appeared that this effect was not maximal when using this model; therefore the response could potentially be decreased if the VZV virus had any effect.

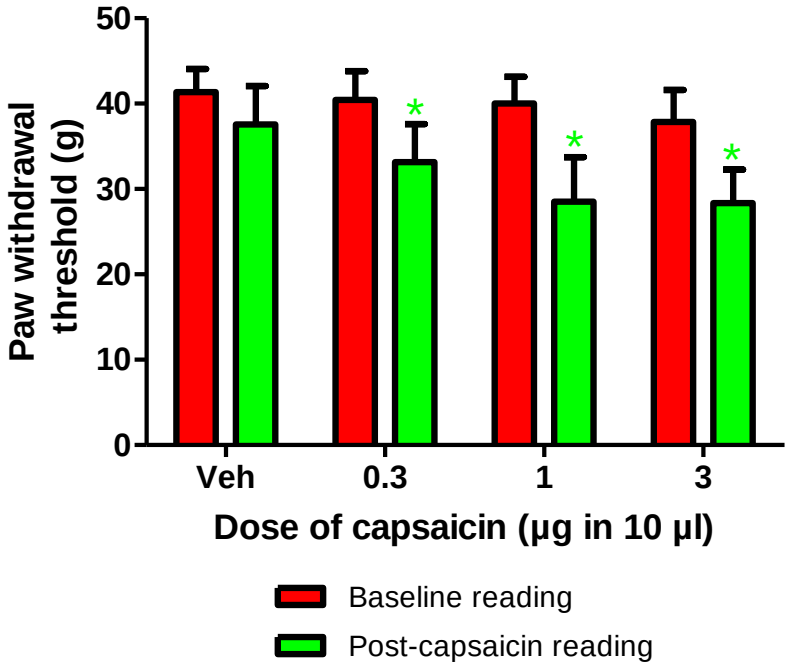

*Figure 44. Effect of injecting capsaicin (0.3-3 µg in a 10 µl volume) on paw withdrawal thresholds of Sprague-Dawley rats using a Dynamic Plantar Aesthesiometer. Data are mean ±SEM with n=7 for each group. *p<0.05 using Repeated Measures ANOVA followed by Fisher's LSD post hoc test comparing to treatment-matched baseline reading.*

4.2.2.10 Effect of VZV on the PWT of rats pre-dosed, via intra-plantar route, with capsaicin

Male Wistar rats (240-260 g prior to inoculation; Charles River, UK) were used. Rats received VZV-infected (Ellen strain) cells (MRC-5 strain) and 10 rats received uninfected cells. The cell suspension was as concentrated as possible and the cytopathic profile remained at approximately 60%.

Prior to inoculation, hyperalgesia was assessed in all rats using the DPA. Further readings were taken on day 8 and 14 post-inoculation. After the reading on day 14, rats were anaesthetised and dosed with either capsaicin (3 µg in a 10 µl dosing

volume) or vehicle (10% (v/v) ethanol, 10% (v/v) Tween, 80% (v/v) saline in a 10 µl dosing volume). Twenty minutes after the injection the rats were placed in the testing chambers for the 10 minute habituation period before PWTs we re-taken.

The average baseline PWT for all rats was approximately 37 g (Figure 45). On day 14 post-inoculation, PWTs remained at this level and were approximately 42 g, with no statistical difference between rats injected with VZV or uninfected cells. A lack of effect was also seen on day 14 when readings were taken 30 minutes after the vehicle for capsaicin was administered to rats previously inoculating with VZV, producing a PWT of 38.9 ±2.4 g. In rats dosed with capsaicin following inoculation with uninfected cells however, PWTs significantly reduced to 30.3 ±3.9 g. Similarly, PWTs from VZV-inoculated rats receiving capsaicin also significantly decreased producing thresholds of 32.9 ±2.6 g. There was however no difference between PWT reductions between the two groups suggesting that VZV had no effect on capsaicin-induced secondary hyperalgesia.

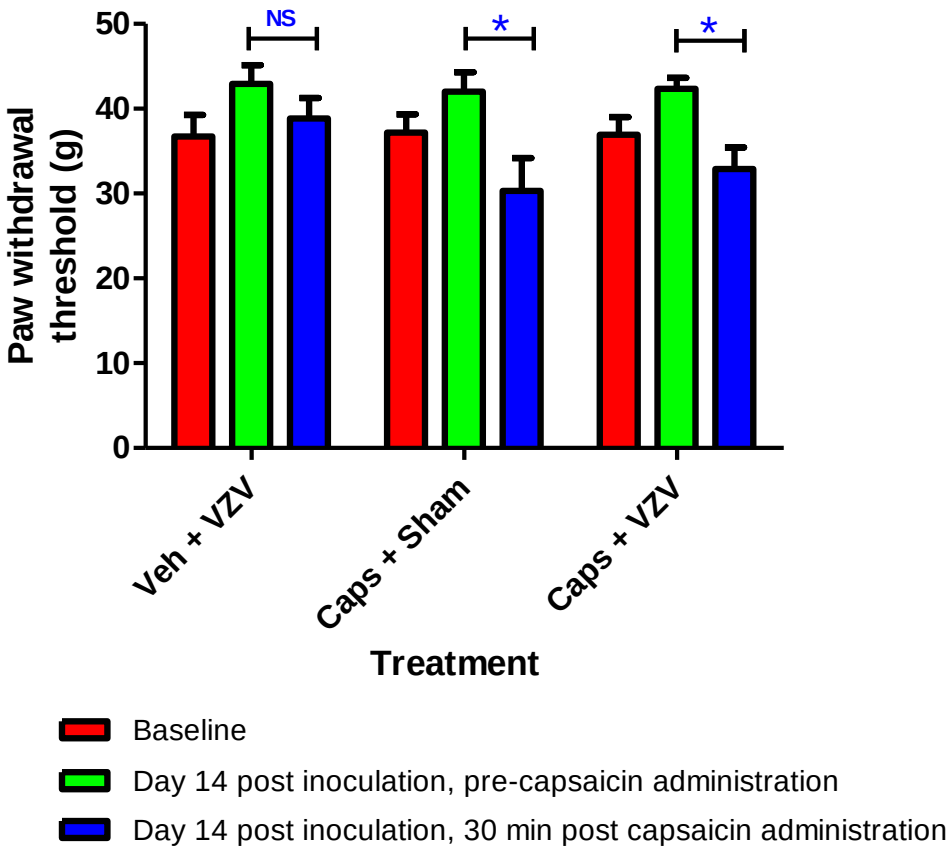

*Figure 45. Effect of injecting capsaicin (3 µg in a 10 µl volume) on paw withdrawal thresholds, using a Dynamic Plantar Aesthesiometer, of Wistar rats injected with VZV (Ellen strain)-infected MRC5 cells. Data are mean ±SEM with n=10 for each group. *p<0.05 using Repeated Measures ANOVA followed by Fisher's LSD post hoc test comparing to 'day 14 post-inoculation pre-capsaicin' readings. NS denotes a non-significant effect.*

4.3 Expression of VZV mRNA in host cells and in DRGs of inoculated rats

4.3.1 Introduction

Due to the inability of translating the *in vitro* actions of VZV on cells within a flask to *in vivo* actions of VZV on native cells within a rat, it was decided to investigate the status of the infected cells post-inoculation. The first approach was to establish the presence of viral genetic material in the DRG of inoculated rats.

The complete DNA sequence of the VZV Dumas strain was first reported, in 1986 (Davison et al., 1986), as a linear double-stranded DNA of about 124 884 base pairs. The genome is composed of 71 open reading frames (ORFs) encoding 68 proteins. To date, transcripts encoding VZV ORFs 4, 21, 29, 62, 63, 66 have been detected in human ganglia (Kennedy et al., 2000; Cohrs and Gilden, 2003). All but ORF66 have been detected in the rat model of VZV latency (Sadzot-Delvaux et al., 1995; Kennedy et al., 2001) and ORF21 and ORF66 have been shown to be dispensable *in vitro* (Sato et al., 2003). From the few studies which have investigated VZV gene translation, ORF63-coded immediate-early protein is most established in both human and rat (Sadzot-Delvaux et al., 1995; Fleetwood-Walker et al., 1999; Kennedy et al., 2000; Kennedy et al., 2001). ORF63-coded protein will be used in the current studies as a marker for viral presence in the DRGs of rats inoculated with VZV.

4.3.2 Method

Before investigating the presence of viral material in the rat tissue, it was necessary to validate the method and the reagents by assessing the content of viral material in the host cells contained within flasks.

4.3.2.1 Sample preparation

4.3.2.1.1 Cells

VZV-infected MRC5 cells (~80% cytopathic) and non-infected cells were gently scraped off two T175 flasks, spun down and the supernatant discarded. 600 µl of RLT lysing buffer (Qiagen, Germany; comprising of 10 µl mercaptoethanol to 1 ml of RCT buffer (e.g. 50 µl + 4950 µl) was added to each pellet. This mixture was then put into a Qiashredder (Qiagen, Germany) tube and spun for 2 minutes at 12000 x gravity and then stored at -80 °C.

4.3.2.1.2 DRGs

After rats had been euthanised at the end of time course study 8, ipsilateral and contralateral L4 and L5 dorsal root ganglions (DRG's) were removed and stored in 2 ml screw-cap tubes on cardice prior to placing in -80 °C freezer. Samples were taken from 2 rats that had been injected with VZV-infected cells and 2 rats that had been injected with non-infected cells 26 days after inoculation.

DRGs were homogenised using a tissue lyser (Qiagen, Germany), a laboratory vibration mill used to homogenize biological samples using stainless steel beads. The milling process was brought about by the beating effect of a steel grinding ball on the material the friction between the grinding ball and the wall of the tube.

Steel cone balls were washed in 70% (v/v) alcohol and then washed in diethylpyrocarbonate (DEPC) water before being transferred into the tubes with DRGs using clean forceps. 200 µl QIAzol lysis reagent was added and tubes were kept on ice. Tubes were transferred to both racks of the Mixer Mill Adapter Set with a cover being placed on the top and bottom of each rack before inserting them into the holding positions in the Mixer Mill. The frequency was set to 30 Hz, the time was set to 5 min and the start button was pressed. Once the machine had stopped, samples were removed and put on ice.

After mixer milling, the tubes were spun at 13000 x gravity for 15 mins at 4 °C, before taking off supernatant avoiding the layer of fat at the top and debris at the bottom of the tube. The tube containing the homogenate was then placed on the benchtop at room temperature for 5 min.

Chloroform (200 µl) was then added in the fume hood to separate homogenate into aqueous phase while DNA partitioned to the interphase and proteins to the lower, organic phase or the interphase. The tube containing the homogenate was capped securely and vortexed vigourously before being placed on the benchtop at room temperature for 2-3 min. The tube was then centrifuged at 12,000 x gravity for 15 min at 4 °C before the upper aqueous phase was transferred to a new collection tube.

4.3.2.2 Purification of genetic material for both cells and DRGs

Purification of genetic material was done using the RNeasy mini protocol, as detailed in the manufacturers instructions. 1 volume of 70% (v/v) ethanol was added to provide appropriate binding conditions and mixed thoroughly. The sample was added to an RNeasy mini spin column in a 2 ml collection tube. The tube was closed gently and centrifuged at 12,000 x gravity for 15 s at room temperature, discarding the flow-through and reusing collection tube. 100 µl buffer RW1 was then added to the RNeasy mini spin column and centrifuged for 15 s at 12,000 x gravity to wash the column. The flow-through was discarded and the collection tube re-used. 10 µl DNase I stock solution was added to 70 µl buffer RDD per reaction. The tube contents was gently mixed and kept on ice. DNase I incubation mix (80 µl) was pipetted directly onto the RNeasy silica-gel membrane, and placed on the bench-top at room temperature for 15 min. 100 µl buffer RW1 was then pipetted into the RNeasy mini spin column, and centrifuged for 15 s at 12,000 x gravity, discarding the flow-through and collection tube. The RNeasy spin column was transferred into a new 2 ml collection tube and 500 µl buffer RPE was pipetted onto the RNeasy spin column before being centrifuge for 15 s at 12,000 x gravity to wash the column. The flow-through was discarded and the collection tube was re-used. Another 500 µl buffer RPE was added to the RNeasy column and centrifuged for 2 min at 12,000 x gravity to dry the RNeasy silica-gel membrane. The RNeasy spin column was placed into a new 2 ml collection tube, and the old collection tube discarded with the flow-through before being centrifuged in a microcentrifuge at full speed for 1 min. To elute, the RNeasy mini spin column was transferred to a new 1.5 ml collection tube and 50 µl RNase-free water was pipetted directly onto the RNeasy silica-gel

membrane which was centrifuged for 1 min at 12,000 x gravity. The elution step was repeated using the eluate. All extracted RNA was kept on ice.

4.3.2.3 Quantification of nucleic acids from cells and DRG samples

The quantification of nucleic acids was done using the nanodrop machine (Labtech International Ltd) which is a full spectrum (220-750 nm) spectrophotometer. Using a pipette, 1.2 µl of water was loaded onto the pedestal to allow calibration of the nanodrop machine. After wiping off water from both surfaces using a soft tissue, 1.2 µl of blank was loaded (water, elution buffer) onto the pedestal. After wiping off the blank, 1.2 µl of each sample was loaded onto the pedestal in turn, wiping the previous sample off the pedestals each time.

Using example data the following calculation matrix was created with the data generated from the nanodrop machine.

Sample no.	[RNA] ng/µl	µl for 1 µg RNA	X4 (triplicate + -R)	In 40 µl H_20
A	330	1000/330	(1000/330)x4	40-((1000/330)x4)
B	450	1000/450	(1000/450)x4	40-((1000/450)x4)

4.3.2.4 Conversion of RNA to cDNA from cell and DRG samples

RNA was converted to cDNA for amplification of the specific gene sequences via reverse transcription (RT) using Omniscript reverse transcriptase kit (Qiagen, Germany). Diluted RNA was aliquoted into 96 well plates whilst keeping samples on ice.

The RT mastermix was made up as detailed below:

	Volume/reaction (generic, µl)		x total no. Reactions (µl)	
	+RT	-RT	+RT (e.g.20x)	-RT (e.g. 8x)
10 x buffer RT	2	2	40	16
dNTP mix	2	2	40	16
oligodT (10 µM)	1	1	20	8
RnaseOut* (10 µM/µl)	1	1	20	8
Omniscript RT	1	-	20	-
dH_2O	3	4	60	32

** Dilute RNaseOUT to 10 units/ul in 1 x buffer RT (1:4 dilution):*

RT mastermix (10 µl) was aliquoted into each well (i.e. 3 RT+ and 1 RT- for each sample) into a 96 well plate, a foil lid was added and the plate was spun down briefly. The plate was incubated at 37 °C for 60 min and at 93 °C for 5 min in a PCR system (GeneAmp 9700, Applied Biosystems) before being spun for 1 minute. Finally, 60 µl RNase free water was added to each well, the foil was replaced and vortexed and spun for 1 min. To prepare test plates, 4 µl of each sample was added to each well before the plates are stored in -80 °C.

4.3.2.5 Quantitative measurement of gene expression

4.3.2.5.1 Quantitative measurement of ORF63 expression in cells and DRGs and GAPDH expression in cells using SYBR green RT-PCR

Quantitative measurement of ORF63 expression was performed using SYBR green RT-PCR, a technique which enables the measurement of an accumulating PCR product in real time using only 2 primers. This method uses SYBR Green I dye to detect PCR products by binding to double stranded DNA formed during PCR. When

SYBR Green PCR Master Mix is added to a sample, SYBR Green I dye immediately binds to all double stranded DNA. During the PCR, AmpliTaq Gold DNA Polymerase amplifies the target sequence, which creates the PCR product. The SYBR Green I dye then binds to each new copy of double stranded DNA. As the PCR progresses, more product is created. Since the SYBR Green I dye binds to all double stranded DNA, the result is an increase in fluorescence intensity proportional to the amount of double stranded PCR product produced.

The SYBR green master mix was first made up:

	For 1 well (µl)	For 40 wells (µl)
Syber mastermix (2x)	10	400
DEPC H_20	4.8	192
Forward primer (10 µM)	0.6	24
Reverse primer (10 µM	0.6	24

The primers for ORF63 was kindly donated by Dr. R Dalziel, University of Edinburgh and are listed in the appendix. In order to control for variations in the quality and quantity of mRNA between samples, the commonly used housekeeping gene, GAPDH was included. The primers for GAPDH were purchased from Sigma Genosys as bespoke oligos..

16 µl of mix was transferred to reservoir, an optical adhesive cover was stuck on the top before the plate was spun at 134 x gravity for 1 min and placed on ice. The plate was placed into the 7500 fast system PCR machine.

The programme involved incubating the plate for 10 minutes at 95 °C before 40 cycles were commenced. A cycle consisted of 15 seconds at 95 °C followed by 1 minutes at 60 °C.

When data was retrieved the following formula was used.

10^((40-Ct)/3.3)

Key: Ct is cycle time, ^ is 'to the power of'.

Once calculated the –RT values were taken from the 3 +RT values before data was averaged and presented as copies per 1 µg RNA ±SD.

4.3.2.5.2 Quantitative measurement of GAPDH expression in DRGs using Taqman RT-PCR

Quantitative measurement of gene expression of GAPDH was performed using Taqman RT-PCR, an alternative technique to Syber green RT-PCR which uses a flurogenic probe in addition to primers for measuring PCR product in real time.

The oligonucleotide probe is constructed with a florescent reporter dye bound to the 5' end and a quencher on the 3' end. When the probe is intact, the proximity of the quencher greatly reduces the fluorescence emitted by the reporter dye. However when cleaved the reporter dye signal increases which forms the method of quantitative measurement of mRNA. Figure 46 illustrates the process which is followed by a brief description.

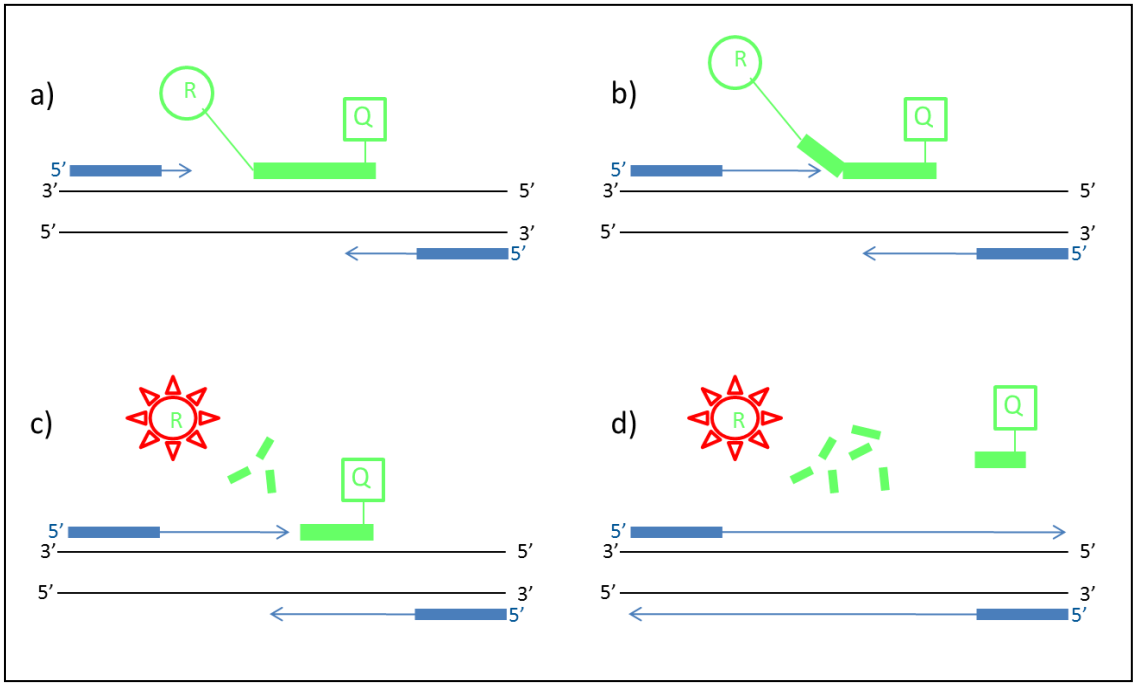

Figure 46. Schematic representation of Taqman PCR (Medhurst et al., 2000).

During PCR if the target sequence is present, the probe anneals between the forward and reverse PCR primers (a) and is displaced by the Taq polymerase during amplification (b). The endogenous 5'-3' nuclease activity of Taq polymerase then

cleaves the probe separating the reporter dye from the quencher dye, thereby increasing the fluorescence (c). The remaining probe dissociates from the target sequence allowing the polymerase reaction to continue (d). This process occurs each cycle resulting in an increase in fluorescence intensity which accumulates over time. The intensity of fluorescence is directly related to the amount of target DNA and the higher the starting copy number of the target sequence the sooner a significant increase in fluorescence is observed. For each sample an amplification plot is generated showing the increase in fluorescence with each cycle of PCR. From each amplification plot a threshold cycle time was calculated which represents the PCR cycle number at which the fluorescence was detectable above an arbitrary threshold. By using the cycle times of known quantities of genomic DNA, the initial quantity of cDNA template per well can be estimated. In order to control for variations in the quality of mRNA between samples, internal control genes were used, known as 'housekeeping'genes. Data generated from the housekeeping genes was also used for normalising the data from the genes of interest to correct for variations in RNA and/or cDNA quality and quantity.

In the current study, a genomic DNA standard was prepared in DEPC H_2O: 100 µl of each total: 1, 1/10, 1/100, 1/1000, 1/10000 (1/10 serial dilution: 10 µl gDNA, 90 µl H_2O and vortexed and centrifuged briefly.

The RT plate was then removed from -20 °C and left to defrost before being centrifuged and placed on ice. 7500 Taqman master mix was prepared in a 15 ml falcon, mixed and spun

The Taqman master mix was first made up:

	For 1 well (µl)	For 40 wells (µl)
Taqman Universal PCR mastermix	10	400
DEPC H_20	4.4	176
Forward primer (10 µM)	0.6	24
Reverse primer (10 µM	0.6	24
Taqman probe (5 µM)	0.4	16

Primers and probes are listed in the appendix and were purchased from Sigma Genosys as bespoke oligos. 4 µl gDNA (i.e. standard) dilutions was pipetted into appropriate wells and H_2O into a spare well. The mix was transferred to a reservoir, 16 µl was dispensed into each appropriate well, including gDNA wells and an optical adhesive cover was stuck over the plate. The plate was centrifuged at 134 x gravity for 1 min and placed into the 7500 fast system PCR machine.

The programme involved incubating the plate for 20 seconds at 95 °C before 40 cycles were commenced. A cycle consisted of 3 seconds at 95 °C followed by 30 seconds at 60 °C.

When the programme had completed the data was exported into Microsoft Office Excel, the –RT values were taken from the 3 +RT values before data was averaged and presented as copies per 1 µg RNA ±SD.

4.3.3 Results

4.3.3.1 Expression of ORF63 in infected cells pre-inoculation.

Before investigating the presence of viral material in rat tissue, it was necessary to validate the method and the primers. This was done by determining the content of viral material within the host cells contained within the cell culture flasks. ORF63 was abundant in VZV-infected cells (~$1.0x10^{07}$ copies) whereas there was less than 100 copies in the sham treated cells (Figure 47).

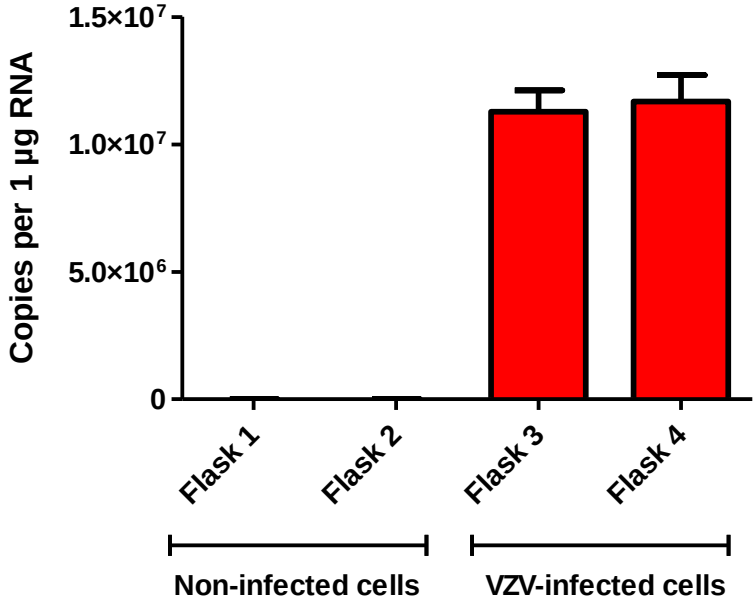

*Figure 47. ORF63 expression in VZV-infected and uninfected cells pre-inoculation. Data is represented as mean ±SD. *p<0.05 using one-way ANOVA comparing both flasks 3 and 4 to flasks 1+2.*

The housekeeper gene GAPDH was present in all flasks, however it appeared that a significantly less amount was found in the VZV-infected cells than the non-infected cells, ~100000 to 50000 (Figure 48). When the expression of VZV- and non VZV- flasks were added together and compared, a statistically significant difference was observed ($p<0.05$). This might be due to a large number of dead cells present post-VZV-infection. On this occasion, the presence of GAPDH in all flasks was sufficient information to validate the method.

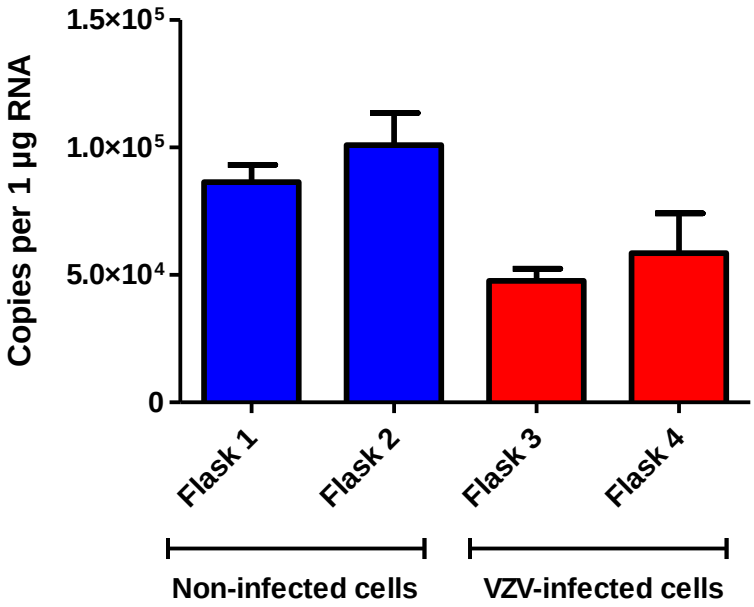

Figure 48. Housekeeping gene GAPDH expression in VZV-infected and non-infected cells pre-inoculation. Data is represented as mean ±SD.

This positive expression data validates the method, primers and reagents in preparation to investigate ORF63 expression in rat tissue.

4.3.3.2 Expression of ORF63 in VZV-infected rat DRGs

Expression of ORF63 was variable, very low and was no different between the ipsilateral and contralateral DRGs in VZV-injected rat or the DRGs in sham treated rats (Figure 49).

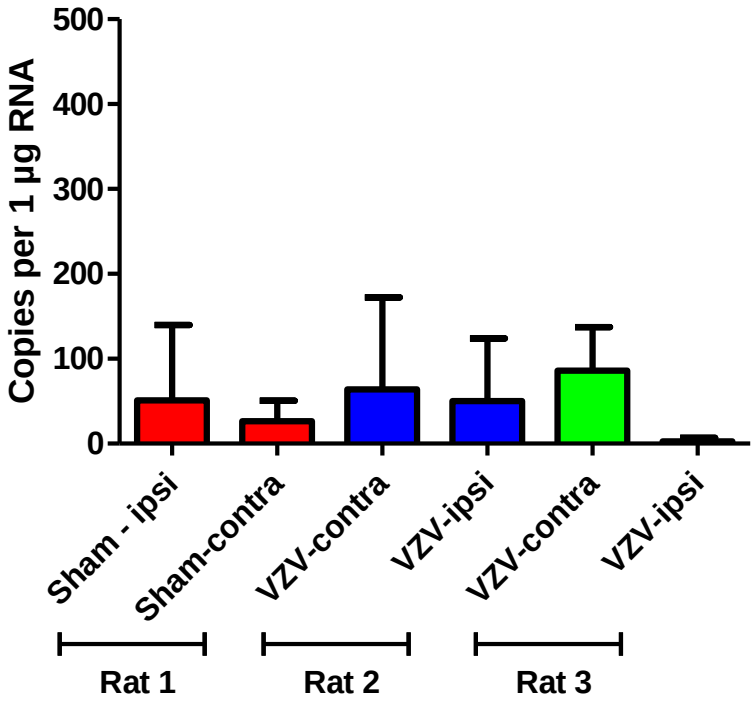

Figure 49. ORF63 expression in infected dorsal root ganglions in VZV-inoculated rats and sham treated rats. Data is represented as mean ±SD.

Copies of the house hold gene GAPDH were variable, producing around 30000 copies per 1 µg of RNA (Figure 50). GAPDH was included in the study to act as a control and this data suggested that RNA integrity was unchanged with treatment.

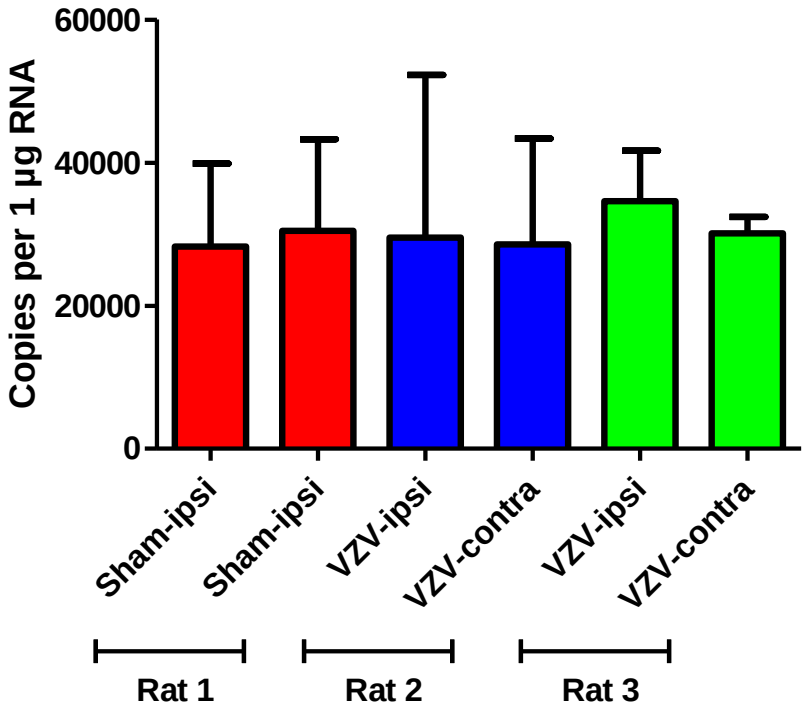

Figure 50. GAPDH expression in infected dorsal root ganglions in VZV-inoculated rats and sham treated rats. Data is represented as mean ±SD.

In summary, this data suggests that there was no VZV present in the DRG of rats injected with the virus via the intra-plantar route.

4.4 Discussion

The aim of this chapter was to compare the potentiating effects of combining a P2X7 receptor antagonist and morphine demonstrated in the nerve injury model, to the effects observed in a disease-induced neuropathic pain model. It was then intended to investigate any differences in microglia and IL-1β involvement for each of the models to ascertain the importance of the neuronal-glial interaction in the mechanism of action of P2X7 receptor antagonists.

Prior to any exploratory study using novel compounds, characterisation of the model was first required to confirm reproducibility from study to study and to allow comparison with the literature. With negative results in the first time course study it was decided to optimise the method to ensure the model was robust enough to test compounds.

Optimisation consisted of changing several variables in a systematic way from one study to the next. One consideration throughout this process was not to change too many variables at once, thereby complicating the interpretation of any positive result. This approach however needed to be balanced with the ethical awareness of keeping the number of animals used to a minimum and yet obtaining the most information from one study.

The decision of which variables to change came from a number of sources;

- considering the literature (e.g. change of rat strain, virus strain, strain of host cell, behavioural readouts)
- considering the clinical disease (e.g. increasing the age of rats)
- considering inherent experimental differences between labs (e.g. running study in Edinburgh, increasing von Frey cut-off pressure to 60 g)
- considering the knowledge of the virus itself (e.g. use of Accutase, levels of confluency of host cells prior to infection, level of cytopathic effect)
- considering the host cell (e.g. number of passages)
- considering the inoculum (e.g. increasing the volume and concentration)
- considering the inoculation procedure (e.g. reducing the size of the needle)

- considering the problem from a different perspective (e.g. incorporating a secondary insult).

After changing many variables and not observing any allodynic effects, it was important to establish where the virus was located post-inoculation. Although there were several publications reporting the presence of virus in the DRG (Dalziel et al., 2004; Garry et al., 2005; Hasnie et al., 2007), it was not possible to confirm the presence of viral genetic material in the current studies. To confirm the lack of viral genetic material a subsequent study could be run looking at DNA, as opposed to RNA, which is more abundant and more robust.

There is currently no explanation for the lack of infection resulting in the lack of behavioural effect. What is confusing are the several reports, albeit from just two laboratories, of robust allodynia when VZV is injected this way (Fleetwood-Walker et al., 1999; Dalziel et al., 2004; Hasnie et al., 2007; Wallace et al., 2007b).

Other labs have also shown, using *in vivo* and *in vitro* methods, that VZV can infect rat cells (Merville-Louis et al., 1989; Sadzot-Delvaux et al., 1990; Sadzot-Delvaux et al., 1995; Kennedy et al., 2001; Kress and Fickenscher, 2001), however only two labs have shown this effect is translated to allodynic responses. It is unfortunate that other groups have not published on this model to build up a larger dataset to assess the reproducibility more satisfactorily. One potential explanation why so few groups use this model could be the lack of reproducibility. Given the known species selectivity of the virus and the lack of other disease-induced symptoms; maybe it is not surprising that this model is less reproducible than previously reported. It is also worth noting that between the two labs who have published on this model, differences exist. Hasnie et al. (2007) were not able to reproduce the thermal hyperalgesia that was reported by Fleetwood-Walker et al. (1999). The explanation given for this difference was ‘due in part to experimental differences e.g. in viral inoculum concentration’, which was a variable already considered in the current studies.

For ethical reasons it was decided that optimisation of the model would stop. If optimisation was to be continued however, the following studies would have been considered. Plaque titration would be performed in order to accurately determine the

quantity of infectious virus,. Briefly this involves serial dilutions of viral inoculum propagated onto a cell line and allowed to form plaques. The number of 'plaque forming units' (pfu) determined would allow a retrospective estimate of the amount of virus in the inoculums to be calculated (pfu/ml). This would allow more accurate assessments between experiments and avoid a potential area of subjectivity when assessing the cytopathic effect.

It would also be recommended to analyse different samples, other than just DRGs, post-inoculation, to establish exactly where the virus was located once injected into the rat. For example, samples from the paw, the sciatic nerve and the spinal cord could be analysed to determine how far the virus had progressed from the injection site. The dorsal horn of the spinal cord would be one area of particular importance (Fields et al., 1998).

Further recommendations would be to look at other strains of the virus, including a fresh clinical isolate at a very low passage, to ensure that method was not strain specific. Finally, it would be recommended to analyse DRGs and spinal cord immunohistochemically to identify the location of IE62 protein, a protein which is commonly used as a marker for VZV, as opposed to viral genetic material, to compare directly with literature (Fleetwood-Walker et al., 1999; Kress and Fickenscher, 2001; Hasnie et al., 2007).

In conclusion, this chapter has demonstrated that the VZV-induced allodynia rat model of post herpetic neuralgia – like pain could not be reproduced using methods published by other laboratories. The model was therefore not characterised sufficiently for a comparison of the P2X7 receptor antagonist and morphine combination effects with the CCI to be investigated.

Chapter 5

Effect of P2X7 antagonism on other actions of morphine

5. Effect of P2X7 antagonism on other actions of morphine

5.1 Introduction

Previously in Chapter 3 it was demonstrated, using the CCI rat model of neuropathic pain, that P2X7 receptor antagonists may have the ability to enhance the analgesic properties of repeatedly dosed morphine. The hypothesis for this was that the P2X7 receptor antagonist inhibited the counteracting activity of proinflammatory cytokines released from microglia allowing morphine to act more effectively.

This chapter focuses on whether P2X7 receptor blockade of microglia activity influences other actions of morphine, including those that are desirable and those that are not (i.e. side-effects).

Firstly, this chapter investigates whether the potentiating effect observed with repeated co-dosing of a P2X7 antagonist and morphine in CCI-induced allodynia are also observed in a single dose acute pain paradigm in naive rats. This data is important, as it may suggest that even a single dose of morphine, which is often administered in the clinic for acute pain, could be made more effective.

Initially the majority of research in this field focused on the elevation of microglia and proinflammatory mediators following only the repeated administration of morphine (Song and Zhao, 2001; Raghavendra et al., 2002; Johnston et al., 2004). In 2005 however, it was demonstrated that analgesia produced by an acute dose of morphine in mice was abolished with a single administration of IL-1β, and that analgesia was re-instated and potentiated when IL-1β was co-dosed with IL-1 receptor antagonist (Shavit et al., 2005). These findings were then extended in rat studies producing data that suggested that the opposing action of proinflammatory cytokines in morphine analgesia was likely to be dependent on spinal microglia (Hutchinson et al., 2008a). The data therefore suggested that even in non-sensitised, naïve rats, analgesia induced by acute morphine may also be enhanced with co-administration of a P2X7 receptor antagonist.

The second part of this chapter focuses on how a combination of P2X7 receptor antagonist and morphine could impact the undesirable effects of morphine. This data is of particular importance. For example, if undesirable effects were also potentiated along with analgesia there would be little gained from combining both compounds. On the other hand, if side effects remained unaffected and the effective analgesic dose of morphine was able to be reduced, the therapeutic window could be widened and the clinical utility of morphine could be increased.

It was at the beginning of the 19th century when one of the most significant side effects of morphine, named after Morpheus the Greek god of dreams, was first realised. Sedation and depression of motor activity in humans is a side effect that continues to confound the use of opioids in the clinic (Hayes and Tyers, 1983; Bowdle, 1998; Meert and Vermeirsch, 2005). In rats it has also been shown that high doses of morphine result in sedation and induce a decrease in motor performance (Meert and Vermeirsch, 2005). Any potential influence that a P2X7 receptor antagonist has on this effect however is unknown and will be investigated in this chapter.

Another morphine-induced action to be considered is reduction in body weight gain. Whilst acute administration of morphine in humans and rats increases food intake and weight gain in a naloxone reversible manner (Shimomura et al., 1982; Levine et al., 1988), repeated administration over a longer period of time lowers food intake and reduces body weight (Levine et al., 1985; Atkinson, 1987). The effect of co-dosing a P2X7 receptor antagonist on morphine-induced 'lack of body weight gain' in rats is currently unknown and is the final aspect considered in this chapter.

5.2 Methods

5.2.1 Paw withdrawal threshold of naive rats

To assess the effect of combining a P2X7 receptor antagonist and morphine on paw withdrawal thresholds (PWTs) of naïve rats to a noxious mechanical stimulus, paw pressure assessments were carried out using an analgesymeter (Ugo Basile, Italy, see previous method section 4.2.1.3.2).

In Chapter 4, the analgesymeter was used to measure paw withdrawal thresholds from rats before and after VZV inoculation with an intention to measure mechanical hyperalgesia. On this occasion however, although the same device is used, there are subtle differences due to naïve rats being used, as opposed to rats that have been manipulated in some way for use in a disease paradigm. Methods were conducted according to Skingle et al. (1990) with an increasing mechanical pressure applied to the left hind paw of naïve rats until paw withdrawal occurred, at which point the force (g) was recorded.

Baseline readings were first taken to assess the 'normal' paw withdrawal reflex of each individual rat. The baseline readings were ranked and randomised, according to Latin square design, in order to assign the rats to dose groups with similar PWTs. After drug administration, a post-dose reading was taken at an appropriate time (see results section 5.3 for individual protocols). A cut off was set at 500 g, as opposed to the cut-off of 250 g used in Chapter 4, and data are presented as PWT (g) with 7 rats in each dosing group. The study was performed with the operator blind to which treatment each group received.

For drug studies, all oral dosing was performed at 5ml/kg and all subcutaneous dosing was performed at 2 ml/kg. Statistical analysis was carried out on PWTs, where post compound readings were compared to baseline readings using ANOVA followed by a Fisher's LSD post hoc test, where $p<0.05$ was considered significant

5.2.2 Motor coordination

The accelerating rota-rod test is a sensitive method for quantifying impaired motor function or changes in co-ordination (Jones and Roberts, 1968). The apparatus consists of a number of chambers attached to a rotating drum which can be rotated at an increasing or constant speed (see Figure 51). The rotating drum is suspended above the base of the apparatus high enough to induce avoidance of fall but not high enough to injure the rat. Rats naturally try and stay on the drum and it is the length of time that the rat remains on the drum that is recorded in seconds.

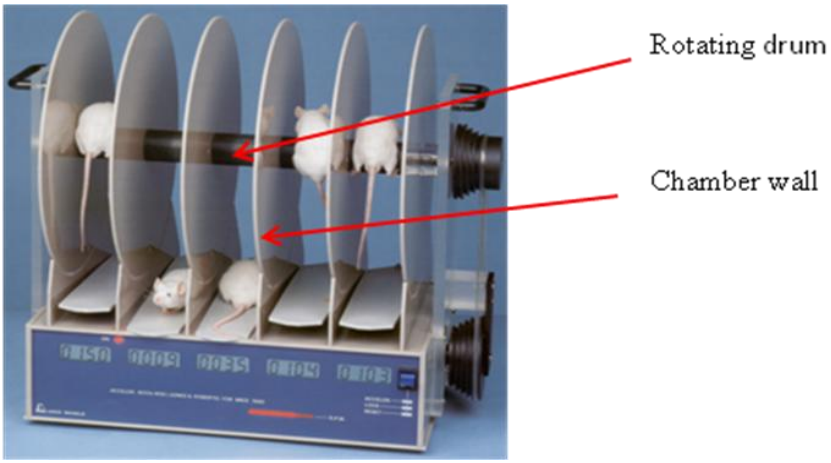

Figure 51 The rota-rod apparatus (Ugo Basile, Italy) was used to assess motor function and changes in co-ordination.

Naïve rats were first acclimatised to the procedure room in their home cage with food and water available *ad libitum*. All rats were trained to remain on the rota-rod at a fixed speed of 2.5 r.p.m. for a minimum period of 90 seconds. Only successfully familiarised rats were used in experiments. Rats were assigned to dosing groups according to a Latin square design. After training, rats were dosed with compound or vehicle and tested for motor coordination at specific times post-dose. During testing all rats were assessed for their ability to remain on the rotating rod while in the acceleration mode from 2.5-20 r.p.m. A cut off of 300 seconds (5 mins) was employed at which time the highest speed had been reached. All studies were performed with the operator blind to which treatment each group received.

Data are presented as mean ±SEM in seconds with n=10 per dosing group. Statistical analysis was carried out on raw data and all drug dose groups were compared with the vehicle treated rats using Repeated Measures ANOVA, followed by Fisher's LSD post hoc test, where $p<0.05$ was considered significant.

5.2.3 Body weight

The effect of co-dosing morphine and GSK1370319 on body weight of rats over time was investigated. Data was generated, using a calibrated balance, from two studies; a CCI study (Section 3.3.3) and a rota-rod study (Section 5.3.2.2).

5.3 Results

5.3.1 Paw withdrawal threshold of naive rats

A morphine dose response study and a P2X7 receptor antagonist study were first carried out to assess the effects of the compound when dosed alone, and to aid the identification of suitable doses for the combination studies.

5.3.1.1 Morphine dose response study

Baseline readings were taken from 28 male Lister hooded rats and dosed with morphine (1, 5, 10 mg/kg) or vehicle (saline) subcutaneously with n=7 in each group. Post-dose readings were taken 30 minutes and 2 hours later.

Mean baseline paw withdrawal thresholds for all rats was 213 ±4 g (Figure 52). When dosed with vehicle, the PWT of the rats remained unchanged from the baseline reading when tested 30 minutes and 2 hours post-dose producing PWTs of 201 ±8 g and 194 ±11 g respectively, suggesting the vehicle had no effect. When rats were dosed with morphine at 1, 5 and 10mg/kg however, PWT increased from the baseline reading producing PWTs of 234 ±12 g, 273 ±20 g and 283 ±17 g respectively. All readings were statistically significant from the corresponding baseline reading suggesting that morphine has significantly increased the pain threshold of naïve rats. At 2 hours this effect was attenuated with readings from each morphine dosed group returning to baseline level.

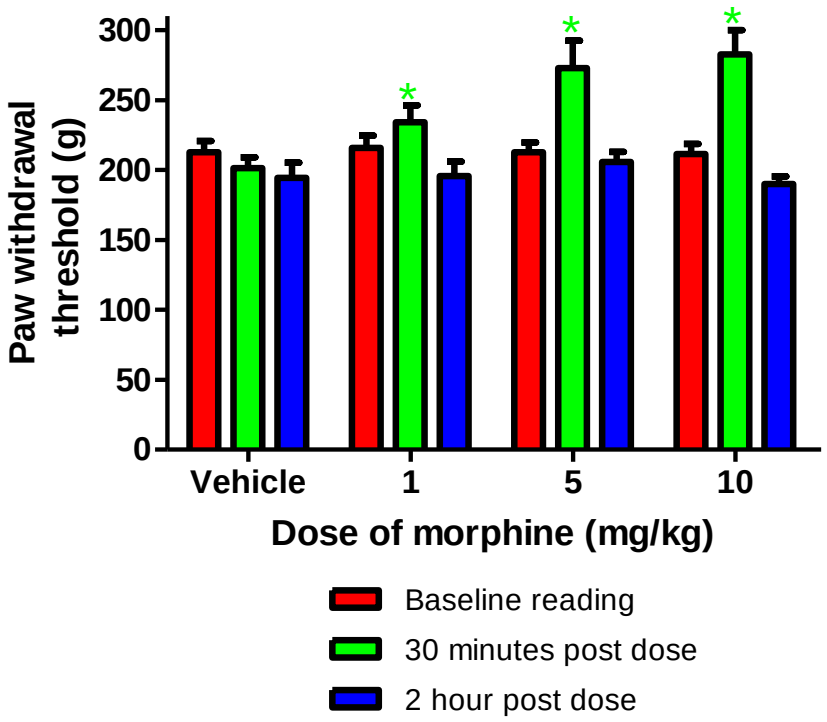

*Figure 52. Effect of μ opioid receptor agonist morphine (1-10 mg/kg, s.c.) on paw withdrawal threshold of rats using an analgesymeter. Data are mean ±SEM with 7 rats in each group. * denotes p<0.05 comparing post-dose readings to baseline readings using Repeated Measures ANOVA followed by Fisher's LSD post hoc test.*

5.3.1.2 P2X7 receptor antagonist alone

Baseline readings were taken from 16 male Lister hooded rats and assigned to 1 of 2 dose groups. P2X7 receptor antagonist, GSK1370319 (100 mg/kg) or vehicle (1% (w/v) methylcellulose) were dosed orally with n=8 in each group. A high dose of P2X7 receptor antagonist was chosen to ensure maximum exposure within the rat. A post-dose reading was taken 90 minutes later before the rats were euthanised using CO_2 inhalation.

The mean baseline readings for all rats was 273 ±7 g (Figure 53). A difference between baseline readings in this study and the previous study was observed. There is no explanation for this difference, apart from unavoidable, subtle environmental

changes which may have affected behaviour. This variation between studies illustrates why baseline readings are essential when performing *in vivo* studies.

A similar level of response was maintained in rats dosed with vehicle, when tested 90 minutes post-dose, producing a PWT of 255 ±11 g. The post-dose reading from rats dosed with 100 mg/kg of GSK1370319 also remained unchanged from the baseline reading, producing a PWT of 283 ±14 g, suggesting that even at a high dose, P2X7 receptor antagonist GSK1370319 had no effect on PWT of naïve rats.

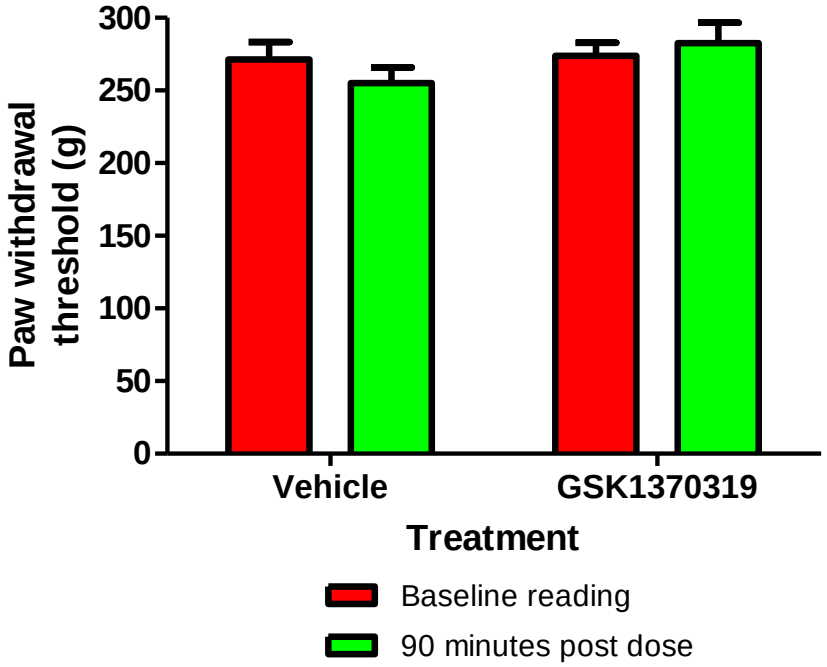

Figure 53. Effect of P2X7 receptor antagonist GSK1370319 (100 mg/kg, p.o.) on paw withdrawal threshold of rats using an analgesymeter. Data are mean ±SEM with 8 rats in each group. Statistical analysis compared post-dose readings to baseline readings using Repeated Measures ANOVA, however there was no significant effect.

5.3.1.3 Combination study 1: GSK1370319 (20 mg/kg) and morphine (0.75 mg/kg)

Having measured the effects of both compounds when dosed alone, combination studies were then carried out to investigate any potential interaction. Before

committing a large number of rats to a full combination study testing several doses of morphine, a smaller 'proof of concept' study was first conducted testing a single dose of GSK1370319 and morphine when dosed alone and dosed together.

Baseline readings were taken from 32 male Lister hooded rats, assigned to 1 of 4 dose groups and dosed with the following combinations:

- Vehicle of GSK1370319 (1% (w/v) methylcellulose, p.o.) and 30 minutes later, the vehicle of morphine (saline, s.c.)
- Vehicle of GSK1370319 (1% (w/v) methylcellulose, p.o.) and 30 minutes later, morphine (0.75 mg/kg, s.c.)
- GSK1370319 (20 mg/kg, p.o.) and 30 minutes later, the vehicle of morphine (saline, s.c.)
- GSK1370319 (20 mg/kg, p.o.) and 30 minutes later, morphine (0.75 mg/kg, s.c.)

The dose of GSK1370319 was chosen as one routinely shown to be efficacious in other single dose behavioural paradigms ran within GSK, for example in the Freunds-complete adjuvant-induced inflammatory pain model (data not shown). The dose of morphine was intended to be 1 mg/kg, but the salt had not been corrected for in the calculation resulting in a lower dose of morphine itself being administered to the rats. A dose of 1mg/kg was the intention as it was shown to have sub-maximal efficacy when dosed alone (figure 52) allowing the opportunity for efficacy to be improved.

A post-dose reading was taken 30 minutes post morphine or saline administration before the rats were euthanised using CO_2 inhalation.

The mean baseline readings for all rats was 285 ±4 g (Figure 54). A similar level of response was maintained from rats dosed with both vehicles producing a PWT of 274 ±13 g. When GSK1370319 and morphine were co-dosed with the appropriate vehicle, PWTs continued to maintain baseline levels producing PWTs of 290 ±17 g and 303 ±15 g respectively, suggesting that neither compound had an effect when dosed alone.

In contrast to this, when the GSK1370319 and morphine were dosed in combination, PWT increased to 349 ±18 g which was significantly different from the corresponding baseline reading.

These data imply that efficacy of morphine had been enhanced by the presence of P2X7 receptor antagonist, GSK1370319. This positive result suggested that a more extensive study combining several doses of morphine with GSK1370319 would be worthwhile.

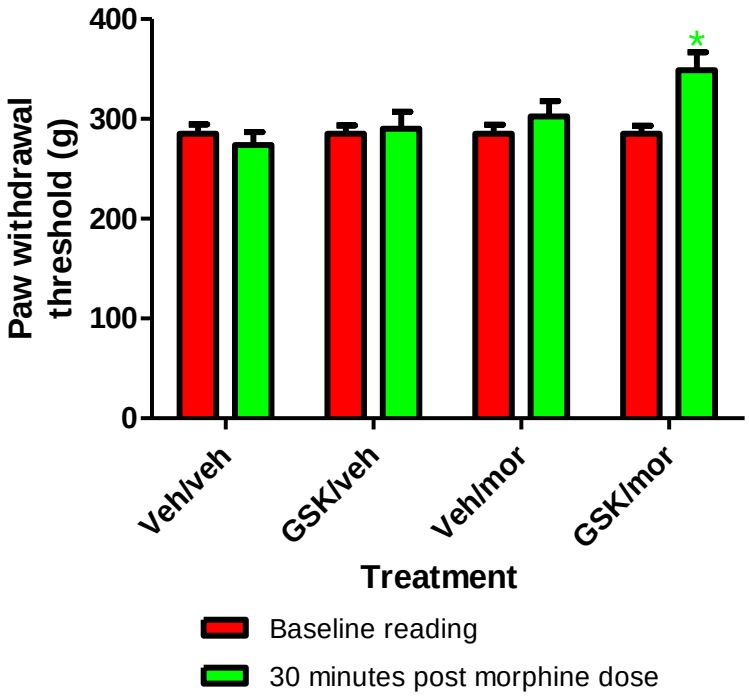

*Figure 54. Effect of co-dosing P2X7 receptor antagonist GSK1370319 (20 mg/kg, p.o., 'GSK') and μ opioid receptor agonist morphine (0.75 mg/kg, s.c., 'mor') on paw withdrawal threshold of rats using an analgesymeter. Data are mean ±SEM with 8 rats in each group. * denotes p<0.05 comparing post-dose readings to baseline readings using Repeated Measures ANOVA followed by Fisher's LSD post hoc test (*p<0.05)*

5.3.1.4 Combination study 2: GSK1370319 (20 mg/kg) and morphine (0.3, 1, 3, 10 mg/kg)

Baseline readings were taken from 80 male Lister hooded rats and assigned to 1 of 10 dose groups and dosed with the following combinations (n=8 per group):

- Vehicle of GSK1370319 (1% (w/v) methylcellulose, p.o.) and 30 minutes later, the vehicle of morphine (saline, s.c.)
- Vehicle of GSK1370319 (1% (w/v) methylcellulose, p.o.,) and 30 minutes later, morphine (0.3 mg/kg, s.c.)
- Vehicle of GSK1370319 (1% (w/v) methylcellulose, p.o.,) and 30 minutes later, morphine (1 mg/kg, s.c.)
- Vehicle of GSK1370319 (1% (w/v) methylcellulose, p.o.) and 30 minutes later, morphine (3 mg/kg, s.c.)
- Vehicle of GSK1370319 (1% (w/v) methylcellulose, p.o.) and 30 minutes later, morphine (10 mg/kg, s.c.)
- GSK1370319 (20 mg/kg, p.o.) and 30 minutes later, the vehicle of morphine (saline, s.c.)
- GSK1370319 (20 mg/kg, p.o.) and 30 minutes later, morphine (0.3 mg/kg, s.c.)
- GSK1370319 (20 mg/kg, p.o.) and 30 minutes later, morphine (1 mg/kg, s.c.)
- GSK1370319 (20 mg/kg, p.o) and 30 minutes later, morphine (3 mg/kg, s.c.)
- GSK1370319 (20 mg/kg, p.o.) and 30 minutes later, morphine (10 mg/kg, s.c.)

A reading was taken 30 minutes post morphine or saline administration before the rats were euthanised using CO_2 inhalation. When the rats were euthanised, 1 cm long sections of lumbar spinal cord were removed, snap frozen in liquid nitrogen and stored in a -80 °C freezer until RT-PCR analysis was carried out (Section 6.2.3.2).

Mean baseline PWTs for all 80 rats was 280 ±3 g (Figure 55). When rats were dosed with both vehicles, the PWT decreased from the baseline level to 251 ±13 g, but this difference was not statistically significant. A lack of effect was also seen in rats dosed with 0.3 and 1 mg/kg morphine when co-dosed with GSK1370319,

producing PWTs of 316 ±15 g and 300 ±26 g respectively, or with the vehicle of GSK1370931, producing PWTs of 289 ±26 g and 271 ±14 g respectively. The lack of effect at 1 and 3 mg/kg is inconsistent with data reported earlier in combination study 1 (section 5.3.1.3). Possible explanations for this discrepancy could be differential sensitivities between different batches of rats or the inherent variability that exists in performing *in vivo* studies.

When responses from rats dosed with morphine (3 mg/kg) were compared to baseline readings, a significantly higher PWT was only produced from rats that were co-dosed with GSK1370319 (PWT of 336 ±29 g), as opposed to those co-dosed with vehicle (PWT of 295 ±24 g). Although this data suggests a potentiation in the efficacy of morphine at this dose, a direct comparison between post-dose readings from groups dosed with morphine + vehicle and morphine + GSK1370319 (3 mg/kg) was not significantly different, putting doubt into this interpretation.

When rats were dosed with 10 mg/kg morphine, an increase in PWT from baseline was also observed in rats co-dosed with both GSK1370319 and the vehicle of GSK1370319, producing PWTs of 487 ±13 g and 437 ±23 g respectively. The post-dose readings from both groups of rats were not only significantly different to their corresponding baseline readings, but also significantly different from each other, suggesting that GSK1370319 may have the ability of modulating the effects of morphine in naïve rats.

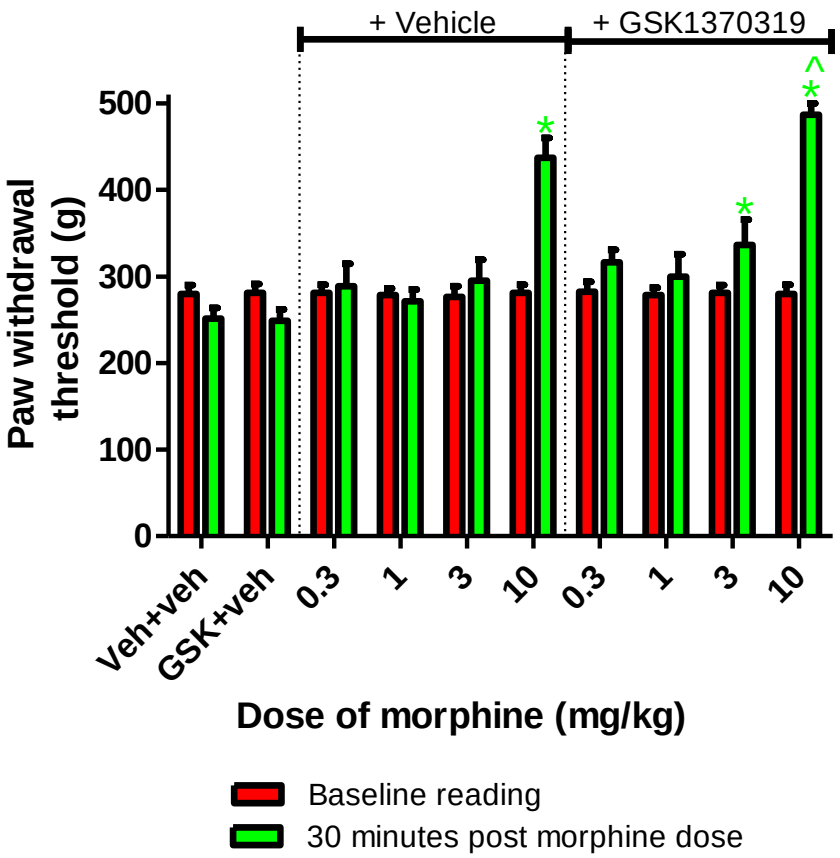

*Figure 55. Effect of co-dosing P2X7 receptor antagonist GSK1370319 (20 mg/kg, p.o, 'GSK'.) and μ opioid receptor agonist morphine (0.3-10 mg/kg, s.c.) on paw withdrawal threshold of rats using an analgesymeter. Data are mean ±SEM with 8 rats in each group. *p<0.05 comparing post-dose readings to baseline readings using Repeated Measures ANOVA followed by Fisher's LSD post hoc test. ^p<0.05 comparing groups of rats treated with morphine + vehicle and equivalent dose of morphine + GSK1370319.*

5.3.2 Motor coordination

To investigate whether GSK1370319 influences the effects of morphine on motor-coordination, rats were co-dosed with both compounds and tested on the rota-rod apparatus. Before embarking on a study testing novel compounds the model was first characterised by testing pregabalin, a compound known to produce motor impairment at high doses, to compare with previous in-house data (not shown).

5.3.2.1 The effect of pregabalin on motor-coordination in rats

Thirty male Sprague-Dawley rats (220-250 g, Charles River) were trained on the rota-rod apparatus. All rats successfully remained on the apparatus for 90 seconds and were therefore included in the study. Rats were assigned to 2 groups and dosed with pregabalin (100 mg/kg, p.o.) or vehicle (1% (w/v) methylcellulose, p.o.) with n=10 for each group. Rats were then assessed for their ability to remain on the accelerating rota-rod apparatus at 1, 2 and 4 hours post-dose with 'fall times' being recorded.

When rats were dosed with vehicle, the time spent on the rota-rod apparatus significantly increased over time, producing 'fall times' of 114 ±20 secs (1 hour), 175 ±21 secs (2 hour) and 191 ±28 secs (4 hours) (Figure 56). The reason for this was likely to be a learning effect as the rats acclimatised to the rotarod apparatus. In this study and the subsequent study, drug responses were compared to time-matched vehicle response implying that the increase in vehicle 'fall time' had less significance.

In contrast, rats dosed with 100 mg/kg pregabalin (p.o.) stayed on the rota-rod apparatus for less time, producing 'fall times' of 94 ±14 secs (1 hour), 38 ±8 secs (2 hour) and 54 ±12 secs (4 hour). The difference between drug and vehicle responses were significantly different at 2 and 4 hours post-dose but not at 1 hour post-dose.

This data suggested that pregabalin (100 mg/kg, p.o.) caused motor-impairment in rats when tested 2 and 4 hours post-dose. This response was very similar to data produced by other operators within GSK inferring that the model was validated and that the method was suitable to test novel compounds.

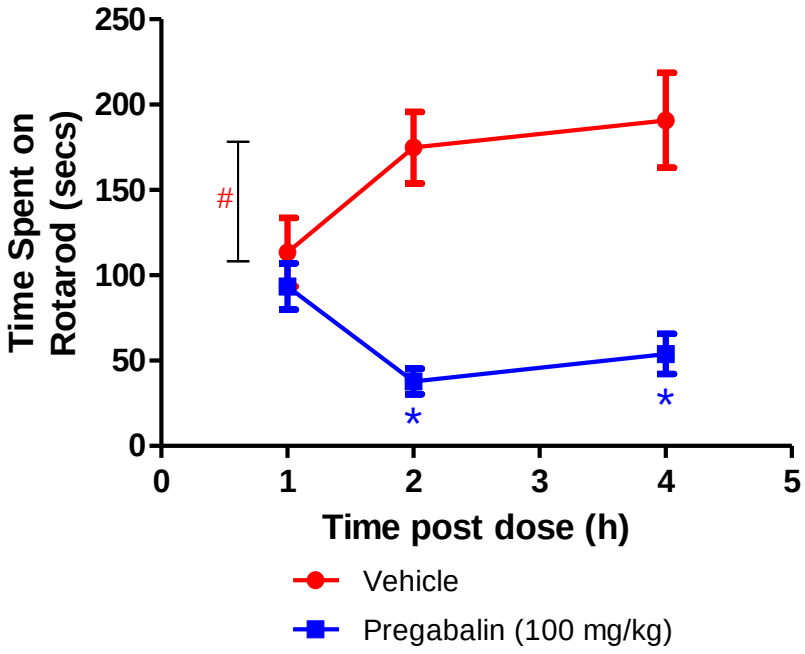

*Figure 56. Effect of dosing pregabalin (100 mg/kg, p.o.) on motor coordination measured using a rotarod. Data are mean ±SEM with 10 rats in each group. # denotes p<0.05 using Repeated Measures ANOVA followed by Fisher's LSD post hoc test comparing vehicle responses at 1 and 2 hours post-dose. * denotes p<0.05 using Repeated Measures ANOVA followed by Fisher's LSD post hoc test comparing to the vehicle dosed group.*

5.3.2.2 Effect of co-dosing P2X7 receptor antagonist and morphine on motor coordination in rats

40 male SD rats were first trained on the rota-rod apparatus, with all rats successfully remaining on the apparatus for 90 seconds and thereby being included in the study. Rats were assigned to 4 groups and dosed chronically with the following combination of compounds or vehicle twice a day for 8 days with n=10 in each group.

- Vehicle of GSK1370319 (1% (w/v) methylcellulose, p.o.) and 30 minutes later, the vehicle of morphine (saline, s.c.)
- Vehicle of GSK1370319 (1% (w/v) methylcellulose, p.o.) and 30 minutes later, morphine (10 mg/kg, s.c.)

- GSK1370319 (5 mg/kg, p.o.) and 30 minutes later, the vehicle of morphine (saline, s.c.)
- GSK1370319 (5 mg/kg, p.o.) and 30 minutes later, morphine (10 mg/kg, s.c.)

The dose regimen of GSK1370319 was chosen as the most commonly used in the combination studies run in the CCI model in Chapter 3.

Rats were assessed for their ability to remain on the accelerating rota-rod apparatus 30 minutes and 2 hours after the morning dose of morphine or saline on day 1 and 8. An additional test was also conducted 30 minutes after the morning dose of morphine or saline on day 4 of the dosing period. Body weight readings were taken from all rats during the morning dosing period for future analysis (see section 5.3.3).

When rats were dosed with both vehicles the time spent on the rota-rod apparatus significantly increased over time, producing a minimal 'fall time' of 117 ±19 seconds on day 1 of dosing (30 minutes post-dose) and a maximum 'fall time' of 180 ±20 seconds on day 8 of dosing (2 hours post-dose) (Figure 57). As already explained this 'effect' had little significance as all responses were compared to the time-matched vehicle response.

There was no significant difference in 'fall times' from rats dosed with GSK1370319 and saline when compared to the responses from both vehicles at any time-point producing a range of 'fall times' of 107-149 seconds. This suggests that GSK1370319 alone has no effect on motor coordination of rats when dosed at 20 mg/kg b.i.d for 8 days. This is not surprising given the lack of literature detailing any effect of glial modulators on motor-coordination.

In contrast, 'fall times' from rats dosed with the vehicle of GSK1370319 and morphine were significantly less than those produced by rats dosed with both vehicles. A statistically significant difference was observed on every test day during the 8 day dosing period. For example, the first assessment on day 1 produced a 'fall time' of 24 ±7 seconds, compared to the vehicle response of 117 ±19 seconds; and the first assessment on day 8 produced a 'fall time' of 60 ±13 seconds compared to

the vehicle response of 148 ±27 seconds. This data suggested that morphine (10 mg/kg) dosed alone significantly induced motor impairment.

Finally, when rats were co-dosed with GSK1370319 and morphine the 'fall times' were also significantly reduced from responses from vehicle-treated rats. 'Fall times' on assessment on days 1 and 8 were of 15 ±3 and 50 ±9 seconds respectively.

As Figure 57 illustrates, the overall profile of responses from rats dosed with morphine in the presence and absence of GSK1370319 were very similar. This was also borne out in statistical analysis which confirmed there was no significant difference between the responses from either group. This data suggests there is no interaction between morphine and GSK1370319 in morphine-induced motor impairment.

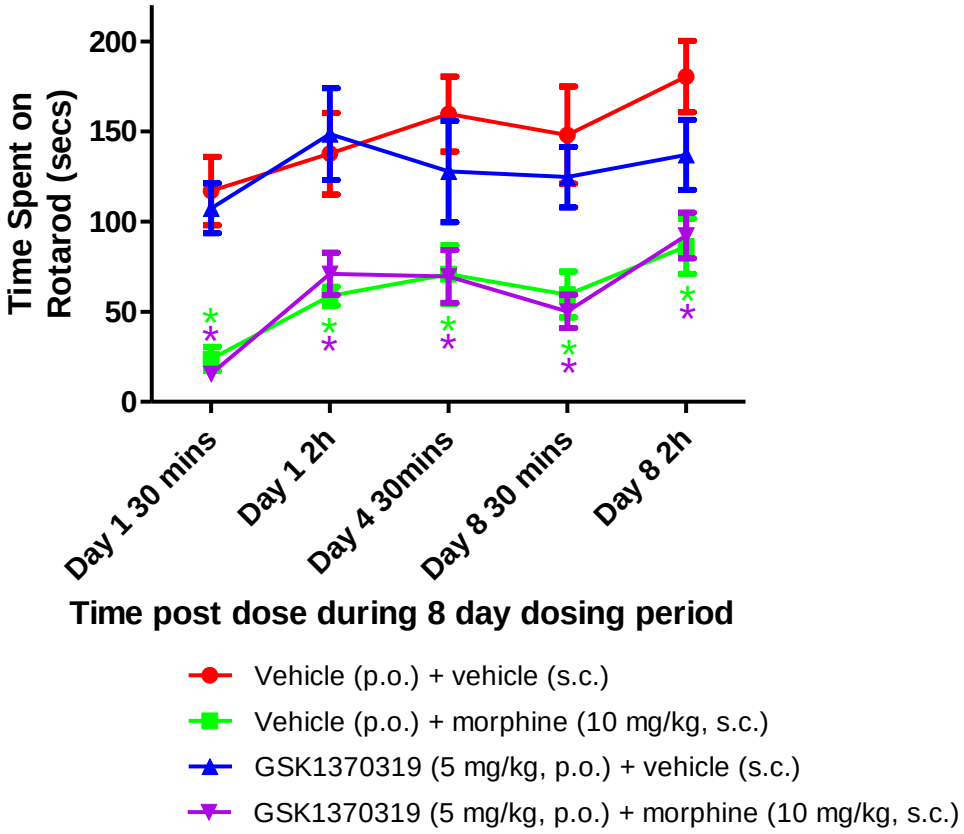

*Figure 57. Effect of co-dosing P2X7 receptor antagonist GSK1370319 (5 mg/kg, p.o., b.i.d for 8 days) and μ opioid receptor agonist morphine (10 mg/kg, s.c., b.i.d. for 8 days) on motor impairment measured using the rotarod apparatus. Data are mean ±SEM with 10 rats in each group. *denotes p<0.05 using Repeated Measures*

ANOVA followed by Fisher's LSD post hoc test comparing all groups to 'vehicle+vehicle' group.

5.3.3 Body weight

To investigate whether GSK1370319 influenced the effects of chronically dosed morphine on other behaviours, body weight of rats were recorded from two studies previously described; from CCI operated rats (Section 3.3.3.) and from rats dosed for a rota-rod study (Section 5.3.2.2).

5.3.3.1 Body weight measurements from CCI-operated rats chronically co-dosed with morphine and GSK1370319

Body weights of Random-hooded rats dosed with 1) both vehicles, 2) GSK1370319 (1 and 5 mg/kg) and saline, 3) 1% (w/v) methylcellulose and morphine (10 mg/kg) and 4) GSK1370319 (1 and 5 mg/kg) and morphine (10 mg/kg) were taken prior to surgery and on the morning of days 9, 11 and 12 of the 12 day dosing period.

The mean body weight for all rats was 225 ±2 g prior to surgery (Figure 58). In rats dosed with both vehicles, this value increased to approximately 240 g over the dosing period. The increase of 10-15 g was also observed in rats dosed with GSK1370319 (1 and 5 mg/kg) and 1% (w/v) methylcellulose, suggesting that the P2X7 receptor antagonist alone had no effect on body weight. Having found no reports of microglia modulators having any adverse effects on body weight, the lack of effect with a P2X7 receptor antagonist is not surprising.

In contrast, body weights of rats dosed with 1% methylcellulose and morphine (10 mg/kg) did not increase over time, but remained at approximately 225 g on the three test days. On each of the post-dose time-points there was a significant difference between this group and the group dosed with both vehicles, suggesting that morphine prevented the rats from gaining weight.

Interestingly, a similar profile was observed in rats dosed with morphine (10 mg/kg) in the presence of GSK1370319 (5 mg/kg) with body weights remaining at approximately 220 g on the three test days. This data suggests that the P2X7 receptor antagonist had no effect on morphine-induced 'lack of body weight gain', as

body weights in morphine-dosed rats remained low whether rats were co-dosed with GSK1370319 or not.

It is worth noting that the 'lack of body weight gain' was well within the acceptable boundaries set in the Home Office project licence. The 'lack of body weight gain' was not considered severe enough to be concerned for the welfare of the rats, especially as Random-hooded rats are known to gain weight slowly.

Rats co-dosed with GSK1370319 (1 mg/kg) and morphine also showed less weight gain than the group dosed with both vehicles, but this was only significantly different on the final day, with a body weight of 227 ±4 g.

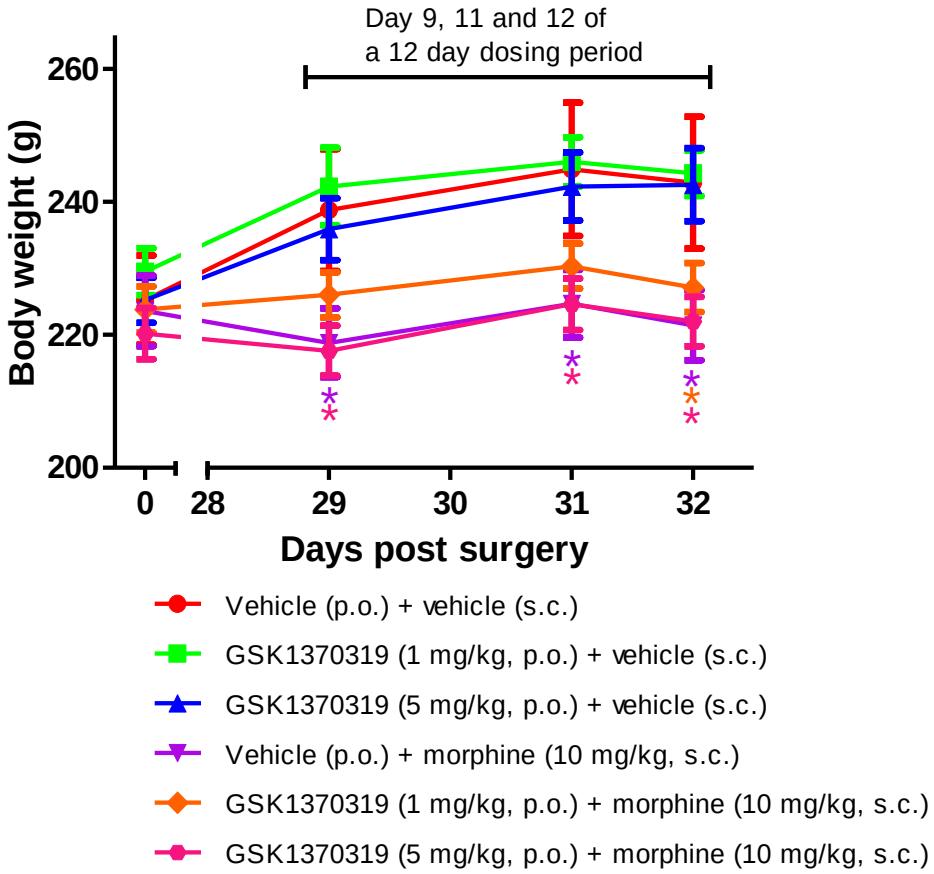

*Figure 58. Effect of co-dosing P2X7 receptor antagonist GSK1370319 (1 and 5 mg/kg, p.o., b.i.d for 12 days) and μ opioid receptor agonist morphine (10 mg/kg, s.c., b.i.d. for 12 days) on body weight of CCI-operated Random hooded rats. Data are mean ±SEM with 10 rats in each group (n=9 for vehicle treated group). *p<0.05 using Repeated Measures ANOVA followed by Fisher's LSD post hoc test comparing all groups to 'vehicle+vehicle' group.*

5.3.3.2 Body weight measurements from naive rats chronically co-dosed with morphine and GSK1370319

Body weights were also taken from Lister hooded naive rats used for the rota-rod study described in section 5.3.2.2. Measurements were taken from rats dosed with both vehicles, GSK1370319 (5 mg/kg) and saline, 1% (w/v) methylcellulose and morphine (10 mg/kg) and finally, GSK1370319 (5 mg/kg) and morphine (10 mg/kg) on each morning of the 8 day dosing period.

The mean body weight for all rats prior to treatment was 243 ±2 g (Figure 59). When rats were dosed with both vehicles this value gradually increased by approximately 8 g every day resulting in a mean body weight of approximately 300 g on day 8 of dosing. A very similar profile was observed in rats dosed with GSK1370319 and saline, suggesting that GSK1370319 had no effect on 'body weight gain'.

In rats co-dosed with morphine and saline however, the body weights increased at a slower rate, increasing by about 3 or 4 g each day and resulting in a body weight of approximately 277 g on day 8. When compared to the group receiving both vehicles there was a significant difference on days 4, 6, 7 and 8 of the 8 day dosing period, therefore confirming morphine-induced 'lack of body weight gain'.

Interestingly, when rats were dosed with morphine in the presence of GSK1370319, a similar body weight profile was observed to rats dosed with morphine and 1% (w/v) methylcellulose. In this group, body weight increased by about 3-4 g each day and the resultant body weight on day 8 was 277 ±5 g. This data therefore suggests that the P2X7 receptor antagonist had no effect on morphine-induced lack of 'body weight gain'.

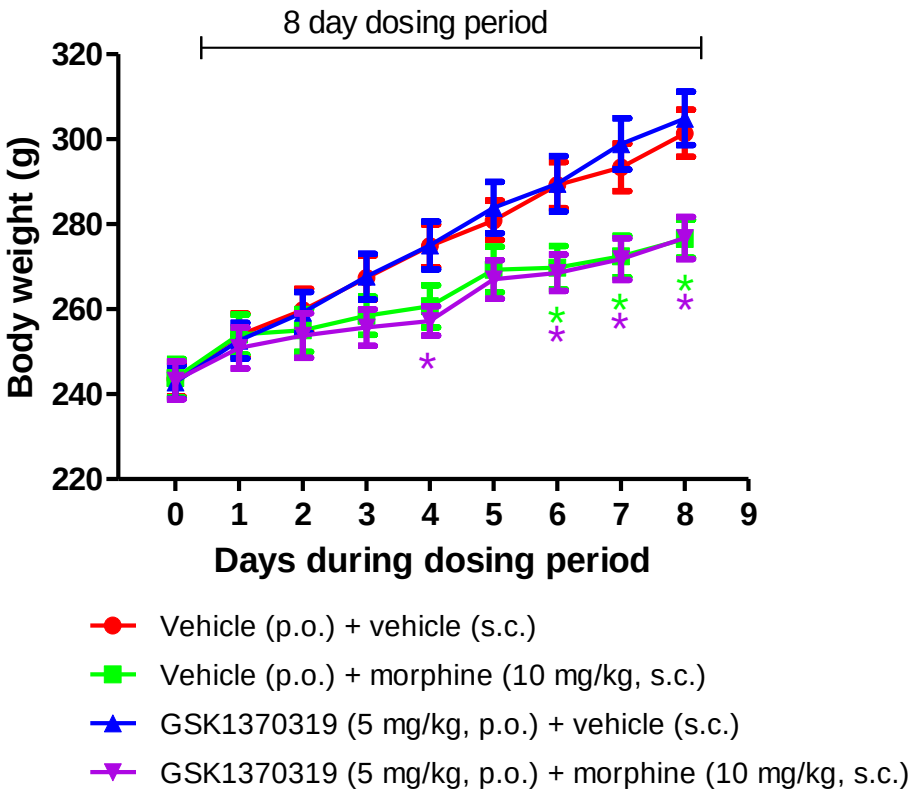

*Figure 59. Effect of co-dosing P2X7 receptor antagonist GSK1370319 (5 mg/kg, p.o., b.i.d for 8 days) and μ opioid receptor agonist morphine (10 mg/kg, s.c., b.i.d. for 8 days) on body weight of Lister-hooded rats . Data are mean ±SEM with 10 rats in each group. *p<0.05 using Repeated Measures ANOVA followed by Fisher's LSD post hoc test comparing all groups to 'vehicle+vehicle' group.*

5.4 Discussion

This chapter explored whether an enhancement of morphine-induced analgesia was possible in unsensitised rats (i.e. 'naive' rats) after a single administration of morphine, in a similar way to that previously suggested in CCI treated rats after repeated administration of morphine.

The behavioural readout used in these studies was paw withdrawal threshold obtained using an analgesymeter. Von Frey filaments, that were used in the CCI studies, were not used for this paradigm for practical reasons. For studies using naïve rats the filament pressures necessary to produce a paw withdrawal post-dose would require filaments that were too thick to bend. The large intervals between the higher hairs would also make it difficult to differentiate efficacy between different compounds.

To obtain the most appropriate dose of morphine for subsequent studies, morphine was first tested alone. Morphine increased paw withdrawal threshold in naïve rats 30 minutes post-dose. The analgesic effect of acutely dosed morphine using this paradigm was in agreement with literature (Skingle et al., 1990). The mechanism for the 'classical' analgesic activity of morphine is well known. Briefly, at the spinal level, opioid receptor activation inhibits ascending signal transmission; whereas at the supraspinal level, opioids activate interneurones, which produce descending inhibition (Benedetti, 1987; Porreca et al., 1987; Yeung and Rudy, 1980; Lipp, 1991).

When P2X7 receptor antagonist GSK1370319 was tested in the acute pain paradigm there was no effect on paw withdrawal thresholds of naïve rats, even at a dose approximately 800 times the pIC50 at the rat receptor. Although there is no literature testing a P2X7 receptor antagonist in a mechanically stimulated acute pain test, there are two studies showing a lack of effect the with P2X7 receptor antagonists A-740003 and BBG, in a thermally stimulated acute pain test (Honore et al., 2006; Ando et al., 2010). Electrophysiolgical recordings also support this data with spontaneous and evoked firing being diminished or absent when P2X7 receptor antagonist A-438079 was dosed to sham-operated rats (McGaraughty et al., 2007).

The biggest difference between the CCI-operated rats and the 'naïve' rats used in the acute pain assays are that the rats themselves are not sensitised. Under 'normal' conditions, microglia will assume a resting/ inactive state providing active surveillance, rapidly extending and retracting processes to constantly sample the microenvironment. Under these conditions, microglia do not appear to be important regulators of pain transmission (Raivich, 2005). This is supported by the fact that drugs that suppress glial function or block the actions of various glial products do not alter responses to heat or mechanical stimuli in normal animals (Meller et al., 1994; Hashizume et al., 2000; Ledeboer et al., 2005a). This therefore explains why P2X7 receptor antagonists have no effect on normal rats; microglia are not activated, therefore IL-1β and other proinflammatory cytokines are not released and the P2X7 receptor antagonist has nothing to inhibit. The situation changes however when microglia are activated, for example in response to a nerve injury, producing a change in morphology, proliferation, up-regulated receptor expression and function. It is these changes that the P2X7 receptor antagonists are influencing to produce efficacy, as seen in Chapter 2. The difference in P2X7 receptor response to the two states of microglia can also be illustrated from P2X7 KO studies in which neuropathic hypersensitivity was completely abolished, whereas normal nociceptive processing still remained (Chessell et al., 2005). Additionally, the negative data with the P2X7 receptor antagonist in the acute pain assay also suggests that efficacy in the CCI model was not due to any anti-nociceptive property of the compound *per se*, but is reliant on the neuropathic condition of the rats.

When the 10 mg/kg dose of morphine was combined with GSK1370319 a potentiation of efficacy was observed. In the smaller 'proof of concept' study, there was also a significant increase in response between morphine alone and morphine in the presence of GSK1370319 when morphine was dosed at 0.75 mg/kg, however this was not reproduced in the larger study.

Although this is the first report showing an enhancement of opioid-induced acute analgesia by a P2X7 receptor antagonist, there are reports showing similar effects using the glial activation inhibitors, minocycline (Cui et al., 2008; Hutchinson et al., 2008b) and ibudilast (Hutchinson et al., 2009).

Other supporting evidence comes from earlier studies suggesting the direct involvement of proinflammatory cytokines and in particular IL-1. Co-administration of IL-1 and morphine abolished morphine analgesia, whereas co-administration with Il-1 receptor antagonist enhanced the magnitude and duration of analgesia (Shavit et al., 2005). Interestingly, administration of Il-1ra when morphine analgesia had dissipated re-instated efficacy, suggesting that endogenous IL-1 is masking ongoing morphine analgesia by exerting an opposing effect (Watkins et al., 2009). To support this further, morphine analgesia was potentiated in mice with impaired IL-1 signalling, whether it was over expression of IL-1ra, deletion of IL-1 receptor type 1 or deletion of IL-1 receptor accessory protein (Shavit et al., 2005).

From the data described in this report and supporting literature, it can be hypothesised that the counteracting IL-1 must be released from microglia which have become activated by morphine, as it has been highlighted that insufficient IL-1 would be in the system under normal conditions. This hypothesis is confirmed by literature showing morphine-induced up-regulation of markers for activated microglia (Cui et al., 2006; Hutchinson et al., 2009) and morphine-induced up-regulation of proinflammatory cytokine and chemokines (Johnston et al., 2004; Raghavendra et al., 2004a; Hutchinson et al., 2008a; Hutchinson et al., 2009).

While it is widely known that cytokines are released in response to pathological conditions, the role of cytokines in normal physiology is now being realised. Cytokines have been implicated in many CNS processes including regulation of the arousal state, modulation of mood, feeding, thermoregulation, sexual behaviour, regulating sleep, learning and memory (Maier and Watkins, 2003; Kapsimalis et al., 2005; Hutchinson et al., 2008a). The release of cytokines in the CNS is therefore not considered to be triggered only in response to pathology. The second part of this chapter focuses on the contribution that activated microglia may have on non-analgesic actions of morphine, by assessing the responses on morphine-induced motor impairment/ sedation and loss in weight gain when in the presence of GSK1370319.

The loss of motor coordination is a common characteristic of many neurological disorders and is one of the most readily observable adverse effects of drugs (Rustay

et al., 2003). The rotarod apparatus is widely used in research for evaluating motor coordination in a number of different paradigms, for example assessing differences between wild-type and knock-out mice (Read et al., 2010), assessing effectiveness of drugs in animals models (Liu et al., 2010), and the most commonly used function, assessing adverse effects of compounds (Spetea et al., 2010). One caveat to the device is that it is unable to distinguish between the reasons for the motor-impairment, e.g. sedation versus cognitive deficits versus joint injury, however the device is well recognised to be a very useful tool to quickly measure any overt motor-impairment regardless of the mechanism.

Pregabalin was used to validate the model, which robustly caused motor-impairment producing similar results to other in-house operators when tested in a similar way (data not shown). Having characterised the rota-rod methodology, the effect of morphine was investigated in the absence and presence of P2X7 receptor antagonist, GSK1370319. The results showed that morphine (10 mg/kg), co-dosed with the vehicle of GSK1370319, reduced the performance of the rats on the apparatus. This data is in agreement with other literature, using the same dose of morphine (Meert and Vermeirsch, 2005; Spetea et al., 2010). This was not unexpected as μ opioid analgesics, including morphine, are known to depress motor activity in humans and is a side effect that often limits their usefulness in the clinic (Hayes and Tyers, 1983; Bowdle, 1998; Meert and Vermeirsch, 2005).

When co-dosed with saline, GSK1370319 had no effect on motor-coordination producing similar readings to rats dosed with both vehicles. This lack of effect is consistent with reports in the literature testing P2X7 receptor antagonist in this way. P2X7 receptor antagonists A-438079 and A-740003 (Honore et al., 2006; McGaraughty et al., 2007) also had no effect motor coordination at analgesic doses. The lack of effect is also not surprising as the rats are not sensitised and microglia would be in resting state, however it was a necessary control to perform.

When morphine was co-dosed with GSK1370319, a very similar reduction in performance was observed in rats dosed with morphine alone, suggesting that the P2X7 receptor antagonist had no effect on the morphine-induced motor impairment. This suggests that microglia are not involved in the mechanism driving morphine-

induced motor impairment and/or not being activated by the dose of morphine used in this study. The finding that compounds can modulate morphine-induced analgesia, but not motor coordination has been reported elsewhere in the literature with other targets. For examples the combination of BIM-46187, an inhibitor of heterotrimeric G-protein complex signalling, strongly synergized with morphine in inflammatory and neuropathic pain models, but did not exacerbate the locomotor deficits observed with morphine alone (Favre-Guilmard et al., 2008). Flupirtine, the potassium channel opener, increased the anti-nociceptive effect of morphine without effecting morphine-induced motor-impairment (Goodchild et al., 2008).

The mechanism responsible for the impairment of normal motor function by opioids has been proposed to be linked to the μ opioid receptor activation in specific brain regions, namely basal ganglia, nuclea raphe pontis, periaqueductal gray and locus coerules (Havemann et al., 1980; Havemann et al., 1982; Vankova et al., 1996; Bowdle, 1998). This supra-spinal site of action may involve microglia to a lesser degree which might explain why there is little impact on these actions when morphine is co-dosed with a P2X7 receptor antagonist.

The final morphine-induced action to be considered is the reduction of body weight gain. This has been demonstrated using a plethora of different routes of administration; implantation of slow release pellets (Ferenczi et al., 2010), infusion with micro-pumps (Gosnell and Krahn, 1993) as well as more traditional subcutaneous and intra-peritoneal routes (Boghossian et al., 2001). Intriguingly however, it has also been widely demonstrated that morphine can also increase food intake and weight gain, but only when morphine is dosed acutely (Shimomura et al., 1982; Levine et al., 1988).

This contradiction is a good illustration of how complex the central regulation of food intake and metabolism is, involving both homeostatic and reward-related components in central structures (Ragnauth et al., 2000; Ferenczi et al., 2010).

The data presented here has shown that chronic morphine treatment reduces body weight gain in both naïve Lister hooded rats and CCI-operated Random-hooded rats. The endogenous opioid system is one of the key mechanisms that affects food intake in the brain via direct inhibition of the anorexigenic neuron population

(Bodnar and Hadjimarkou, 2003). It has been repeatedly shown that exogenous opioid compounds, such as excess morphine administration, results in the dysregulation of morphine receptors signalling in several brain regions (He et al., 2009) therefore reducing opioid receptor signalling and inhibitory opioid tone (Garcia de and Pelletier, 1993; Wardlaw et al., 1996). It is therefore reasonable to assume that the lack of body weight gain from chronic morphine is due to the fall in the activity of the endogenous regulatory system.

It is also important to acknowledge that the lack of body weight gain might be related to other morphine-induced side effects e.g. sedation, constipation, respiratory depression which might indirectly decrease feeding frequency or food intake. For example decrease in feeding frequency might be a result from a decrease in locomotion, which is also seen after morphine treatment, or due to the peripheral actions of opioids on gut function known to cause constipation. One other less reported confounding factor is morphine-induced taste aversion (Nader et al., 1996). It is out of the scope of this dissertation to explore these avenues in more detail, suffice to say that it appears that morphine-induced decrease in body weight gain is attributed to deregulatory activities on endogenous opioids in the brain, as well as indirect factors associated with other morphine-induced side effects.

The finding that P2X7 receptor antagonist has had no effect on morphine-induced lack of weight gain, suggests that microglia, whether activated by morphine or a neuropathic insult, have little influence on any of the mechanisms proposed. This is in contrast to the interaction the receptors has with analgesic properties of morphine re-iterating the fact that morphine has supraspinal activities which maybe independent to those related to the activation of spinal microglia.

In summary, this chapter has demonstrated that the blockade of P2X7 receptors on microglia can enhance morphine acute dose-induced analgesia, but has no influence on some of the undesirable actions of morphine, like motor-impairment and lack of body weight gain. This contrasting relationship may be related to the different sites of action that the morphine-induced effects originate from. Although more is being learnt about potential advantages of co-dosing opioids with compounds to enhance efficacy or to reduce tolerance, what is less known is how the combinations

might affect morphine-related side effects. The data in this chapter illustrates for the first time, that co-dosing morphine with a P2X7 receptor antagonist, not only potentiates morphine analgesia in naïve rats, but has little influence on two morphine-induced side effects. This data suggests that the therapeutic window of morphine could be increased, suggesting the therapeutic benefit of morphine, and maybe other opioids, could also be increased which in turn could have significant clinical implications.

Chapter 6

Investigating the role of microglia in P2X7 receptor mediated activities

6. Investigating the role of microglia in P2X7 receptor mediated activities

6.1 Introduction

Having demonstrated the involvement of P2X7 receptors in neuropathic pain (Chapter 2) and in morphine-induced tolerance and morphine-induced analgesia (Chapters 3 and 5), it was important to investigate the possible mechanisms of action. As P2X7 receptors are primarily expressed on microglia it was hypothesised that these cells play a central role in P2X7 receptor function. This chapter investigates this hypothesis using *in vivo*, immunohistochemical and molecular techniques.

Evidence supporting the role of microglia in neuropathic pain has been acquired from *in vivo* studies demonstrating anti-allodynic properties of drugs that interfere with microglia function (Raghavendra et al., 2003b; Ledeboer et al., 2005a; Clark et al., 2007; Tawfik et al., 2007). In this chapter, minocycline, a semisynthetic antibiotic that selectively inhibits microglial activation, was dosed to CCI-operated rats after allodynia had been established. Minocycline has previously been shown to prevent the development of neuropathic pain after pre-emptive dosing (Raghavendra et al., 2003b; Ledeboer et al., 2005a) although evidence for it reducing established allodynia is less well established.

Glial activation is a process that involves morphological changes, proliferation and up-regulation of surface antigens. Immunohistochemistry (IHC) has been used extensively to monitor this transformation and uses the up-regulated surface antigens as markers of activation. The cell surface molecules most commonly used in IHC for identifying activated microglia include:

- Integrin alpha M (ITGAM) [also known as complement receptor 3 (CR3) or cluster determinant 11b (CD11b) or MAC-1] a transmembrane protein with an extracellular domain that is expressed on the outer membrane of microglia. The antibody OX-42 recognises this protein and although it is one of the most commonly used microglial markers, there are doubts about its selectivity. For

example, OX-42 staining is observed in sham-operated rats. In addition, there is some confusion as to whether OX-42 is a marker for behavioural hypersensitivity or of CNS injury due to a mismatch between staining and behavioural responses (Colburn et al., 1997).

- Cluster of differentiation 14 (CD14) was the first of the pattern recognition receptor and are proteins expressed by cells of the innate immune system to identify pathogen-associated molecular patterns associated with cellular stress.
- Major histocompatibilty complex (MHC-I and II) have a role in antigen presentation to T lymphocytes.
- Ionised calcium-binding adapter molecule (Iba-1) is a calcium-binding protein that is specifically expressed in microglia (Narita et al., 2006; Jergova and Cizkova, 2007).
- Peripheral benzodiazepine receptor (PBR) is expressed on the outer mitochondrial membrane of activated microglia. The development of radiolabeled ligands for PBR has enabled positron emission tomography (PET) imaging of the PBR to be used in *in vivo* human studies investigating neuroinflammatory and neurodegenerative conditions (Banati, 2002) making this marker particularly relevant for drug discovery programmes.

In terms of astrocytes, glial fibrillary acidic proteins (GFAP) is selectively increased when this cell type is activated and is widely accepted to be an astrocytic differentiation marker (Garrison et al., 1991; Sweitzer et al., 2001).

The majority of published IHC studies in the pain area have focused on the role of microglia in the induction of chronic pain rather than its maintenance (Svensson et al., 1993; Eriksson et al., 1997; Raghavendra et al., 2004b). Other IHC studies have demonstrated an up-regulation of GFAP during established neuropathic pain (Hajos et al., 1990; Murray et al., 1990; Garrison et al., 1994). However few studies have demonstrated changes in microglia markers at later time-points when the nerve-injury-induced allodynia is established. It is these changes that are investigated in the current study using the microglia marker Iba-1.

The involvement of P2X7 receptors in microglial activation in established neuropathic pain was also investigated by comparing Iba-1 expression in the dorsal horn of CCI-operated rats dosed with P2X7 receptor antagonist GSK1370319 and CCI-operated rats dosed with vehicle. Although the same tissue types and the same marker were used for both IHC studies, a different experimental method with higher throughput was used in the second study. In study 1 a traditional method was used whereby dewaxing, buffer/ antibody application and washing steps were performed manually. In study 2 however a robotic platform called Ventana Discovery was used which completed all the same steps automatically. The overall principle for both manual and automated studies was similar and followed the avidin-biotin method, however there were several differences between the experimental methods involved which are discussed in the section 6.2.2.3.

As previously described the mechanisms underlying neuropathic pain and morphine tolerance are strikingly similar. Since the initial report in 2001 showing extensive GFAP staining in the spinal cord of morphine-dosed rats (Song and Zhao, 2001), evidence has rapidly accumulated showing that microglia and astrocytes are involved in the development of morphine tolerance (Deleo et al., 1996; Song and Zhao, 2001; Johnston et al., 2004; Raghavendra et al., 2004a; Watkins et al., 2005; Watkins, 2007). For example, morphine tolerance was shown to be blocked by inhibiting glial activation using glial inhibitors such as fluorocitrate (Song and Zhao, 2001) or propentofylline (Raghavendra et al., 2004a). It is now widely hypothesised that chronic morphine is able to activate microglia which counter-regulates the analgesic properties of morphine and thus manifesting into tolerance (Watkins et al., 2005; Watkins et al., 2007a).

As demonstrated in Chapter 3, morphine tolerance in CCI rats was delayed when morphine was co-dosed with GSK1370319, suggesting that the P2X7 receptor antagonist might also be working in this way. To investigate this further, mRNA expression of ITGAM and PBR was measured in the lumbar region of the spinal cord of CCI-operated rats co-dosed with morphine and GSK1370319. Having shown transcriptional changes it was then intended to confirm the findings, using IHC, in protein expression studies.

To identify an involvement of astrocytes and proinflammatory cytokines during repeated morphine administration in the CCI model, the levels of mRNA expression of GFAP, IL-1β and TNF were determined. Furthermore, mRNA expression of the μ opioid receptor was assessed to investigate the validity of the 'receptor down-regulation theory' of tolerance explained in Chapter 1. This data may also confirm findings that glial exposure to morphine enhances the constitutive expression of the μ opioid receptor (Mahajan et al., 2002).

Finally, as demonstrated in Chapter 5, GSK1370319 also significantly enhanced the efficacy of a single dose of morphine in naïve rats suggesting microglia may have a regulatory role in efficacy of acute administration of morphine as well as chronic administration. To investigate this hypothesis further, the mRNA expression of ITGAM and PBR were measured in the spinal cord of naive rats co-dosed with a single administration of morphine and GSK1370319.

Changes in gene expression have traditionally been studied using Northern blot analysis, competitive PCR or in situ hybridisation. Although these techniques have proven successful and reliable, they can require large amounts of RNA, can be difficult to optimise and quantify, may require time consuming downstream processing of samples and are not amenable to large sample numbers. Taqman RT-PCR however enables the measurement of an accumulating PCR product in real time by utilising a dual-labelled Taqman fluorogenic probe (Heid et al., 1996; Lang et al., 1997; Lie and Petropoulos, 1998).

By using *in vivo*, IHC and molecular techniques the experimental objectives in this chapter were three fold; (1) to investigate the role of microglia in established CCI-induced allodynia, (2) to investigate the role of the P2X7 receptor in microglial activation induced by CCI injury, (3) to investigate interaction of P2X7 and microglia in morphine-induced tolerance in CCI-operated rats and morphine-induced analgesia in naïve rats.

6.2 Methods

6.2.1 The effect of minocycline on CCI-induced allodynia in rats

To investigate the involvement of microglia in CCI-induced allodynia, rats were dosed with minocycline, and paw withdrawal thresholds to von Frey hairs were assessed.

6.2.1.1 CCI model

Sixty male Random-hooded rats underwent CCI surgery following the methods detailed in section 2.2. For details of the surgical procedure and the methodology for the behavioural testing with von Frey hairs please refer to sections 2.2.2.1 and 2.2.2.2 respectively.

6.2.1.2 Testing compounds

Minocycline was obtained from Sigma (M9511) and made up in 1% (w/v) saline for intra-peritoneal dosing at a dosing volume of 3 ml/kg or in 1% (w/v) methylcellulose for oral dosing at a dosing volume of 5 ml/kg.

6.2.1.3 Data analysis

Data are presented as mean ±SEM in grams and statistical analysis was carried out on PWTs. All drug dose groups were compared with the vehicle treated rats using Repeated Measures ANOVA, followed by Planned LSD comparisons, where $p<0.05$ was considered significant.

6.2.2 The expression of Iba-1 in spinal cord sections of CCI-operated rats dosed with P2X7 receptor antagonist using two immunohistochemical techniques

6.2.2.1 Preparation of tissue

Lumbar spinal cord sections of 1 cm length, were dissected from 6 CCI operated rats, 6 un-operated rats and 6 CCI operated rats treated with P2X7 receptor antagonist GSK1370319 (50 mg/kg, p.o., b.i.d. for 8 days) on day 34 post-surgery. This time-point post-surgery was chosen as it followed the 8 day dosing period when CCI-

induced allodynia was robust. The tissue was placed in 4% paraformaldehyde (PFA) and left at room temperature for 2 days before being washed in saline. 4% PFA was made up in a specific way in which 1000 ml of distilled water was heated to 56-58 °C before 42 g PFA was added with continuous stirring. One pellet of sodium hydroxide was added until the solution became clear before the solution was cooled and filtered. The pH was then lowered to 7.4 using 0.1M HCl before 5 PBS tablets (Sigma) were added. The final pH was then adjusted to 7.4.

Cord samples were placed in fully labelled tissue cassettes, dehydrated and processed into paraffin wax using a Shandon Citadel 2000 tissue processor. In summary, the cord samples were placed in the following environments for the following times, which included different concentrations of industrial methylated spirit (IMS).

70% IMS (1.5 hours) → 80% IMS (1 hour) → 90% IMS (1 hour) → 100% IMS (1 hour) → absolute ethanol I (1.5 hours) → absolute ethanol II (2 hours) → isobutyl alcohol I (1.5 hours) → isobutyl alcohol II (1.5 hours) → xylene I (2 hours) → xylene II (2 hours) → paraffin I (2 hours) → paraffin I (2 hours).

At the end of the programme, the cords were marked by a cut by a sharp blade on the ventral area of the contralateral side to aid orientation for subsequent steps.

To embed the tissues within a wax block, the Shandon Histocentre tissue embedding centre was used. The device is a workstation made up of a heated embedding centre, consisting of vessels of heated wax, and a cold plate used for setting the wax in the final stages.

The cord samples were first divided into 3 segments ensuring that each cut end was inverted and orientated correctly in base moulds taken from the pre-warming area. Wax was dispensed into the mould ensuring the cord remained in the correct orientation, with the surfaces to be sectioned placed downwards. The processing cassette, labelled with sample details, was placed on the top of the cord in the base mould and more wax was dispensed on the top of the cassette. After being placed on the cold plate the blocks were removed from the mould and trimmed in preparation for sectioning.

6.2.2.2 Sectioning

The block of embedded tissue was placed onto a Leica microtome chuck and secured. The section thickness was set to 5 µm and sections showing the characteristic shape of L4 and L5 (see Figure 60) were cut and removed from the knife edge. The sections were then stretched in a pre-heated (45 °C) water bath containing 2 L of distilled water. 3 serial sections were mounted onto each microscope slides (Superfrost plus, VWR) and placed on a slide drying tray set at approximately 35-40 °C to dry overnight.

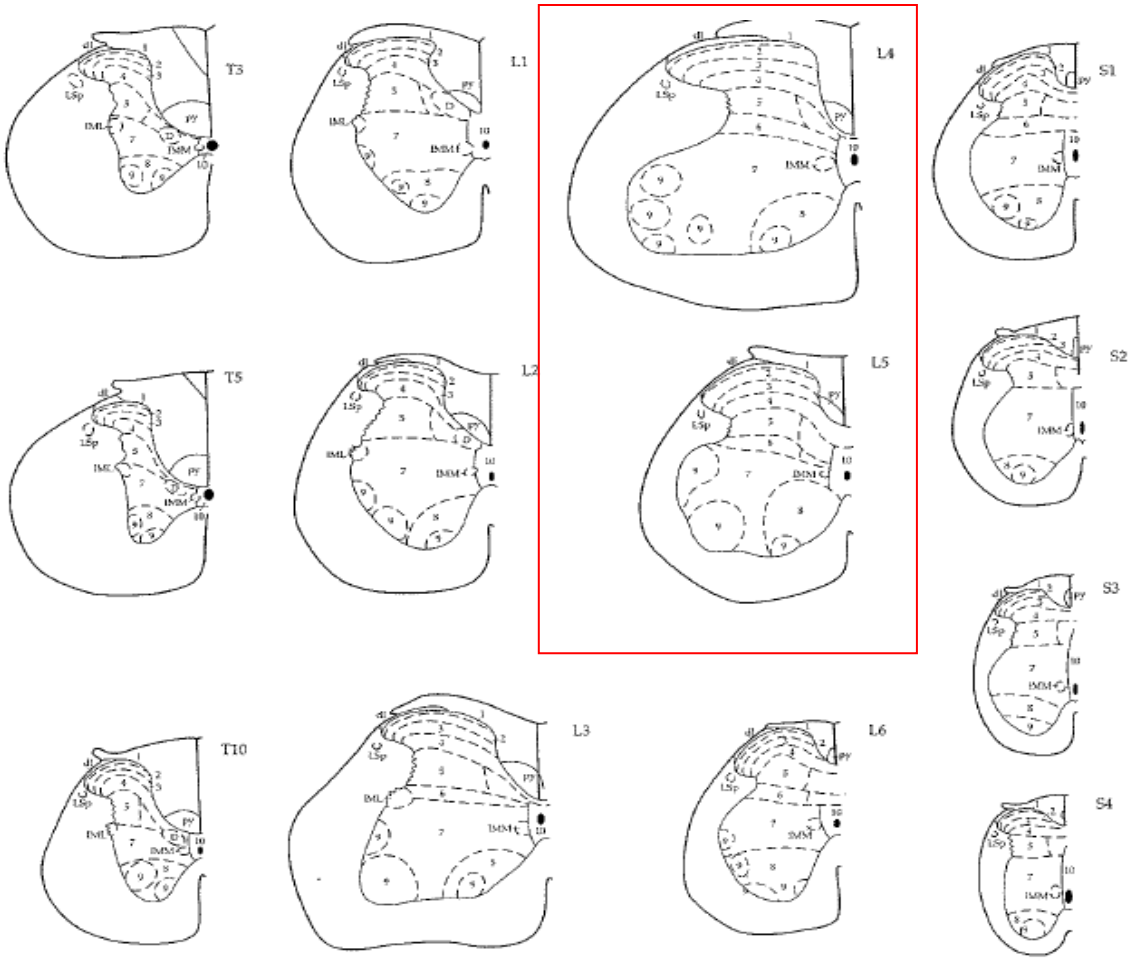

Figure 60. Spinal cord cytoarchitecture (Molander and Grant, 1995) 1-10: spinal cord layers, CeCv: central cervical nucleus, dl: dorsolateral fasciculus, IML: intermediolateral cell column, IMM: intermediomedial cell column, LatC: lateral cervical nucleus, LSp: lateral spinal nucleus, py: pyramidal tract.

6.2.2.2.1 Cresyl violet staining

To aid identification of the spinal cord region, slides were stained with cresyl violet using the following protocol. The sections were first dewaxed by placing the slides in the following sequence of liquids for 5 minutes each step.

Xylene → Xylene → Xylene → Absolute ethanol → 90% IMS → 70% IMS → distilled water

The slides were then placed in 1% Fast Cresyl Violet solution for 5 minutes and then washed twice in tap water. The slides were then dehydrated, placing the slides in the following sequence of liquids for the specified times.

70% (v/v) Ethanol (20-30 sec) → 90% Ethanol (1 min) → Absolute ethanol (3-5 min) → Absolute ethanol (3-5 min) → Xylene (5 min) → Xylene (5min)

Finally, coverslips were put on the slides, mounted with DPX, and dried overnight on a hot plate at 35 ºC.

6.2.2.3 Immunostaining

Immunostaining for activated microglia was performed using two different methods: manually or by using a Ventana Discovery XT robotic platform (Roche). Before investigating the effect of GSK1370319 on CCI-induced microglia activation it was important to confirm sufficient microglia activation was apparent in CCI-operated rats compared to un-operated rats. The manual method was used for the initial study and the automated method was used for the compound dose study.

The overall principle for both manual and automated studies was similar and followed the avidin-biotin method. However there were some differences between the two methods including reagents used (e.g. buffers, blockers and washing solutions) as well as the incubation times for each step. The differences are illustrated in two diagrams below and described in the method sections.

6.2.2.3.1 Manual staining method for identifying activated microglia in the spinal cord of CCI-operated rats and un-operated rats

2 sections from 1 slide per rat were used for this study comparing 6 CCI operated rats and 6 sham operated rats.

The sections were first dewaxed by placing the slides in the following sequence of liquids for 5 minutes each step.

Dewax histoclear → I Histoclear → II Histoclear → Absolute ethanol → 90% IMS → 70% IMS → distilled water

Figure 61 illustrates each step of the staining method. The numbers below correspond to the numbers on the diagram.

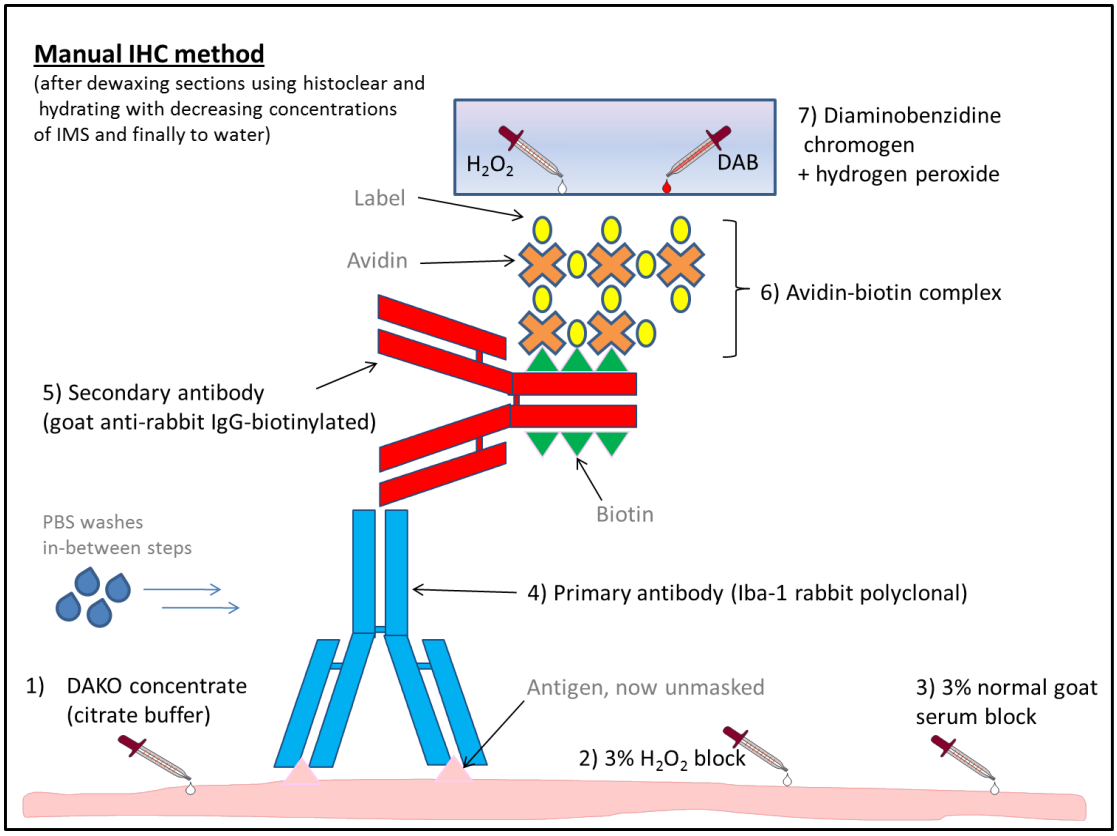

Figure 61. A diagram summarising the method used for manually staining spinal cord.

1) To unmask the antigen from cross-links which may have occurred during the processing stage, an antigen retrieval buffer was prepared. 100 x DAKO concentrate (HD supplies) was diluted 1:10 and pH adjusted to 6.0. The buffer was heated in a microwave at 750 W for 4 minutes. The slides were placed in the hot buffer and placed in the microwave and heated at 300 W for 5 minutes. The slides were then cooled for 10 minutes in gentle running cold water, before being transferred to the microwave and heated again for 5 minutes at 300 W.

2) Having completed the antigen retrieval step the slides were washed in PBS twice. 3% (v/v) hydrogen peroxide (BDH) in PBS was added to the slides and left for 30 minutes. The slides were then washed with PBS twice before the sections were circled using a 'pap pen'. The hydrophobic properties of the ink allow a barrier to be drawn on the glass slide to confine the flow of reagents to a defined area.

3) The slides were incubated for 45 minutes with 3% (v/v) normal goat serum 1% (v/v) bovine serum albumin (BSA) which acted as a 'blocking' solution.

4) The slides incubated overnight at 4 °C in the primary antibody, Iba-1 (rabbit polyclonal, 1:2000, Wako Chemicals, GMBH), which was then diluted in 1% BSA.

5) After 3 washes in PBS the slides were incubated for 30 minutes in the secondary antibody, goat anti-rabbit, IgG- biotinylated (1:200, Vector BA-1000).

6) The ABC vector kit (Vector PK6100) was prepared by mixing avidin and biotin together and left for 30 minutes. After being washed in PBS three times, the slides were incubated in the ABC mix for 45 minutes, before being washed again in PBS three times.

7) The DAB-chromagen reaction was completed by preparing a buffer containing 100 ml Tris buffer and 0.5 ml aliquot DAB (Sigma D5637 50 mg) and adding 20 µl 30% hydrogen peroxide. The slides were incubated in the buffer for 5 minutes before the reaction was stopped with PBS and then water.

Following the staining protocol, sections were dehydrated following the steps below (3 minutes for each) before being coverslipped using DPX medium.

70% Ethanol → 90% IMS → Absolute ethanol → Absolute Ethanol

A Leica DMR microscope equipped with colour camera DFC500 was used for image acquisition. To quantify the images, analysis was completed using Karl Zeiss Vision KS300 and the Media cybernetic imaging software.

In brief, 4 sections from each rat (8 images) were uploaded and the grey matter in ipsilateral and contralateral dorsal horn was manually 'drawn around'. The threshold of brown colour to match colour of activated microglia was set to avoid background. The software then calculated the % area containing the stipulated intensity of the brown staining. Artefacts having dark brown colour intensity were manually excluded from count. Each area of interest was drawn with the operator

blind to the treatment the rat had received. After the % area containing Iba-1 stained activated microglia had been calculated, statistical comparisons were made using repeated measures ANOVA followed by Planned LSD comparisons comparing responses from CCI operated rats and responses from un-operated rats.

6.2.2.3.2 Automated method for identifying activated microglia in the spinal cord of CCI-operated rats dosed with GSK1370319

Slides were placed on the Ventana Discovery platform and the programme was initiated. All staining procedure from dewaxing the slides to final DAB detection system was performed by the Ventana Discovery XT robotic platform (Roche). A detergent (EZPrep, Ventana 950-102) was used to wash off the wax after the slide had automatically been heated to 75 °C, a liquid 'coverslip' (Ventana 650-010) was applied which consists of a drop of liquid which protects the samples (see Figure 62), but allows application of substances by passing through the liquid.

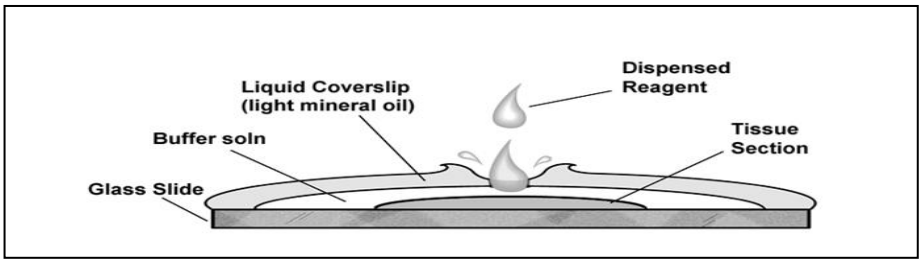

Figure 62. Diagram illustrating the liquid coverslip

Figure 63 illustrates each step of the staining method. The numbers below correspond to the numbers on the diagram.

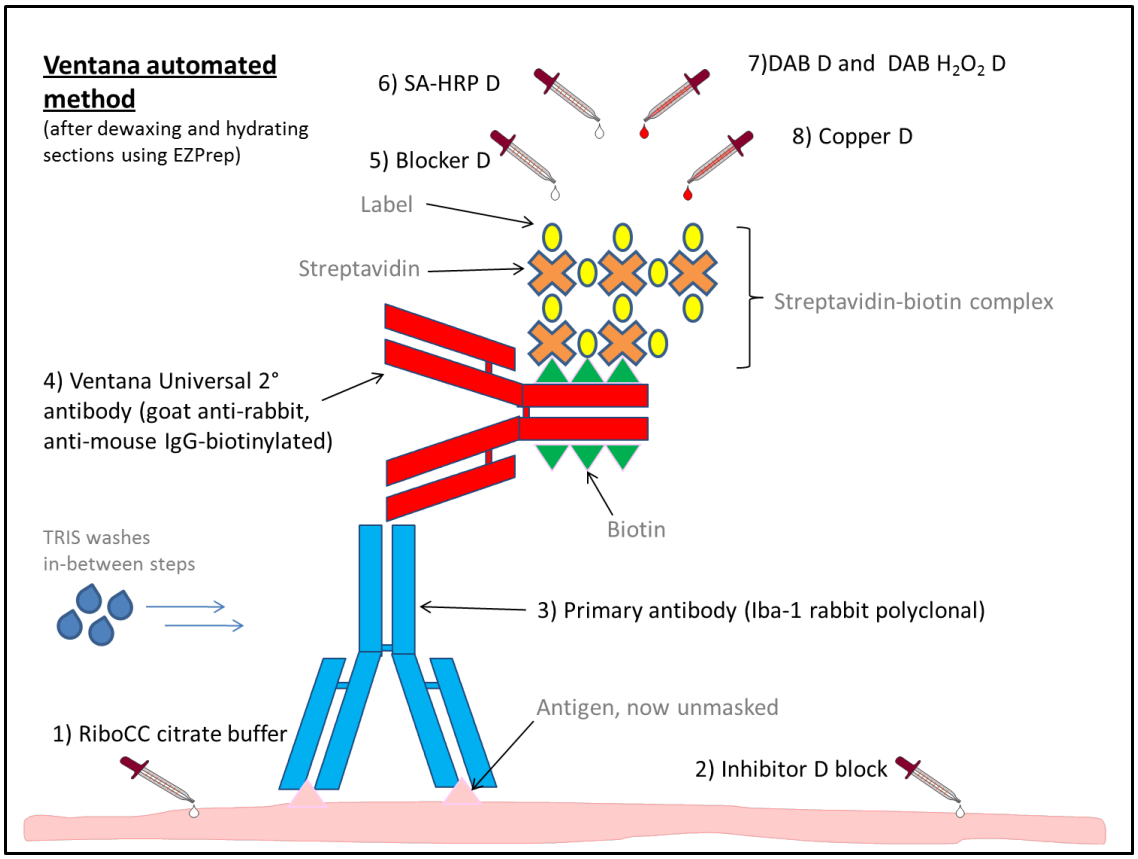

Figure 63. A diagram summarising the method used for staining spinal cord using the Ventana Discovery platform

1) Antigen retrieval was accomplished by adding RiboCC citrate pH 6.0 (Ventana 760-107) for 32 minutes at 95-100 ºC.

2) Hydrogen peroxide block followed by applying one drop of 'inhibitor D' for 4 minutes before the slide was washed with TRIS buffer.

3) The primary antibody was a rabbit polyclonal to Iba-1 (Wako 019-19741) applied at 1:500 for 2 hour before being washed with TRIS buffer.

4) After several washing steps and heating the slides to 37 °C the Ventana universal secondary antibody (biotinylated anti rabbit + mouse IgGs, Ventana 760-4205) was applied and left for 32 minutes before being washed by TRIS buffer.

5) 'Blocker D' was then applied, however due to the commercial reasons the identify of this blocker is unknown.

6) 1 drop of streptavidin-horseradish peroxide D (SA-HRP D) was applied and left for 16 minutes to initiate amplification.

7) DAB D (enzyme) and DAB H2020 D (substrate) (DAM Map kit; Ventana 760-124), was applied and incubated for 8 minutes in each.

8) To enhance the signal, one drop of copper D was applied before slides were incubated for 4 minutes.

When the programme had finished, the slides were taken out of the robot, dehydrated through the ethanol series detailed below, cleared with xylene and coverslipped.

70% Ethanol → 90% IMS → Absolute Ethanol → II Absolute Ethanol

The slides were scanned in Hamamatsu NanoZoomer under 20 x objective size. Image quantification was conducted using Image-pro. The grey matter in ipsilateral and contralateral dorsal horn was manually drawn around and the threshold of brown colour to match colour of activated microglia was set to avoid background. The software calculated the % area containing the stipulated intensity of the brown staining. Artefacts having intense dark brown colour were manually excluded from the count. After the % area containing Iba-1 stained activated microglia had been calculated statistical comparisons were made using repeated measures ANOVA followed by Planned LSD comparisons. Responses from CCI operated rats and responses from un-operated rats were first compared followed by a comparison between CCI operated rats dosed with vehicle and CCI operated rats dosed with GSK1370319.

6.2.3 Quantitative real-time RT-PCR assessment of specific gene expression in rat spinal cord

mRNA expression of specific genes were assessed, using Taqman quantitative real-time RT-PCR, in spinal cord samples taken from Random-hooded rats used in a CCI study and naïve Lister hooded rats used in acute pain study. Two housekeeping genes were used in these studies: Cyclophilin and β- actin.

6.2.3.1 mRNA expression of ITGAM, PBR, GFAP, IL-1β, TNF-α and μ opioid receptors in the spinal cord of CCI operated rats chronically co-dosed with GSK1370319 and morphine

6.2.3.1.1 Sample dissection and storage

After rats had been euthanised at the end of CCI combination study detailed in section 3.3.3, a 1 cm section of lumbar spinal cord was removed, placed on foil and stored at -80 °C until used. Samples were taken from 3 rats treated with vehicle (p.o.) + vehicle (s.c.), vehicle (p.o.) + morphine (10 mg/kg, s.c.), GSK1370319 (5 mg/kg, p.o.) + vehicle (s.c.) and GSK1370319 (5 mg/kg, p.o.) + morphine (10 mg/kg, s.c.).

6.2.3.1.2 Purification of genetic material

Purification of genetic material was carried out using the RNeasy lipid tissue mini protocol (Qiagen, Germany) using the method detailed in section 4.3.2.2.

6.2.3.1.3 Quantification of nucleic acids

The quantification of nucleic acids was done using the nanodrop machine (Labtech International Ltd) using the method detailed in section 4.3.2.3.

6.2.3.1.4 Conversion of RNA to cDNA

Conversion of RNA to cDNA for amplification of specific gene sequences was completed using a reverse transcriptase kit (High capacity cDNA kit, Applied Biosystems). 10 µl of prepared RNA were placed into appropriate wells and the RT mastermix was made up as detailed below:

	For 1 well (µl)	For 115wells (µl)
Mastermix	4	460
H_20	6	690
RNA	10	-
Total volume	20	1150

10 µl RT mastermix was aliquoted into each well and a foil lid was added before the plate was spun down briefly. The plate was incubated at 25 °C for 5 minutes, 42 °C for 30 minutes, 85 °C for 5 minutes and then held at 4°C using a PCR system (GeneAmp 9700, Applied Biosystems). Finally, 50 µl RNase free water was added to each well, the foil was replaced and vortexed and spun for 1 min. To prepare test plates, 5 µl of each sample was added to each well of a Fast Optical plate (MicroAmp before the plates are stored in -80 °C.

6.2.3.1.5 Quantitative measurement of gene expression

Measurement of gene expression was performed by Quantitative RT-PCR using Taqman^{TM} fluorogenic probes, a technique which enables the measurement of an accumulating PCR product in real time, and hence a precise determination of the initial number of copies of a PCR template.

Firstly, genomic a DNA standard was prepared in DEPC H_2O: 100 µl of each total: 1, 1/10, 1/100, 1/1000, 1/10000 (1/10 serial dilution: 10 µl gDNA, 90 µl H_2O) and vortexed and centrifuged briefly.

5 µl of cDNA, genomic standards and a no template control (NTC) were used per Taqman PCR reaction. MicroAmp® Fast Optical 96-Well Reaction Plate with Barcode (Applied Biosystems) were used for running the Taqman reaction.

In this study, the housekeeping genes were cyclophilin and β-actin, and the genes of interest were PBR, ITGAM, GFAP, IL-1β, TNF-α and µ opioid receptor. Primers and probes are listed in the appendix and were purchased from Sigma Genosys as bespoke oligos. The Taqman master mix was made up for each primer set as follows.

	For 1 well (µl)	For 120 wells (µl)
Taqman Universal PCR mastermix	10	1200
DEPC H_20	3.4	408
Forward primer (10 µM)	0.6	72
Reverse primer (10 µM	0.6	72
Taqman probe (5 µM)	0.4	48

The mix was transferred to a reservoir, 15 µl was dispensed into each appropriate well, including genomic DNA and NTC wells and an optical adhesive cover (Applied Biosystems) was applied to the top of the plate. The plate was centrifuged at 134 x gravity for 1 min and placed into the 7500 fast system.

The programme involved incubating the plate for 20 seconds at 95 °C before 40 cycles were commenced. A cycle consisted of 3 seconds at 95 °C followed by 30 seconds at 60 °C.

When the programme had completed, the data was exported into Microsoft Office Excel and statistically analysed using Omicsoft array studio v3.6. which generated data for the genes of interest which were normalised by both housekeepers. Statistical analysis was one-way ANOVA comparing the rats administered orally dosed vehicle and subcutaneously dosed vehicle producing 95% confidence intervals.

6.2.3.2 mRNA expression of ITGAM and PBR in the spinal cord of naïve Lister-hooded rats co-dosed with morphine and GSK1370319

6.2.3.2.1 Sample dissection and storage

After rats had been euthanised at the end of an acute pain study detailed in section 5.3.1.4, a 1 cm section of lumbar spinal cord was removed, placed on foil and stored in -80 °C freezer. Samples were taken from 3 rats treated with vehicle 1 (p.o.) + vehicle 2 (s.c.), 2 rats treated with GSK1370319 (20 mg/kg, p.o.) and morphine (0.3 mg/kg, s.c.) and 4 rats from each of the following groups: GSK1370319 (20mg/kg, p.o.) + vehicle (p.o.), GSK1370319 (20 mg/kg, p.o.) + morphine (3 and 10 mg/kg, s.c.) and vehicle (p.o.) + morphine (0.3, 3 and 10 mg/kg, s.c.)

6.2.3.2.2 Purification of genetic material and RNA extraction

The protocol detailed in section 4.3.2.2 was followed.

6.2.3.2.3 Quantification of nucleic acids

The protocol detailed in section 4.3.2.3. was followed.

6.2.3.2.4 Conversion of RNA to cDNA

The protocol detailed in section 4.3.2.4 was followed.

6.2.3.2.5 Quantitative measurement of gene expression

The protocol detailed in section 4.3.2.5 was followed. The genes of interest in this study were PBR and ITGAM.

6.3 Results

6.3.1 The effect of minocycline on CCI-induced allodynia in rats

In this study, one dose of minocycline was tested alongside a GSK compound from a programme unrelated to this thesis. Only the method and results from rats dosed with minocycline, its associated vehicle and the positive control pregabalin will be reported.

Von Frey hair testing was carried out on the day prior to surgery and on day 19 post- surgery. On day 20, after rats had been ranked and assigned to a dose group they were repeatedly dosed with minocycline (30 mg/kg, intra-peritoneally, b.i.d., n=9) or the associated vehicle (saline, n=9) and pregabalin (30 mg/kg, p.o., b.i.d., n=9) for 8 days. The dose of 30 mg/kg was chosen as a dose commonly used in the literature (Zanjani et al., 2006; Mika et al., 2009b). After the first intra-peritoneal dose of minocycline was administered however the rats appeared to show signs of distress (vocalisation and hunching) which lasted for 2-3 minutes. It was decided to not dose these rats for 3 dosing sessions before continuing to dose via an alternative route. It is important to emphasize that the adverse effects were within the acceptable boundaries of the Home Office Project licence. When dosing commenced, rats were administered with minocycline via the oral route for the 6 remaining days of the dosing period. A group of rats orally dosed with pregabalin (30 mg/kg) for the entire 8 day dosing period was included as a study control.

Testing was conducted 1 hour post-morning dose on day 1 (pregabalin dosed rats only), 3, 5 and 8 of the dosing period which corresponded to days 20, 22, 25 and 27 post-surgery.

Prior to surgery, all rats produced a mean PWT of 24.4 ±0.8 g which decreased dramatically to 4.6 ±0.4 g 19 days post CCI surgery demonstrating an allodynic response. On day 19 there were 5 CCI-operated rats that met the exclusion criteria of PWT > 10 g and so were not included in the study.

Throughout the dosing period, rats dosed with vehicle continued to show allodynia as expected, producing PWTs with a range of 4.0-4.8 g, which were not significantly different to the pre-dose PWT (Figure 64). PWTs from rats dosed with

pregabalin significantly increased on day 3, 5 and 8 producing PWTs of approximately 14 g.

When rats were dosed with minocycline for 6 days the PWT also increased and was significantly different from the vehicle response on all days of dosing period, producing PWTs of approximately 12 g. It is worth noting that minocycline was active on the first day of dosing, whereas pregabalin required 4 doses before efficacy was observed. The efficacy shown with minocycline in this study implicates the involvement of microglia in CCI-induced allodynia in rats.

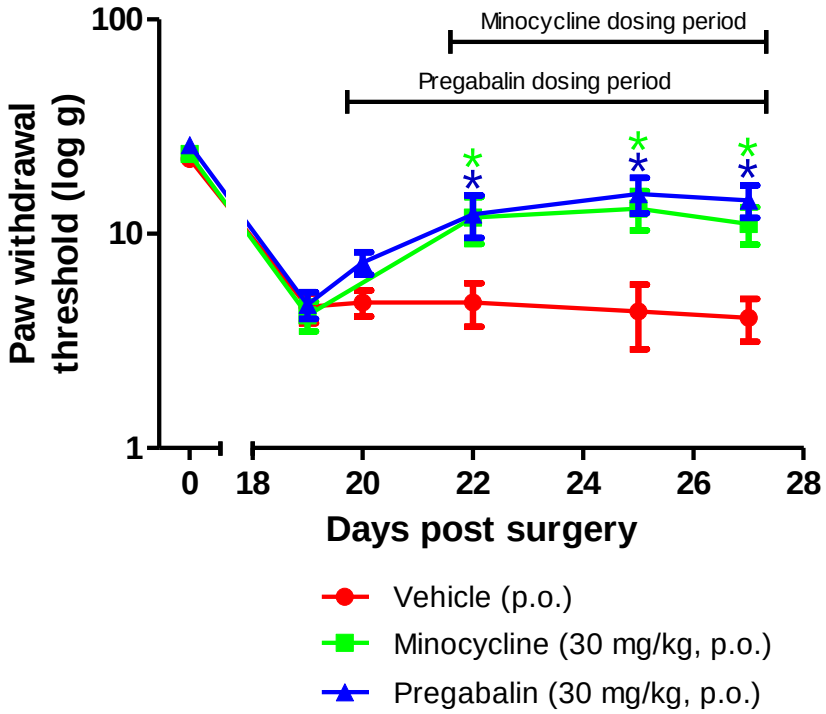

*Figure 64. Effect of microglia inhibitor, minocycline (30 mg/kg, p.o., b.i.d. for 6 days) on paw withdrawal threshold of CCI-operated rats following von Frey filament application. Pregabalin (30 mg/kg, p.o., b.i.d. for 8 days) was included as a positive control. Data are log mean ±SEM with 9 rats in each group. * denotes $p<0.05$ comparing drug treated rats with vehicle treated rats using Repeated Measures ANOVA followed by Planned LSD comparisons.*

6.3.2 The expression of activated microglia in spinal cord sections of CCI-operated rats dosed with P2X7 receptor antagonist using two immunohistochemical techniques

6.3.2.1 Manual staining method for identifying activated microglia in the spinal cord of CCI-operated rats and un-operated rats

To identify the presence of microglia in CCI-induced allodynia 34 days post-surgery, spinal cords of CCI and naïve rats were taken, processed and stained with antibody for Iba-1.

To aid identification of the spinal cord regions sections were stained with cresyl violet. Figure 65 shows two representative images showing the lumbar L4 and the L5 regions. In this initial study, sections of both L4 and L5 regions were used and combined.

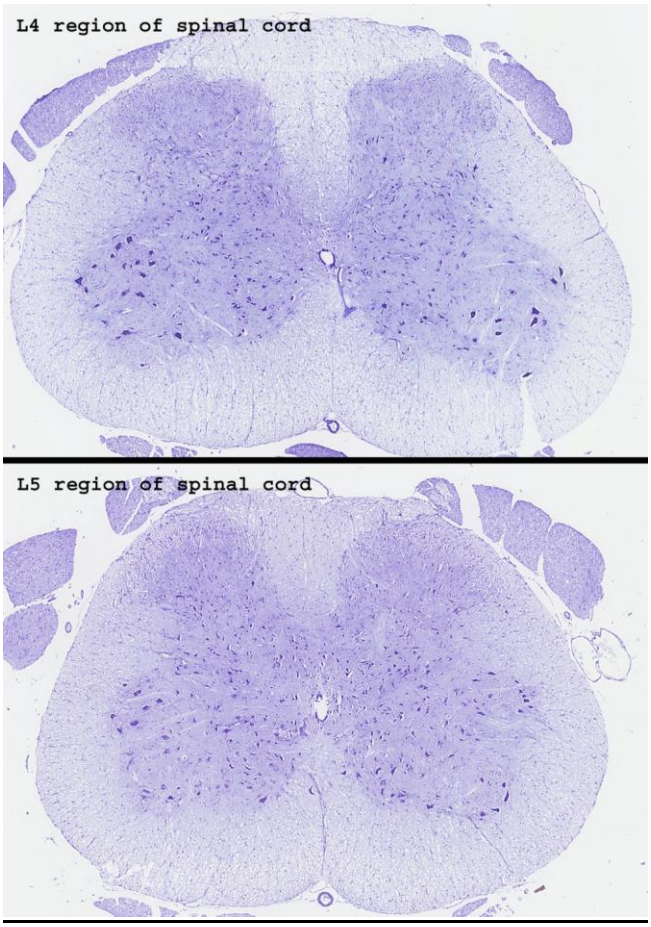

Figure 65. Representative images showing cresyl violet staining of the lumbar L4 and L5 spinal cord of male rats. [Scale: 1 mm]

Data from all sections stained with Iba-1 antibody are represented as a scatter plot (Figure 66a). There was no observed difference in staining between the ipsilateral and the contralateral dorsal horns in un-operated rats producing values of 1.7-3.0% and 1.6-2.9% respectively. In contrast, when ipsilateral and contralateral sides were compared in CCI-operated rats there was a difference producing values of 2.9-5.3% and 1.7-2.5% respectively. There also appears to be a difference in staining between the ipsilateral dorsal horns of un-operated and CCI-operated rats.

When mean data was calculated the difference between the ipsilateral or the contralateral dorsal horns in CCI rats was statistically significant producing values of 3.96% (95% conf. limits 3.26-4.67) and 2.26% (95% conf. limits 1.86-2.67) respectively (Figure 66b). There was also a significant difference between the ipsilateral dorsal horns of un-operated rats and CCI-operated rats. There was no significant difference between the ipsilateral and contralateral dorsal horns of un-operated rats producing values of 2.42% (95% conf. limits 1.71-3.12) and 2.22% (95% conf. limits 1.81-2.63) respectively.

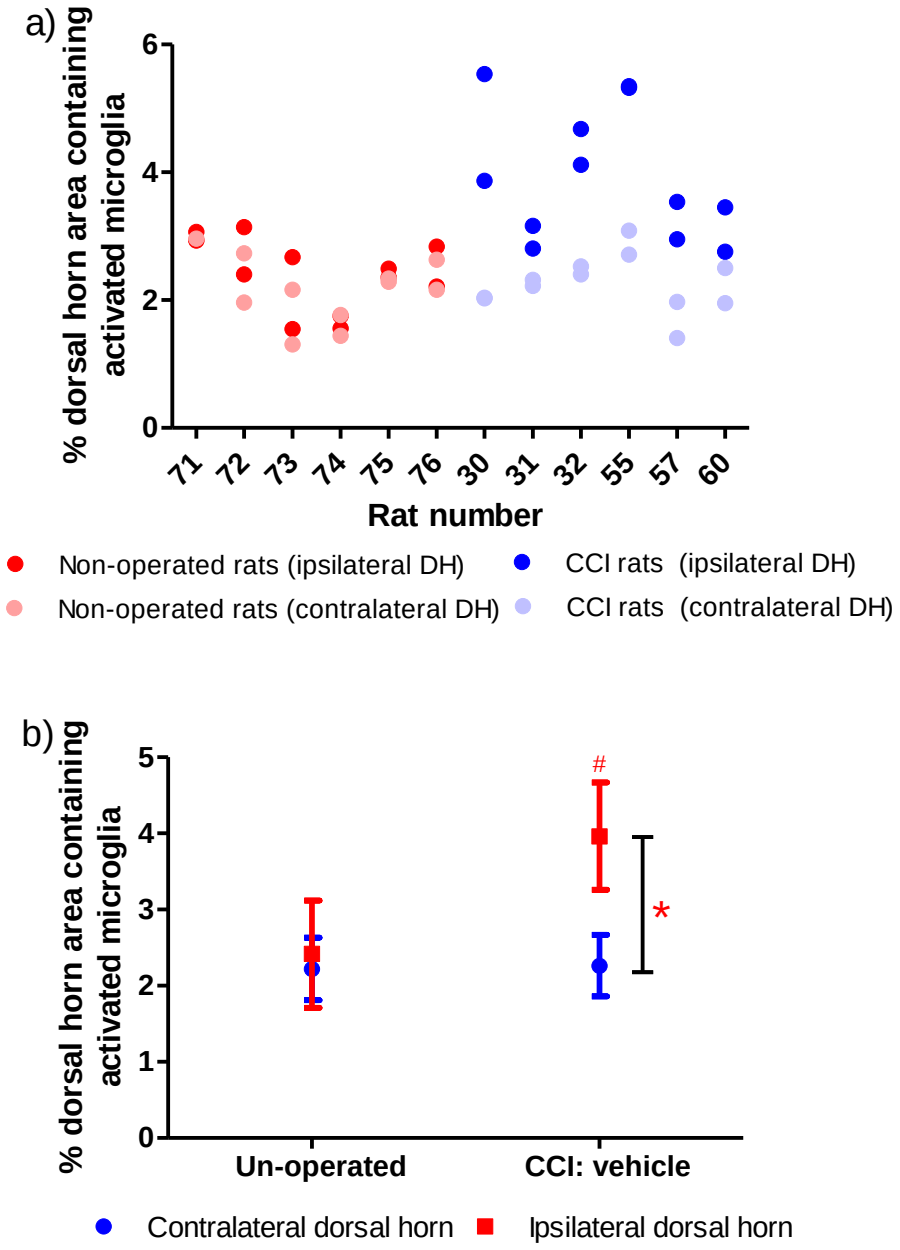

*Figure 66. % area of the ipsi- and contralateral dorsal horn containing Iba-1 stained activated microglia from 6 CCI-operated rats and 6 un-operated rats with 2 sections from each rat. Data are individual % areas containing Iba-1 stained activated microglia within a manually marked area of interest (a) and mean ±95% confidence limits (b.) Statistical analysis used repeated Measures ANOVA followed by Planned LSD comparisons of ipsilateral and contralateral dorsal horn (*p<0.05) and CCI operated rats and un-operated rats responses (# p<0.05).*

Figure 67 shows representative images of Iba-1 staining in the lumbar regions of the dorsal horn. The brown particles are activated microglia which appear most numerous in the ipsilateral dorsal horn from CCI-operated rats compared to un-operated (naïve) rats.

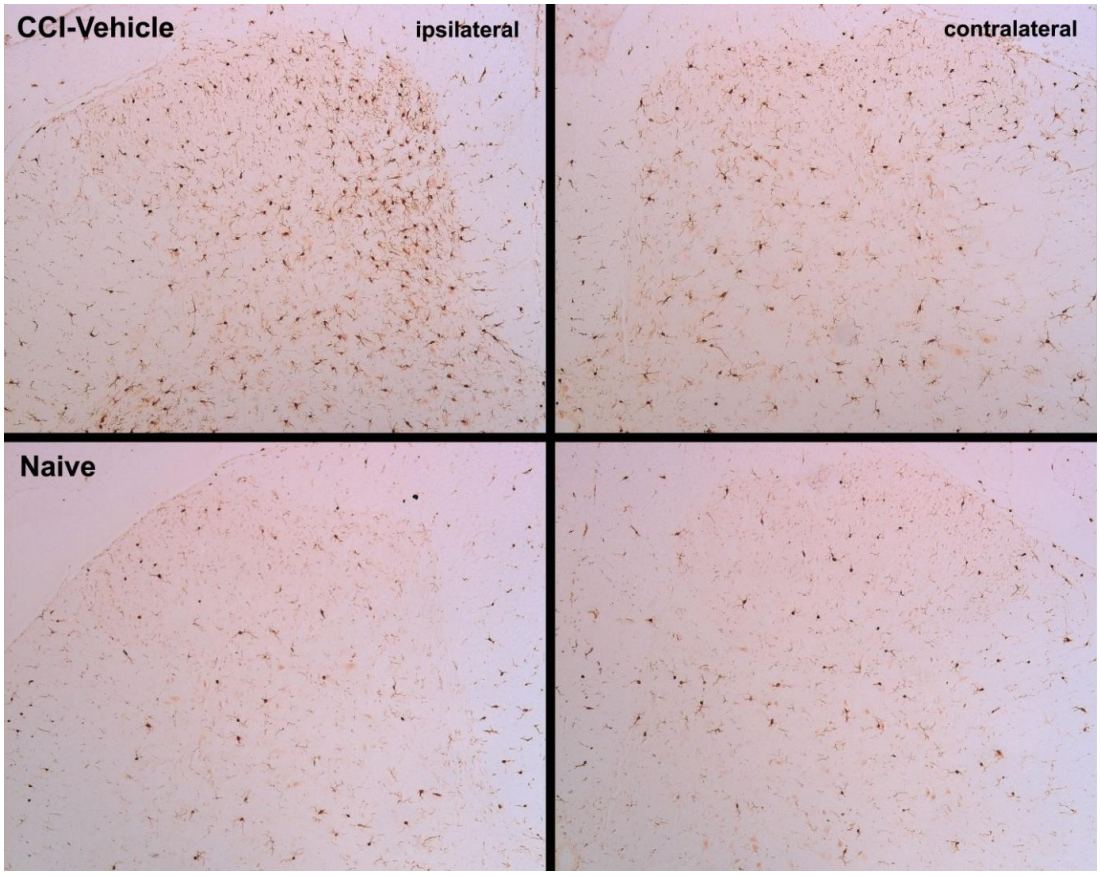

Figure 67. Representative images showing Iba-1 staining of the lumbar (L4-L5) spinal cord of male rats 34 days after CCI surgery and age-matched un-operated rats. The upper two panels show the ipsilateral and contralateral superficial dorsal horns of CCI-operated rats dosed with vehicle (1% methylcellulose, p.o., b.i.d. for 8 days). The lower two panels show the similar cord regions in un-operated ('naïve') and untreated age-matched rats. [Scale: 500µm]

6.3.2.2 Automated method for identifying activated microglia in the spinal cord of CCI-operated rats dosed with GSK1370319

The effect of P2X7 receptor antagonist GSK1370319 on CCI-induced increase in activated microglia was investigated by comparing the levels of Iba-1 staining in

dorsal horn sections from the L4 lumbar region in CCI-operated rats dosed with GSK1370319 or vehicle.

When data from all sections were represented as a scatter plot (Figure 68a) it appeared there was no difference in staining between the ipsilateral or the contralateral dorsal horns in un-operated rats producing a range of 1.4-2.6% and 1.2-2.4% respectively. In contrast, when the different sides were compared in CCI-operated rats dosed with vehicle, there was a clear separation producing values of 4.5-7.2% and 2.2-3.4% respectively. There was also a difference between ipsilateral and contralateral sides in CCI-operated rats dosed with GSK1370319 producing values of 1.7-6.5% and 0.4-3.6%. Finally, there appears to be a difference in staining between the ipsilateral dorsal horns of un-operated and CCI-operated rats.

Meaned data showed a difference between the ipsilateral and the contralateral dorsal horns in vehicle treated CCI rats was statistically significant producing values of 5.72% (95% conf. limits 4.73-6.71) and 2.86% (95% conf. limits 2.16-3.55) respectively (Figure 68b). There was also a significant difference between dorsal horns in GSK1370319 treated CCI rats producing values of 4.07% (95% conf. limits 3.08-5.05) and 2.35% (95% conf. limits 1.65-3.05) respectively. There was no difference between the dorsal horns of naïve rats producing values of 1.86% (95% conf. limits 0.87-2.85) and 1.77% (95% conf. limits 1.07-2.47) respectively.

When considering alternative comparisons there was a significant difference between the ipsilateral dorsal horns of un-operated rats and both groups of CCI-operated rats. Interestingly there was also a significant difference between the contralateral dorsal horn staining of vehicle treated CCI-operated rats and un-operated rats, but not between the GSK1370319 treated CCI-operated rats and un-operated rats.

The final comparison with this data is the difference in staining in the CCI-operated rats dosed with vehicle and GSK1370319. There was no significant difference in the staining of the contralateral dorsal horn between the two groups. In contrast the dorsal horn regions of the GSK1370319 dosed CCI-operated rats had a significantly smaller % area containing Iba-1 stained activated microglia than CCI-operated rats dosed with vehicle.

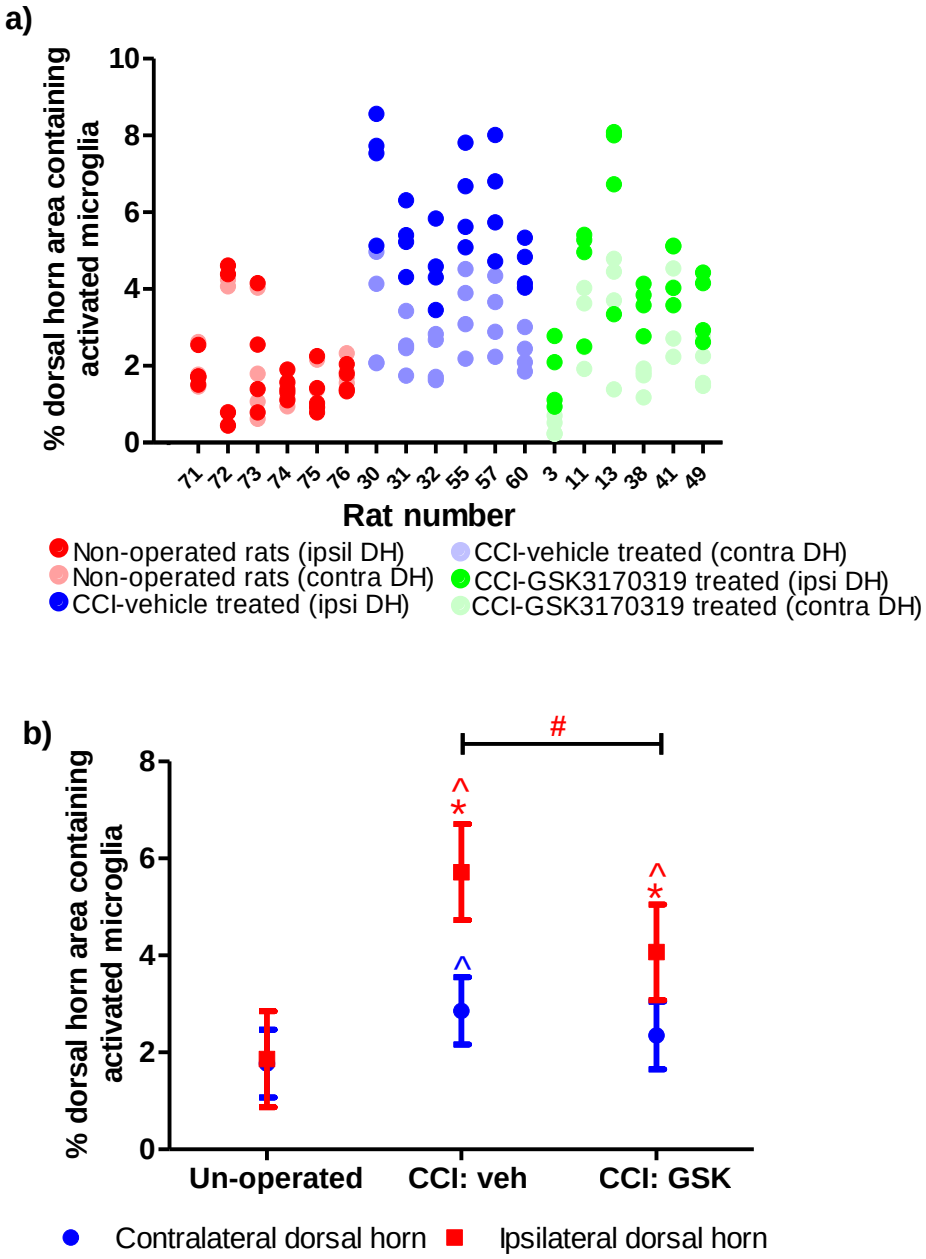

Figure 68. % area of the ipsi- and contralateral dorsal horn containing Iba-1 stained activated microglia from 6 non-operated rats and CCI operated rats dosed with vehicle and P2X7 receptor antagonist GSK1370319 (50 mg/kg, p.o., b.i.d. x 8 days) with 4 sections from each side from each rat. Data are individual % areas containing Iba-1 stained activated microglia within a manually marked area of interest (a) and mean ±95% confidence limits (b). Statistical analysis was completed using repeated Measures ANOVA followed by Planned LSD comparisons comparing responses from CCI operated rats and un-operated rats (^$p<0.05$), responses from ipsilateral and contralateral dorsal horn within the same group of rats ($p<0.05$) and CCI operated rats dosed with vehicle and GSK1370319 (#$p<0.05$).*

Figure 69 shows representative images of Iba-1 staining in the lumbar regions of the dorsal horn. The brown particles are activated microglia which appear most numerous in the ipsilateral dorsal horn from CCI-operated rats dosed with vehicle.

This data using the automated Ventana Discovery platform confirms the increase in activated microglia in the ipsilateral dorsal horn of to CCI-operated rats reported in the previous section. In addition, this data suggests that the CCI-induced increase in activated microglia was significantly reduced in rat treated with P2X7 receptor antagonist GSK1370319.

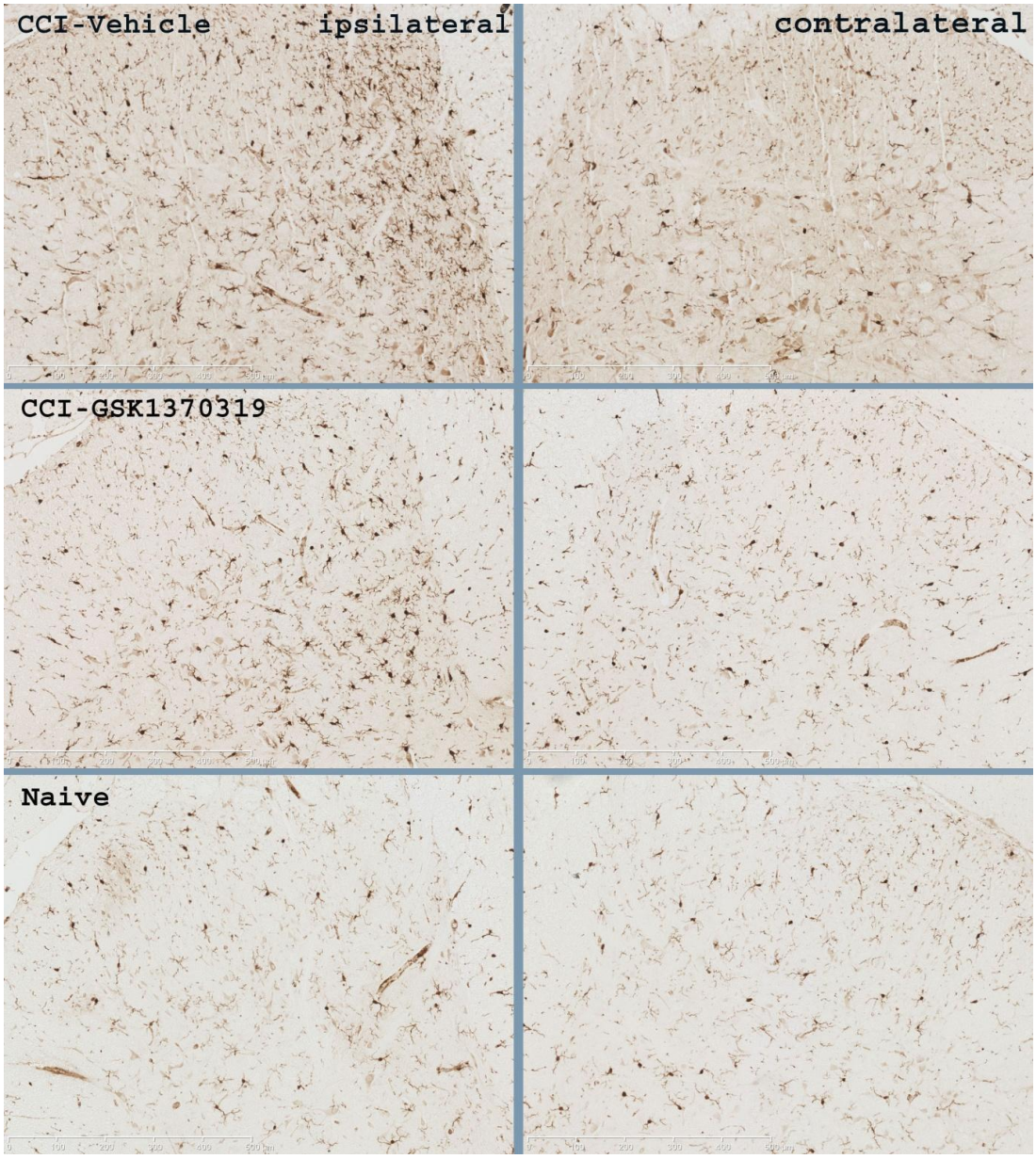

[Scale: 500µm]

Figure 69. Representative images showing Iba-1 staining of the lumbar (L4 region) spinal cord of male rats 34 days after CCI surgery after being dosed with P2X7 receptor antagonist GSK1370319 (50 mg/kg, p.o., b.i.d. for 8 days) or vehicle (1% methylcellulose, p.o., b.i.d. for 8 days) and age-matched un-operated rats. The upper two panels show the ipsi-and contralateral superficial dorsal horns of CCI-operated rats dosed with vehicle ('CCI – Veh'). The middle two panels show the ipsi- and contralateral superficial dorsal horns of CCI-operated rats dosed with GSK1370319 ('50 mg/kg'). The lower two panels show the similar cord regions in un-operated ('naïve') and untreated age-matched rats.

6.3.3 Quantitative real-time RT-PCR assessment of specific gene expression in rat spinal cord

Two RT-PCR studies were conducted to investigate the role of microglia in the P2X7-induced enhancement of morphine efficacy in naïve rats and the role of microglia in morphine-induced tolerance in CCI-operated rats.

6.3.3.1 mRNA expression of ITGAM, PBR, GFAP, IL-1β, TNF-α and μ opioid receptors in the spinal cord of CCI operated rats repeatedly co-dosed with GSK1370319 and morphine

When mRNA expression was quantified in spinal cord sections from CCI rats dosed with morphine and GSK1370319 for 8 days, there was no difference in expression in either of the housekeeping genes cyclophilin and β-actin (Figure 70), suggesting that the quality of the mRNA was similar across the majority of samples and these genes were not affected by treatment.

The mRNA coding for PBR, ITGAM, GFAP, μ opioid receptor, IL-1β and TNF also remained unchanged regardless of the treatment when compared to the expression levels of rats dosed with both vehicles.

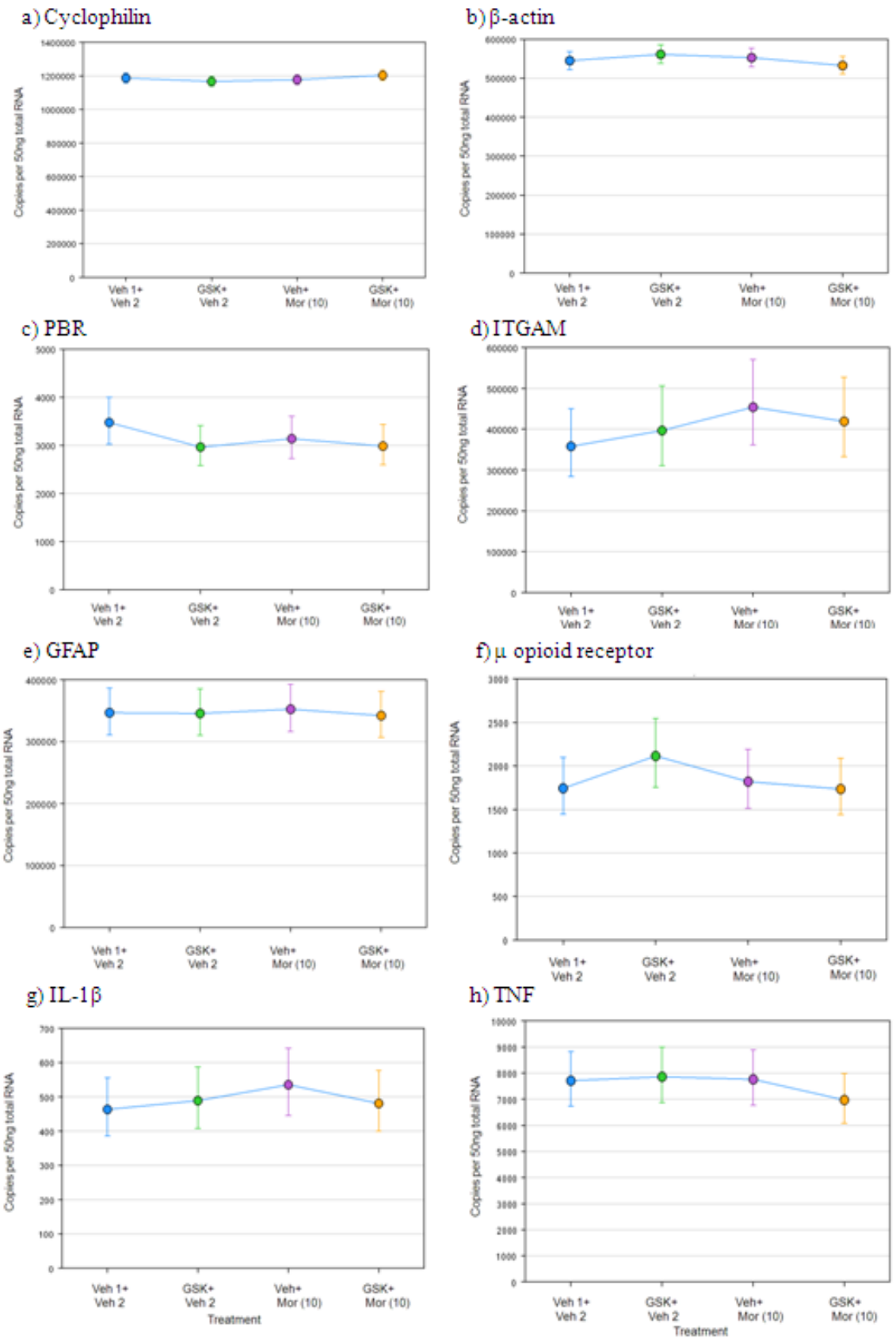
a) Cyclophilin
b) β-actin
c) PBR
d) ITGAM
e) GFAP
f) μ opioid receptor
g) IL-1β
h) TNF
Copies per 50ng total RNA
Veh 1+ Veh 2
GSK+ Veh 2
Veh+ Mor (10)
GSK+ Mor (10)
Treatment

Figure 70. mRNA expression of cyclophilin (a), β-actin (b) PBR (c), ITGAM (d), GFAP (e), μ opioid receptor (f), IL-1β (g) and TNF-α (h) in the lumbar region of spinal cord of CCI-operated male Random hooded rats co-dosed with GSK1370319 and morphine for 12 days (b.i.d.) between days 21-32 post-surgery . This data was taken from 3 rats treated with vehicle (1% methylcellulose, p.o., 'Veh 1') + vehicle (saline, s.c., 'Veh 2'); GSK1370319 (5mg/kg, p.o., 'GSK') + vehicle (saline, s.c., 'Veh 2'); vehicle (1% methylcellulose, p.o., 'Veh 1') + morphine (10 mg/kg, s.c., 'Mor 10'); GSK1370319 (5 mg/kg, p.o., 'GSK') + morphine (10 mg/kg, s.c., 'Mor 10'). The house keeper genes were β-actin and cyclophilin.

6.3.3.2 mRNA expression of ITGAM and PBR in the spinal cord of naïve Lister hooded rats co-dosed with morphine and GSK1370319

To investigate the role of microglia in P2X7-induced enhancement of morphine analgesia in naïve rats, mRNA expression of PBR and ITGAM were assessed in the lumbar spinal cord region of naïve Lister-hooded rats.

Two housekeeper genes were used in this study, cyclophilin and β-actin, both of which showed no difference in expression regardless of the treatment that the rats received (Figure 71). This suggests that the quality of the mRNA was similar across the majority of samples and these genes were not affected by treatment.

There was no difference in the expression of PBR or ITGAM gene in the cord of naïve rats injected with morphine (0.3, 3, 10 mg/kg) in the presence or absence of P2X7 receptor antagonist GSK1370319.

Interestingly it appeared that as the morphine dose increased, in the absence of P2X7 receptor antagonist, the expression of ITGAM decreased. This pattern however was not present when the opioid was dosed in the presence of P2X7 receptor antagonist, however the expression level was extremely low and this could be due to a background signal.

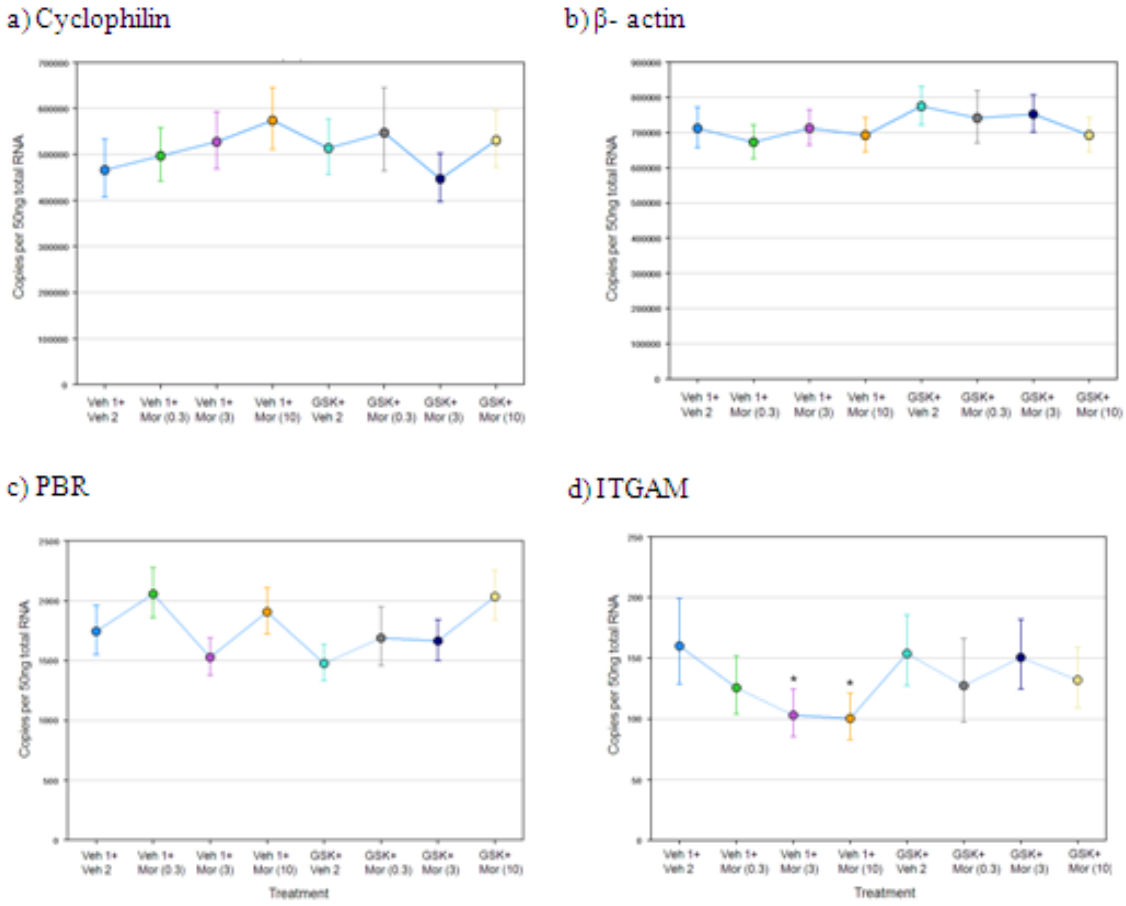

Figure 71. mRNA expression of cyclophilin (a), β-actin (b) PBR (c), ITGAM (d) in the lumbar region of spinal cord of naive male Lister hooded rats co-dosed with GSK1370319 and morphine. This data is taken from 3 rats treated with vehicle (1% methylcellulose, p.o., 'Veh 1') + vehicle (saline, s.c., 'Veh 2'); 2 rats treated with GSK1370319 (20 mg/kg, p.o., 'GSK') and morphine (0.3 mg/kg, s.c., 'Mor 0.3'); 4 rats from each of the following groups: GSK1370319 (20 mg/kg, p.o., 'GSK') + vehicle (saline, s.c., 'Veh 2'); GSK1370319 (20 mg/kg, p.o., 'GSK') + morphine (3 and 10 mg/kg, s.c., 'Mor 3' and 'Mor 10'); vehicle (1% methylcellulose, p.o., 'Veh 1') + morphine (0.3, 3 and 10 mg/kg, s.c., 'Mor 0.3', 'Mor 3', 'Mor 10').

6.4 Discussion

In the present study it was demonstrated that minocycline, a selective inhibitor of microglia, attenuated mechanical allodynia 22 days following CCI surgery. Maximum efficacy was observed after the first dose with a similar level of efficacy continuing throughout the dosing period. This data was in contrast to data produced from rats dosed with the clinically used drug pregabalin, which required 5 doses before reaching a similar level of efficacy.

Although there are several reports detailing efficacy with minocycline in neuropathic pain models, some reports show efficacy is only observed with pre-emptive dosing, and that no effect occurs when the compound is dosed after allodynia has been established (Raghavendra et al., 2003a; Ledeboer et al., 2005a). These findings led to the hypothesis that different glial cell types played distinct roles at different stages of disease progression. Those that suggested that microglia only participate in the initiation of chronic pain; also proposed that microglia drove subsequent astrocyte activation (Svensson et al., 1993; Raghavendra et al., 2003a). Support for these findings also came from studies using real time RT-PCR demonstrating that peripheral nerve injury induced an early microglial activation (4 hours post-surgery), followed by a delayed (day 4) but sustained (> day 28) GFAP expression (Tanga et al., 2004). The data presented in this chapter is therefore in contrast to these previous published findings as minocycline was efficacious when CCI-induced allodynia was established.

Reasons for the contrasting results might be due to the difference in models and dosing routes used. Data reported by Raghavendra et al. (2003a) used the spinal nerve model with minocycline being dosed intra-peritoneally, whilst Ledeboer et al. (2005a) used a spinal injection of HIV-1 envelope glycoprotein gp-120 to induce neuropathic pain and minocycline was dosed intrathecally.

In terms of the dosing route used, there is little explanation why side effects were seen when minocycline was initially dosed intra-peritoneally at 30 mg/kg. This is a dose and route commonly used in the literature and no publications describing side effects have been identified. One possible explanation however could be the

strain of rat used. It is possible that Random-hooded rats may be more sensitive to this compound than other strains, although evidence for this has not been identified.

There are other reports suggesting that microglial activation does occur at later time-points following nerve injury. Recently it has been shown that nerve injury-induced increase in microglial marker expression have been pharmacologically inhibited using fluorocitrate and propentofylline on days 28 and 50 post-surgery (Clark et al., 2007; Tawfik et al., 2007), thus supporting an active role of microglia in established nerve-injury induced allodynia.

In terms of the mechanism of action for minocycline, it has recently been proposed that the efficacy of minocycline seen in neuropathic pain models is achieved by decreasing mRNA expression of IL-1β, TNF-α, each of their converting enzymes, and IL-10 in the dorsal spinal cord; reducing IL-1β and TNF-α in the cerebrospinal fluid; and decreasing serum IL-6 (Ledeboer et al., 2005a; Zanjani et al., 2006). It has also been shown that minocycline can increase p38 MAPK activation in spinal microglia (Cui et al., 2008).

In summary, the current data demonstrates a role of activated microglia in established allodynia after nerve injury. Further studies to compare different doses of minocycline administered orally at different time-points during the development of allodynia would be worth investigating further.

The first evidence that glial cells were involved in pain modulation came from an immunohistochemistry study by Garrison et al. (1991) who showed that activated astrocytes, identified by GFAP staining, were present in the spinal cord of nerve-injured rats. These findings have since been extended to show robust activation of microglia at the lumbar spinal cord in a variety of rodent models of neuropathic pain (Deleo et al., 1996; Colburn et al., 1997; Sweitzer et al., 1999; Hashizume et al., 2000; Sweitzer et al., 2001; Raghavendra et al., 2002; Jin et al., 2003; Milligan et al., 2003a; Tsuda et al., 2003; Tanga et al., 2005; Clark et al., 2007). The majority of reported IHC studies focus on microglial involvement in the initiation of pain as opposed to the maintenance of pain. The current study however assesses microglial expression at a late time-point post-surgery thereby investigating the role of microglia in maintained pain.

Immunohistochemical analysis of L4/L5 spinal cord revealed an increase in microglial activation at 34 days post CCI- surgery. Other studies have shown that microglial expression can be observed as late as 28, 33, 42, 50, 84 and 150 days after nerve injury (Svensson et al., 1993; Coyle, 1998; Hains and Waxman, 2006; Zhang and De, 2006; Clark et al., 2007; Tawfik et al., 2007), although the current data appears to be the first data generated using Iba-1 marker in the CCI model.

The current IHC data also corresponded well with the behavioural data generated with these rats. Activated spinal microglia were observed in tissue of CCI-operated rats that demonstrated allodynia, producing paw withdrawal thresholds of approximately 5 g. In comparison, non-operated rats had minimal microglia activation and produced withdrawal thresholds of approximately 20 g.

In reported studies comparing behavioural responses with activation however, there have been several cases in which the neuropathic pain has not been associated with the expression of microglial markers (Colburn et al., 1997; Tsuda et al., 2003; Tanga et al., 2004; Zhuang et al., 2007) . This led to concerns that commonly used markers like Iba-1 may be demonstrating existence of an injury rather than the presence of neuropathic pain (Ji and Suter, 2007). Tanga et al. (2004) showed decreased expression of microglia markers at day 28 which was not accompanied by a decrease in tactile hypersensitivity in spinal nerve ligation animals. It has also been shown that OX42 immunoreactivity did not correlate with mechanical allodynia in a lumbar radiculopathy model (Winkelstein et al., 2001). In direct comparison to the current study, Colburn et al. (1997) found a dis-association between hyperalgesia in CCI-operated rats and microglia activation, however this discrepancy could be explained by protocol, for example a different marker was used (OX-42), a different time-point was assessed (day 10 post-surgery) and a different behavioural readout was used (thermal).

In the present study, there were no differences in Iba-1 expression in the contralateral dorsal horns of CCI-operated and non-operated rats. This agrees with previous studies which routinely show the unilateral effect in an array of neuropathic models, for example spinal nerve transection (Sweitzer et al., 2001), partial ligation

(Clark et al., 2007) , gp-120-induced neuropathic pain (Ledeboer et al., 2005a) and spared nerve injury model (Scholz et al., 2008).

Having demonstrated a CCI-induced increase in Iba-1 expression in spinal cord at day 34, the effect of P2X7 antagonism on this increase was investigated. This study used the same naïve and CCI rats as the previous study, but only the L4 regions were analysed, as opposed to both L4 and L5.

In this study an increase in IBA-1 staining was again observed in CCI-operated rats dosed with vehicle compared to non-operated rats, although the % area of Iba-1 staining was higher than the previous study. This was most likely due to different scanning systems being used and different thresholds being set for the identification of the Iba-1 stained cells.

Discrepancy between studies was also observed in the contralateral dorsal horn. In contrast to the previous study there was a significant increase in Iba-1 staining when compared to the same region in the non-operated group. This data suggests a potential bilateral effect and although this has not been previously reported in the CCI model using immunohistochemical methods, mirror-image neuropathic pain has been illustrated using a sciatic inflammatory neuropathy model in which hyperalgesia from a contralateral paw had been reversed by fluorocitrate (Milligan et al., 2003b). Alternatively, although statistically significant, the increase in staining was very small and there is the possibility that the ‘contralateral effect’ was due to experimental variability between sections. It would be recommended to repeat the study with larger group sizes to confirm the results.

A significant reduction in ipsilateral staining was observed in CCI-operated rats dosed with GSK1370319 compared to CCI-operated rats dosed with vehicle. This data suggests that established microglia activation can be inhibited by blocking the P2X7 receptor. As already described, there is IHC evidence that microglial inhibitors can prevent established microglial activation, however this is the first time that a selective P2X7 receptor antagonist has been shown to inhibit microglial activation using these techniques.

Since completing this data, a study has been published supporting the involvement of P2X7 receptors in microglial activation. It has been shown, using

double-immunofluorescence staining methods, that P2X7 receptors are not only expressed on microglia, but that P2X7 receptor antagonist BBG, suppressed the up-regulation of microglia induced by tetanic stimulation of the sciatic nerve, a method known to produce long-lasting hyperalgesia and allodynia in rats (Chu et al., 2010). Other recent supporting studies showed the modulation of LPS-induced IL-1β release from microglia in the dorsal horn of the spinal cord by selective P2X7 receptor antagonist A-438079 (Clark et al., 2007). These results are also consistent with a previous report that oxATP blocks LPS stimulation-induced increase in expression of microglial P2X7 receptors (Choi et al., 2007).

To fully investigate the relationship between P2X7 receptors and CCI-induced microglial activation, samples could be taken from nerve-injured rats at different time-points after surgery to establish the profile of microglia activation and to establish how the interaction changes over time.

Having demonstrated that protein levels of activated microglia were up-regulated in the spinal cord of CCI-operated rats, it was intended to investigate the role of microglia in morphine tolerance by analysing spinal cord samples from CCI-operated rats that had received morphine. Before proceeding with this it was decided to first investigate changes in mRNA expression in these rats.

In the current study however, there was no change in PBR, ITGAM, GFAP or cytokines in CCI-operated rats that had been repeatedly dosed with morphine compared to CCI-operated rats dosed with vehicle. As this study did not include a non-operated group it was not possible to observe any changes in mRNA due to neuropathic surgery. The objective of this study was to investigate the effect of P2X7 receptor antagonist on morphine-induced gene changes in CCI-operated rats, therefore a control group was not deemed necessary. It was also thought unnecessary given the amount of literature available detailing microglial activation in neuropathic rats, as well as the increase in ITGAM staining showed in an earlier study.

Additionally, there was no difference in cytokine mRNA levels between CCI-operated rats dosed with morphine and those dosed with vehicle. This was also unexpected as literature suggests that cytokines can modulate opioid actions (Raffa et al., 1993). This has been confirmed by observations that administration of IL-1β can

reduce the analgesic effect of morphine (Gul et al., 2000; Rady and Fujimoto, 2001). Selective inhibition of IL-1β or collective inhibition of proinflammatory cytokines during chronic morphine treatment has also been shown to attenuate the expression of morphine tolerance (Raghavendra et al., 2002; Johnston et al., 2004).

Finally, mRNA levels of μ opioid receptor also remained unchanged in CCI-operated rat repeatedly dosed with morphine. This may suggest that the receptor was not down-regulated, however mRNA levels do not always correlate with protein levels and without the inclusion of a non-operated group in place the data is difficult to interpret. There are recent reports that total μ opioid receptor expression in the dorsal horn of the spinal cord may be enhanced following repeated morphine administration (Horvath et al., 2010b). It was postulated that this could be an adaptive response to tolerance formation or a response to enhanced receptor internalisation.

With no difference in mRNA levels in rats treated with chronic morphine, the effect that P2X7 receptor antagonist would have on morphine tolerance is difficult to examine. It may have been expected that rats treated with P2X7 alone would show a decrease in mRNA expression of ITGAM, PBR, IL-1β and TNF, however interpretation is difficult without comparative data from non-operated rats. Since completing this work it has been published that P2X7 receptors and Iba-1 expression are up-regulated in the spinal cord in rats chronically dosed with morphine and that antagonism of the P2X7 receptor also reduced the up-regulation of Iba-1 (Zhou et al., 2010). This data therefore implicates P2X7 receptors being involved in the generation of morphine tolerance.

It has also recently been reported that the inhibition of spinal microglial P2X4 receptor expression inhibited morphine-induced increases in Iba-1 and GFAP expression (Horvath et al., 2010b) confirming the involvement of an alternative purinergic receptor. Reduction of morphine-induced spinal CD11b and GFAP expression have been demonstrated using glial modulators propentofylline (Raghavendra et al., 2004a) and minocycline (Cui et al., 2008), however these studies used naïve rats and microglial activation was only due to the chronic morphine administration alone as opposed to both morphine administration and neuropathy.

It is possible that the lack of up-regulation of any marker in the current study could be due to activated microglia already being at a maximum as a result of the neuropathic surgery. When comparing the mRNA expression of ITGAM in CCI-operated rats to the naïve rats, results of which are to be discussed subsequently, there is a 2400 times increase in the CCI rats compared to naïve rats (naïve ITGAM = ~150copies; CCI ITGAM = ~360,000 copies). Whilst there are limitations to comparing different Taqman datasets, these results may still suggest that microglia levels have increased dramatically due to CCI surgery and it is possible that levels have reached a maximum. PBR expression in CCI rats was also higher than in naïve rats by approximately double (naïve PBR = ~1800 copies; CCI PBR = ~3500).

The other possibility is that the time-point for this study was too late. Although behavioural efficacy was seen, the transcriptional changes may have occurred earlier in the time-course and returned to normal by day 34. To support this theory, Tanga et al. (2004) found spinal lumbar mRNA of ITGAM up-regulated at 4 hour post L5 nerve transection surgery, but had returned to normal by postoperative day 28 although this was not accompanied by a decrease in tactile hypersensitivity. Inhibition of ITGAM levels by minocycline have also been shown to be dependent on the time-point post-surgery with a reduced effect being observed 5 days after surgery (Raghavendra et al., 2003a). If this hypothesis was correct however, one might still expect chronic morphine administration to have more of an effect if CCI-induced activated microglia levels had reduced at the later time-point.

To investigate this data further, future studies would require the inclusion of an un-operated control group, as well as a gene known to increase under these conditions, to act as a positive control. Although transcriptional data did not demonstrate the involvement of microglia in morphine tolerance it would still be recommended to investigate changes at the protein level using immunohistochemistry.

While research relating glia to morphine-induced actions began with a focus on morphine tolerance, it soon became apparent that glia may modulate the acute analgesic effects of morphine as well (Watkins et al., 2005). Although it has been shown that blockade of cytokines known to be released from activated microglia,

increases the magnitude and duration of acute analgesia to morphine (Johnston et al., 2004; Shavit et al., 2005), the author has not found any literature implicating microglia directly.

In the present study however, although it was shown behaviourally that P2X7 receptor antagonism enhanced morphine analgesia in naïve rats thus implicating the involvement of microglia, this was not reflected in the transcriptional analysis. Morphine administration had no effect on mRNA levels of PBR and ITGAM in naïve rats, therefore an effect of GSK1370319 was also not seen.

A lack of OX42 immunoreactivity has been reported in control rats in a neuropathic study, although data was not included in the manuscript (Raghavendra et al., 2002) . This data suggests that the enhancement of efficacy seen behaviourally in naïve rats after acute co-administration of morphine and GSK1370319 may be independent of microglial activation, or that the signal was not robust enough to be identified transcriptionally.

In summary, this chapter has demonstrated that microglia play a role in established allodynia induced by CCI-surgery and that P2X7 receptors directly influence microglia-activation induced by CCI surgery. Data is also presented that suggests that P2X7 receptor-mediated enhancement of morphine analgesia in naïve rats may be independent of microglia activation although further work is required to confirm this. Further work is also required to investigate the role of P2X7 and microglia in morphine-induced tolerance.

Chapter 7

General Discussion

7. General Discussion

7.1 The efficacy of P2X7 receptor antagonists and the association with microglia

The therapeutic potential of P2X7 receptor antagonists in pain was first suggested by the work of Dell'Antonio and colleagues who demonstrated that oxidised ATP was efficacious in pain models (Dell'Antonio et al., 2002a; Dell'Antonio et al., 2002b). In the work detailed in this thesis, efficacy with the selective P2X7 receptor antagonist GSK1370319 in the CCI model of neuropathic pain confirms these original suggestions and adds to the growing pool of literature showing efficacy with several chemically distinct, selective P2X7 receptor antagonists (Honore et al., 2006; Donnelly-Roberts et al., 2009; Chambers et al., 2010; Chen et al., 2010).

To increase confidence that this efficacy was relevant to different neuropathic pain states it was intended to test GSK1370319 in another model of neuropathic pain. Unfortunately the VZV-induced allodynia model was not found to be sufficiently reproducible to test novel compounds, even after a very considered, systematic and thorough attempt at validating the model. It was considered unethical to continue to use rats in further studies to understand the reasons for the lack of phenotype, although a number of potential studies were suggested in Chapter 5. A suggestion not listed, was to use an alternative way of delivering VZV into the spinal cord. One possibility would be to inject the virus directly into a peripheral nerve, as demonstrated in a previous study using adeno-associated viral vector (Boulis et al., 2003). Presumably the virus could also be administered directly into the spinal cord, potentially using methods detailed in section 2.2.2.3. However it must be recognised that these approaches focus away from the aetiology of the clinical condition which is being modeled.

Nonetheless, data obtained with GSK1370319 in the CCI model supported the rationale that inhibiting P2X7 receptors pharmacologically represents a novel therapeutic approach for treating pain caused by nerve damage, for which there is

currently no effective therapy. Other data also showed that the blockade of these receptors in naive rats did not affect pain responses thereby adding the additional therapeutic benefit that normal pain sensitivity would be unaffected.

Although pre-clinical evidence for the involvement of the P2X7 receptor in pain processing is accumulating, evidence for the relevance of this receptor for a pain indication in humans is limited. Currently, only two P2X7 receptor antagonists have been tested in man for two pain indications: osteoarthritis and rheumatoid arthritis (source: 'Pipeline', a 'new drug intelligent service', search date 7th January 2011). Both AZD-9056 and CE-224535 however failed and development of both antagonists has been discontinued. The reasons for the lack of efficacy remain unreported. Possible explanations however include a lack of CNS penetration of the compounds or an inability of the compounds to reach a level of CNS penetration required in humans, which may be different to that in pre-clinical species. An alternative explanation for the negative clinical results is that neither compound produced a sufficient effect on the cytokine balance to be useful clinically. To date, the clinical effect of P2X7 receptor antagonists on neuropathic pain remains untested.

The significance of central penetration for the efficacious effects of P2X7 receptor antagonists was also demonstrated, the importance of which is now slowly being realised. A paper has recently been published which alludes to the potential benefits of a centrally-penetrant P2X7 receptor antagonist, although the authors do not include any *in vivo* data to support this claim (Chen et al., 2010). To extend the site of action studies further, supraspinal influences could also be explored by injecting P2X7 receptor antagonist intra-cerebroventricularly. This would be particularly relevant given the proposed role of this receptor in the brain in neurodegenerative diseases, such as Alzheimers disease (McLarnon et al., 2006), Huntingdons disease (Diaz-Hernandez et al., 2009) and Prion diseases (Takenouchi et al., 2007). Other studies indicate that supraspinal glial-neuronal interactions at the level of the RVM may promote descending pain facilitation following peripheral nerve injury (Wei et al., 2008). After chronic constriction of the rat intra-orbital nerve, microglia and astrocyte activation was evident in the RVM, associated with local elevation of IL-1β and TNFα levels.

Using immunohistochemistry, it was confirmed that P2X7 receptors and microglia are closely associated. Alternative approaches which could have been considered include autoradiography or positron emission tomography (PET), the latter can also be used in a clinical setting. The peripheral benzodiazepine receptor (PBR) is expressed on the outer mitchochondrial membrane of only activated microglia (Banati, 2002). PBR ligands, which can be radiolabelled, therefore make ideal biomarkers allowing the number and location of activated microglia to be measured *in vivo*, when in the presence and absence of glial-modulating agents, such as P2X7 receptor antagonists.

Although the involvement of microglia in the development of neuropathic pain is well established, the relevance of microglia to pain states in humans will only be fully realised when microglial-modifying drugs are tested in clinical trials. To date two drugs that interfere with glial function have been put into clinical trials for neuropathic pain. SLC-022 (propentofylline) failed in Phase 2a in PHN patients and AV-411 (ibudilast) is currently suspended in Phase 2a for unknown reasons (source: 'Pipeline', a 'new drug intelligent service', search date 7th January 2011). The actual reasons for the failure of both compounds is not reported, however it might be due to the mixed pharmacology of each compound not being appropriate for humans. Both compounds act on many systems, for example propentofylline is known to be a phophodiesterase inhibitor (Frampton et al., 2003) and an adenosine reuptake inhibitor (Frampton et al., 2003). It is possible that the multiple actions of these compounds might be confounding the benefits of inhibiting glia. This would suggest there is an advantage for developing compounds, like P2X7 receptor antagonists, which are more specific to modulating glial cells. The lack of clinical efficacy may again be due to the level of required CNS penetration being different in humans than in pre-clinical species. It appears that understanding the role of microglia in human pain remains an area of great untapped potential.

7.2 Actions of morphine and the association with P2X7 receptors and microglia

In the present studies it was demonstrated that GSK1370319 delayed morphine tolerance in CCI-operated rats, adding confidence to the glial-related theory of morphine-induced tolerance (Section 1.7.4.3.4). A proposed study to support this finding would be to measure the expression of activated microglia, using IHC, in spinal cords of CCI-operated rats that were repeatedly co-dosed with morphine and GSK1370319. If the hypothesis of an association is correct, a difference in protein expression would be evident between CCI-operated rats dosed with morphine+vehicle and CCI-operated rats dosed with vehicle+vehicle, as well as a difference between CCI-operated rats dosed with morphine+vehicle and CCI-operated rats dosed with morphine+GSK1370319. Related to this, data has recently been published in which protein levels of P2X7 receptor were up-regulated after chronic exposure to morphine with these levels being reduced when the P2X7 receptor antagonist BBG was administered (Zhou et al., 2010). These authors also showed that spinal P2X7 receptor protein only co-localised with the microglial marker OX42 and not the astrocytic maker GFAP, confirming the greater significance of microglia over astrocytes to the current studies.

The association between P2X7 receptors, microglia and morphine tolerance could be further validated by running a morphine tolerance study in P2X7 KO mice. It would be expected that tolerance is reduced in P2X7 KO compared to WTs. However, as with any study using KO mice, experimental and interpretational caveats apply, including the recognised problem of compensation by other genes which may confound the data (Lariviere et al., 2002; Hatcher and Chessell, 2006).

Studies could also be performed to confirm the central site of action for the P2X7-morphine interaction by using peripherally restricted compounds. Using this approach, one could investigate the effects of a peripherally-restricted P2X7 receptor antagonist, like GSK2039841 or a peripherally-restricted opioid, like loperamide. Loperamide has previously been shown to inhibit herpetic-induced allodynia in mice with no development of tolerance (Sasaki et al., 2007) confirming the proposed role of microglia in tolerance. Caution is required when using this opioid however, as the

interaction between this peripheral agonist and central opioid receptors is still unclear. One report suggests that loperamide is able to modulate the central mechanisms of perception of painful stimuli, cause hyperalgesia and partially prevent the development of morphine-induced tolerance, by suppressing central μ opioid receptors (Sudakov and Trigub, 2008).

By virtue of the large number of mechanisms that glia are linked to, it is also possible that glia are associated with several of the theories of tolerance discussed in Chapter 1. This is particularly the case for the 'opioid-induced facilitation mechanism hypothesis' (section 1.7.4.3). For example, there is evidence in the literature for morphine tolerance being associated with the down regulation of glial GLAST and GLT-1 glutamate transporters leading to an up-regulation of excitatory amino acids (Mao et al., 2002; Tai et al., 2006). Pain enhancing effects of neuronally derived spinal dynorphin have also been linked to selective activation of microglial p38 MAPK leading to the release of PGE2 and IL-1 (Laughlin et al., 2000; Svensson et al., 2005). Recently, data has been published, using an RNA interference approach, showing that P2X7 siRNA injection inhibited the up-regulation of phosphorylated p38 MAPK by chronic morphine, suggesting a further link to this signalling pathway (Zhou et al., 2010). The other possibility is that all the suggested mechanisms, including opioid signal transduction, desensitisation of opioid receptors and involvement of descending pain facilitatory systems, contribute to the phenomenon of tolerance but to differing degrees. More research in this field however is required to understand the relationships between them.

Data has been presented suggesting that P2X7 antagonism can influence morphine efficacy when morphine is repeatedly dosed to CCI-operated rats and when morphine is singly dosed to naive rats. As with tolerance studies, it would be interesting to see whether this also occurs when peripherally restricted tools are tested. These findings could be extended by testing opioid agonists which act at different opioid receptors to identify any involvement of receptors other than the μ receptor. As well as expressing μ receptors (Chao et al., 1997), microglial cells are also known to express kappa and delta receptors (Chao et al., 1996; Calvo et al.,

2000; Turchan-Cholewo et al., 2008) although the relevance of their expression to the functions of microglia are unknown.

Throughout this thesis putative mechanisms for how purinergic-activated glia can impact on morphine's activities have been discussed, whether this includes direct ATP-related mechanisms, or indirect mechanisms involving the glutaminergic NMDA receptor or enhanced p38 MAPK signalling. What is less well understood however, is how the μ opioid and P2X7 purinergic receptor pathways interact.

One possibility is that the P2X7 receptor antagonist may be inhibiting morphine-induced enhancement of microglial migration. This has recently been shown with P2X4 antagonism using an *in vitro* culture system (Horvath and Deleo, 2009). These authors proposed that when morphine is given repeatedly and in high doses, it binds to μ receptors in microglia, inducing migration which leads to an elevated local concentration of proinflammatory cytokines and chemokines resulting in neuronal sensitisation. This sensitisation then counteracts the analgesic effect of morphine manifesting into morphine tolerance or reduction in morphine efficacy. This hypothesis has yet to be proven for P2X7 receptors and the microglial migration theory itself has yet to be confirmed *in vivo*.

An alternative theory concerns the opioid receptors located on microglia. It has recently been postulated that opioids cause direct glial activation in a 'non-classical opioid receptor fashion' via the activation of the Toll-like receptor TLR4 (Hutchinson and Somogyi, 2004a; Hutchinson and Somogyi, 2004b; Hutchinson and Somogyi, 2005). TLR4 is only expressed by microglia (Lehnardt et al., 2002) and is upregulated in microglia in response to spinal nerve injury correlating with enhanced pain (Tanga et al., 2004). TLR4 has been extensively characterised, and is the receptor that recognises lipopolysaccharide (LPS), a component of bacterial cell walls. It was the early findings that naloxone could block microglial activation by LPS (Liu et al., 2000) that initiated further investigation. Liu et al. found that the actions of naloxone were not mediated by the classical neuronal opioid receptors as both the opioid-active (-)-isomer and the opioid-inactive (+)-isomer of naloxone exerted identical inhibitory effects. This therefore suggested that naloxone was acting through a receptor other than the classical opioid receptor. Hutchinson extended

these findings firstly showing that opioid agonists activated TLR4 and secondly, that opioid antagonists non-stereoselectively blocked TLR4 activation (Hutchinson and Somogyi, 2005). Supporting data for a non-classical opioid receptor being responsible for microglial activities has also arisen from triple μ, δ and κ opioid receptor KO mice in which opioid-induced hyperalgesia was still observed (Juni et al., 2007).

Suggestions that P2X7 receptors are potentially involved with the TLR4 theory has recently been proposed. It has been shown that the LPS-induced release of IL-1β and phosphorylation of p38 MAPK in microglial cells is mediated by P2X7 receptors (Clark et al., 2010). They showed this by blocking LPS-induced release of IL-1β in dorsal horn slices with the P2X7 receptor A-438079. This *ex vivo* approach was also demonstrated *in vivo*, by blocking LPS-induced mechanical hyperalgesia with a P2X7 receptor antagonist and demonstrating that LPS-induced hypersensitivity did not occur in P2X7 KO mice.

Taking all the evidence together, it is feasible that morphine-induced microglial activation via TLR4, might be blocked by a P2X7 receptor antagonist in a similar way than LPS-induced microglia activation. This suggests that P2X7 receptor antagonist may be interacting with TLR4 on microglia, as opposed to μ opioid receptors. Developing drugs that could differentiate between classical opioid receptors and TLR4 receptors, or combining opioids with compounds that interact with TLR4 receptors, like P2X7 receptor antagonists, could potentially separate the desirable (analgesia) and undesirable (tolerance, reduction in efficacy) actions of opioids, thereby improving the safety and efficacy of their use.

How morphine-induced microglial activation impacts effects of morphine beyond analgesia was also addressed in this thesis. Data suggested that morphine-induced motor impairment and loss of body weight gain were not effected by P2X7 receptor antagonism. Although clinically this would be considered a benefit as the side effects had not been potentiated in a similar way to efficacy, it is also interesting that these side effects were not improved or abolished. To explore this area further, the effect of P2X7 antagonism and microglial inhibition on other side effects of morphine could be tested, for example respiratory depression and constipation or

morphine-induced dependence, reward and hyperalgesia. Studies investigating some of these actions using other glial modulators have already been reported. For example, ibudilast has been shown to significantly reduce naloxone-precipitated withdrawal behaviours suggesting that opioid-induced glial activation is involved in morphine dependence (Hutchinson et al., 2009). This mechanism was also shown to be TLR4 driven as co-administration of (+)-naloxone reduced withdrawal behaviours. Propenofylline and ibudilast have been shown to reduce conditioned place preferences induced by morphine, suggesting the involvement of glial activation in the rewarding and reinforcing actions of morphine (Narita et al., 2006; Hutchinson et al., 2007). This finding led to the initiation of a Phase 2a trial with ibudilast in 30 heroin-dependent volunteers, although this trial has been suspended for unknown reasons (source: 'Pipeline', a 'new drug intelligent service', search date 7th January 2011). Further rationale for non-analgesic associations between morphine and glia, includes the reduction of morphine-induced respiratory depression by minocycline and ibudilast (Hutchinson et al., 2007; Hutchinson et al., 2009). It would be very interesting to see whether these effects are reciprocated with P2X7 receptor antagonists.

7.3 Clinical implications

Neuropathic pain is estimated to afflict as much as 7-8% of the general population in Europe (Torrance et al., 2006; Bouhassira et al., 2008). The management of patients with chronic neuropathic pain continues to be challenging (Attal et al., 2010; Dworkin et al., 2010; Finnerup et al., 2010). Most clinical trials, which have been run in patients with post-herpetic neuralgia or peripheral diabetic neuropathy, mainly study the effects of mono-therapy (Attal et al., 2010; Finnerup et al., 2010; Dworkin et al., 2010) with only a few considering poly-pharmacology (Gilron et al., 2005; Hanna et al., 2008; Agrawal et al., 2009; Gilron et al., 2009). There are many benefits to a multidrug regimen, particularly considering that neuropathic pain has many causes, resultant symptoms, and diverse underlying mechanisms. The data in this thesis suggests that the combination of a P2X7 receptor antagonist and morphine is a combination worth consideration for further clinical exploration.

Although the use of opioids for the treatment of chronic pain has increased dramatically over the past decade they remain the second or third line treatment (Attal et al., 2010; Dworkin et al., 2010). This is due to a narrow therapeutic index as a result of side effects, such as constipation, sedation, nausea, dizziness and vomiting and the associated problems with long-term opioid use like the risk of misuse/ addiction, and opioid-induced hyperalgesia (Crofford, 2010). Table 6 lists the recommended drug treatments for the two most common neuropathic pain conditions and highlights the recommended stage at which opioids are considered. The table also indicates the lack of clinically used treatments which are known to work via glial modulation. ‘Numbers needed to treat’ (NNT) values are included in the table, which is a useful method to assess clinical analgesic efficacy and refers to the number of patients that have to be treated before one patient experiences more than 50% pain relief.

Etiology	Recommendations as First-Line Treatment (number needed to treat values)	Recommendations as Second- or Third-Line Treatment (number needed to treat values)
Diabetic neuropathy/ painful polyneuropathy	Duloxetine (5[#]) Gabapentin (6.4) Pregabalin (4.5) TCAs (2.1) Venlafaxine (5[#])	Opioids (2.6) Tramadol (4.9)
Postherpetic neuralgia	Gabapentin (4.3) Pregabalin (4.2) TCAs (2.8) Lidocaine plasters	Capsaicin Opioids (2.6)

Table 6. Recommendations of drug treatments in the two most common neuropathic pain conditions. Treatments are presented in alphabetical order. Only drugs used in repeated dosages and available for use are shown. Adapted from Attal et al., (2010). Number needed to treat values adapted from Finnerup et al., (2010). # this value relates to 'Serotonin–norepinephrine reuptake inhibitor' generally as opposed to duloxetine and venlafaxine individually.

Comparing the NNT values for each drug, illustrates the effectiveness of opioids, at doses which are limited by side effects. If a combination with a P2X7 receptor antagonist could increase efficacy of morphine, or other opioids, at lower doses which do not carry side effects, the NNT could be reduced further and opioids could then perhaps be re-considered as an effective first line treatment.

Reference list

Reference List

Abberley L, Bebius A, Beswick PJ, Billinton A, Collis KL, Dean DK, Gleave RJ, Medhurst SJ, Michel AD, Moses AP, Patel S, Scoccitti T, Smith B, Steadman JGA, Walter DS (2010) Identification of 2-oxo-N-(phenylmethyl)-4-imidazolidinecarboxamide antagonists of the P2X7 receptor. Bioorganic and Medicinal Chemistry Letters 20:6370-6374.

Abbott NJ, Ronnback L, Hansson E (2006) Astrocyte-endothelial interactions at the blood-brain barrier. [Review] [163 refs]. Nature Reviews Neuroscience 7:41-53.

Abdelhamid EE, Takemori AE (1991) Characteristics of mu and opioid binding sites in striatal slices of morphine-tolerant and -dependent mice. European Journal of Pharmacology 198:157-163.

Abdi MH, et al. (2010) Discovery and structure-activity relationships of a series of pyroglutamic acid amide antagonists of the P2X7 receptor. Bioorganic and Medicinal Chemistry Letters 20:5080-5084.

Abdi S, Lee DH, Chung JM (1998) The anti-allodynic effects of amitriptyline, gabapentin, and lidocaine in a rat model of neuropathic pain. Anesthesia & Analgesia 87:1360-1366.

Aga M, Johnson CJ, Hart AP, Guadarrama AG, Suresh M, Svaren J, Bertics PJ, Darien BJ (2002) Modulation of monocyte signaling and pore formation in response to agonists of the nucleotide receptor P2X(7). Journal of Leukocyte Biology 72:222-232.

Agrawal RP, Goswami J, Jain S, Kochar DK (2009) Management of diabetic neuropathy by sodium valproate and glyceryl trinitrate spray: A prospective double-blind randomized placebo-controlled study. Diabetes Research and Clinical Practice 83:371-378.

Aicher SA, Sharma S, Cheng PY, Pickel VM (1997) The N-methyl-D-aspartate (NMDA) receptor is postsynaptic to substance P-containing axon terminals in the rat superficial dorsal horn. Brain Research 772:71-81.

Anderson CM, Nedergaard M (2006) Emerging challenges of assigning P2X7 receptor function and immunoreactivity in neurons. [Review] [50 refs]. Trends in Neurosciences 29:257-262.

Andersson AK, Ronnback L, Hansson E (2005) Lactate induces tumour necrosis factor-alpha, interleukin-6 and interleukin-1beta release in microglial- and astroglial-enriched primary cultures. Journal of Neurochemistry 93:1327-1333.

Ando RD, Mehesz B, Gyires K, Illes P, Sperlagh B (2010) A comparative analysis of the activity of ligands acting at P2X and P2Y receptor subtypes in models of neuropathic, acute and inflammatory pain. Br J Pharmacol 159:1106-1117.

Andrei C, Dazzi C, Lotti L, Torrisi MR, Chimini G, Rubartelli A (1999) The secretory route of the leaderless protein interleukin 1beta involves exocytosis of endolysosome-related vesicles. Molecular Biology of the Cell 10:1463-1475.

Appleyard SM, Celver J, Pineda V, Kovoor A, Wayman GA, Chavkin C (1999) Agonist-dependent desensitization of the opioid receptor by G protein receptor kinase and beta-arrestin. Journal of Biological Chemistry 274:23802-23807.

Araque A, Sanzgiri RP, Parpura V, Haydon PG (1999) Astrocyte-induced modulation of synaptic transmission. Canadian Journal of Physiology and Pharmacology 77:699-706.

Argoff CE, Katz N, Backonja M (2004) Treatment of postherpetic neuralgia: a review of therapeutic options. J Pain Symptom Manage 28:396-411.

Atkinson RL (1987) Opioid regulation of food intake and body weight in humans. Fed Proc 46:178-182.

Attal N, Chen YL, Kayser V, Guilbaud G (1991) Behavioural evidence that systemic morphine may modulate a phasic pain-related behaviour in a rat model of peripheral mononeuropathy. Pain 47:65-70.

Attal N, Cruccu G, Baron R, Haanpaa M, Hansson P, Jensen TS, Nurmikko T (2010) EFNS guidelines on the pharmacological treatment of neuropathic pain: 2010 revision. European Journal of Neurology 17:1113-1123.

Attal N, Jazat F, Kayser V, Guilbaud G (1990) Further evidence for 'pain-related' behaviours in a model of unilateral peripheral mononeuropathy. Pain 41:235-251.

Baba H, Doubell TP, Woolf CJ (1999) Peripheral inflammation facilitates Abeta fiber-mediated synaptic input to the substantia gelatinosa of the adult rat spinal cord. Journal of Neuroscience 19:859-867.

Backonja M, Beydoun A, Edwards KR, Schwartz SL, Fonseca V, Hes M, LaMoreaux L, Garofalo E (1998) Gabapentin for the symptomatic treatment of painful neuropathy in patients with diabetes mellitus: a randomized controlled trial. JAMA 280:1831-1836.

Backonja MM, Miletic G, Miletic V (1995) The effect of continuous morphine analgesia on chronic thermal hyperalgesia due to sciatic constriction injury in rats. Neuroscience Letters 196:61-64.

Bagley EE, Chieng BC, Christie MJ, Connor M (2005) Opioid tolerance in periaqueductal gray neurons isolated from mice chronically treated with morphine. British Journal of Pharmacology 146:68-76.

Bal-Price A, Brown GC (2001) Inflammatory neurodegeneration mediated by nitric oxide from activated glia-inhibiting neuronal respiration, causing glutamate release and excitotoxicity. Journal of Neuroscience 21:6480-6491.

Banati RB (2002) Visualising microglial activation in vivo. [Review] [72 refs]. GLIA 40:206-217.

Barbe MT, Monyer H, Bruzzone R (2006) Cell-cell communication beyond connexins: the pannexin channels. [Review] [111 refs]. Physiology 21:103-114.

Basbaum AI, Fields HL (1984) Endogenous pain control systems: brainstem spinal pathways and endorphin circuitry. [Review] [182 refs]. Annual Review of Neuroscience 7:309-338.

Bassani F, Bergamaschi M, Tonino BP, Villetti G (2005) CHF3381, a novel antinociceptive agent, attenuates capsaicin-induced pain in rats. Eur J Pharmacol 519:231-236.

Beck PW, Handwerker HO, Zimmermann M (1974) Nervous outflow from the cat's foot during noxious radiant heat stimulation. Brain Research 67:373-386.

Benedetti C (1987) Intraspinal analgesia: an historical overview. Acta Anaesthesiol Scand Suppl 85:17-24.

Bennett GJ, Xie Y-K (1988) A peripheral mononeuropathy in rat that produces disorders of pain sensation like those seen in man. Pain 33:87-107.

Besse D, Lombard MC, Zajac JM, Roques BP, Besson JM (1990) Pre- and postsynaptic distribution of mu, delta and kappa opioid receptors in the superficial layers of the cervical dorsal horn of the rat spinal cord. Brain Research 521:15-22.

Bessou P, Perl ER (1969) Response of cutaneous sensory units with unmyelinated fibers to noxious stimuli. Journal of Neurophysiology 32:1025-1043.

Bhargava HN (1994) Diversity of agents that modify opioid tolerance, physical dependence, abstinence syndrome, and self-administrative behavior. [Review] [371 refs]. Pharmacological Reviews 46:293-324.

Bhargava HN, Gulati A (1990) Down-regulation of brain and spinal cord mu-opiate receptors in morphine tolerant-dependent rats. European Journal of Pharmacology 190:305-311.

Bhargava HN, Thorat SN (1996) Evidence for a role of nitric oxide of the central nervous system in morphine abstinence syndrome. Pharmacology 52:86-91.

Bianchi BR, Lynch KJ, Touma E, Niforatos W, Burgard EC, Alexander KM, Park HS, Yu H, Metzger R, Kowaluk E, Jarvis MF, van BT (1999) Pharmacological characterization of recombinant human and rat P2X receptor subtypes. European Journal of Pharmacology 376:127-138.

Bianchi M, Dib B, Panerai AE (1998) Interleukin-1 and nociception in the rat. [Review] [67 refs]. Journal of Neuroscience Research 53:645-650.

Bianco F, Ceruti S, Colombo A, Fumagalli M, Ferrari D, Pizzirani C, Matteoli M, Di VF, Abbracchio MP, Verderio C (2006) A role for P2X7 in microglial proliferation. Journal of Neurochemistry 99:745-758.

Blanchet C, Scher C (2002) Desensitization of mu-opioid receptor-evoked potassium currents: initiation at the receptor, expression at the effector. Proceedings of the National Academy of Sciences of the United States of America 99:4674-4679.

Blomstrand F, Giaume C, Hansson E, Ronnback L (1999) Distinct pharmacological properties of ET-1 and ET-3 on astroglial gap junctions and Ca(2+) signaling. American Journal of Physiology 277:C616-C627.

Bodnar RJ, Hadjimarkou MM (2003) Endogenous opiates and behavior: 2002. Peptides 24:1241-1302.

Boghossian S, Jourdan D, Dacher M, Alliot J (2001) Effect of morphine on caloric intake and macronutrient selection in male and female Lou/c/jall rats during ageing. Mech Ageing Dev 122:1825-1839.

Bohn LM, Lefkowitz RJ, Caron MG (2002) Differential mechanisms of morphine antinociceptive tolerance revealed in (beta)arrestin-2 knock-out mice. Journal of Neuroscience 22:10494-10500.

Bolser DC (2006) Current and future centrally acting antitussives. [Review] [50 refs]. Respiratory Physiology & Neurobiology 152:349-355.

Bonica JJ (1990) Biochemistry and modulation of nociception and pain. In: The Management of Pain (Bonica JJ, ed), pp 95-121.

Bouhassira D, Lanteri-Minet M, Attal N, Laurent B, Touboul C (2008) Prevalence of chronic pain with neuropathic characteristics in the general population. Pain 136:380-387.

Boulis NM, Noordmans AJ, Song DK, Imperiale MJ, Rubin A, Leone P, During M, Feldman EL (2003) Adeno-associated viral vector gene expression in the adult rat spinal cord following remote vector delivery. Neurobiology of Disease 14:535-541.

Bowdle TA (1998) Adverse effects of opioid agonists and agonist-antagonists in anaesthesia. Drug Saf 19:173-189.

Broom DC, Matson DJ, Bradshaw E, Buck ME, Meade R, Coombs S, Matchett M, Ford KK, Yu W, Yuan J, Sun SH, Ochoa R, Krause JE, Wustrow DJ, Cortright DN (2008) Characterization of N-(adamantan-1-ylmethyl)-5-[(3R-amino-pyrrolidin-1-yl)methyl]-2-chloro-ben zamide, a P2X7 antagonist in animal models of pain and inflammation. J Pharmacol Exp Ther 327:620-633.

Bu SZ, Huang Q, Jiang YM, Min HB, Hou Y, Guo ZY, Wei JF, Wang JW, Ni X, Zheng SS (2006) p38 Mitogen-activated protein kinases is required for counteraction of 2-methoxyestradiol to estradiol-stimulated cell proliferation and induction of apoptosis in ovarian carcinoma cells via phosphorylation Bcl-2. Apoptosis 11:413-425.

Burke BL, Steele RW, Beard OW, Wood JS, Cain TD, Marmer DJ (1982) Immune responses to varicella-zoster in the aged. Arch Intern Med 142:291-293.

Burnstock G (1972) Purinergic nerves. [Review] [582 refs]. Pharmacological Reviews 24:509-581.

Burnstock G (1990) Overview: Purinergic mechanisms. Annals of the New York Academy of Sciences 603:1-18.

Burnstock G (2007) Physiology and pathophysiology of purinergic neurotransmission. [Review] [1987 refs]. Physiological Reviews 87:659-797.

Burnstock G (2009) Purinergic receptors and pain. Curr Pharm Des 15:1717-1735.

Burnstock G, Campbell G, Satchell D, Smythe A (1970) Evidence that adenosine triphosphate or a related nucleotide is the transmitter substance released by non-adrenergic inhibitory nerves in the gut. British Journal of Pharmacology 40:668-688.

Burnstock G, Knight GE (2004) Cellular distribution and functions of P2 receptor subtypes in different systems. International Review of Cytology 240:31-304.

Bushong EA, Martone ME, Jones YZ, Ellisman MH (2002) Protoplasmic astrocytes in CA1 stratum radiatum occupy separate anatomical domains. Journal of Neuroscience 22:183-192.

Calvo CF, Cesselin F, Gelman M, Glowinski J (2000) Identification of an opioid peptide secreted by rat embryonic mixed brain cells as a promoter of macrophage migration. European Journal of Neuroscience 12:2676-2684.

Carroll WA, Kalvin DM, Perez MA, Florjancic AS, Wang Y, Donnelly-Roberts DL, Namovic MT, Grayson G, Honore P, Jarvis MF (2007) Novel and potent 3-(2,3-dichlorophenyl)-4-(benzyl)-4H-1,2,4-triazole P2X7 antagonists. Bioorg Med Chem Lett 17:4044-4048.

Catheline G, Kayser V, Guilbaud G (1996) Further evidence for a peripheral component in the enhanced antinociceptive effect of systemic morphine in mononeuropathic rats: involvement of kappa-, but not delta-opioid receptors. European Journal of Pharmacology 315:135-143.

Celerier E, Rivat C, Jun Y, Laulin J-P, Larcher A, Reynier P, Simonnet G. (2000) Long-lasting hyperalgesia induced by fentanyl in rats: Preventive effect of ketamine. Anesthesiology 92:465-472.

Chakrabarti S, Gintzler AR (2003) Phosphorylation of Gbeta is augmented by chronic morphine and enhances Gbetagamma stimulation of adenylyl cyclase activity. Brain research Molecular brain research 119:144-151.

Chakrabarti S, Oppermann M, Gintzler AR (2001) Chronic morphine induces the concomitant phosphorylation and altered association of multiple signaling proteins: A novel mechanism for modulating cell signaling. Proceedings of the National Academy of Sciences of the United States of America 98:4209-4214.

Chakrabarti S, Regec A, Gintzler AR (2005) Chronic morphine acts via a protein kinase Cgamma-G(beta)-adenylyl cyclase complex to augment phosphorylation of G(beta) and G(betagamma) stimulatory adenylyl cyclase signaling. Brain Research Molecular Brain Research. 138:94-103.

Chakrabarti S, Rivera M, Yan S-Z, Tang W-J, Gintzler AR (1998) Chronic morphine augments G(beta)/G(salpha) stimulation of adenylyl cyclase: Relevance to opioid tolerance. Molecular pharmacology 54:655-662.

Chakrabarti S, Yang W, Law PY, Loh HH (1997) The mu-opioid receptor down-regulates differently from the delta-opioid receptor: requirement of a high affinity receptor/G protein complex formation. Molecular pharmacology 52:105-113.

Chambers LJ, Stevens AJ, Moses AP, Michel AD, Walter DS, Davies DJ, Livermore DG, Fonfria E, Demont EH, Vimal M, Theobald PJ, Beswick PJ, Gleave RJ, Roman SA, Senger S (2010) Synthesis and structure-activity relationships of a series of (1H-pyrazol-4-yl)acetamide antagonists of the P2X7 receptor. Bioorganic & Medicinal Chemistry Letters 20:3161-3164.

Chang KJ, Eckel RW, Blanchard SG (1982) Opioid peptides induce reduction of enkephalin receptors in cultured neuroblastoma cells. Nature 296:446-448.

Chang SL, Wu GD, Patel NA, Vidal EL, Fiala M (1998) The effects of interaction between morphine and interleukin-1 on the immune response. [Review] [19 refs]. Advances in Experimental Medicine & Biology 437:67-72.

Chao CC, Gekker G, Hu S, Sheng WS, Shark KB, Bu D-F, Archer S, Peterson PK (1996) opioid receptors in human microglia downregulate human immunodeficiency virus 1 expression. Proceedings of the National Academy of Sciences of the United States of America 93:8051-8056.

Chao CC, Gekker G, Sheng WS, Hu S, Tsang M, Peterson PK (1994) Priming effect of morphine on the production of tumor necrosis factor-alpha by microglia: implications in respiratory burst activity and human immunodeficiency virus-1 expression. Journal of Pharmacology & Experimental Therapeutics 269:198-203.

Chao CC, Hu S, Shark KB, Sheng WS, Gekker G, Peterson PK (1997) Activation of mu opioid receptors inhibits microglial cell chemotaxis. Journal of Pharmacology & Experimental Therapeutics 281:998-1004.

Chaplan SR, Bach FW, Pogrel JW, Chung JM, Yaksh TL (1994) Quantitative assessment of tactile allodynia in the rat paw. J Neurosci Methods 53:55-63.

Chapman CR, Casey KL, Dubner R, Foley KM, Gracely RH, Reading AE (1985) Pain measurement: an overview. Pain 22:1-31.

Chapman GA, Moores K, Harrison D, Campbell CA, Stewart BR, Strijbos P.J. (2000) Fractalkine cleavage from neuronal membranes represents an acute event in the inflammatory response to excitotoxic brain damage. The Journal of neuroscience : the official journal of the Society for Neuroscience 20:RC87.

Chauvet N, Palin K, Verrier D, Poole S, Dantzer R, Lestage J (2001) Rat microglial cells secrete predominantly the precursor of interleukin-1beta in response to lipopolysaccharide. European Journal of Neuroscience 14:609-617.

Chen X, Pierce B, Naing W, Grapperhaus ML, Phillion DP (2010) Discovery of 2-chloro-N-((4,4-difluoro-1-hydroxycyclohexyl)methyl)-5-(5-fluoropyrimidin -2-yl)benzamide as a potent and CNS penetrable P2X7 receptor antagonist. Bioorg Med Chem Lett 20:3107-3111.

Cherny NI, Thaler HT, Friedlander-Klar H, Lapin J, Foley KM, Houde R, Portenoy RK (1994) Opioid responsiveness of cancer pain syndromes caused by neuropathic or

nociceptive mechanisms: a combined analysis of controlled, single-dose studies. Neurology 44:857-861.

Chessell IP, Grahames CBA, Michel AD, Humphrey PPA (2001) Dynamics of p2x7 receptor pore dilation: Pharmacological and functional consequences. Drug Development Research 53:60-65.

Chessell IP, Hatcher JP, Bountra C, Michel AD, Hughes JP, Green P, Egerton J, Murfin M, Richardson J, Peck WL, Grahames CB, Casula MA, Yiangou Y, Birch R, Anand P, Buell GN (2005) Disruption of the P2X7 purinoceptor gene abolishes chronic inflammatory and neuropathic pain. Pain 114:386-396.

Chessell IP, Michel AD, Humphrey PPA (1997) Properties of the pore-forming P2X7 purinoceptor in mouse NTW8 microglial cells. British Journal of Pharmacology 121:1429-1437.

Chessell IP, Simon J, Hibell AD, Michel AD, Barnard EA, Humphrey PP (1998) Cloning and functional characterisation of the mouse P2X7 receptor. FEBS Letters 439:26-30.

Choi HB, Ryu JK, Kim SU, McLarnon JG (2007) Modulation of the purinergic P2X7 receptor attenuates lipopolysaccharide-mediated microglial activation and neuronal damage in inflamed brain. Journal of Neuroscience 27:4957-4968.

Christensen D, Kayser V (2000) The development of pain-related behaviour and opioid tolerance after neuropathy-inducing surgery and sham surgery. Pain 88:231-238.

Christrup LL, Lundorff L, Werner M (2009) Novel formulations and routes of administration for opioids in the treatment of breakthrough pain. Therapy 6:695-706.

Chu Y-X, Zhang Y, Zhang Y-Q, Zhao Z-Q (2010) Involvement of microglial P2X7 receptors and downstream signaling pathways in long-term potentiation of spinal nociceptive responses. Brain, behavior, and immunity 24:1176-1189.

Clark AK, Gentry C, Bradbury EJ, McMahon SB, Malcangio M (2007) Role of spinal microglia in rat models of peripheral nerve injury and inflammation. European Journal of Pain 11:223-230.

Clark AK, Staniland AA, Marchand F, Kaan TK, McMahon SB, Malcangio M (2010) P2X7-dependent release of interleukin-1beta and nociception in the spinal cord following lipopolysaccharide. Journal of Neuroscience 30:573-582.

Cockcroft S, Gomperts BD (1980) The ATP4- receptor of rat mast cells. Biochemical Journal 188:789-798.

Coggeshall RE, Hong KA, Langford LA, Schaible HG, Schmidt RF (1983) Discharge characteristics of fine medial articular afferents at rest and during passive movements of inflamed knee joints. Brain Research 272:185-188.

Cohrs RJ, Gilden DH (2003) Varicella zoster virus transcription in latently-infected human ganglia. Anticancer Res 23:2063-2069.

Cohrs RJ, Gilden DH, Mahalingam R (2004) Varicella zoster virus latency, neurological disease and experimental models: an update. Front Biosci 9:751-762.

Colburn RW, Deleo JA (1999) The effect of perineural colchicine on nerve injury-induced spinal glial activation and neuropathic pain behavior. Brain Research Bulletin 49:419-427.

Colburn RW, Deleo JA, Rickman AJ, Yeager MP, Kwon P, Hickey WF (1997) Dissociation of microglial activation and neuropathic pain behaviors following peripheral nerve injury in the rat. Journal of Neuroimmunology 79:163-175.

Colburn RW, Rickman AJ, Deleo JA (1999) The effect of site and type of nerve injury on spinal glial activation and neuropathic pain behavior. Experimental Neurology 157:289-304.

Collins SD, Chessell IP (2005) Emerging therapies for neuropathic pain. [Review] [136 refs]. Expert Opinion on Emerging Drugs 10:95-108.

Colomar A, Amedee T (2001) ATP stimulation of P2X(7) receptors activates three different ionic conductances on cultured mouse Schwann cells. European Journal of Neuroscience 14:927-936.

Colpaert FC (1996) System theory of pain and of opiate analgesia: no tolerance to opiates. [Review] [408 refs]. Pharmacological Reviews 48:355-402.

Cotrina ML, Nedergaard M (2009) Physiological and pathological functions of P2X7 receptor in the spinal cord. Purinergic Signalling 5:223-232.

Coull JA, Beggs S, Boudreau D, Boivin D, Tsuda M, Inoue K, Gravel C, Salter MW, De KY (2005) BDNF from microglia causes the shift in neuronal anion gradient underlying neuropathic pain. Nature 438:1017-1021.

Courteix C, Eschalier A, Lavarenne J (1993) Streptozocin-induced diabetic rats: behavioural evidence for a model of chronic pain. Pain 53:81-88.

Coyle DE (1998) Partial peripheral nerve injury leads to activation of astroglia and microglia which parallels the development of allodynic behavior. GLIA 23:75-83.

Crofford LJ (2010) Adverse effects of chronic opioid therapy for chronic musculoskeletal pain. [Review] [49 refs]. Nature Reviews Rheumatology 6:191-197.

Cui Y, Chen Y, Zhi JL, Guo RX, Feng JQ, Chen PX (2006) Activation of p38 mitogen-activated protein kinase in spinal microglia mediates morphine antinociceptive tolerance. Brain Res 1069:235-243.

Cui Y, Liao XX, Liu W, Guo RX, Wu ZZ, Zhao CM, Chen PX, Feng JQ (2008) A novel role of minocycline: attenuating morphine antinociceptive tolerance by inhibition of p38 MAPK in the activated spinal microglia. Brain Behav Immun 22:114-123.

Cvejic S, Trapaidze N, Cyr C, Devi LA (1996) Thr353, located within the COOH-terminal tail of the delta opiate receptor, is involved in receptor down-regulation. Journal of Biological Chemistry 271:4073-4076.

D'Amour FE, Smith DL (1941) A method of determining loss of pain sensation. Journal of Pharmacology & Experimental Therapeutics 72:74-78.

Dalziel RG, Bingham S, Sutton D, Grant D, Champion JM, Dennis SA, Quinn JP, Bountra C, Mark MA (2004) Allodynia in rats infected with varicella zoster virus--a small animal model for post-herpetic neuralgia. Brain Res Brain Res Rev 46:234-242.

Davalos D, Grutzendler J, Yang G, Kim JV, Zuo Y, Jung S, Littman DR, Gan WB (2005) ATP mediates rapid microglial response to local brain injury in vivo. Nature neuroscience 8:752-758.

Davison AJ, Scott JE (1986) The complete DNA sequence of varicella-zoster virus. J Gen Virol 67 (Pt 9):1759-1816.

Dayer JM, de RB, Burrus B, Demczuk S, Dinarello CA (1986) Human recombinant interleukin 1 stimulates collagenase and prostaglandin E2 production by human synovial cells. Journal of Clinical Investigation 77:645-648.

De VJ, Kuhl E, Franken-Kunkel P, Eckel G (2004) Pharmacological characterization of the chronic constriction injury model of neuropathic pain. European Journal of Pharmacology 491:137-148.

Deciga-Campos M, Guevara LU, Diaz Reval MI, Lopez-Munoz FJ (2003) Enhancement of antinociception by co-administration of an opioid drug (morphine) and a preferential cyclooxygenase-2 inhibitor (rofecoxib) in rats. European Journal of Pharmacology 460:99-107.

Decosterd I, Woolf CJ (2000) Spared nerve injury: an animal model of persistent peripheral neuropathic pain. Pain 87:149-158.

Delaney A, Colvin LA, Fallon MT, Dalziel RG, Mitchell R, Fleetwood-Walker SM (2009) Postherpetic neuralgia: from preclinical models to the clinic. Neurotherapeutics 6:630-637.

Deleo JA, Colburn RW, Nichols M, Malhotra A (1996) Interleukin-6-mediated hyperalgesia/allodynia and increased spinal IL-6 expression in a rat mononeuropathy model. Journal of Interferon & Cytokine Research 16:695-700.

Dell'Antonio G, Quattrini A, Cin ED, Fulgenzi A, Ferrero ME (2002a) Relief of inflammatory pain in rats by local use of the selective P2X7 ATP receptor inhibitor, oxidized ATP. Arthritis & Rheumatism 46:3378-3385.

Dell'Antonio G, Quattrini A, Dal CE, Fulgenzi A, Ferrero ME (2002b) Antinociceptive effect of a new P(2Z)/P2X7 antagonist, oxidized ATP, in arthritic rats. Neuroscience Letters 327:87-90.

Di VF (2006) Purinergic signalling between axons and microglia. Novartis Foundation Symposium 276:253-258.

Di VF, Ceruti S, Bramanti P, Abbracchio MP (2009) Purinergic signalling in inflammation of the central nervous system. [Review] [86 refs]. Trends in Neurosciences 32:79-87.

Diaz-Hernandez M, Diez-Zaera M, Sanchez-Nogueiro J, Gomez-Villafuertes R, Alberch J, Miras-Portugal MT, Lucas JJ (2009) Altered P2X7-receptor level and function in mouse models of Huntington's disease and therapeutic efficacy of antagonist administration. FASEB Journal 23:1893-1906.

Dickenson AH, Suzuki R (2005) Opioids in neuropathic pain: Clues from animal studies. European Journal of Pain 9:113-116.

Ding XZ, Bayer BM (1993) Increases of CCK mRNA and peptide in different brain areas following acute and chronic administration of morphine. Brain Research 625:139-144.

Dogrul A, ilyurt O, imer A, zeldemir ME (2001) L-type and T-type calcium channel blockade potentiate the analgesic effects of morphine and selective mu opioid agonist, but not to selective delta and kappa agonist at the level of the spinal cord in mice. Pain 93:61-68.

Dogrul A, Yesilyurt O (1998) Effects of intrathecally administered aminoglycoside antibiotics, calcium-channel blockers, nickel and calcium on acetic acid-induced writhing test in mice. Vascular Pharmacology 30:613-616.

Dogrul A, Yesilyurt O, Deniz G, Isimer A (1997) Analgesic effects of amlodipine and its interaction with morphine and ketorolac-induced analgesia. Vascular Pharmacology 29:839-845.

Dogrul A, Zagli U, Tulunay FC (2002) The role of T-type calcium channels in morphine analgesia, development of antinociceptive tolerance and dependence to morphine, and morphine abstinence syndrome. Life Sciences 71:725-734.

Donnelly-Roberts DL, Jarvis MF (2007) Discovery of P2X7 receptor-selective antagonists offers new insights into P2X7 receptor function and indicates a role in chronic pain states. Br J Pharmacol 151:571-579.

Donnelly-Roberts DL, Namovic MT, Faltynek CR, Jarvis MF (2004) Mitogen-activated protein kinase and caspase signaling pathways are required for P2X7 receptor (P2X7R)-induced pore formation in human THP-1 cells. Journal of Pharmacology & Experimental Therapeutics 308:1053-1061.

Donnelly-Roberts DL, Namovic MT, Surber B, Vaidyanathan SX, Perez-Medrano A, Wang Y, Carroll WA, Jarvis MF (2009) [3H]A-804598 ([3H]2-cyano-1-[(1S)-1-phenylethyl]-3-quinolin-5-ylguanidine) is a novel, potent, and selective antagonist radioligand for P2X7 receptors. Neuropharmacology 56:223-229.

Dourish CT, Hawley D, Iversen SD (1988) Enhancement of morphine analgesia and prevention of morphine tolerance in the rat by the cholecystokinin antagonist L-364,718. European Journal of Pharmacology 147:469-472.

Doverty M, White JM, Somogyi AA, Bochner F, Ali R, Ling W (2001) Hyperalgesic responses in methadone maintenance patients. Pain 90:91-96.

Dowdall T, Robinson I, Meert TF (2005) Comparison of five different rat models of peripheral nerve injury. Pharmacol Biochem Behav 80:93-108.

Dray A, Perkins MN (2010) New Pain Treatments in Late Development. pp 383-401.

Duan S, Anderson CM, Keung EC, Chen Y, Chen Y, Swanson RA (2003) P2X7 receptor-mediated release of excitatory amino acids from astrocytes. Journal of Neuroscience 23:1320-1328.

Dubner R, Ruda MA (1992) Activity-dependent neuronal plasticity following tissue injury and inflammation. [Review] [59 refs]. Trends in Neurosciences 15:96-103.

Dubuisson D, Dennis SG (1977) The formalin test: a quantitative study of the analgesic effects of morphine, meperidine, and brain stem stimulation in rats and cats. Pain 4:161-174.

Ducreux D, Attal N, Parker F, Bouhassira D (2006) Mechanisms of central neuropathic pain: a combined psychophysical and fMRI study in syringomyelia. Brain 129:963-976.

Dworkin RH, et al. (2010) Recommendations for the pharmacological management of neuropathic pain: an overview and literature update. [Review] [113 refs]. Mayo Clinic Proceedings 85:S3-14.

Dworkin RH, Portenoy RK (1996) Pain and its persistence in herpes zoster. Pain 67:241-251.

Dworkin RH, Schmader KE (2003) Treatment and prevention of postherpetic neuralgia. Clin Infect Dis 36:877-882.

Echeverry S, Shi XQ, Zhang J (2008) Characterization of cell proliferation in rat spinal cord following peripheral nerve injury and the relationship with neuropathic pain. Pain 135:37-47.

Elliott K, Minami N, Kolesnikov YA, Pasternak GW, Inturrisi CE (1994) The NMDA receptor antagonists, LY274614 and MK-801, and the nitric oxide synthase inhibitor, NG-nitro-L-arginine, attenuate analgesic tolerance to the mu-opioid morphine but not to kappa opioids. Pain 56:69-75.

Ennion S, Hagan S, Evans RJ (2000) The role of positively charged amino acids in ATP recognition by human P2X(1) receptors. Journal of Biological Chemistry 275:29361-29367.

Eriksson NP, Persson JKE, Aldskogius H, Svensson M (1997) A quantitative analysis of the glial cell reaction in primary sensory termination areas following sclatic nerve injury and treatment with nerve growth factor in the adult rat. Experimental Brain Research 114:393-404.

Eriksson NP, Persson JKE, Svensson N, Arvidsson J, Molander C (1993) A quantitative analysis of the microglial cell reaction in central primary sensory projection territories following peripheral nerve injury in the adult rat. Experimental Brain Research 96:19-27.

Esser MJ, Sawynok J (2000) Caffeine blockade of the thermal antihyperalgesic effect of acute amitriptyline in a rat model of neuropathic pain. European Journal of Pharmacology 399:131-139.

Evans RJ, Lewis C, Virginio C, Lundstrom K, Buell G, Surprenant A, North RA (1996) Ionic permeability of, and divalent cation effects on, two ATP-gated cation channels (P2X receptors) expressed in mammalian cells. Journal of Physiology 497:413-422.

Faden AI (1992) Dynorphin increases extracellular levels of excitatory amino acids in the brain through a non-opioid mechanism. Journal of Neuroscience 12:425-429.

Faria RX, Cascabulho CM, Reis RA, Alves LA (2010) Large-conductance channel formation mediated by P2X7 receptor activation is regulated through distinct intracellular signaling pathways in peritoneal macrophages and 2BH4 cells. Naunyn-Schmiedebergs Archives of Pharmacology 382:73-87.

Faris PL (1985) Opiate antagonistic function of cholecystokinin in analgesia and energy balance systems. Annals of the New York Academy of Sciences 448:437-447.

Favre-Guilmard C, Zeroual-Hider H, Soulard C, Touvay C, Chabrier PE, Prevost G, Auguet M (2008) The novel inhibitor of the heterotrimeric G-protein complex, BIM-46187, elicits anti-hyperalgesic properties and synergizes with morphine. Eur J Pharmacol 594:70-76.

Ferenczi S, Nunez C, Pinter-Kubler B, Foldes A, Martin F, Ladnyanszky M, V, Milanes MV, Kovacs KJ (2010) Changes in metabolic-related variables during chronic morphine treatment. Neurochem Int.

Ferguson SS, Barak LS, Zhang J, Caron MG (1996) G-protein-coupled receptor regulation: role of G-protein-coupled receptor kinases and arrestins. [Review] [137 refs]. Canadian Journal of Physiology & Pharmacology 74:1095-1110.

Ferrari D, Chiozzi P, Falzoni S, Dal SM, Melchiorri L, Baricordi OR, Di VF (1997a) Extracellular ATP triggers IL-1 beta release by activating the purinergic P2Z receptor of human macrophages. Journal of Immunology 159:1451-1458.

Ferrari D, Pizzirani C, Adinolfi E, Lemoli RM, Curti A, Idzko M, Panther E, Di VF (2006) The P2X7 receptor: a key player in IL-1 processing and release. J Immunol 176:3877-3883.

Ferrari D, Villalba M, Chiozzi P, Falzoni S, Ricciardi-Castagnoli P, Di VF (1996) Mouse microglial cells express a plasma membrane pore gated by extracellular ATP. Journal of Immunology 156:1531-1539.

Ferrari D, Wesselborg S, Bauer MK, Schulze-Osthoff K (1997b) Extracellular ATP activates transcription factor NF-kappaB through the P2Z purinoreceptor by selectively targeting NF-kappaB p65. Journal of Cell Biology 139:1635-1643.

Ferreira SH, Lorenzetti BB, Bristow AF, Poole S (1988) Interleukin-1beta as a potent hyperalgesic agent antagonized by a tripeptide analogue. Nature 334:698-700.

Field MJ, Bramwell S, Hughes J, Singh L (1999a) Detection of static and dynamic components of mechanical allodynia in rat models of neuropathic pain: are they signalled by distinct primary sensory neurones? Pain 83:303-311.

Field MJ, Holloman EF, McCleary S, Hughes J, Singh L (1997) Evaluation of gabapentin and S-(+)-3-isobutylgaba in a rat model of postoperative pain. Journal of Pharmacology & Experimental Therapeutics 282:1242-1246.

Field MJ, McCleary S, Hughes J, Singh L (1999b) Gabapentin and pregabalin, but not morphine and amitriptyline, block both static and dynamic components of mechanical allodynia induced by streptozocin in the rat. Pain 80:391-398.

Fields HL (2000) Pain modulation: Expectation, opioid analgesia and virtual pain. Progress in Brain Research 122:245-253.

Fields HL, Bry J, Hentall I, Zorman G (1983) The activity of neurons in the rostral medulla of the rat during withdrawal from noxious heat. Journal of Neuroscience 3:2545-2552.

Fields HL, Heinricher MM, Mason P (1991) Neurotransmitters in nociceptive modulatory circuits. [Review] [190 refs]. Annual Review of Neuroscience 14:219-245.

Fields HL, Rowbotham M, Baron R (1998) Postherpetic neuralgia: irritable nociceptors and deafferentation. Neurobiol Dis 5:209-227.

Finn AK, Whistler JL (2001) Endocytosis of the mu opioid receptor reduces tolerance and a cellular hallmark of opiate withdrawal. Neuron 32:829-839.

Finnerup NB, Sindrup SH, Jensen TS (2010) The evidence for pharmacological treatment of neuropathic pain. Pain 150:573-581.

Fleetwood-Walker SM, Quinn JP, Wallace C, Blackburn-Munro G, Kelly BG, Fiskerstrand CE, Nash AA, Dalziel RG (1999) Behavioural changes in the rat following infection with varicella-zoster virus. J Gen Virol 80 (Pt 9):2433-2436.

Foley KM (1995) Misconceptions and controversies regarding the use of opioids in cancer pain. Anti-Cancer Drugs 6:4-13.

Fonnum F, Johnsen A, Hassel B (1997) Use of fluorocitrate and fluoroacetate in the study of brain metabolism. [Review] [58 refs]. GLIA 21:106-113.

Frampton M, Harvey RJ, Kirchner V (2003) Propentofylline for dementia. [Review] [32 refs]. Cochrane Database of Systematic Reviews2853.

Freye E, Latasch L (2003) Development of opioid tolerance - Molecular mechanisms and clinical consequences. Anasthesiologie Intensivmedizin Notfallmedizin Schmerztherapie 38:14-26.

Friedle SA, Curet MA, Watters JJ (2010) Recent patents on novel P2X(7) receptor antagonists and their potential for reducing central nervous system inflammation. [Review] [157 refs]. Recent Patents on CNS Drug Discovery 5:35-45.

Fukuhara N, Imai Y, Sakakibara A, Morita K, Kitayama S, Tanne K, Dohi T (2000) Regulation of the development of allodynia by intrathecally administered P2 purinoceptor agonists and antagonists in mice. Neurosci Lett 292:25-28.

Fundytus ME, Yashpal K, Chabot J-G, Osborne MG, Lefebvre CD, Dray A, Coderre TJ (2001) Knockdown of spinal metabotropic glutamate receptor 1 (mGluR1) alleviates pain and restores opioid efficacy after nerve injury in rats. British Journal of Pharmacology 132:354-367.

Gao Y-J, Ji R-R (2010) Chemokines, neuronal-glial interactions, and central processing of neuropathic pain. Pharmacology and Therapeutics 126:56-68.

Garcia de YE, Pelletier G (1993) Opioid regulation of proopiomelanocortin (POMC) gene expression in the rat brain as studied by in situ hybridization. Neuropeptides 25:91-94.

Gardell LR, Wang R, Burgess SE, Ossipov MH, Vanderah TW, Malan J, Lai J, Porreca F (2002) Sustained morphine exposure induces a spinal dynorphin-dependent enhancement of excitatory transmitter release from primary afferent fibers. Journal of Neuroscience 22:6747-6755.

Gargett CE, Cornish EJ, Wiley JS (1996) Phospholipase D activation by P(2Z)-purinoceptor agonists in human lymphocytes is dependent on bivalent cation influx. Biochemical Journal 313:529-535.

Garrison CJ, Dougherty PM, Carlton SM (1994) GFAP expression in lumbar spinal cord of naive and neuropathic rats treated with MK-801. Experimental Neurology 129:237-243.

Garrison CJ, Dougherty PM, Kajander KC, Carlton SM (1991) Staining of glial fibrillary acidic protein (GFAP) in lumbar spinal cord increases following a sciatic nerve constriction injury. Brain Research 565:1-7.

Garry EM, Delaney A, Anderson HA, Sirinathsinghji EC, Clapp RH, Martin WJ, Kinchington PR, Krah DL, Abbadie C, Fleetwood-Walker SM (2005) Varicella zoster virus induces neuropathic changes in rat dorsal root ganglia and behavioral reflex sensitisation that is attenuated by gabapentin or sodium channel blocking drugs. Pain 118:97-111.

Garzon J, Rodriguez-Munoz M, Lopez-Fando A, Sanchez-Blazquez P (2005) Activation of mu-opioid receptors transfers control of Galpha subunits to the regulator of G-protein signaling RGS9-2: Role in receptor desensitization. Journal of Biological Chemistry 280:8951-8960.

Gauriau C, Bernard J-F (2004) A Comparative Reappraisal of Projections from the Superficial Laminae of the Dorsal Horn in the Rat: The Forebrain. Journal of Comparative Neurology 468:24-56.

Gebhart GF (1990) Some mechanistic insights into opioid tolerance. Anesthesiology 73:1065-1066.

Gendron FP, Neary JT, Theiss PM, Sun GY, Gonzalez FA, Weisman GA (2003) Mechanisms of P2X7 receptor-mediated ERK1/2 phosphorylation in human astrocytoma cells. American journal of physiology Cell physiology 284:C571-C581.

Gershon AA, Steinberg SP (1979) Cellular and humoral immune responses to varicella-zoster virus in immunocompromised patients during and after varicella-zoster infections. Infect Immun 25:170-174.

Ghilardi JR, Allen CJ, Vigna SR, McVey DC, Mantyh PW (1992) Trigeminal and dorsal root ganglion neurons express CCK receptor binding sites in the rat, rabbit, and monkey: possible site of opiate-CCK analgesic interactions. Journal of Neuroscience 12:4854-4866.

Gilchrist HD, Allard BL, Simone DA (1996) Enhanced withdrawal responses to heat and mechanical stimuli following intraplantar injection of capsaicin in rats. Pain 67:179-188.

Gilron I, Bailey JM, Tu D, Holden RR, Jackson AC, Houlden RL (2009) Nortriptyline and gabapentin, alone and in combination for neuropathic pain: a double-blind, randomised controlled crossover trial. Lancet 374:1252-1261.

Gilron I, Bailey JM, Tu D, Holden RR, Weaver DF, Houlden RL (2005) Morphine, gabapentin, or their combination for neuropathic pain. New England Journal of Medicine 352:1324-1334.

Gintzler AR, Chakrabarti S (2006) Post-opioid receptor adaptations to chronic morphine; Altered functionality and associations of signaling molecules. Life Sciences 79:717-722.

Gintzler AR, Chan WC, Glass J (1987) Evoked release of methionine enkephalin from tolerant/dependent enteric ganglia: paradoxical dependence on morphine. Proceedings of the National Academy of Sciences of the United States of America 84:2537-2539.

Gintzler AR, Xu H (1991) Different G proteins mediate the opioid inhibition or enhancement of evoked [5-methionine]enkephalin release. Proceedings of the National Academy of Sciences of the United States of America 88:4741-4745.

Gleave RJ, Walter DS, Beswick PJ, Fonfria E, Michel AD, Roman SA, Tang SP (2010) Synthesis and biological activity of a series of tetrasubstituted-imidazoles as P2X(7) antagonists. Bioorganic & Medicinal Chemistry Letters 20:4951-4954.

Go VL, Yaksh TL (1987) Release of substance P from the cat spinal cord. Journal of Physiology 391:141-167.

Goodchild CS, Kolosov A, Tucker AP, Cooke I (2008) Combination therapy with flupirtine and opioid: studies in rat pain models. Pain Medicine 9:928-938.

Goodwin JS (1987) Toxicity of nonsteroidal anti-inflammatory drugs. Archives of Internal Medicine 147:34-35.

Gordon JL (1986) Extracellular ATP: effects, sources and fate. [Review] [160 refs]. Biochemical Journal 233:309-319.

Gosnell BA, Krahn DD (1993) The effects of continuous morphine infusion on diet selection and body weight. Physiology & Behavior 54:853-859.

Griffin RS, Costigan M, Brenner GJ, Ma CH, Scholz J, Moss A, Allchorne AJ, Stahl GL, Woolf CJ (2007) Complement induction in spinal cord microglia results in anaphylatoxin C5a-mediated pain hypersensitivity. Journal of Neuroscience 27:8699-8708.

Gu JG, MacDermott AB (1997) Activation of ATP P2X receptors elicits glutamate release from sensory neuron synapses. Nature 389:749-753.

Gul H, Yildiz O, Dogrul A, Yesilyurt O, Isimer A (2000) The interaction between IL-1beta and morphine: possible mechanism of the deficiency of morphine-induced analgesia in diabetic mice. Pain 89:39-45.

Guo JD, Wang H, Zhang YQ, Zhao ZQ (2006) Distinct effects of D-serine on spinal nociceptive responses in normal and carrageenan-injected rats. Biochemical & Biophysical Research Communications 343:401-406.

Guthrie PB, Knappenberger J, Segal M, Bennett MV, Charles AC, Kater SB (1999) ATP released from astrocytes mediates glial calcium waves. Journal of Neuroscience 19:520-528.

Hack SP, Vaughan CW, Christie MJ (2003) Modulation of GABA release during morphine withdrawal in midbrain neurons in vitro. Neuropharmacology 45:575-584.

Hains BC, Waxman SG (2006) Activated microglia contribute to the maintenance of chronic pain after spinal cord injury. Journal of Neuroscience 26:4308-4317.

Hajos F, Csillik B, Knyihar-Csillik E (1990) Alterations in glial fibrillary acidic protein immunoreactivity in the upper dorsal horn of the rat spinal cord in the course of transganglionic degenerative atrophy and regenerative proliferation. Neuroscience Letters 117:8-13.

Hamon Y, Luciani MF, Becq F, Verrier B, Rubartelli A, Chimini G (1997) Interleukin-1beta secretion is impaired by inhibitors of the Atp binding cassette transporter, ABC1. Blood 90:2911-2915.

Han DW, Kweon TD, Lee JS, Lee YW (2007) Antiallodynic effect of pregabalin in rat models of sympathetically maintained and sympathetic independent neuropathic pain. Yonsei Med J 48:41-47.

Hanisch UK (2002) Microglia as a source and target of cytokines. [Review] [170 refs]. GLIA 40:140-155.

Hanna M, O'Brien C, Wilson MC (2008) Prolonged-release oxycodone enhances the effects of existing gabapentin therapy in painful diabetic neuropathy patients. European Journal of Pain 12:804-813.

Harada H, Ueda H, Katada T, Ui M, Satoh M (1990) Phosphorylated mu-opioid receptor purified from rat brains lacks functional coupling with G(i)1, a GTP-binding protein in reconstituted lipid vesicles. Neuroscience Letters 113:47-49.

Hargreaves K, Dubner R, Brown F, Flores C, Joris J (1988) A new and sensitive method for measuring thermal nociception in cutaneous hyperalgesia. Pain 32:77-88.

Harrison LM, Kastin AJ, Zadina JE (1998) Opiate tolerance and dependence: Receptors, G-proteins, and antiopiates. Peptides 19:1603-1630.

Hart RP, Shadiack AM, Jonakait GM (1991) Substance P gene expression is regulated by interleukin-1 in cultured sympathetic ganglia. Journal of Neuroscience Research 29:282-291.

Hashizume H, Rutkowski MD, Weinstein JN, Deleo JA (2000) Central administration of methotrexate reduces mechanical allodynia in an animal model of radiculopathy/sciatica. Pain 87:159-169.

Hasnie FS, Breuer J, Parker S, Wallace V, Blackbeard J, Lever I, Kinchington PR, Dickenson AH, Pheby T, Rice AS (2007) Further characterization of a rat model of varicella zoster virus-associated pain: Relationship between mechanical hypersensitivity and anxiety-related behavior, and the influence of analgesic drugs. Neuroscience 144:1495-1508.

Hatcher JP, Chessell IP (2006) Transgenic models of pain: a brief review. [Review] [68 refs]. Current Opinion in Investigational Drugs 7:647-652.

Havemann U, Turski L, Kuschinsky K (1982) Role of opioid receptors in the substantia nigra in morphine-induced muscular rigidity. Life Sci 31:2319-2322.

Havemann U, Winkler M, Kuschinsky K (1980) Opioid receptors in the caudate nucleus can mediate EMG-recorded rigidity in rats. Naunyn Schmiedebergs Arch Pharmacol 313:139-144.

Hayes AG, Tyers MB (1983) Determination of receptors that mediate opiate side effects in the mouse. Br J Pharmacol 79:731-736.

Hayes GM, Woodroofe MN, Cuzner ML (1987) Microglia are the major cell type expressing MHC class II in human white matter. Journal of the Neurological Sciences 80:25-37.

He L, Fong J, von ZM, Whistler JL (2002) Regulation of opioid receptor trafficking and morphine tolerance by receptor oligomerization. Cell 108:271-282.

He L, Kim JA, Whistler JL (2009) Biomarkers of morphine tolerance and dependence are prevented by morphine-induced endocytosis of a mutant mu-opioid receptor. FASEB J 23:4327-4334.

Heid CA, Stevens J, Livak KJ, Williams PM (1996) Real time quantitative PCR. Genome Research 6:986-994.

Heinricher MM, Neubert MJ (2004) Neural basis for the hyperalgesic action of cholecystokinin in the rostral ventromedial medulla. Journal of Neurophysiology 92:1982-1989.

Heinricher MM, Roychowdhury SM (1997) Reflex-related activation of putative pain facilitating neurons in rostral, ventromedial medulla requires excitatory amino acid transmission. Neuroscience 78:1159-1165.

Hibell AD, Thompson KM, Xing M, Humphrey PP, Michel AD (2001) Complexities of measuring antagonist potency at P2X(7) receptor orthologs. Journal of Pharmacology & Experimental Therapeutics 296:947-957.

Hide I, Tanaka M, Inoue A, Nakajima K, Kohsaka S, Inoue K, Nakata Y (2000) Extracellular ATP triggers tumor necrosis factor-alpha release from rat microglia. J Neurochem 75:965-972.

Holguin A, O'Connor KA, Biedenkapp J, Campisi J, Wieseler-Frank J, Milligan ED, Hansen MK, Spataro L, Maksimova E, Bravmann C, Martin D, Fleshner M, Maier SF, Watkins LR (2004) HIV-1 gp120 stimulates proinflammatory cytokine-mediated pain facilitation via activation of nitric oxide synthase-I (nNOS). Pain 110:517-530.

Holt M, Cooke A, Wu MM, Lagnado L (2003) Bulk membrane retrieval in the synaptic terminal of retinal bipolar cells. Journal of Neuroscience 23:1329-1339.

Holzer P, Ahmedzai SH, Niederle N, Leyendecker P, Hopp M, Bosse B, Spohr I, Reimer K (2009) Opioid-induced bowel dysfunction in cancer-related pain: causes, consequences, and a novel approach for its management. [Review] [48 refs]. Journal of Opioid Management 5:145-151.

Hong EK, Takemori AE (1989) Indirect involvement of delta opioid receptors in cholecystokinin octapeptide-induced analgesia in mice. Journal of Pharmacology & Experimental Therapeutics 251:594-598.

Honore P, Donnelly-Roberts D, Namovic M, Zhong C, Wade C, Chandran P, Zhu C., Carroll W, Perez-Medrano A, Iwakura Y, Jarvis MF (2009) The antihyperalgesic activity of a selective P2X7 receptor antagonist, A-839977, is lost in IL-1alphabeta knockout mice. Behavioural Brain Research 204:77-81.

Honore P, Donnelly-Roberts D, Namovic MT, Hsieh G, Zhu CZ, Mikusa JP, Hernandez G, Zhong C, Gauvin DM, Chandran P, Harris R, Medrano AP, Carroll W, Marsh K, Sullivan JP, Faltynek CR, Jarvis MF (2006) A-740003 [N-(1-{[(cyanoimino)(5-quinolinylamino) methyl]amino}-2,2-dimethylpropyl)-2-(3,4-dimethoxyphenyl)acetamide], a novel and selective P2X7 receptor antagonist, dose-dependently reduces neuropathic pain in the rat. J Pharmacol Exp Ther 319:1376-1385.

Horvath RJ, Deleo JA (2009) Morphine enhances microglial migration through modulation of P2X4 receptor signaling. Journal of Neuroscience 29:998-1005.

Horvath RJ, Landry RP, Romero-Sandoval EA, Deleo JA (2010a) Morphine tolerance attenuates the resolution of postoperative pain and enhances spinal microglial p38 and extracellular receptor kinase phosphorylation. Neuroscience 169:843-854.

Horvath RJ, Romero-Sandoval EA, Leo JAD (2010b) Inhibition of microglial P2X4 receptors attenuates morphine tolerance, Iba1, GFAP and mu opioid receptor protein expression while enhancing perivascular microglial ED2. Pain 150:401-413.

Hsieh GC, Chandran P, Salyers AK, Pai M, Zhu CZ, Wensink EJ, Witte DG, Miller TR, Mikusa JP, Baker SJ, Wetter JM, Marsh KC, Hancock AA, Cowart MD, Esbenshade TA, Brioni JD, Honore P (2010) H4 receptor antagonism exhibits anti-nociceptive effects in inflammatory and neuropathic pain models in rats. Pharmacol Biochem Behav 95:41-50.

Hu H, Hoylaerts MF (2010) The P2X1 ion channel in platelet function. Platelets 21:153-166.

Humphreys BD, Dubyak GR (1996) Induction of the P2z/P2X7 nucleotide receptor and associated phospholipase D activity by lipopolysaccharide and IFN-gamma in the human THP-1 monocytic cell line. Journal of Immunology 157:5627-5637.

Humphreys BD, Virginio C, Surprenant A, Rice J, Dubyak GR (1998) Isoquinolines as antagonists of the P2X7 nucleotide receptor: high selectivity for the human versus rat receptor homologues. Molecular pharmacology 54:22-32.

Hunt SP, Mantyh PW (2001) The molecular dynamics of pain control. [Review] [98 refs]. Nature Reviews Neuroscience 2:83-91.

Hunter JC, Gogas KR, Hedley LR, Jacobson LO, Kassotakis L, Thompson J, Fontana DJ (1997) The effect of novel anti-epileptic drugs in rat experimental models of acute and chronic pain. European Journal of Pharmacology 324:153-160.

Hutchinson MR, Bland ST, Johnson KW, Rice KC, Maier SF, Watkins LR (2007) Opioid-induced glial activation: mechanisms of activation and implications for opioid analgesia, dependence, and reward. [Review] [65 refs]. Thescientificworldjournal 7:98-111.

Hutchinson MR, Coats BD, Lewis SS, Zhang Y, Sprunger DB, Rezvani N, Baker EM, Jekich BM, Wieseler JL, Somogyi AA, Martin D, Poole S, Judd CM, Maier SF, Watkins LR (2008a) Proinflammatory cytokines oppose opioid-induced acute and chronic analgesia. Brain, Behavior, & Immunity 22:1178-1189.

Hutchinson MR, Lewis SS, Coats BD, Skyba DA, Crysdale NY, Berkelhammer DL, Brzeski A, Northcutt A, Vietz CM, Judd CM, Maier SF, Watkins LR, Johnson KW (2009) Reduction of opioid withdrawal and potentiation of acute opioid analgesia by systemic AV411 (ibudilast). Brain Behav Immun 23:240-250.

Hutchinson MR, Northcutt AL, Chao LW, Kearney JJ, Zhang Y, Berkelhammer DL, Loram LC, Rozeske RR, Bland ST, Maier SF, Gleeson TT, Watkins LR (2008b) Minocycline suppresses morphine-induced respiratory depression, suppresses morphine-induced reward, and enhances systemic morphine-induced analgesia. Brain Behav Immun 22:1248-1256.

Hutchinson MR, Somogyi AA (2004a) (S)-(+)-methadone is more immunosuppressive than the potent analgesic (R)-(--)-methadone. International Immunopharmacology 4:1525-1530.

Hutchinson MR, Somogyi AA (2004b) Relationship between 4,5-epoxymorphinan structure and in vitro modulation of cell proliferation. European Journal of Pharmacology 494:251-262.

Hutchinson MR, Somogyi AA (2005) Characterisation of the in vitro modulation of splenocyte proliferation by non-4,5-epoxymorphinan opioids. International Immunopharmacology 5:1713-1722.

Hylden JL, Nahin RL, Dubner R (1987) Altered responses of nociceptive cat lamina I spinal dorsal horn neurons after chronic sciatic neuroma formation. Brain Research 411:341-350.

Hylden JL, Wilcox GL (1980) Intrathecal morphine in mice: a new technique. Eur J Pharmacol 67:313-316.

Ikeda K, Kobayashi T, Kumanishi T, Yano R, Sora I, Niki H (2002) Molecular mechanisms of analgesia induced by opioids and ethanol: Is the GIRK channel one of the keys? Neuroscience research 44:121-131.

Ingram SL, Vaughan CW, Bagley EE, Connor M, Christie MJ (1998) Enhanced opioid efficacy in opioid dependence is caused by an altered signal transduction pathway. Journal of Neuroscience 18:10269-10276.

Inoue K (2006) The function of microglia through purinergic receptors: neuropathic pain and cytokine release. [Review] [162 refs]. Pharmacology & Therapeutics 109:210-226.

Inoue K, Koizumi S, Nakajima K, Hamanoue M, Kohsaka S (1994) Modulatory effect of plasminogen on NMDA-induced increase in intracellular free calcium concentration in rat cultured hippocampal neurons. Neuroscience Letters 179:87-90.

Jabs R, Matthias K, Grote A, Grauer M, Seifert G, Steinhauser C (2007) Lack of P2X receptor mediated currents in astrocytes and GluR type glial cells of the hippocampal CA1 region. GLIA 55:1648-1655.

Jamieson GP, Snook MB, Thurlow PJ, Wiley JS (1996) Extracellular ATP causes of loss of L-selectin from human lymphocytes via occupancy of P2Z purinocepters. Journal of Cellular Physiology 166:637-642.

Jarvis MF (2003) Contributions of P2X3 homomeric and heteromeric channels to acute and chronic pain. [Review] [76 refs]. Expert Opinion on Therapeutic Targets 7:513-522.

Jeftinija S, Miletic V, Randic M (1981) Cholecystokinin octapeptide excites dorsal horn neurons both in vivo and in vitro. Brain Research 213:231-236.

Jergova S, Cizkova D (2007) Microglial activation in different models of peripheral nerve injury of the rat. Journal of Molecular Histology 38:245-251.

Ji RR, Suter MR (2007) p38 MAPK, microglial signaling, and neuropathic pain. [Review] [68 refs]. Molecular pain 3:33.

Ji RR, Woolf CJ (2001) Neuronal plasticity and signal transduction in nociceptive neurons: implications for the initiation and maintenance of pathological pain. Neurobiol Dis 8:1-10.

Jiang LH (2009) Inhibition of P2X(7) receptors by divalent cations: old action and new insight. [Review] [88 refs]. European Biophysics Journal 38:339-346.

Jiang LH, Mackenzie AB, North RA, Surprenant A (2000a) Brilliant blue G selectively blocks ATP-gated rat P2X(7) receptors. Molecular pharmacology 58:82-88.

Jiang LH, Rassendren F, MacKenzie A, Zhang YH, Surprenant A, North RA (2005) N-methyl-D-glucamine and propidium dyes utilize different permeation pathways at rat P2X(7) receptors. American Journal of Physiology - Cell Physiology 289:C1295-C1302.

Jiang LH, Rassendren F, Surprenant A, North RA (2000b) Identification of amino acid residues contributing to the ATP-binding site of a purinergic P2X receptor. Journal of Biological Chemistry 275:34190-34196.

Jin SX, Zhuang ZY, Woolf CJ, Ji RR (2003) p38 mitogen-activated protein kinase is activated after a spinal nerve ligation in spinal cord microglia and dorsal root ganglion neurons and contributes to the generation of neuropathic pain. Journal of Neuroscience 23:4017-4022.

Jo YH, Schlichter R (1999) Synaptic corelease of ATP and GABA in cultured spinal neurons. Nature neuroscience 2:241-245.

John GR, Simpson JE, Woodroofe MN, Lee SC, Brosnan CF (2001) Extracellular nucleotides differentially regulate interleukin-1beta signaling in primary human astrocytes: Implications for inflammatory gene expression. Journal of Neuroscience 21:4134-4142.

Johnson RW, Whitton TL (2004) Management of herpes zoster (shingles) and postherpetic neuralgia. Expert Opin Pharmacother 5:551-559.

Johnston IN, Milligan ED, Wieseler-Frank J, Frank MG, Zapata V, Campisi J, Langer S, Martin D, Green P, Fleshner M, Leinwand L, Maier SF, Watkins LR (2004) A role for proinflammatory cytokines and fractalkine in analgesia, tolerance, and subsequent pain facilitation induced by chronic intrathecal morphine. J Neurosci 24:7353-7365.

Jonakait GM, Schotland S, Hart RP (1990) Interleukin-1 specifically increases substance P in injured sympathetic ganglia. Annals of the New York Academy of Sciences 594:222-230.

Jones BJ, Roberts DJ (1968) The quantiative measurement of motor inco-ordination in naive mice using an acelerating rotarod. J Pharm Pharmacol 20:302-304.

Jones CA, Vial C, Sellers LA, Humphrey PP, Evans RJ, Chessell IP (2004) Functional regulation of P2X6 receptors by N-linked glycosylation: identification of a novel alpha beta-methylene ATP-sensitive phenotype. Molecular pharmacology 65:979-985.

Juni A, Klein G, Pintar JE, Kest B (2007) Nociception increases during opioid infusion in opioid receptor triple knock-out mice. Neuroscience 147:439-444.

Kahlenberg JM, Dubyak GR (2004) Mechanisms of caspase-1 activation by P2X7 receptor-mediated K+ release. American Journal of Physiology - Cell Physiology 286:C1100-C1108.

Kalso E, Edwards JE, Moore RA, McQuay HJ (2004) Opioids in chronic non-cancer pain: systematic review of efficacy and safety. [Review] [46 refs]. Pain 112:372-380.

Kapsimalis F, Richardson G, Opp MR, Kryger M (2005) Cytokines and normal sleep. Curr Opin Pulm Med 11:481-484.

Kawai S (1998) Cyclooxygenase selectivity and the risk of gastro-intestinal complications of various non-steroidal anti-inflammatory drugs: A clinical consideration. Inflammation Research 47:S102-S106.

Keceli B, Kubo Y (2009) Functional and structural identification of amino acid residues of the P2X2 receptor channel critical for the voltage- and [ATP]-dependent gating. Journal of Physiology 587:5801-5818.

Kellstein DE, Mayer DJ (1991) Spinal co-administration of cholecystokinin antagonists with morphine prevents the development of opioid tolerance. Pain 47:221-229.

Kennedy PG, Grinfeld E, Bell JE (2000) Varicella-zoster virus gene expression in latently infected and explanted human ganglia. J Virol 74:11893-11898.

Kennedy PG, Grinfeld E, Bontems S, Sadzot-Delvaux C (2001) Varicella-Zoster virus gene expression in latently infected rat dorsal root ganglia. Virology 289:218-223.

Kennedy PG, Grinfeld E, Gow JW (1998) Latent varicella-zoster virus is located predominantly in neurons in human trigeminal ganglia. Proc Natl Acad Sci U S A 95:4658-4662.

Kest B, McLemore G, Kao B, Inturrisi CE (1997) The competitive alpha-amino-3-hydroxy-5-methylisoxazole-4-propionate receptor antagonist LY293558 attenuates and reverses analgesic tolerance to morphine but not to Delta or Kappa opioids. Journal of Pharmacology and Experimental Therapeutics 283:1249-1255.

Khakh BS, Proctor WR, Dunwiddie TV, Labarca C, Lester HA (1999) Allosteric control of gating and kinetics at P2X4 receptor channels. Journal of Neuroscience 19:7289-7299.

Kieffer BL, Evans CJ (2002) Opioid tolerance-in search of the holy grail. [Review] [20 refs]. Cell 108:587-590.

Kim KJ, Yoon YW, Chung JM (1997) Comparison of three rodent neuropathic pain models. Exp Brain Res 113:200-206.

Kim SH, Chung JM (1992) An experimental model for peripheral neuropathy produced by segmental spinal nerve ligation in the rat. Pain 50:355-363.

King T, Ossipov MH, Vanderah TW, Porreca F, Lai J (2005) Is paradoxical pain induced by sustained opioid exposure an underlying mechanism of opioid antinociceptive tolerance? NeuroSignals 14:194-205.

Koerber HR, Mirnics K, Brown PB, Mendell LM (1994) Central sprouting and functional plasticity of regenerated primary afferents. Journal of Neuroscience 14:3655-3671.

Koetzner L, Hua XY, Lai J, Porreca F, Yaksh T (2004) Nonopioid actions of intrathecal dynorphin evoke spinal excitatory amino acid and prostaglandin E2 release mediated by cyclooxygenase-1 and -2. Journal of Neuroscience 24:1451-1458.

Kohno T, Kumamoto E, Higashi H, Shimoji K, Yoshimura M (1999) Actions of opioids on excitatory and inhibitory transmission in substantia gelatinosa of adult rat spinal cord. Journal of Physiology 518:803-813.

Konsman JP, Kelley K, Dantzer R (1999) Temporal and spatial relationships between lipopolysaccharide-induced expression of Fos, interleukin-1beta and inducible nitric oxide synthase in rat brain. Neuroscience 89:535-548.

Kostura MJ, Tocci MJ, Limjuco G, Chin J, Cameron P, Hillman AG, Schmidt JA (1989) Identification of a monocyte specific pre-interleukin 1beta convertase activity. Proceedings of the National Academy of Sciences of the United States of America 86:5227-5231.

Kovelowski CJ, Ossipov MH, Sun H, Lai J, Malan J, T.P., Porreca F (2000) Supraspinal cholecystokinin may drive tonic descending facilitation mechanisms to maintain neuropathic pain in the rat. Pain 87:265-273.

Kovoor A, Nappey V, Kieffer BL, Chavkin C (1997) Mu and delta opioid receptors are differentially desensitized by the coexpression of beta-adrenergic receptor kinase 2 and beta-arrestin 2 in xenopus oocytes. Journal of Biological Chemistry 272:27605-27611.

Kress M, Fickenscher H (2001) Infection by human varicella-zoster virus confers norepinephrine sensitivity to sensory neurons from rat dorsal root ganglia. FASEB Journal 15:1037-1043.

Kress M, Reeh PW (1996) More sensory competence for nociceptive neurons in culture. [Review] [35 refs]. Proceedings of the National Academy of Sciences of the United States of America 93:14995-14997.

Kreutzberg GW (1996) Microglia: a sensor for pathological events in the CNS. [Review] [75 refs]. Trends in Neurosciences 19:312-318.

Kukley M, Stausberg P, Adelmann G, Chessell IP, Dietrich D (2004) Ecto-nucleotidases and nucleoside transporters mediate activation of adenosine receptors on hippocampal mossy fibers by P2X7 receptor agonist 2'-3'-O-(4-benzoylbenzoyl)-ATP. Journal of Neuroscience 24:7128-7139.

Labasi JM, Petrushova N, Donovan C, McCurdy S, Lira P, Payette MM, Brissette W, Wicks JR, Audoly L, Gabel CA (2002) Absence of the P2X7 receptor alters leukocyte function and attenuates an inflammatory response. Journal of Immunology 168:6436-6445.

LaMotte RH, Lundberg LE, Torebjork HE (1992) Pain, hyperalgesia and activity in nociceptive C units in humans after intradermal injection of capsaicin. Journal of Physiology 448:749-764.

Lang E, Hord AH, Denson D (1996) Venlafaxine hydrochloride (Effexor) relieves thermal hyperalgesia in rats with an experimental mononeuropathy. Pain 68:151-155.

Lang R, Pfeffer K, Wagner H, Heeg K (1997) A rapid method for semiquantitative analysis of the human V beta-repertoire using TaqManR PCR. Journal of Immunological Methods 203:181-192.

Lariviere WR, Wilson SG, Laughlin TM, Kokayeff A, West EE, Adhikari S.M., Wan Y, Mogil JS (2002) Heritability of nociception. III. Genetic relationships among commonly used assays of nociception and hypersensitivity. Pain 97:75-86.

Laughlin TM, Bethea JR, Yezierski RP, Wilcox GL (2000) Cytokine involvement in dynorphin-induced allodynia. Pain 84:159-167.

Laughlin TM, Vanderah TW, Lashbrook J, Nichols ML, Ossipov M, Porreca F, Wilcox GL (1997) Spinally administered dynorphin A produces long-lasting allodynia: involvement of NMDA but not opioid receptors. Pain 72:253-260.

Laulin JP, Celerier E, Larcher A, Le MM, Simonnet G (1999) Opiate tolerance to daily heroin administration: An apparent phenomenon associated with enhanced pain sensitivity. Neuroscience 89:631-636.

Le BD, Gozariu M, Cadden SW (2001) Animal models of nociception. [Review] [500 refs]. Pharmacological Reviews 53:597-652.

Ledeboer A, Liu T, Shumilla JA, Mahoney JH, Vijay S, Gross MI, Vargas J.A., Sultzbaugh L, Claypool MD, Sanftner LM, Watkins LR, Johnson KW (2006) The glial modulatory drug

AV411 attenuates mechanical allodynia in rat models of neuropathic pain. Neuron Glia Biology 2:279-291.

Ledeboer A, Sloane EM, Milligan ED, Frank MG, Mahony JH, Maier SF, Watkins LR (2005a) Minocycline attenuates mechanical allodynia and proinflammatory cytokine expression in rat models of pain facilitation. Pain 115:71-83.

Ledeboer A, Sloane EM, Milligan ED, Frank MG, Mahony JH, Maier SF, Watkins LR (2005b) Minocycline attenuates mechanical allodynia and proinflammatory cytokine expression in rat models of pain facilitation. Pain 115:71-83.

Lehnardt S, Lachance C, Patrizi S, Lefebvre S, Follett PL, Jensen FE, Rosenberg PA, Volpe JJ, Vartanian T (2002) The toll-like receptor TLR4 is necessary for lipopolysaccharide-induced oligodendrocyte injury in the CNS. Journal of Neuroscience 22:2478-2486.

Leon A, Buriani A, Dal TR, Fabris M, Romanello S, Aloe L (1994) Mast cells synthesize, store, and release nerve growth factor. Proceedings of the National Academy of Sciences of the United States of America 91:3739-3743.

Levine AS, Grace M, Billington CJ, Gosnell BA, Krahn DD, Brown DM, Morley JE (1988) Effect of morphine and nalmefene on energy balance in diabetic and non-diabetic rats. Pharmacol Biochem Behav 29:495-500.

Levine AS, Morley JE, Gosnell BA, Billington CJ, Bartness TJ (1985) Opioids and consummatory behavior. Brain Res Bull 14:663-672.

Lewis C, Neidhart S, Holy C, North RA, Buell G, Surprenant A (1995) Coexpression of P2X2 and P2X3 receptor subunits can account for ATP-gated currents in sensory neurons. Nature 377:432-435.

Li J, Wang G, Wang C, Zhao Y, Zhang H, Tan Z, Song Z, Ding M, Deng H (2007) MEK/ERK signaling contributes to the maintenance of human embryonic stem cell self-renewal. Differentiation 75:299-307.

Lie YS, Petropoulos CJ (1998) Advances in quantitative PCR technology: 5' nuclease assays. [Review] [13 refs]. Current Opinion in Biotechnology 9:43-48.

Lifschitz MD (1983) Renal effects of nonsteroidal anti-inflammatory agents. [Review] [53 refs]. Journal of Laboratory & Clinical Medicine 102:313-323.

Lindia JA, McGowan E, Jochnowitz N, Abbadie C (2005) Induction of CX3CL1 expression in astrocytes and CX3CR1 in microglia in the spinal cord of a rat model of neuropathic pain. Journal of Pain 6:434-438.

Ling GS, Spiegel K, Lockhart SH, Pasternak GW (1985) Separation of opioid analgesia from respiratory depression: evidence for different receptor mechanisms. Journal of Pharmacology & Experimental Therapeutics 232:149-155.

Lipp J (1991) Possible mechanisms of morphine analgesia. Clin Neuropharmacol 14:131-147.

Littleton J (2001) Receptor regulation as a unitary mechanism for drug tolerance and physical dependence--not quite as simple as it seemed!. [Review] [24 refs]. Addiction 96:87-101.

Liu AM, Lu G, Tsang KS, Li G, Wu Y, Huang ZS, Ng HK, Kung HF, Poon WS (2010) Umbilical cord-derived mesenchymal stem cells with forced expression of hepatocyte growth factor enhance remyelination and functional recovery in a rat intracerebral hemorrhage model. Neurosurgery 67:357-365.

Liu B, Du L, Kong LY, Hudson PM, Wilson BC, Chang RC, Abel HH, Hong JS (2000) Reduction by naloxone of lipopolysaccharide-induced neurotoxicity in mouse cortical neuron-glia co-cultures. Neuroscience 97:749-756.

Liu HT, Toychiev AH, Takahashi N, Sabirov RZ, Okada Y (2008) Maxi-anion channel as a candidate pathway for osmosensitive ATP release from mouse astrocytes in primary culture. Cell Research 18:558-565.

Liu J-G, Anand KJS (2001) Protein kinases modulate the cellular adaptations associated with opioid tolerance and dependence. Brain Research Reviews 38:1-19.

Liu W, Wang CH, Cui Y, Mo LQ, Zhi JL, Sun SN, Wang YL, Yu HM, Zhao CM, Feng JQ, Chen PX (2006) Inhibition of neuronal nitric oxide synthase antagonizes morphine antinociceptive tolerance by decreasing activation of p38 MAPK in the spinal microglia. Neurosci Lett 410:174-177.

Locovei S, Scemes E, Qiu F, Spray DC, Dahl G (2007) Pannexin1 is part of the pore forming unit of the P2X(7) receptor death complex. FEBS Letters 581:483-488.

Ma L, Pei G (2007) Beta-arrestin signaling and regulation of transcription. [Review] [42 refs]. Journal of Cell Science 120:213-218.

MacKenzie A, Wilson HL, Kiss-Toth E, Dower SK, North RA, Surprenant A (2001) Rapid secretion of interleukin-1beta by microvesicle shedding. Immunity 15:825-835.

Mahajan SD, Schwartz SA, Shanahan TC, Chawda RP, Nair MPN (2002) Morphine regulates gene expression of alpha- and beta-chemokines and their receptors on astroglial cells via the opioid mu receptor. Journal of Immunology 169:3589-3599.

Maier SF, Watkins LR (2003) Immune-to-central nervous system communication and its role in modulating pain and cognition: Implications for cancer and cancer treatment. Brain Behav Immun 17 Suppl 1:S125-S131.

Maier SF, Wiertelak EP, Martin D, Watkins LR (1993) Interleukin-1 mediates the behavioral hyperalgesia produced by lithium chloride and endotoxin. Brain Research 623:321-324.

Malan TP, Ossipov MH, Gardell LR, Ibrahim M, Bian D, Lai J, Porreca F (2000) Extraterritorial neuropathic pain correlates with multisegmental elevation of spinal dynorphin in nerve-injured rats. Pain 86:185-194.

Mao J, Mayer DJ (2001) Spinal cord neuroplasticity following repeated opioid exposure and its relation to pathological pain. [Review] [44 refs]. Annals of the New York Academy of Sciences 933:175-184.

Mao J, Price DD, Mayer DJ (1994) Thermal hyperalgesia in association with the development of morphine tolerance in rats: Roles of excitatory amino acid receptors and protein kinase C. Journal of Neuroscience 14:2301-2312.

Mao J, Price DD, Mayer DJ (1995a) Mechanisms of hyperalgesia and morphine tolerance: A current view of their possible interactions. Pain 62:259-274.

Mao J, Price DD, Phillips LL, Lu J, Mayer DJ (1995b) Increases in protein kinase C gamma immunoreactivity in the spinal cord of rats associated with tolerance to the analgesic effects of morphine. Brain Research 677:257-267.

Mao J, Sung B, Ji R-R, Lim G (2002) Chronic morphine induces downregulation of spinal glutamate transporters: Implications in morphine tolerance and abnormal pain sensitivity. Journal of Neuroscience 22:8312-8323.

Marchand F, Alloui A, Pelissier T, Hernandez A, Authier N, Alvarez P, Eschalier A, Ardid D (2003) Evidence for an antihyperalgesic effect of venlafaxine in vincristine-induced neuropathy in rat. Brain Research 980:117-120.

Marker CL, Lujan R, Loh HH, Wickman K (2005) Spinal G-protein-gated potassium channels contribute in a dose-dependent manner to the analgesic effect of mu- and delta- but not kappa-opioids. Journal of Neuroscience 25:3551-3559.

Marriott I (2004) The role of tachykinins in central nervous system inflammatory responses. Front Biosci 9:2153-2165.

Martinez-Francois JR, Morales-Tlalpan V, Vaca L (2002) Characterization of the maitotoxin-activated cationic current from human skin fibroblasts. Journal of Physiology 538:79-86.

Marvizon JC, Ma Y-Y, Charles AC, Walwyn W, Evans CJ (2010) Pharmacology of the opioid system. Pharmacology of pain textbook. pp 87-110.

Matthews EA, Dickenson AH (2002) A combination of gabapentin and morphine mediates enhanced inhibitory effects on dorsal horn neuronal responses in a rat model of neuropathy. Anesthesiology 96:633-640.

Matute C, Torre I, Perez-Cerda F, Perez-Samartin A, Alberdi E, Etxebarria E, Arranz AM, Ravid R, Rodriguez-Antiguedad A, Sanchez-Gomez M, Domercq M (2007) P2X(7) receptor blockade prevents ATP excitotoxicity in oligodendrocytes and ameliorates experimental autoimmune encephalomyelitis. Journal of Neuroscience 27:9525-9533.

Mayer DJ, Mao J, Holt J, Price DD (1999) Cellular mechanisms of neuropathic pain, morphine tolerance, and their interactions. [Review] [47 refs]. Proceedings of the National Academy of Sciences of the United States of America 96:7731-7736.

Mayer DJ, Mao J, Price DD (1995) The association of neuropathic pain, morphine tolerance and dependence, and the translocation of protein kinase C. [Review] [111 refs]. NIDA Research Monograph 147:269-298.

Mayer DJ, Price DD (1976) Central nervous system mechanisms of analgesia. [Review] [128 refs]. Pain 2:379-404.

McCleane G, Smith HS (2007) Opioids for persistent noncancer pain. [Review] [73 refs]. Medical Clinics of North America 91:177-197.

McCleane GJ, Suzuki R, Dickenson AH (2003) Does a single intravenous injection of the 5HT3 receptor antagonist ondansetron have an analgesic effect in neuropathic pain? A double-blinded, placebo-controlled cross-over study. Anesthesia & Analgesia 97:1474-1478.

McGaraughty S, Chu KL, Namovic MT, Donnelly-Roberts DL, Harris RR, Zhang XF, Shieh CC, Wismer CT, Zhu CZ, Gauvin DM, Fabiyi AC, Honore P, Gregg RJ, Kort ME, Nelson DW, Carroll WA, Marsh K, Faltynek CR, Jarvis MF (2007) P2X7-related modulation of pathological nociception in rats. Neuroscience 146:1817-1828.

McGaraughty S, Jarvis MF (2005) Antinociceptive properties of a non-nucleotide P2X3/P2X2/3 receptor antagonist. [Review] [61 refs]. Drug News & Perspectives 18:501-507.

McLarnon JG, Ryu JK, Walker DG, Choi HB (2006) Upregulated expression of purinergic P2X(7) receptor in Alzheimer disease and amyloid-beta peptide-treated microglia and in peptide-injected rat hippocampus. Journal of Neuropathology & Experimental Neurology 65:1090-1097.

McLaughlin JP, Myers LC, Zarek PE, Caron MG, Lefkowitz RJ, Czyzyk T.A., Pintar JE, Chavkin C (2004) Prolonged Kappa Opioid Receptor Phosphorylation Mediated by G-protein Receptor Kinase Underlies Sustained Analgesic Tolerance. Journal of Biological Chemistry 279:1810-1818.

McMahon SB, Bennet DLH, Bevan S (2006) New Pain Treatments in Late Development. Wall and Malzack's textbook of pain. pp 49-72.

McNally GP (1999) Pain facilitatory circuits in the mammalian central nervous system: their behavioral significance and role in morphine analgesic tolerance. [Review] [264 refs]. Neuroscience & Biobehavioral Reviews 23:1059-1078.

McQuay HJ (2002) Neuropathic pain: evidence matters. [Review] [30 refs]. European Journal of Pain: Ejp 6 Suppl A:11-18.

Medhurst AD, et al. (2007) Structurally novel histamine H3 receptor antagonists GSK207040 and GSK334429 improve scopolamine-induced memory impairment and capsaicin-induced secondary allodynia in rats. Biochem Pharmacol 73:1182-1194.

Medhurst AD, Harrison DC, Read SJ, Campbell CA, Robbins MJ, Pangalos MN (2000) The use of TaqMan RT-PCR assays for semiquantitative analysis of gene expression in CNS tissues and disease models. Journal of Neuroscience Methods 98:9-20.

Medhurst SJ, Collins SD, Billinton A, Bingham S, Dalziel RG, Brass A, Roberts JC, Medhurst AD, Chessell IP (2008) Novel histamine H3 receptor antagonists GSK189254 and GSK334429 are efficacious in surgically-induced and virally-induced rat models of neuropathic pain. Pain 138:61-69.

Medhurst SJ, Walker K, Bowes M, Kidd BL, Glatt M, Muller M, Hattenberger M, Vaxelaire J, O'Reilly T, Wotherspoon G, Winter J, Green J, Urban L (2002) A rat model of bone cancer pain. Pain 96:129-140.

Meert TF, Vermeirsch HA (2005) A preclinical comparison between different opioids: antinociceptive versus adverse effects. Pharmacol Biochem Behav 80:309-326.

Meller ST, Dykstra C, Grzybycki D, Murphy S, Gebhart GF (1994) The possible role of glia in nociceptive processing and hyperalgesia in the spinal cord of the rat. Neuropharmacology 33:1471-1478.

Merville-Louis MP, Sadzot-Delvaux C, Delree P, Piette J, Moonen G, Rentier B (1989) Varicella-zoster virus infection of adult rat sensory neurons in vitro. J Virol 63:3155-3160.

Michel AD, Chessell IP, Humphrey PP (1999) Ionic effects on human recombinant P2X7 receptor function. Naunyn-Schmiedebergs Archives of Pharmacology 359:102-109.

Michel AD, Clay WC, Ng SW, Roman S, Thompson K, Condreay JP, Hall M, Livermore D, Senger S (2008) Identification of regions of the P2X7 receptor that contribute to human and rat species differences in antagonist effects. British Journal of Pharmacology 155:738-751.

Michel AD, Xing M, Thompson KM, Jones CA, Humphrey PP (2006) Decavanadate, a P2X receptor antagonist, and its use to study ligand interactions with P2X7 receptors. European Journal of Pharmacology 534:19-29.

Mico JA, Ardid D, Berrocoso E, Eschalier A (2006) Antidepressants and pain. [Review] [73 refs]. Trends in Pharmacological Sciences 27:348-354.

Mika J (2008) Modulation of microglia can attenuate neuropathic pain symptoms and enhance morphine effectiveness. Pharmacological Reports 60:297-307.

Mika J, Osikowicz M, Makuch W, Przewlocka B (2007) Minocycline and pentoxifylline attenuate allodynia and hyperalgesia and potentiate the effects of morphine in rat and mouse models of neuropathic pain. European Journal of Pharmacology 560:142-149.

Mika J, Osikowicz M, Rojewska E, Korostynski M, Wawrzczak-Bargiela A, Przewlocki R, Przewlocka B (2009a) Differential activation of spinal microglial and astroglial cells in a mouse model of peripheral neuropathic pain. European Journal of Pharmacology 623:65-72.

Mika J, Wawrzczak-Bargiela A, Osikowicz M, Makuch W, Przewlocka B (2009b) Attenuation of morphine tolerance by minocycline and pentoxifylline in naive and neuropathic mice. Brain, Behavior, & Immunity 23:75-84.

Millan MJ (1999) The induction of pain: an integrative review. [Review] [1895 refs]. Progress in Neurobiology 57:1-164.

Millan MJ (2002) Descending control of pain. Progress in Neurobiology 66:355-474.

Miller G (2005) Neuroscience. The dark side of glia. Science 308:778-781.

Milligan ED, Maier SF, Watkins LR (2003a) Review: Neuronal-glial interactions in central sensitization. Seminars in Pain Medicine 1:171-183.

Milligan ED, Mehmert KK, Hinde JL, Harvey LO, Martin D, Tracey KJ, Maier SF, Watkins LR (2000) Thermal hyperalgesia and mechanical allodynia produced by intrathecal administration of the human immunodeficiency virus-1 (HIV-1) envelope glycoprotein, gp120. Brain Research 861:105-116.

Milligan ED, O'Connor KA, Nguyen KT, Armstrong CB, Twining C, Gaykema R.P.A., Holguin A, Martin D, Maier SF, Watkins LR (2001) Intrathecal HIV-1 envelope glycoprotein gp120 induces enhanced pain states mediated by spinal cord proinflammatory cytokines. Journal of Neuroscience 21:2808-2819.

Milligan ED, Sloane EM, Watkins LR (2008) Glia in pathological pain: a role for fractalkine. [Review] [94 refs]. Journal of Neuroimmunology 198:113-120.

Milligan ED, Twining C, Chacur M, Biedenkapp J, O'Connor K, Poole S, Martin D, Maier SF, Watkins LR (2003b) Spinal glia and proinflammatory cytokines mediate mirror-image neuropathic pain in rats. Journal of Neuroscience 23:1026-1040.

Min KJ, Pyo HK, Yang MS, Ji KA, Jou I, Joe EH (2004) Gangliosides activate microglia via protein kinase C and NADPH oxidase. GLIA 48:197-206.

Mingam R, De S, V, Amedee T, Bluthe RM, Kelley KW, Dantzer R, Laye S (2008) In vitro and in vivo evidence for a role of the P2X7 receptor in the release of IL-1 beta in the murine brain. Brain, Behavior, & Immunity 22:234-244.

Moffat JF, Zerboni L, Kinchington PR, Grose C, Kaneshima H, Arvin AM (1998) Attenuation of the vaccine Oka strain of varicella-zoster virus and role of glycoprotein C in alphaherpesvirus virulence demonstrated in the SCID-hu mouse. J Virol 72:965-974.

Mogil JS (2009) Animal models of pain: progress and challenges. Nat Rev Neurosci 10:283-294.

Molander C, Grant G (1995) The Nervous System. The Nervous System, 2nd Edition, Academic Press, San Diego.

Morgan MM, Tierney BW, Ingram SL (2005) Intermittent dosing prolongs tolerance to the antinociceptive effect of morphine microinjection into the periaqueductal gray. Brain Research 1059:173-178.

Morioka N, Abdin M, Kitayama T, Morita K, Nakata Y, Dohi T (2008) P2X7 receptor stimulation in primary cultures of rat spinal microglia induces downregulation of the activity for glutamate transport. GLIA 56:528-538.

Murray M, Wang SD, Goldberger ME, Levitt P (1990) Modification of astrocytes in the spinal cord following dorsal root or peripheral nerve lesions. Experimental Neurology 110:248-257.

Murray RB, Adler MW, Korczyn AD (1983) The pupillary effects of opioids. [Review] [84 refs]. Life Sciences 33:495-509.

Nader K, Bechara A, van der KD (1996) Lesions of the lateral parabrachial nucleus block the aversive motivational effects of both morphine and morphine withdrawal but spare morphine's discriminative properties. Behav Neurosci 110:1496-1502.

Nakazato-Imasato E, Kurebayashi Y (2009) Pharmacological characteristics of the hind paw weight bearing difference induced by chronic constriction injury of the sciatic nerve in rats. Life Sciences 84:622-626.

Narcisse L, Scemes E, Zhao Y, Lee SC, Brosnan CF (2005) The cytokine IL-1beta transiently enhances P2X7 receptor expression and function in human astrocytes. GLIA 49:245-258.

Narita M, Yoshida T, Nakajima M, Narita M, Miyatake M, Takagi T, Yajima Y, Suzuki T (2006) Direct evidence for spinal cord microglia in the development of a neuropathic pain-like state in mice. Journal of Neurochemistry 97:1337-1348.

Nasu-Tada K, Koizumi S, Tsuda M, Kunifusa E, Inoue K (2006) Possible involvement of increase in spinal fibronectin following peripheral nerve injury in upregulation of microglial P2X4, a key molecule for mechanical allodynia. GLIA 53:769-775.

Nelson DW, Gregg RJ, Kort ME, Perez-Medrano A, Voight EA, Wang Y, Grayson G, Namovic MT, Donnelly-Roberts DL, Niforatos W, Honore P, Jarvis MF, Faltynek CR, Carroll WA (2006) Structure-activity relationship studies on a series of novel, substituted 1-benzyl-5-phenyltetrazole P2X7 antagonists. Journal of Medicinal Chemistry 49:3659-3666.

Nelson DW, Sarris K, Kalvin DM, Namovic MT, Grayson G, Donnelly-Roberts DL, Harris R, Honore P, Jarvis MF, Faltynek CR, Carroll WA (2008) Structure-activity relationship studies on N'-aryl carbohydrazide P2X7 antagonists. Journal of Medicinal Chemistry 51:3030-3034.

Neumann S, Doubell TP, Leslie T, Woolf CJ (1996) Inflammatory pain hypersensitivity mediated by phenotypic switch in myelinated primary sensory neurons. Nature 384:360-364.

Nichols ML, Allen BJ, Rogers SD, Ghilardi JR, Honore P, Luger NM, Finke MP, Li J, Lappi DA, Simone DA, Mantyh PW (1999) Transmission of chronic nociception by spinal neurons expressing the substance P receptor. Science 286:1558-1561.

Nichols ML, Bian D, Ossipov MH, Lai J, Porreca F (1995) Regulation of morphine antiallodynic efficacy by cholecystokinin in a model of neuropathic pain in rats. Journal of Pharmacology and Experimental Therapeutics 275:1339-1345.

North RA (2002) Molecular physiology of P2X receptors. Physiological Reviews 82:1013-1067.

North RA, Surprenant A (2000) Pharmacology of cloned P2X receptors. [Review] [89 refs]. Annual Review of Pharmacology & Toxicology 40:563-580.

Novakovic SD, Kassotakis LC, Oglesby IB, Smith JAM, Eglen RM, Ford A.P.D.W., Hunter JC (1999) Immunocytochemical localization of P(2X3) purinoceptors in sensory neurons in naive rats and following neuropathic injury. Pain 80:273-282.

Nozaki-Taguchi N, Yaksh TL (1998) A novel model of primary and secondary hyperalgesia after mild thermal injury in the rat. Neuroscience Letters 254:25-28.

Nurmikko T (1995) Clinical features and pathophysiologic mechanisms of postherpetic neuralgia. Neurology 45:S54-S55.

Oatway MA, Chen Y, Weaver LC (2004) The 5-HT3 receptor facilitates at-level mechanical allodynia following spinal cord injury. Pain 110:259-268.

Ohgo S, Nakatsuru K, Ishikawa E, Matsukura S (1992) Stimulation of cholecystokinin (CCK) release from superfused rat hypothalamo-neurohypophyseal complexes by interleukin-1 (IL-1). Brain Research 593:25-31.

Okada M, Nakagawa T, Minami M, Satoh M (2002) Analgesic effects of intrathecal administration of P2Y nucleotide receptor agonists UTP and UDP in normal and neuropathic pain model rats. Journal of Pharmacology & Experimental Therapeutics 303:66-73.

Ono K, Han J (2000) The p38 signal transduction pathway: activation and function. [Review] [185 refs]. Cellular Signalling 12:1-13.

Ossipov MH, Kovelowski CJ, Vanderah T, Porreca F (1994) Naltrindole, an opioid delta antagonist, blocks the enhancement of morphine-antinociception induced by a CCKB antagonist in the rat. Neuroscience Letters 181:9-12.

Ossipov MH, Lai J, King T, Vanderah TW, Malan TP, Jr., Hruby VJ, Porreca F (2004) Antinociceptive and nociceptive actions of opioids. [Review] [250 refs]. Journal of Neurobiology 61:126-148.

Ossipov MH, Lai J, Vanderah TW, Porreca F (2003) Induction of pain facilitation by sustained opioid exposure: relationship to opioid antinociceptive tolerance. [Review] [156 refs]. Life Sciences 73:783-800.

Owens T, Babcock AA, Millward JM, Toft-Hansen H (2005) Cytokine and chemokine inter-regulation in the inflamed or injured CNS. [Review] [39 refs]. Brain Research - Brain Research Reviews 48:178-184.

Ozawa T, Nakagawa T, Shige K, Minami M, Satoh M (2001) Changes in the expression of glial glutamate transporters in the rat brain accompanied with morphine dependence and naloxone-precipitated withdrawal. Brain Research 905:254-258.

Panchin Y, Kelmanson I, Matz M, Lukyanov K, Usman N, Lukyanov S (2000) A ubiquitous family of putative gap junction molecules. Current Biology 10:R473-R474.

Panchin YV (2005) Evolution of gap junction proteins--the pannexin alternative. [Review] [54 refs]. Journal of Experimental Biology 208:1415-1419.

Panenka W, Jijon H, Herx LM, Armstrong JN, Feighan D, Wei T, Yong VW, Ransohoff RM, MacVicar BA (2001) P2X7-like receptor activation in astrocytes increases chemokine monocyte chemoattractant protein-1 expression via mitogen-activated protein kinase. Journal of Neuroscience 21:7135-7142.

Papp L, Vizi ES, gh B (2004) Lack of ATP-evoked GABA and glutamate release in the hippocampus of P2X7 receptor-/- mice. NeuroReport 15:2387-2391.

Parkitna JR, Obara I, Wawrzczak-Bargiela A, Makuch W, Przewlocka B, Przewlocki R (2006) Effects of glycogen synthase kinase 3beta and cyclin-dependent kinase 5 inhibitors on morphine-induced analgesia and tolerance in rats. Journal of Pharmacology & Experimental Therapeutics 319:832-839.

Parvathenani LK, Tertyshnikova S, Greco CR, Roberts SB, Robertson B, Posmantur R (2003) P2X7 mediates superoxide production in primary microglia and is up-regulated in a transgenic mouse model of Alzheimer's disease. Journal of Biological Chemistry 278:13309-13317.

Pelegrin P, Surprenant A (2006) Pannexin-1 mediates large pore formation and interleukin-1beta release by the ATP-gated P2X7 receptor. EMBO Journal 25:5071-5082.

Pelissier T, Laurido C, Kramer V, ndez A, Paeile C (2003) Antinociceptive interactions of ketamine with morphine or methadone in mononeuropathic rats. European Journal of Pharmacology 477:23-28.

Perez-Medrano A, Donnelly-Roberts DL, Honore P, Hsieh GC, Namovic MT, Peddi S, Shuai Q, Wang Y, Faltynek CR, Jarvis MF, Carroll WA (2009) Discovery and biological evaluation of novel cyanoguanidine P2X(7) antagonists with analgesic activity in a rat model of neuropathic pain. J Med Chem 52:3366-3376.

Pernia A, Mico JA, Calderon E, Torres LM (2000) Venlafaxine for the treatment of neuropathic pain. J Pain Symptom Manage 19:408-410.

Perregaux D, Gabel CA (1994) Interleukin-1 beta maturation and release in response to ATP and nigericin. Evidence that potassium depletion mediated by these agents is a necessary and common feature of their activity. Journal of Biological Chemistry 269:15195-15203.

Persson M, Brantefjord M, Hansson E, Ronnback L (2005) Lipopolysaccharide increases microglial GLT-1 expression and glutamate uptake capacity in vitro by a mechanism dependent on TNF-alpha. GLIA 51:111-120.

Peters A (1964) Further observations on the structure of myelin sheaths in the central nervous system. Journal of Cell Biology 20:281-296.

Piao ZG, Cho IH, Park CK, Hong JP, Choi SY, Lee SJ, Lee S, Park K, Kim JS, Oh SB (2006) Activation of glia and microglial p38 MAPK in medullary dorsal horn contributes to tactile hypersensitivity following trigeminal sensory nerve injury. Pain 121:219-231.

Pitcher JA, Freedman NJ, Lefkowitz RJ (1998) G protein-coupled receptor kinases. [Review] [255 refs]. Annual Review of Biochemistry 67:653-692.

Porreca F, Mosberg HI, Omnaas JR, Burks TF, Cowan A (1987) Supraspinal and spinal potency of selective opioid agonists in the mouse writhing test. J Pharmacol Exp Ther 240:890-894.

Porreca F, Ossipov MH, Gebhart GF (2002) Chronic pain and medullary descending facilitation. [Review] [76 refs]. Trends in Neurosciences 25:319-325.

Porreca F, Tang QB, Bian D, Riedl M, Elde R, Lai J (1998) Spinal opioid mu receptor expression in lumbar spinal cord of rats following nerve injury. Brain Research 795:197-203.

Powell KJ, Hosokawa A, Bell A, Sutak M, Milne B, Quirion R, Jhamandas K (1999) Comparative effects of cyclo-oxygenase and nitric oxide synthase inhibition on the development and reversal of spinal opioid tolerance. British Journal of Pharmacology 127:631-644.

Powell KJ, Ma W, Sutak M, Doods H, Quirion R, Jhamandas K (2000) Blockade and reversal of spinal morphine tolerance by peptide and non-peptide calcitonin gene-related peptide receptor antagonists. British Journal of Pharmacology 131:875-884.

Pradhan AA, Yu XH, Laird JM (2010) Modality of hyperalgesia tested, not type of nerve damage, predicts pharmacological sensitivity in rat models of neuropathic pain. Eur J Pain 14:503-509.

Priller J, Haas CA, Reddington M, Kreutzberg GW (1995) Calcitonin gene-related peptide and ATP induce immediate early gene expression in cultured rat microglial cells. GLIA 15:447-457.

Przewlocki R, Przewlocka B (2001) Opioids in chronic pain. [Review] [150 refs]. European Journal of Pharmacology 429:79-91.

Przewlocki R, Przewlocka B (2005) Opioids in neuropathic pain. [Review] [222 refs]. Current Pharmaceutical Design 11:3013-3025.

Rady JJ, Fujimoto JM (2001) Confluence of antianalgesic action of diverse agents through brain interleukin-1beta in mice. Journal of Pharmacology and Experimental Therapeutics 299:659-665.

Raffa RB, Mathiasen JR, Kimball ES, Vaught JL (1993) The combined immunological and antinociceptive defects of beige-J mice: The possible existence of a 'mu-repressin'. Life Sciences 52:1-8.

Raghavendra V, Rutkowski MD, Deleo JA (2002) The role of spinal neuroimmune activation in morphine tolerance/hyperalgesia in neuropathic and sham-operated rats. J Neurosci 22:9980-9989.

Raghavendra V, Tanga F, Deleo JA (2003a) Inhibition of microglial activation attenuates the development but not existing hypersensitivity in a rat model of neuropathy. Journal of Pharmacology and Experimental Therapeutics 306:624-630.

Raghavendra V, Tanga F, Rutkowski MD, Deleo JA (2003b) Anti-hyperalgesic and morphine-sparing actions of propentofylline following peripheral nerve injury in rats: Mechanistic implications of spinal glia and proinflammatory cytokines. Pain 104:655-664.

Raghavendra V, Tanga FY, Deleo JA (2004a) Attenuation of morphine tolerance, withdrawal-induced hyperalgesia, and associated spinal inflammatory immune responses by propentofylline in rats. Neuropsychopharmacology 29:327-334.

Raghavendra V, Tanga FY, Deleo JA (2004b) Complete Freunds adjuvant-induced peripheral inflammation evokes glial activation and proinflammatory cytokine expression in the CNS. European Journal of Neuroscience 20:467-473.

Ragnauth A, Moroz M, Bodnar RJ (2000) Multiple opioid receptors mediate feeding elicited by mu and delta opioid receptor subtype agonists in the nucleus accumbens shell in rats. Brain Res 876:76-87.

Raivich G (2005) Like cops on the beat: the active role of resting microglia. Trends Neurosci 28:571-573.

Rappold PM, Lynd-Balta E, Joseph SA (2006) P2X7 receptor immunoreactive profile confined to resting and activated microglia in the epileptic brain. Brain Research 1089:171-178.

Rassendren F, Buell GN, Virginio C, Collo G, North RA, Surprenant A (1997) The permeabilizing ATP receptor, P2X7. Cloning and expression of a human cDNA. Journal of Biological Chemistry 272:5482-5486.

Read R, Savelieva K, Baker K, Hansen G, Vogel P (2010) Histopathological and Neurological Features of Atg4b Knockout Mice. Vet PatholEpub ahead of print.

Reichling DB, Levine JD (1999) The primary afferent nociceptor as pattern generator. [Review] [99 refs]. Pain Suppl 6:S103-S109.

Rexed B (1952) The cytoarchitectonic organization of the spinal cord in the cat. Journal of Comparative Neurology 96:414-495.

Reynolds DV (1969) Surgery in the rat during electrical analgesia induced by focal brain stimulation. Science 164:444-445.

Rhee JS, Wang ZM, Nabekura J, Inoue K, Akaike N (2000) ATP facilitates spontaneous glycinergic IPSC frequency at dissociated rat dorsal horn interneuron synapses. Journal of Physiology 524:471-483.

Rincon M, Flavell RA, Davis RA (2000) The JNK and p38 MAP kinase signaling pathways in T cell-mediated immune responses. Free Radical Biology and Medicine 28:1328-1337.

Rivera M, Gintzler AR (1998) Differential effect of chronic morphine on mRNA encoding adenylyl cyclase isoforms: Relevance to physiological sequela of tolerance/dependence. Molecular Brain Research 54:165-169.

Romagnoli R, Baraldi PG, Cruz-Lopez O, Lopez-Cara C, Preti D, Borea PA, Gessi S (2008) The P2X7 receptor as a therapeutic target. [Review] [80 refs]. Expert Opinion on Therapeutic Targets 12:647-661.

Ronnback L, Hansson E (1988) Modulation of astrocyte activity. One way to reinforce morphine effects? Cellular and Molecular Biology 34:337-349.

Rosenblum A, Marsch LA, Joseph H, Portenoy RK (2008) Opioids and the Treatment of Chronic Pain: Controversies, Current Status, and Future Directions. Experimental and Clinical Psychopharmacology 16:405-416.

Rothman RB, Long JB, Bykov V, Xu H, Jacobson AE, Rice KC, Holaday J.W. (1991) Upregulation of the opioid receptor complex by the chronic administration of morphine: A biochemical marker related to the development of tolerance and dependence. Peptides 12:151-160.

Rowbotham M, Harden N, Stacey B, Bernstein P, Magnus-Miller L (1998) Gabapentin for the treatment of postherpetic neuralgia: a randomized controlled trial. JAMA 280:1837-1842.

Rowbotham MC, Fields HL (1996) The relationship of pain, allodynia and thermal sensation in post-herpetic neuralgia. Brain 119 (Pt 2):347-354.

Ruan HZ, Burnstock G (2005) The distribution of P2X5 purinergic receptors in the enteric nervous system of mouse. Cell and tissue research 319:191-200.

Rustay NR, Wahlsten D, Crabbe JC (2003) Influence of task parameters on rotarod performance and sensitivity to ethanol in mice. Behav Brain Res 141:237-249.

Sabatowski R, Galvez R, Cherry DA, Jacquot F, Vincent E, Maisonobe P, Versavel M (2004) Pregabalin reduces pain and improves sleep and mood disturbances in patients with post-herpetic neuralgia: results of a randomised, placebo-controlled clinical trial. Pain 109:26-35.

Sadzot-Delvaux C, Debrus S, Nikkels A, Piette J, Rentier B (1995) Varicella-zoster virus latency in the adult rat is a useful model for human latent infection. Neurology 45:S18-S20.

Sadzot-Delvaux C, Merville-Louis MP, Delree P, Marc P, Piette J, Moonen G, Rentier B (1990) An in vivo model of varicella-zoster virus latent infection of dorsal root ganglia. J Neurosci Res 26:83-89.

Safieh-Garabedian B, Poole S, Allchorne A, Winter J, Woolf CJ (1995) Contribution of interleukin-1beta to the inflammation-induced increase in nerve growth factor levels and inflammatory hyperalgesia. British Journal of Pharmacology 115:1265-1275.

Sagen J, Proudfit HK (1987) Release of endogenous monoamines into spinal cord superfusates following the microinjection of phentolamine into the nucleus raphe magnus. Brain Research 406:246-254.

Samad TA, Moore KA, Sapirstein A, Billet S, Allchorne A, Poole S, Bonventre JV, Woolf CJ (2001) Interleukin-1beta-mediated induction of Cox-2 in the CNS contributes to inflammatory pain hypersensitivity. Nature 410:471-475.

Sasaki A, Nakashima Y, Takasaki I, Andoh T, Shiraki K, Kuraishi Y (2007) Effects of loperamide on mechanical allodynia induced by herpes simplex virus type-1 in mice. Journal of Pharmacological Sciences 104:218-224.

Sato H, Pesnicak L, Cohen JI (2003) Varicella-zoster virus ORF47 protein kinase, which is required for replication in human T cells, and ORF66 protein kinase, which is expressed during latency, are dispensable for establishment of latency. J Virol 77:11180-11185.

Sawynok J, Downie JW, Reid AR, Cahill CM, White TD (1993) ATP release from dorsal spinal cord synaptosomes: characterization and neuronal origin. Brain Research 610:32-38.

Schachtele SJ, Hu S, Little MR, Lokensgard JR (2010) Herpes simplex virus induces neural oxidative damage via microglial cell Toll-like receptor-2. J Neuroinflammation 7:35.

Schaible H-G, Schmidt RF (1988) Time course of mechanosensitivity changes in articular afferents during a developing experimental arthritis. Journal of Neurophysiology 60:2180-2195.

Scholz J, Abele A, Marian C, Haussler A, Herbert TA, Woolf CJ, Tegeder I. (2008) Low-dose methotrexate reduces peripheral nerve injury-evoked spinal microglial activation and neuropathic pain behavior in rats. Pain 138:130-142.

Schultz JJ, Hsu AK, Gross GJ (1997) Ischemic preconditioning and morphine-induced cardioprotection involve the delta (delta)-opioid receptor in the intact rat heart. Journal of Molecular & Cellular Cardiology 29:2187-2195.

Schwei MJ, Honore P, Rogers SD, Salak-Johnson JL, Finke MP, Ramnaraine ML, Clohisy DR, Mantyh PW (1999) Neurochemical and cellular reorganization of the spinal cord in a murine model of bone cancer pain. Journal of Neuroscience 19:10886-10897.

Seltzer Z, Dubner R, Shir Y (1990) A novel behavioral model of neuropathic pain disorders produced in rats by partial sciatic nerve injury. Pain 43:205-218.

Shan S, Hong C, Mei H, Ting-Ting L, Hai-Li P, Zhi-Qi Z, Yu-Qiu Z (2007) New evidence for the involvement of spinal fractalkine receptor in pain facilitation and spinal glial activation in rat model of monoarthritis. Pain 129:64-75.

Shavit Y, Wolf G, Goshen I, Livshits D, Yirmiya R (2005) Interleukin-1 antagonizes morphine analgesia and underlies morphine tolerance. Pain 115:50-59.

Shimomura Y, Oku J, Glick Z, Bray GA (1982) Opiate receptors, food intake and obesity. Physiol Behav 28:441-445.

Sim JA, Young MT, Sung HY, North RA, Surprenant A (2004) Reanalysis of P2X7 receptor expression in rodent brain. J Neurosci 24:6307-6314.

Skingle M, Birch PJ, Leighton GE, Humphrey PP (1990) Lack of antinociceptive activity of sumatriptan in rodents. Cephalalgia 10:207-212.

Smart ML, Gu B, Panchal RG, Wiley J, Cromer B, Williams DA, Petrou S (2003) P2X7 receptor cell surface expression and cytolytic pore formation are regulated by a distal C-terminal region. Journal of Biological Chemistry 278:8853-8860.

Snyder SH, Kim S (2004) No glial death with NO. Nature Cell Biology 6:17-18.

Solle M, Labasi J, Perregaux DG, Stam E, Petrushova N, Koller BH, Griffiths RJ, Gabel CA (2001) Altered cytokine production in mice lacking P2X(7) receptors. Journal of Biological Chemistry 276:125-132.

Soltys Z, Ziaja M, Pawlinski R, Setkowicz Z, Janeczko K (2001) Morphology of reactive microglia in the injured cerebral cortex. Fractal analysis and complementary quantitative methods. Journal of Neuroscience Research 63:90-97.

Sommer C, Petrausch S, Lindenlaub T, Toyka KV (1999) Neutralizing antibodies to interleukin 1-receptor reduce pain associated behavior in mice with experimental neuropathy. Neuroscience Letters 270:25-28.

Song P, Zhao ZQ (2001) The involvement of glial cells in the development of morphine tolerance. Neurosci Res 39:281-286.

Sperlagh B, Vizi ES, Wirkner K, Illes P (2006) P2X7 receptors in the nervous system. Progress in Neurobiology 78:327-346.

Spetea M, Bohotin CR, Asim MF, Stubegger K, Schmidhammer H (2010) In vitro and in vivo pharmacological profile of the 5-benzyl analogue of 14-methoxymetopon, a novel mu opioid analgesic with reduced propensity to alter motor function. Eur J Pharm Sci 41:125-135.

Speth C, Dierich MP, Gasque P (2002) Neuroinvasion by pathogens: a key role of the complement system. [Review] [87 refs]. Molecular Immunology 38:669-679.

Srivastava RK, Gombar KK, Kaur AH, Khosla P (1995) Attenuation of morphine-induced antinociception by L-glutamic acid at the spinal site in rats. Canadian Journal of Anaesthesia 42:541-546.

Stanfa LC, Dickenson AH (1993) Cholecystokinin as a factor in the enhanced potency of spinal morphine following carrageenin inflammation. British Journal of Pharmacology 108:967-973.

Stefano GB, Salzet M, Hughes TK, Bilfinger TV (1998) Delta2 opioid receptor subtype on human vascular endothelium uncouples morphine stimulated nitric oxide release. International Journal of Cardiology 64 Suppl 1:S43-S51.

Sternini C, Spann M, Anton B, Keith J, D.E., Bunnett NW, von ZM, Brecha NC (1996) Agonist-selective endocytosis of mu opioid receptor by neurons in vivo. Proceedings of the National Academy of Sciences of the United States of America 93:9241-9246.

Stokes L, Jiang LH, Alcaraz L, Bent J, Bowers K, Fagura M, Furber M, Mortimore M, Lawson M, Theaker J, Laurent C, Braddock M, Surprenant A (2006) Characterization of a selective and potent antagonist of human P2X(7) receptors, AZ11645373. British Journal of Pharmacology 149:880-887.

Stoll G, Jander S (1999) The role of microglia and macrophages in the pathophysiology of the CNS. [Review] [187 refs]. Progress in Neurobiology 58:233-247.

Suadicani SO, Brosnan CF, Scemes E (2006) P2X7 receptors mediate ATP release and amplification of astrocytic intercellular Ca2+ signaling. Journal of Neuroscience 26:1378-1385.

Sudakov SK, Trigub MM (2008) Hypothesis on reciprocal interactions between the central and peripheral components of the endogenous opioid system. Bulletin of Experimental Biology and Medicine 146:663-666.

Suh BC, Kim JS, Namgung U, Ha H, Kim KT (2001) P2X7 nucleotide receptor mediation of membrane pore formation and superoxide generation in human promyelocytes and neutrophils. Journal of Immunology 166:6754-6763.

Sumpton JE, Moulin DE (2001) Treatment of neuropathic pain with venlafaxine. Ann Pharmacother 35:557-559.

Sung B, Lim G, Mao J (2003) Altered expression and uptake activity of spinal glutamate transporters after nerve injury contribute to the pathogenesis of neuropathic pain in rats. Journal of Neuroscience 23:2899-2910.

Surprenant A (1996) Functional properties of native and cloned P2X receptors. [Review] [40 refs]. Ciba Foundation symposium 198:208-219.

Surprenant A, Rassendren F, Kawashima E, North RA, Buell G (1996) The cytolytic P2Z receptor for extracellular ATP identified as a P2X receptor (P2X7). Science 272:735-738.

Suzuki T, Hide I, Ido K, Kohsaka S, Inoue K, Nakata Y (2004) Production and release of neuroprotective tumor necrosis factor by P2X7 receptor-activated microglia. Journal of Neuroscience 24:1-7.

Svensson CI, Schafers M, Jones TL, Powell H, Sorkin LS (2005) Spinal blockade of TNF blocks spinal nerve ligation-induced increases in spinal P-p38. Neuroscience Letters 379:209-213.

Svensson M, Eriksson P, Persson JK, Molander C, Arvidsson J, Aldskogius H (1993) The response of central glia to peripheral nerve injury. [Review] [61 refs]. Brain Research Bulletin 30:499-506.

Sweitzer SM, Colburn RW, Rutkowski M, Deleo JA (1999) Acute peripheral inflammation induces moderate glial activation and spinal IL-1beta expression that correlates with pain behavior in the rat. Brain Research 829:209-221.

Sweitzer SM, Schubert P, Deleo JA (2001) Propentofylline, a glial modulating agent, exhibits antiallodynic properties in a rat model of neuropathic pain. Journal of Pharmacology and Experimental Therapeutics 297:1210-1217.

Tai YH, Wang YH, Tsai RY, Wang JJ, Tao PL, Liu TM, Wang YC, Wong CS (2007) Amitriptyline preserves morphine's antinociceptive effect by regulating the glutamate transporter GLAST and GLT-1 trafficking and excitatory amino acids concentration in morphine-tolerant rats. Pain 129:343-354.

Tai YH, Wang YH, Wang JJ, Tao PL, Tung CS, Wong CS (2006) Amitriptyline suppresses neuroinflammation and up-regulates glutamate transporters in morphine-tolerant rats. Pain 124:77-86.

Takayama N, Ueda H (2005) Morphine-induced overexpression of prepro-nociceptin/orphanin FQ in cultured astrocytes. Peptides 26:2513-2517.

Takemori AE, Loh HH, Lee NM (1992) Suppression by dynorphin A-(1-13) of the expression of opiate withdrawal and tolerance in mice. European Journal of Pharmacology 221:223-226.

Takenouchi T, Iwamaru Y, Imamura M, Kato N, Sugama S, Fujita M, Hashimoto M, Sato M, Okada H, Yokoyama T, Mohri S, Kitani H (2007) Prion infection correlates with hypersensitivity of P2X7 nucleotide receptor in a mouse microglial cell line. FEBS Letters 581:3019-3026.

Takenouchi T, Sugama S, Iwamaru Y, Hashimoto M, Kitani H (2009) Modulation of the ATP-lnduced release and processing of IL-1beta in microglial cells. [Review] [73 refs]. Critical Reviews in Immunology 29:335-345.

Tanga FY, Nutile-McMenemy N, Deleo JA (2005) The CNS role of Toll-like receptor 4 in innate neuroimmunity and painful neuropathy. Proceedings of the National Academy of Sciences of the United States of America 102:5856-5861.

Tanga FY, Raghavendra V, Deleo JA (2004) Quantitative real-time RT-PCR assessment of spinal microglial and astrocytic activation markers in a rat model of neuropathic pain. Neurochemistry International 45:397-407.

Tatham PE, Lindau M (1990) ATP-induced pore formation in the plasma membrane of rat peritoneal mast cells. Journal of General Physiology 95:459-476.

Tawfik VL, LaCroix-Fralish ML, Nutile-McMenemy N, Deleo JA (2005) Transcriptional and translational regulation of glial activation by morphine in a rodent model of neuropathic pain. Journal of Pharmacology & Experimental Therapeutics 313:1239-1247.

Tawfik VL, Nutile-McMenemy N, LaCroix-Fralish ML, Deleo JA (2007) Reprint of "Efficacy of propentofylline, a glial modulating agent, on existing mechanical allodynia following peripheral nerve injury" [Brain Behav. Immun. 21 (2007) 238-246]. Brain, behavior, and immunity 21:677-685.

Thornberry NA, Bull HG, Calaycay JR, Chapman KT, Howard AD, Kostura M.J., Miller DK, Molineaux SM, Weidner JR, Aunins J, Elliston KO, Casano FJ, Chin J, Ding GJF, Egger LA, Gaffney EP, Palyha OC (1992) A novel heterodimeric cysteine protease is required for interleukin-1beta processing in monocytes. Nature 356:768-774.

Tikka TM, Koistinaho JE (2001) Minocycline provides neuroprotection against N-methyl-D-aspartate neurotoxicity by inhibiting microglia. Journal of Immunology 166:7527-7533.

Torrance N, Smith BH, Bennett MI, Lee AJ (2006) The epidemiology of chronic pain of predominantly neuropathic origin. Results from a general population survey. Journal of Pain 7:281-289.

Tortorici V, Robbins CS, Morgan MM (1999) Tolerance to the antinociceptive effect of morphine microinjections into the ventral but not lateral-dorsal periaqueductal gray of the rat. Behavioral Neuroscience 113:833-839.

Trang T, Beggs S, Salter MW (2006) Purinoceptors in microglia and neuropathic pain. [Review] [73 refs]. Pflugers Archiv - European Journal of Physiology 452:645-652.

Trang T, Beggs S, Wan X, Salter MW (2009) P2X4-receptor-mediated synthesis and release of brain-derived neurotrophic factor in microglia is dependent on calcium and p38-mitogen-activated protein kinase activation. Journal of Neuroscience 29:3518-3528.

Trang T, Sutak M, Quirion R, Jhamandas K (2002) The role of spinal neuropeptides and prostaglandins in opioid physical dependence. British Journal of Pharmacology 136:37-48.

Tremont-Lukats IW, Megeff C, Backonja MM (2000) Anticonvulsants for neuropathic pain syndromes: mechanisms of action and place in therapy. [Review] [161 refs]. Drugs 60:1029-1052.

Trujillo KA, Akil H (1991) Opiate tolerance and dependence: recent findings and synthesis. [Review] [80 refs]. New Biologist 3:915-923.

Tsuda M, Inoue K, Salter MW (2005) Neuropathic pain and spinal microglia: a big problem from molecules in "small" glia. [Review] [70 refs]. Trends in Neurosciences 28:101-107.

Tsuda M, Kuboyama K, Inoue T, Nagata K, Tozaki-Saitoh H, Inoue K (2009) Behavioral phenotypes of mice lacking purinergic P2X4 receptors in acute and chronic pain assays. Molecular pain 5.

Tsuda M, Shigemoto-Mogami Y, Koizumi S, Mizokoshi A, Kohsaka S, Salter MW, Inoue K (2003) P2X4 receptors induced in spinal microglia gate tactile allodynia after nerve injury. Nature 424:778-783.

Turchan-Cholewo J, Dimayuga FO, Ding Q, Keller JN, Hauser KF, Knapp P.E., Bruce-Keller AJ (2008) Cell-specific actions of HIV-tat and morphine on opioid receptor expression in glia. Journal of Neuroscience Research 86:2100-2110.

Ulmann L, Hatcher JP, Hughes JP, Chaumont S, Green PJ, Conquet F, Buell GN, Reeve AJ, Chessell IP, Rassendren F (2008) Up-regulation of P2X4 receptors in spinal microglia after peripheral nerve injury mediates BDNF release and neuropathic pain. Journal of Neuroscience 28:11263-11268.

Urban MO, Gebhart GF (1998) The glutamate synapse: a target in the pharmacological management of hyperalgesic pain states. [Review] [81 refs]. Progress in Brain Research 116:407-420.

Urban MO, Gebhart GF (1999) Central mechanisms in pain. [Review] [30 refs]. Medical Clinics of North America 83:585-596.

Van HJ, Gybels J (1981) C nociceptor activity in human nerve during painful and non painful skin stimulation. Journal of Neurology, Neurosurgery & Psychiatry 44:600-607.

Vanderah TW, Bernstein RN, Yamamura HI, Hruby VJ, Porreca F (1996) Enhancement of morphine antinociception by a CCK(B) antagonist in mice is mediated via opioid delta receptors. Journal of Pharmacology and Experimental Therapeutics 278:212-219.

Vanderah TW, Gardell LR, Burgess SE, Ibrahim M, Dogrul A, Zhong CM, Zhang ET, Malan TP, Jr., Ossipov MH, Lai J, Porreca F (2000a) Dynorphin promotes abnormal pain and spinal opioid antinociceptive tolerance. Journal of Neuroscience 20:7074-7079.

Vanderah TW, Gardell LR, Burgess SE, Ibrahim M, Dogrul A, Zhong CM, Zhang ET, Malan TP, Jr., Ossipov MH, Lai J, Porreca F (2000b) Dynorphin promotes abnormal pain and spinal opioid antinociceptive tolerance. Journal of Neuroscience 20:7074-7079.

Vanderah TW, Lai J, Yamamura HI, Porreca F (1994) Antisense oligodeoxynucleotide to the CCKB receptor produces naltrindole- and [Leu5]enkephalin antiserum-sensitive enhancement of morphine antinociception. NeuroReport 5:2601-2605.

Vanderah TW, Ossipov MH, Lai J, Malan J, Philip PF (2001a) Mechanisms of opioid-induced pain and antinociceptive tolerance: Descending facilitation and spinal dynorphin. Pain 92:5-9.

Vanderah TW, Ossipov MH, Lai J, Malan TP, Jr., Porreca F (2001b) Mechanisms of opioid-induced pain and antinociceptive tolerance: descending facilitation and spinal dynorphin. [Review] [44 refs]. Pain 92:5-9.

Vanderah TW, Suenaga NM, Ossipov MH, Malan TP, Jr., Lai J, Porreca F (2001c) Tonic descending facilitation from the rostral ventromedial medulla mediates opioid-induced abnormal pain and antinociceptive tolerance. Journal of Neuroscience 21:279-286.

Vane JR (1971) Inhibition of prostaglandin synthesis as a mechanism of action for aspirin-like drugs. Nature - New Biology 231:232-235.

Vanegas H, Schaible HG (2004) Descending control of persistent pain: inhibitory or facilitatory?. [Review] [80 refs]. Brain Research - Brain Research Reviews 46:295-309.

Vankova ME, Weinger MB, Chen DY, Bronson JB, Motis V, Koob GF (1996) Role of central mu, delta-1, and kappa-1 opioid receptors in opioid-induced muscle rigidity in the rat. Anesthesiology 85:574-583.

Verge GM, Milligan ED, Maier SF, Watkins LR, Naeve GS, Foster AC (2004) Fractalkine (CX3CL1) and fractalkine receptor (CX3CR1) distribution in spinal cord and dorsal root ganglia under basal and neuropathic pain conditions. European Journal of Neuroscience 20:1150-1160.

Vergne-Salle P, Beneytout J-L (2010) Targeting the cyclooxygenase pathway. pp 383-401.

Verhoef PA, Estacion M, Schilling W, Dubyak GR (2003) P2X7 receptor-dependent blebbing and the activation of Rho-effector kinases, caspases, and IL-1 beta release. Journal of Immunology 170:5728-5738.

Virginio C, Church D, North RA, Surprenant A (1997) Effects of divalent cations, protons and calmidazolium at the rat P2X7 receptor. Neuropharmacology 36:1285-1294.

Virginio C, MacKenzie A, North RA, Surprenant A (1999a) Kinetics of cell lysis, dye uptake and permeability changes in cells expressing the rat P2X7 receptor. Journal of Physiology 519 Pt 2:335-346.

Virginio C, MacKenzie A, Rassendren FA, North RA, Surprenant A (1999b) Pore dilation of neuronal P2X receptor channels. Nature neuroscience 2:315-321.

Visentin S, Renzi M, Frank C, Greco A, Levi G (1999) Two different ionotropic receptors are activated by ATP in rat microglia. Journal of Physiology 519 Pt 3:723-736.

Voogd TE, Vansterkenburg EL, Wilting J, Janssen LH (1993) Recent research on the biological activity of suramin. [Review] [209 refs]. Pharmacological Reviews 45:177-203.

Wagner R, Deleo JA (1996) Pre-emptive dynorphin and N-methyl-D-aspartate glutamate receptor antagonism alters spinal immunocytochemistry but not allodynia following complete peripheral nerve injury. Neuroscience 72:527-534.

Waksman JC, Brody A, Phillips SD (2007) Nonselective nonsteroidal antiinflammatory drugs and cardiovascular risk: are they safe?. [Review] [69 refs]. Annals of Pharmacotherapy 41:1163-1173.

Waldhoer M, Bartlett SE, Whistler JL (2004) Opioid receptors. [Review] [309 refs]. Annual Review of Biochemistry 73:953-990.

Wall PD, Devor M, Inbal R, Scadding JW, Schonfeld D, Seltzer Z, Tomkiewicz MM (1979) Autotomy following peripheral nerve lesions: experimental anaesthesia dolorosa. Pain 7:103-111.

Wallace VC, Blackbeard J, Pheby T, Segerdahl AR, Davies M, Hasnie F, Hall S, McMahon SB, Rice AS (2007a) Pharmacological, behavioural and mechanistic analysis of HIV-1 gp120 induced painful neuropathy. Pain 133:47-63.

Wallace VC, Segerdahl AR, Lambert DM, Vandevoorde S, Blackbeard J, Pheby T, Hasnie F, Rice AS (2007b) The effect of the palmitoylethanolamide analogue, palmitoylallylamide (L-29) on pain behaviour in rodent models of neuropathy. Br J Pharmacol 151:1117-1128.

Wang L, Gintzler AR (1995) Morphine tolerance and physical dependence: reversal of opioid inhibition to enhancement of cyclic AMP formation. Journal of Neurochemistry 64:1102-1106.

Wang L, Gintzler AR (1997) Altered mu-opiate receptor-G protein signal transduction following chronic morphine exposure. Journal of Neurochemistry 68:248-254.

Wang X, Arcuino G, Takano T, Lin J, Peng WG, Wan P, Li P, Xu Q, Liu QS, Goldman SA, Nedergaard M (2004) P2X7 receptor inhibition improves recovery after spinal cord injury. Nat Med 10:821-827.

Wang Z, Gardell LR, Ossipov MH, Vanderah TW, Brennan MB, Hochgeschwender U, Hruby VJ, Malan TP, Jr., Lai J, Porreca F (2001) Pronociceptive actions of dynorphin maintain chronic neuropathic pain. Journal of Neuroscience 21:1779-1786.

Wardlaw SL, Kim J, Sobieszczyk S (1996) Effect of morphine on proopiomelanocortin gene expression and peptide levels in the hypothalamus. Brain Res Mol Brain Res 41:140-147.

Watanabe N, Kawaguchi M, Kobayashi Y (1998) Activation of interleukin-1beta-converting enzyme by nigericin is independent of apoptosis. Cytokine 10:645-653.

Watkins LR (2007) Immune and glial regulation of pain. Brain, behavior, and immunity 21:519-521.

Watkins LR, Hutchinson MR, Johnston IN, Maier SF (2005) Glia: Novel counter-regulators of opioid analgesia. Trends in Neurosciences 28:661-669.

Watkins LR, Hutchinson MR, Ledeboer A, Wieseler-Frank J, Milligan ED (2007a) Glia as the "bad guys": Implications for improving clinical pain control and the clinical utility of opioids. Brain, behavior, and immunity 21:131-146.

Watkins LR, Hutchinson MR, Milligan ED, Maier SF (2007b) "Listening" and "talking" to neurons: Implications of immune activation for pain control and increasing the efficacy of opioids. Brain Research Reviews 56:148-169.

Watkins LR, Hutchinson MR, Rice KC, Maier SF (2009) The "toll" of opioid-induced glial activation: improving the clinical efficacy of opioids by targeting glia. Trends Pharmacol Sci 30:581-591.

Watkins LR, Kinscheck IB, Mayer DJ (1984) Potentiation of opiate analgesia and apparent reversal of morphine tolerance by proglumide. Science 224:395-396.

Watkins LR, Kinscheck IB, Mayer DJ (1985) Potentiation of morphine analgesia by the cholecystokinin antagonist proglumide. Brain Research 327:169-180.

Watkins LR, Maier SF (2003) Glia: a novel drug discovery target for clinical pain. [Review] [134 refs]. Nature Reviews Drug Discovery. 2:973-985.

Watkins LR, Martin D, Ulrich P, Tracey KJ, Maier SF (1997) Evidence for the involvement of spinal cord glia in subcutaneous formalin induced hyperalgesia in the rat. Pain 71:225-235.

Watkins LR, Milligan ED, Maier SF (2001) Spinal cord glia: new players in pain. [Review] [34 refs]. Pain 93:201-205.

Watson CP, Deck JH, Morshead C, van der KD, Evans RJ (1991) Post-herpetic neuralgia: further post-mortem studies of cases with and without pain. Pain 44:105-117.

Weber E, Evans CJ, Barchas JD (1983) Multiple endogenous ligands for opioid receptors. pp 333-336.

Wei F, Guo W, Zou S, Ren K, Dubner R (2008) Supraspinal glial-neuronal interactions contribute to descending pain facilitation. Journal of Neuroscience 28:10482-10495.

Welch SP, Olson KG (1991) Opiate tolerance-induced modulation of free intracellular calcium in synaptosomes. Life Sciences 48:1853-1861.

Westin BD, Walker SM, Deumens R, Grafe M, Yaksh TL (2010) Validation of a preclinical spinal safety model: effects of intrathecal morphine in the neonatal rat. Anesthesiology 113:183-199.

Whistler JL, Chuang HH, Chu P, Jan LY, von ZM (1999) Functional dissociation of mu opioid receptor signaling and endocytosis: implications for the biology of opiate tolerance and addiction. Neuron 23:737-746.

White JM (2004) Pleasure into pain: The consequences of long-term opioid use. Addictive Behaviors 29:1311-1324.

Wieseler-Frank J, Maier SF, Watkins LR (2004) Glial activation and pathological pain. [Review] [70 refs]. Neurochemistry International 45:389-395.

Williams JT, Christie MJ, Manzoni O (2001) Cellular and synaptic adaptations mediating opioid dependence. [Review] [549 refs]. Physiological Reviews 81:299-343.

Winkelstein BA, Rutkowski MD, Sweitzer SM, Pahl JL, Deleo JA (2001) Nerve injury proximal or distal to the DRG induces similar spinal glial activation and selective cytokine expression but differential behavioral responses to pharmacologic treatment. Journal of Comparative Neurology 439:127-139.

Woodhams PL, MacDonald RE, Collins SD, Chessell IP, Day NC (2007) Localisation and modulation of prostanoid receptors EP1 and EP4 in the rat chronic constriction injury model of neuropathic pain. Eur J Pain 11:605-613.

Woolf CJ (1983) Evidence for a central component of post-injury pain hypersensitivity. Nature 306:686-688.

Woolf CJ (1991) Generation of acute pain: Central mechanisms. British Medical Bulletin 47:523-533.

Woolf CJ, Allchorne A, Safieh-Garabedian B, Poole S (1997) Cytokines, nerve growth factor and inflammatory hyperalgesia: The contribution of tumour necrosis factor alpha. British Journal of Pharmacology 121:417-424.

Woolf CJ, Shortland P, Coggeshall RE (1992) Peripheral nerve injury triggers central sprouting of myelinated afferents. Nature 355:75-78.

Woolf CJ, Thompson SW (1991) The induction and maintenance of central sensitization is dependent on N-methyl-D-aspartic acid receptor activation; implications for the treatment of post-injury pain hypersensitivity states. Pain 44:293-299.

Woolf CJ, Wall PD (1986) Relative effectiveness of C primary afferent fibers of different origins in evoking a prolonged facilitation of the flexor reflex in the rat. Journal of Neuroscience 6:1433-1442.

Woolf CJ, Walters ET (1991) Common patterns of plasticity contributing to nociceptive sensitization in mammals and Aplysia. [Review] [60 refs]. Trends in Neurosciences 14:74-78.

Xie G-X, Palmer PP (2005) RGS proteins: New players in the field of opioid signaling and tolerance mechanisms. Anesthesia and Analgesia 100:1034-1042.

Xie JY, Herman DS, Stiller C-O, Gardell LR, Ossipov MH, Lai J, Vanderah TW (2005) Cholecystokinin in the rostral ventromedial medulla mediates opioid-induced hyperalgesia and antinociceptive tolerance. Journal of Neuroscience 25:409-416.

Xu H, Wang X, Wang J, Rothman RB (2004) Opioid peptide receptor studies. 17. Attenuation of chronic morphine effects after antisense oligodeoxynucleotide knock-down of RGS9 protein in cells expressing the cloned Mu opioid receptor. Synapse 52:209-217.

Xu XJ, Dalsgaard CJ, Wiesenfeld-Hallin Z (1992) Spinal substance P and N-methyl-D-aspartate receptors are coactivated in the induction of central sensitization of the nociceptive flexor reflex. Neuroscience 51:641-648.

Yaksh TL, Harty GJ (1988) Pharmacology of the allodynia in rats evoked by high dose intrathecal morphine. Journal of Pharmacology and Experimental Therapeutics 244:501-507.

Yaksh TL, Harty GJ, Onofrio BM (1986) High dose of spinal morphine produce a nonopiate receptor-mediated hyperesthesia: clinical and theoretic implications. Anesthesiology 64:590-597.

Yan Z, Li S, Liang Z, Tomic M, Stojilkovic SS (2008) The P2X 7 receptor channel pore dilates under physiological ion conditions. Journal of General Physiology 132:563-573.

Yeung JC, Rudy TA (1980) Multiplicative interaction between narcotic agonisms expressed at spinal and supraspinal sites of antinociceptive action as revealed by concurrent intrathecal and intracerebroventricular injections of morphine. J Pharmacol Exp Ther 215:633-642.

Yoshida K, Gage FH (1992) Cooperative regulation of nerve growth factor synthesis and secretion in fibroblasts and astrocytes by fibroblast growth factor and other cytokines. Brain Research 569:14-25.

Yu Y, Ugawa S, Ueda T, Ishida Y, Inoue K, Kyaw NA, Umemura A, Mase M, Yamada K, Shimada S (2008) Cellular localization of P2X7 receptor mRNA in the rat brain. Brain Research 1194:45-55.

Zachariou V, Georgescu D, Sanchez N, Rahman Z, DiLeone R, Berton O, Neve RL, Sim-Selley LJ, Selley DE, Gold SJ, Nestler EJ (2003) Essential role for RGS9 in opiate action. Proceedings of the National Academy of Sciences of the United States of America 100:13656-13661.

Zadina JE, Chang SL, Ge LJ, Kastin AJ (1993) Mu opiate receptor down-regulation by morphine and up-regulation by naloxone in SH-SY5Y human neuroblastoma cells. Journal of Pharmacology & Experimental Therapeutics 265:254-262.

Zanjani TM, Sabetkasaei M, Mosaffa N, Manaheji H, Labibi F, Farokhi B (2006) Suppression of interleukin-6 by minocycline in a rat model of neuropathic pain. European Journal of Pharmacology 538:66-72.

Zanovello P, Bronte V, Rosato A, Pizzo P, Di VF (1990) Responses of mouse lymphocytes to extracellular ATP. II. Extracellular ATP causes cell type-dependent lysis and DNA fragmentation. Journal of Immunology 145:1545-1550.

Zaremba PD, Bialek M, Blaszczyk B, Cioczek P, Czuczwar SJ (2006) Non-epilepsy uses of antiepilepsy drugs. [Review] [101 refs]. Pharmacological Reports: PR 58:1-12.

Zerboni L, Ku CC, Jones CD, Zehnder JL, Arvin AM (2005) Varicella-zoster virus infection of human dorsal root ganglia in vivo. Proc Natl Acad Sci U S A 102:6490-6495.

Zhang J, De KY (2006) Spatial and temporal relationship between monocyte chemoattractant protein-1 expression and spinal glial activation following peripheral nerve injury. Journal of Neurochemistry 97:772-783.

Zhang L, Yu Y, Mackin S, Weight FF, Uhl GR, Wang JB (1996) Differential mu opiate receptor phosphorylation and desensitization induced by agonists and phorbol esters. Journal of Biological Chemistry 271:11449-11454.

Zhang R-X, Liu B, Wang L, Ren K, Qiao J-T, Berman BM, Lao L (2005a) Spinal glial activation in a new rat model of bone cancer pain produced by prostate cancer cell inoculation of the tibia. Pain 118:125-136.

Zhang XF, Han P, Faltynek CR, Jarvis MF, Shieh CC (2005b) Functional expression of P2X7 receptors in non-neuronal cells of rat dorsal root ganglia. Brain Res 1052:63-70.

Zheng LM, Zychlinsky A, Liu CC, Ojcius DM, Young JD (1991) Extracellular ATP as a trigger for apoptosis or programmed cell death. The Journal of cell biology 112:279-288.

Zhou D, Chen M-L, Zhang Y-Q, Zhao Z-Q (2010) Involvement of spinal microglial P2X7 receptor in generation of tolerance to morphine analgesia in rats. Journal of Neuroscience 30:8042-8047.

Zhou HY, Chen SR, Chen H, Pan HL (2008) Sustained inhibition of neurotransmitter release from nontransient receptor potential vanilloid type 1-expressing primary afferents by mu-opioid receptor activation-enkephalin in the spinal cord. Journal of Pharmacology & Experimental Therapeutics 327:375-382.

Zhou Y, Sun Y-H, Zhang Z-W, Han J-S (1993) Increased release of immunoreactive cholecystokinin octapeptide by morphine and potentiation of mu-opioid analgesia by CCK(B) receptor antagonist L-365,260 in rat spinal cord. European Journal of Pharmacology 234:147-154.

Zhuang Z-Y, Kawasaki Y, Tan P-H, Wen Y-R, Huang J, Ji R-R (2007) Role of the CX3CR1/p38 MAPK pathway in spinal microglia for the development of neuropathic pain following nerve injury-induced cleavage of fractalkine. Brain, behavior, and immunity 21:642-651.

Zhuo M, Gebhart GF (1990) Characterization of descending inhibition and facilitation from the nuclei reticularis gigantocellularis and gigantocellularis pars alpha in the rat. Pain 42:337-350.

Zhuo M, Gebhart GF (1991) Spinal serotonin receptors mediate descending facilitation of a nociceptive reflex from the nuclei reticularis gigantocellularis and gigantocellularis pars alpha in the rat. Brain Research 550:35-48.

Zhuo M, Gebhart GF (1992) Characterization of descending facilitation and inhibition of spinal nociceptive transmission from the nuclei reticularis gigantocellularis and gigantocellularis pars alpha in the rat. Journal of Neurophysiology 67:1599-1614.

Zhuo M, Gebhart GF (1997) Biphasic modulation of spinal nociceptive transmission from the medullary raphe nuclei in the rat. Journal of Neurophysiology 78:746-758.

Appendix – probes and primers used

ORF-63 (supplied by Dr. R. Dalziel)
Forward primer: VZV63P1: GCG AGA TTC ACG AAG ATT GCG[a]
Forward primer: VZV63P2: TTA TCT AAT GGG TCG CAC C[a]
Reverse primer: VZV63P3: TCA ATT ACA TCC GAT GGC G[b]

[a]Sense, same direction as the ORF following VZV Dumas strain sequence
[b] Antisense, opposite direction from that of the ORF following VZV Dumas strain sequence

r/m GAPDH
Forward primer: 5'-GAACATCATCCCTGCATCCA-3'
Reverse primer: 5'-CCAGTGAGCTTCCCGTTCA-3'
Probe: 5'- FAM-CTTGCCCACAGCCTTGGCAGC-TAMRA-3'

r Cyclophilin
Forward primer: 5'-TGTGCCAGGGTGGTGACTT-3'
Reverse primer: 5'-TCAAATTTCTCTCCGTAGATGGACTT-3'
Probe: 5'- FAM-CCACCAGTGCCATTATGGCGTGT-TAMRA-3'

r GFAP
Forward primer: 5'-ACCCTCTCGGAAGCTGGTTG -3'
Reverse primer: 5'-TCCTGCCCAGTGAGTAAAGGTG -3'
Probe: 5'- FAM-CCACCAGTGCCATTATGGCGTGT-TAMRA-3'

rβ-Actin
Forward primer: 5'-AGTTTCATGGATGCCACAGGA-3'
Reverse primer: 5'-GAGCTATGAGCTGCCTGAC-3'
Probe: 5'-FAM-CATCACTATCGGCAATGAGCGGTTCC-TAMRA-3'

rITGAM
Forward primer: 5'-ACCACAGTCCCGCAGAGAGC-3'
Reverse primer: 5'-GTTCCGAATGGTATTCAGAGCTTC-3'
Probe: 5'-FAM-TGTCCACTTGGAACACGTGATCACCAG-TAMRA-3'

rPBR
Forward primer: 5'-GGACCTCATGCTTGTCAGTGG-3'
Reverse primer: 5'-CCAGGCCAGGTAAGGATACAGC-3'
Probe: 5'-FAM-ACTACCCTGGCTTGGCACCGAGTGAG-TAMRA-3'

rTNF-RSF1α
Forward primer: 5'-GCAGGGAAGTGTGCCATCTG-3'
Reverse primer: 5'-CTGAGGAGGCCCTGAGAAGC-3'
Probe: 5'-FAM-CTGATACCCACTTGGGATGCAAGGACC-TAMRA-3'

rμOpioid

Forward primer: 5’-GCAGGAAGCCAAGAATTTCGC-3’
Reverse primer: 5’-ATGCTGTTTCATAAGGCATCAGG-3’
Probe: 5’-FAM-TCAGTAATTTCTCCACATGCACGCTC-TAMRA-3’

rIL-1β

Forward primer: 5’-CCCAACTGGTACATCAGCACC-3’
Rerverse primer: 5’-ACACGGGTTCCATGGTGAAGTC-3’
Probe: 5’-FAM-TCCCGACCATTGCTGTTTCCTAGGAAG-TAMRA-3’